Near-ultraviolet radiation-induced damage using an actinic reticuloid strain as a possible sensitive model

Kralli, Aspasia

Award date:
1987

Awarding institution:
University of Bath

NEAR-ULTRAVIOLET RADIATION-INDUCED DAMAGE USING AN ACTINIC RETICULOID STRAIN AS A POSSIBLE SENSITIVE MODEL

Submitted by Aspasia Kralli, B. Pharm., M.P.S.

for the degree of Doctor of Philosophy

of the University of Bath

1987

This research has been carried out in the School of Pharmacy and Pharmacology of the University of Bath under the supervision of S.H. Moss, M.Sc., Ph.D., M.P.S. and D.J.G. Davies, M.Sc., Ph.D., F.P.S.

ProQuest LLC
789 East Eisenhower Parkway
P.O. Box 1346
Ann Arbor, MI 48106-1346

To my family

ACKNOWLEDGMENTS

There are a lot of people who have contributed to the completion of this work, directly or indirectly, which I would like to thank.

My supervisors, Dr. S. H. Moss and Dr. D. J. G. Davies for giving me the opportunity to do this research and for being so helpful and encouraging throughout all stages of the work.

My parents, Elias and Sophia, for their love and wisdom with which they have always guided me. My sister Natasha and my brother Alexis for their moral support. My future husband, Takis, for his great patience, understanding and personal sacrifices made while we were apart to still keep us together. Without the support of my family I would have neither begun nor completed this work, and, in recognition of this I dedicate my thesis to them.

All the technical staff at Bath University, especially Mr. P. Christie for his assistance in the computer room and his helpful advice on statistics and Mr. D. Vinicombe for his help with the figures.

All my colleagues, in particular, Dr. S. P. Moore, Miss. A. Coombs, Mrs. J. Chamberlain and Mr. A. Smith who read through the manuscript and offered their constructive criticism. Also, Miss M. McAleer with whom we shared a lot of early discussions and frustrations and Mr. H. Patel who was most helpful in showing me the use of 'tel-a-graph'.

My overqualified typist who was so professional, patient and helpful throughout all stages of typing.

Last, but not least, Katrina, not only for providing a roof on top of my head, but most importantly, for providing me with such warmth and friendliness when I needed it most.

ABSTRACT

The introduction to this thesis consists of a review of current concepts regarding the effects of ultraviolet radiation on living cells. Emphasis is placed on near-ultraviolet radiation properties and the marked influence of oxygen on its effects. In particular, the possible generation of reactive oxygen species together with their toxicity is discussed. This is followed by a brief review of cellular antioxidant systems to defend the damage and a detailed description of the properties and actions of vitamin E. Actinic reticuloid, a disease condition for which a near-ultraviolet radiation cellular sensitivity has been proposed as an underlying cause, is described.

Chapter 2 lists the materials and methods basic to cell culture procedures and the irradiation procedures used in succeeding chapters.

The experimental work, the broad aim of which is to expand existing knowledge of the effects of near-ultraviolet radiation that may lead to cell lethality has centred upon the irradiation of a normal human skin fibroblast strain, GM730, and a strain derived from an actinic reticuloid patient, AR6LO. It is presented in five parts.

Part 1 examines the effect of the irradiation temperature on the normal human fibroblast sensitivity to specific ultraviolet wavelengths. Part 2 describes the sensitivity of actinic reticuloid fibroblasts to a range of ultraviolet wavelengths under controlled

conditions of irradiation. The next two sections include observations on the protective effect of Trolox-C, a vitamin E analogue and the sensitization resulting by the replacement of the irradiation medium by a deuterated one, using both normal and actinic reticuloid fibroblasts. The final part examines broad-band near- and far-ultraviolet radiation-induced membrane damage by the use of radioactively labelled rubidium as a potassium analogue.

The data obtained in each section have been discussed in the context of current published concepts regarding near-ultraviolet radiation-induced mechanisms of lethality.

CONTENTS

INTRODUCTION

1. ORIGINS OF PRESENT WORK

Living cells are exposed to numerous physical and chemical stresses throughout their life and sunlight has long been recognized as one of them. In order to retain their integrity, cells have evolved methods of preventing or combating potentially damaging effects occurring as a result of exposure to sunlight. These include physical screening of the radiation by a cell wall or membrane, quenching of deleterious photoproducts and means of repairing essential cellular components such as DNA.

Initial studies to elucidate the damaging effects of sunlight and the cellular protective mechanisms originally used artificial sources emitting principally 254 nm wavelength and simple cells such as bacteria. The choice of wavelength was due to the fact that it produced marked biological effects and could be easily generated as a strong emission line of low pressure mercury vapour lamps. The choice of cell type studied was due to its uncomplicated structure and the ease of its manipulation. Much was learnt about the nature of damage clearly implicating DNA as the primary target. Enzymatic repair systems were identified which acted on non-replicating DNA, such as photoreactivation and excision repair, or on replicating DNA, such as postreplication repair. The use of bacterial mutants lacking in one or more repair processes greatly advanced the elucidation of mechanisms leading to lethality and the identification of lethal lesions formed by 254 nm-irradiation.

Later work expanded to include longer wavelengths (290-400 nm) which are more relevant biologically since a layer of ozone in the upper atmosphere shields the earth from wavelengths shorter than 290 nm. It was realized that the mechanisms of damage initiated by monochromatic or polychromatic bands of longer wavelengths were different to those resulting from 254 nm irradiation. In particular, the importance of oxygen became apparent and cellular components in addition to DNA were examined as potential targets of the radiation.

The uncertainties arising as a result of the new proposals were more pronounced in the case of the more advanced cell types studied, such as mammalian cells. Studies with mammalian cells could benefit from the use of cell strains specifically sensitive to irradiation in a manner analogous to the use of bacterial mutants. Indeed, research into the genetic condition xeroderma pigmentosum, characterized by a marked predisposition of patients to develop skin cancers after exposure to sunlight, supported a link between an increase in DNA lesions and tumourigenicity. The most effective wavelength to bring about these particular DNA lesions was found to be 254 nm.

An analogous model to serve as a probe in the damaging effects of longer wavelength radiation would be of value, and this study was designed to investigate near-ultraviolet-induced damage using a mammalian cell line with suspected sensitivity specifically at these wavelengths. Before describing details of the origin of this cell line, the nature of ultraviolet radiation and oxygen toxicity as two major environmental stresses will be discussed. Their impact upon the living cell and the cellular defense systems devised to protect

against their damaging effects will be examined in detail, with emphasis on the longer ultraviolet radiations which are present in our environment. Since the cell type studied in the experimental section will be the skin fibroblast, an effort will be made to view it in relation to its function as part of the human physical screen to ultraviolet radiation i.e. the human skin. Finally, actinic reticuloid, a disease condition characterized by skin sensitivity of patients to solar-ultraviolet radiations, will be described, since investigations into the sensitivity of skin fibroblasts from such a patient will be presented in the experimental section.

2. UV RADIATION EFFECTS ON CELLS

2.1.1 Electromagnetic Spectrum

The radiant energy which originates from continuous thermonuclear reactions in the sun's core is called electromagnetic because it is in the form of oscillating electric and magnetic fields. It exhibits both wave-like (oscillating field) and particle-like (discrete packet) properties. These discrete packets or quanta of energy are called photons.

The relationship between the energy and the wavelength of radiations is given by the following expression:

$$E = \frac{h \times c}{\lambda}$$

where E=energy of the quantum in Joules

h=Planck's constant (6.624×10^{-34} Js)

c=velocity of light (3×10^{10} cm s^{-1})

λ=wavelength in cm

The energy of a quantum (or photon) is, therefore, inversely proportional to the wavelength of the radiation.

2.1.2 Solar Spectrum

In discussing the properties and characteristics of the ultraviolet (UV) spectrum which represents only a small portion of the whole electromagnetic spectrum, it is convenient to distinguish between the regions which have distinct physical and biological properties.

The following breakdown of the UV spectrum is widely accepted and the nomenclature which will be used throughout this work is

Far UV - for radiations of wavelengths between 190 and 290 nm which are the most energetic

Mid UV - for radiations of wavelengths between 290 and 320 nm

Near UV - for radiations of wavelengths longer than 320 nm up to the visible region (400nm)

An alternative nomenclature of UV-C, UV-B, and UV-A is also used in the literature for the corresponding regions.

When considering the effects of sunlight in relation to carcinogenesis or photosensitive conditions, it is important to examine the effects of environmentally relevant wavelengths. Only mid UV and near UV can be considered as such, since a layer of ozone in the upper atmosphere shields the surface of the earth of all radiations below 290 nm. Figure 1 depicts the current solar radiation at the earth's surface. The term solar UV is thus coined to refer collectively to wavelengths longer than 290 nm up to the visible region.

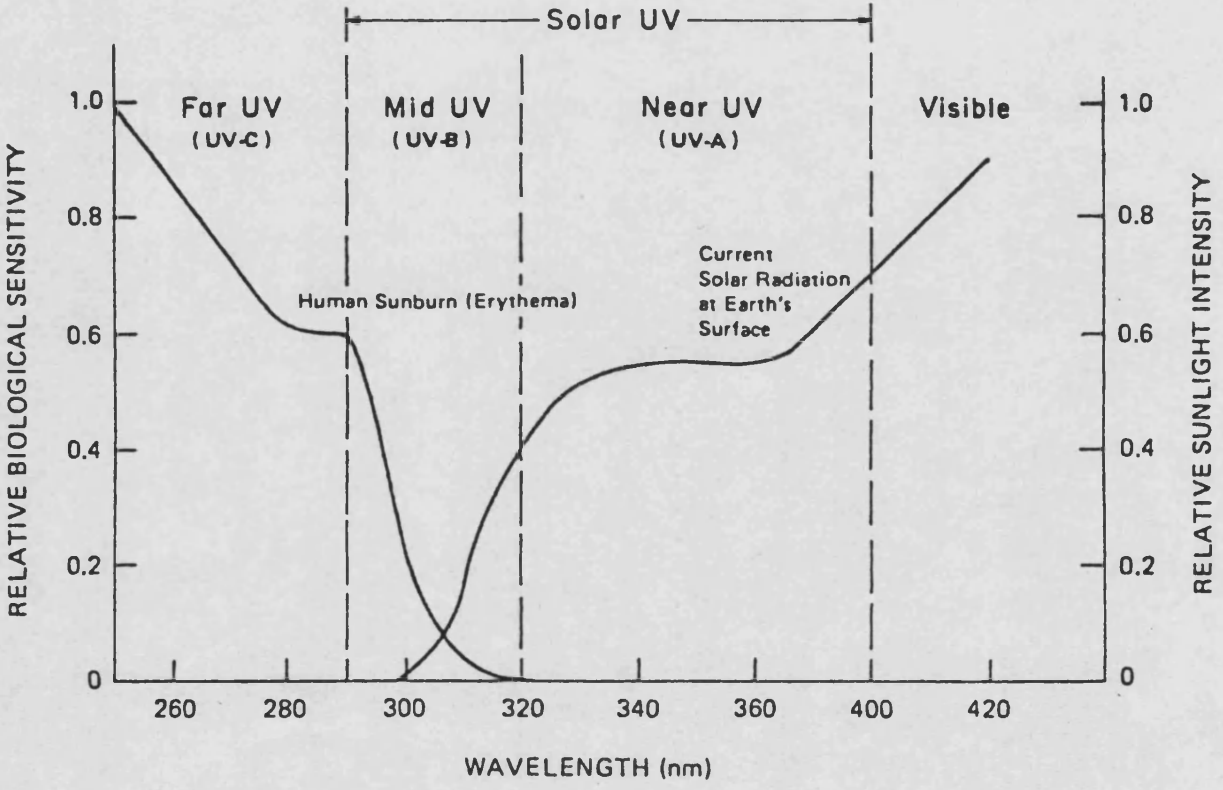

Figure 1. Action spectrum (approximate) for the induction of erythema in human skin, and average intensity of sunlight at the earth's surface. The figure also depicts the ranges of various UV-regions (from Jagger, 1985).

The distinction between mid UV and near UV is less clear. Mid UV is a region of transition, consisting of wavelengths with sufficient energy to interact directly with the DNA. Even though the relative amount of sunlight in this region is low and the absorption of DNA poor, mid-UV is responsible for most deleterious effects of sunlight on humans such as sunburn (Fig. 1) and skin cancer. It is not clear whether the mechanisms of action of mid-UV radiation on biological systems are a mixture of far- and near-UV effects or whether these wavelengths have properties of their own.

This work will be mainly concerned with near-UV light which has relatively recently received attention as having properties distinct from far-UV wavelengths. Near UV is a major component of solar UV and results in multiple biological effects through interactions with several cellular components, details of which remain enigmatic.

2.2 Photobiological Response of Cells to UV Radiation

Although solar-UV radiation effects on human cells are of most interest when considering the potential environmental hazard presented by sunlight to human beings, most of the research originally centered on the biological effects of 254 nm wavelength on bacterial cells. When some of the basic effects of far-UV radiation on bacterial cells became elucidated and the interest shifted to the effects of longer wavelengths, inevitably questions regarding the similarity in the mechanisms of inactivation by wavelengths in the two spectral regions, in terms of lethal target and resultant lesions, arose. Simple comparisons between the effects of far-UV and near-UV radiation formed the basis of further investigations. Hollaender was the first to publish such

comparisons on E. coli cells in 1943. He found that 10^4-10^5 more energy of near-UV radiation (primarily 365 nm) was required to induce the same killing as the shorter wavelengths. This has since been confirmed using monochromatic wavelengths both in bacterial (Webb, 1977) and in human cells (Keyse et al., 1983). Hollaender also reported that survival curves in the near-UV region exhibited much larger shoulders, a finding also confirmed by monochromatic wavelength irradiation of bacterial (Webb, 1977) and mammalian (Keyse et al., 1983) cells. The sensitivity of near-UV irradiated cells to physiological saline observed by Hollaender formed the basis of investigations into the membrane effects of near-UV radiation (Moss and Smith, 1981; Kelland et al., 1983a, b). Hollaender was also the first to report a temperature dependence of near-UV-induced lethality, an observation which forms part of this work.

Another feature specific to near-UV radiation biological effects is a strong dependence on oxygen, studied both in relation to cell killing in bacteria (Webb and Lorenz, 1970), mammalian cells (Danpure and Tyrrell, 1976) and in relation to the induction of possible lethal lesions, as will be discussed later.

Webb and Brown (1979) investigated oxygen dependence in an E. coli strain lacking the ability to repair DNA by the excision pathway and found that for wavelengths longer than 320 nm, cell inactivation was more effective under aerobic than under anaerobic conditions. Danpure and Tyrrell (1976) in a similar study using V-79 Chinese Hamster cells and HeLa cells, showed increased cell sensitivity when the cell suspension was bubbled with air as opposed

to nitrogen. They measured a ratio of doses (anaerobic/aerobic) to give a surviving fraction of 0.8, as 3.5 for Chinese Hamster V-79 cells and 2.9 for HeLa cells. They concluded that although this oxygen dependence could be a reflection of both damage to DNA repair processes and the induction of an oxygen dependent class of lesions in DNA, nothing precluded that instead of a genetic effect there might be damage to the cellular oxidative metabolism.

2.2.1 Energy absorption considerations and chromophores

In order that any intracellular photochemical reaction can take place, radiation must first be absorbed by a molecule or a group of molecules called a chromophore.

The far UV represents a region in which proteins and nucleic acids effectively absorb the incident radiation. Figure 2 shows the absorption spectrum of E. coli DNA (Sutherland and Griffin, 1981) which is due to the absorption of the individual nucleotides, such as the thymidine absorbance depicted on the graph (Webb and Brown, 1979). Since DNA absorbs radiations up to 320 nm, DNA is considered to be the major chromophore in the far- and mid-UV region for cell killing.

Above 320 nm, as can be seen in Fig. 2, the nucleotides like thymidine, show very little absorption. Absorbance of DNA measured by procedures that subtract contributions due to light scattering (Sutherland and Griffin, 1981), is observed out as far as 360 nm, but is very low, and it is not clear how it can take place. It is, therefore, doubtful whether DNA can absorb long wavelength radiation directly. Furthermore, the strong oxygen dependence for near-UV effects suggests that perhaps some other chromophore(s) absorbs the

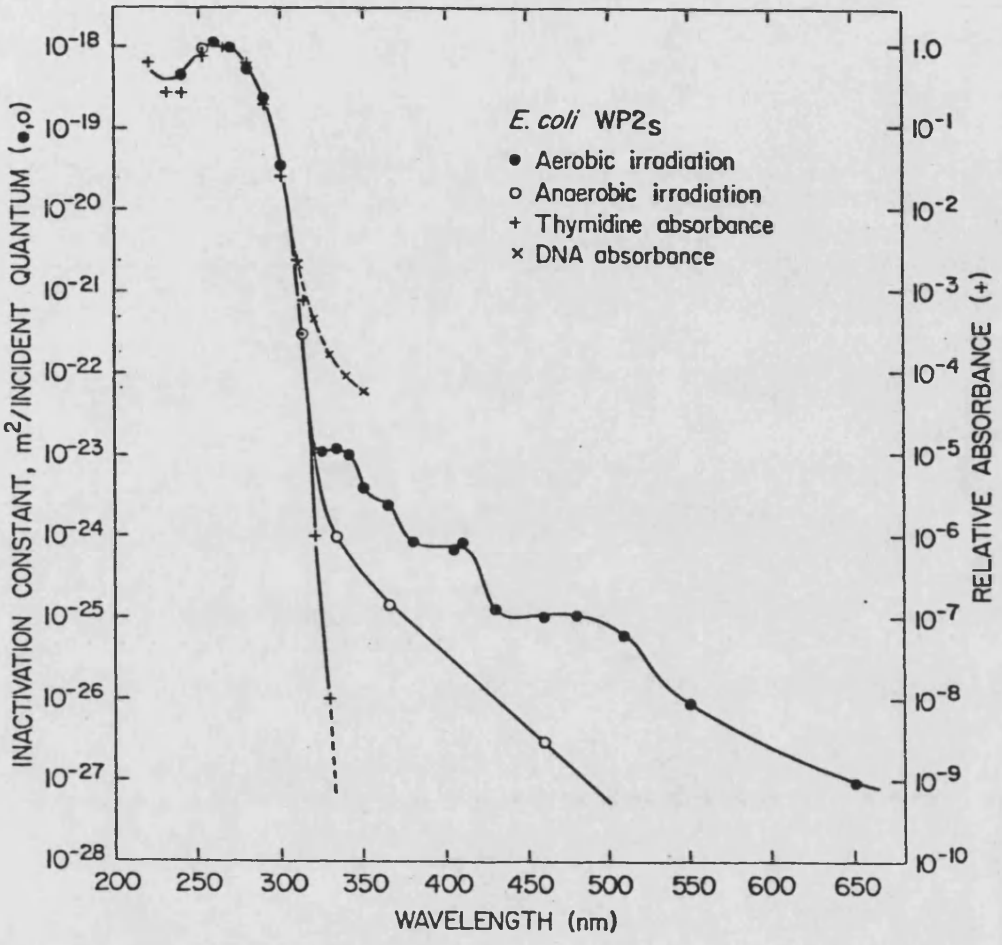

Figure 2. Action spectra for killing of stationary-phase E. coli WP2s uvrA irradiated at 25°C in the presence (●) and absence (○) of oxygen (Webb and Brown, 1979). Also shown are the absorption spectra of thymidine in M9 buffer at pH 7(+) (Webb and Brown, 1979) and of E. coli DNA (Sutherland and Griffin, 1981).

(×)

radiation and in the presence of oxygen transfers its energy to DNA (photodynamic action). This proposal is justified by looking at action spectra such as that composed by Webb and Brown (1979) for E. coli inactivation under aerobic and anaerobic conditions (Fig. 2). There, apart from noting how aerobic killing deviates from that under anaerobic conditions at wavelengths greater than 320 nm, it can also be seen that the action spectrum for aerobic killing shows much more detail and significant plateaux at 340, 365, 410 and 500 nm.

Such evidence has led to the proposal that killing by near-UV radiation is comprised of two modes (Jagger, 1985). These are (1) anaerobic killing which may be due to direct DNA absorption and shows little efficiency for the production of photoproducts (Sutherland and Griffin, 1981) and (2) aerobic killing which is probably due to the absorption of other molecules, bound to DNA, that produce photoproducts through photodynamic action that requires oxygen. However, absorption need not only take place in molecules bound to the DNA. Several compounds with conjugated double bonds present in the respiratory chain, in membranes and in vitamins, such as porphyrins, flavins, quinones and cytochromes, absorb well in the near-UV region and have been suggested as potential chromophores.

The group which belongs to the electron transport chains of mitochondria and bacteria includes porphyrins, flavins and quinones. The porphyrins absorb light strongly in the 350-430 nm range, but do not seem to become inactivated unless very high fluences are used. Riboflavin absorbs at 375 and 450 nm and has been shown to cause photosensitized oxidation of tryptophan and tyrosine as a result of black-light irradiation of tissue-culture medium (Stoein and Wang,

1974) a reaction which could also occur intracellularly. Amongst the quinones, naphthoquinone vitamin K1 has an absorption maximum at 334 nm and is extremely sensitive to near-UV light (Jagger, 1983) so it is regarded as a potential chromophore. Bilirubin which is related in structure to the porphyrins, absorbs maximally at 450 nm and its presence has been shown to increase single-strand break production in human fibroblasts (Rosenstein et al., 1983).

Other molecules considered as possible chromophores of near-UV light include compounds related to nucleic acids such as the base 4-thiouridine (^{4}Srd) that extends the absorption of tRNA into the near-UV region, with a peak at 340 nm. The presence of this base in a solution of bacterial DNA in phosphate buffer resulted in a ten-fold increase in the number of single-strand breaks produced by 334 nm (Peak et al., 1984). Absorption at 360 nm by protein B2, a non-heme iron-containing protein, present in the ribonucleoside diphosphate reductase (RDP reductase) complex, is thought responsible for the inactivation of the complex and the killing of exponentially growing E. coli by near-UV radiation (Peters, 1977). The coenzyme pyridoxal phosphate also absorbs strongly throughout the near-UV region with peaks at 325 and 388 nm, but the biological consequences of the absorption are not clear. Another co-factor nicotinamide adenine dinucleoside in its reduced form (NADH), has an absorption peak at 340 nm and has been implicated in the production of the superoxide ion in an in vitro system (Cunningham et al., 1985)

The conclusions that can be drawn from the above studies are that the diverse actions and locations of the compounds mentioned make it likely that different chromophores are responsible for

different biological effects of near-UV radiation in a particular cell. Additionally different chromophores may be involved in different cell types. For example, ^{4}Srd and protein B2 of ribonucleoside diphosphate reductase might account for the 340 and 410 nm plateau of the E. coli action spectra whereas in the spectra of mammalian cells these plateaux do not exist. Similarly, action spectra for effects such as single-strand break induction in mammalian cells show shoulders in the near-UV region that do not exist in bacterial cells, suggesting chromophores unique to mammalian cells (riboflavin).

2.2.2 DNA as a Target of UV Radiation

DNA has a unique role in the cell carrying the genetic information, and damage to DNA is expected to be of overwhelming importance regarding cell lethality. Evidence that DNA is the molecular target for a particular effect is often sought in comparisons between the action spectrum for the effect and the absorption spectrum of DNA. Such a spectrum for cell lethality in different cell types is shown in Fig. 3. Data for pyrimidine dimer formation, a DNA lesion, is also included for later discussion.

It can be seen that up to 313 nm there is a relatively good correlation between action spectra for lethality and the DNA absorption spectrum, although two differences are apparent: For wavelengths 270-290 nm there is enhanced sensitivity for killing of mammalian and frog cells relative to the absorption spectrum. In contrast, above 300 nm the absorption spectrum has a relatively higher value. Sutherland and Griffin (1981) suggested that the heterogeneous nature of DNA and the fact that photons absorbed by

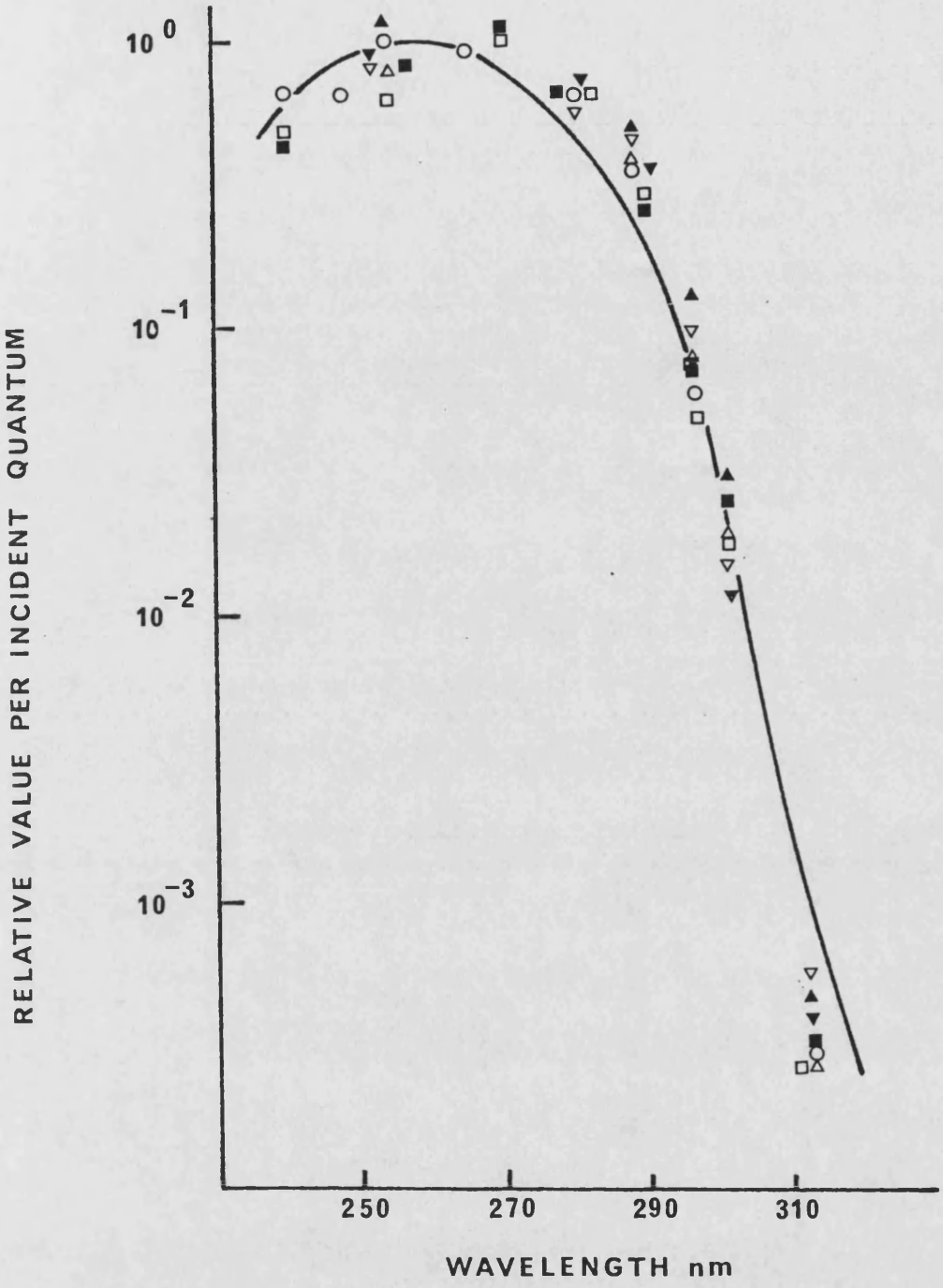

Figure 3. Points on action spectra of a variety of higher organic cells (normalized to 1.0 at 265 nm). Also shown is the absorption spectrum of purified mammalian DNA from Sutherland and Griffin, 1981 (solid line).

Human Cells
○ Killing Kantor et al., 1980)

Chinese Hamster V79 Cells
△ Killing (Rothman and Setlow, 1979)
▲ Dimers (Rothman and Setlow, 1979)

Syrian Hamster Cells
□ Killing (Doniger et al, 1981)
■ Dimers (Doniger et al, 1981)

Frog Cells
▽ Killing (Rosenstein and Setlow, 1980)
▼ Dimers (Rosenstein and Setlow, 1980)

different bases may have different probabilites of giving rise to photoproducts could account for the differences observed between absorption and action spectra and should not establish the significant involvement of other molecules as targets for cell killing. For example, absorption above 300 nm is dominated by regions of DNA rich in guanine-cytosine, and guanine is less likely to give rise to photoproducts. It is important to note that action spectra do not differentiate between the relative contribution of DNA and RNA to effects such as lethality and dimer formation. Only after consideration of its unique role, as a carrier of genetic information, can DNA be regarded as more important and can be assumed to be the major target for the induction of lethality by radiations up to 320 nm.

For wavelengths greater than 320 nm where direct absorption by DNA becomes minimal but still possible, different criteria serve as evidence that damage to DNA continues to be important. Transforming DNA has been inactivated by wavelengths up to 460 nm (Cabrera-Juárez et al., 1976; Peak et al., 1973) showing that it can be a target for near-UV biological effects. However, the protective effect of histidine and the lack of photoreactivation at wavelengths greater than 320 nm, (Cabrera-Juárez et al., 1976) indicate that the mechanism of lethality and the lethal lesions produced are different in the far- and near-UV regions. A number of studies have been done on the modification of sensitivity of transforming DNA by agents such as glycerol, diazobicyclooctane (DABCO), 2-aminoethylisothiouronium bromide hydrobromide (AET) (Peak and Peak, 1980; Peak et al., 1981; Peak and Peak, 1975). Their finding has been that cell survival is also altered in a similar way and

they regard DNA inactivation as important for the induction of lethality. A similar conclusion is reached by Webb et al., 1976) who found increased sensitivity to near-UV irradiation of a strain completely deficient in dark repair (E. coli K-12 AB2480 uvrA recA) relative to the wild type. Additional evidence came from the sensitization of wild-type E. coli to near-UV irradiation when inhibitors of repair of far-UV damage in DNA, such as acriflavine, were used (Peak, 1970; Webb and Brown, 1976).

The conclusion from the above studies is that DNA is the primary lethal target in the far-UV region. In the near-UV region, DNA damage may contribute to lethality but as a result of a different type of damage than that produced by shorter wavelengths. As further evidence will support, non-DNA damage may also contribute to lethality in the near-UV region.

2.2.3 Lethal Lesions in the DNA

Pyrimidine dimers

It is quite well established by now that lethality from far-UV radiations is due to damage in the DNA and in particular due to the formation of pyrimidine dimers. These dimers are produced between adjacent pyrimidines in the same strand of a DNA molecule, and they involve the creation of new covalent bonds between the two 5-positions and the two 6-positions of these adjacent pyrimidines, resulting in a cyclobutane ring. The pyrimidine dimer is a very stable photoproduct but its formation can be reversed by a light catalysed enzymatic process called photoreactivation. The alteration of cell survival as a result of photoreactivation can be

taken as indicative that pyrimidine dimers are a lesion that results in lethality.

As shown in Fig. 3, action spectra for pyrimidine dimer formation are in very good agreement with action spectra for cellular inactivation in mammalian (Rothman and Setlow, 1979; Kantor et al.,1980; Doniger et al., 1981) and frog cells (Rosenstein and Setlow, 1980) as well as with the absorption spectrum of human DNA (Sutherland and Griffin, 1981) for wavelengths up to 313 nm. This finding has strongly implicated DNA as the critical target for this spectral region and pyrimidine dimers as the lethal lesion formed.

Studies using wavelengths longer than 313 nm and in particular, broad-band solar UV, have been more controversial regarding the importance of pyrimidine dimer formation, especially in mammalian cells. In bacterial cells, the use of photoreactivation as a means of indicating the contribution of pyrimidine dimers to cell lethality has ruled out the possibility that these may be a lethal near-UV radiation lesion. Most bacterial strains irradiated under normal conditions (low fluence rate, room temperature, air) show lack of photoreactivability (Jagger, 1983). Similarly, transforming DNA is not photoreactivated following near-UV irradiation (Cabrera-Juárez et al., 1976). In mammalian cells, the use of this method to assess the importance of pyrimidine dimers is not possible since most commonly used cell types have not been shown to use photoreactivation repair effectively. A different approach to this question has been to investigate whether near-UV irradiation results in inactivation which follows kinetics consistent with a dimer-caused mechanism. Although the presence of a constant dose modification factor obtained between 254 nm and

near-UV monochromatic or broad-band wavelengths has been used as an argument that the mechanism of near-UV killing is similar to that of far-UV, i.e. through pyrimidine dimer formation, this is not correct. On the contrary the absence of such a correlation suggests the involvement of other mechanisms in the near-UV induced cell killing.

Unfortunately, this comparison has been complicated by the use of polychromatic sources such as fluorescent sun lamps (FSL) which emit very significantly in the mid-UV region and in which synergistic effects between different wavelengths are possible. Therefore, although a constant dose modification factor has been reported for cultured goldfish cells (Shima and Setlow, 1984) and human fibroblasts (Kantor + Setlow, 1980; Patton et al., 1984) when the effects of 254 nm and FSL were compared, this could be due to the contribution of shorter wavelengths present in the FSL. Support for this suggestion comes from the studies of Shima and Setlow (1984) and Rosenstein (1984). Using goldfish cells which possess photoreactivating enzyme, the first study showed that both 254 nm and FSL-induced dimers were reversed, if photoreactivated, and dimer reversal was paralleled by a reduction in cell killing. However, if progressive filtering of the radiant energy to remove increasing segments of the spectral region below 320 nm was done, as in the second study, a progressive decline in the photoreactivable sector was obtained. A similar conclusion was reached by Zelle et al. (1980) who used filters to separate the effects of mid UV and near UV at 320 nm and found lethality per dimer to be lowest after far-UV irradiation and highest after near-UV irradiation in Chinese hamster cells.

These results show that while dimers are critical photoproducts in cells exposed to far-UV radiation, at longer wavelengths non-dimer photoproducts are also involved and their contribution to cell killing becomes important.

Studies using monochromatic light also agree that the number of pyrimidine dimers induced in cellular DNA by near-UV light of wavelength greater than 320 nm is not sufficient to account for cell killing, and a different lesion must be involved (Smith and Paterson, 1982; Keyse et al., 1983; Wells and Han, 1984). Han et al. (1984) estimated that, in Chinese Hamster cells, pyrimidine dimer formation (measured as endonuclease sensitive sites) following 365 nm irradiation was 4.3 per 2 x 10^8 daltons compared to 30.3 sites per 2 x 10^8 daltons formed by 254 nm. No detectable endonuclease sites were induced following 405 nm irradiation.

Single-Strand breaks (ssb)

A DNA lesion which occurs with greater frequency relative to pyrimidine dimers at longer wavelengths is single-strand break formation (Tyrrell et al., 1974). In E. coli the number of dimers induced for each ssb was measured as 800, 21, 1.8 and <0.1 following irradiation with 254, 313, 365 and 405 nm, respectively (Webb, 1977). In mammalian cells, Han et al. (1984) noted a similar increase in ssb frequency at longer wavelengths. They measured 1, 11.3, and 13.3 single-strand breaks per $2x10^8$ daltons in Chinese hamster cells following doses of 254, 365 and 405 nm which resulted in approximately 10 per cent survival.

Action spectra for DNA single-strand break induction have been obtained by Peak and Peak (1982) for B. subtilis in the 254-434 nm

range and by Rosenstein and Ducore (1983) for normal human fibroblasts in the 240-546 nm range. Both action spectra are similar to each other and to the normalized DNA absorption spectrum (Fig. 4) in the far-UV region, but in the near-UV two significant differences are apparent: Although both action spectra have a peak at 265 nm, the bacterial action spectrum shows a distinct break at 334 nm producing a shoulder in the near UV whereas the human cell action spectrum has a more subtle decrease in slope from 313 to 405 nm and a second peak, three orders of magnitude smaller, at 450 nm. This part is similar to the normalized absorption spectrum for riboflavin or bilirubin. Rosenstein et al., (1983) showed that exogenously added bilirubin greatly enhanced near-UV-induced DNA single-strand breaks in human fibroblasts. Irradiated bilirubin also induced DNA single-strand breaks in the dark, and this effect was eliminated if the irradiated bilirubin was first incubated with catalase. Together with the action spectrum data (Fig. 4) this suggests that the ssb formation at 400 nm is due to hydrogen peroxide production by endogenous bilirubin. This effect is largely eliminated by incubation of the cells in complete medium for 30 min at 37°C (Rosenstein and Ducore, 1984).

In bacterial cells, ssb can also be effectively repaired by the DNA polymerase function (Ley et al., 1978). Evidence for the importance of unrepaired ssb as contributors to lethality comes from comparisons of whether agents that modify ssb induction alter cell survival in a similar way. Oxygen, which sensitizes both bacterial and mammalian cells (Webb and Lorenz, 1970; Danpure and Tyrrell, 1976) and transforming DNA (Peak et al., 1981) to inactivation, also increases ssb induction by 365 nm (Tyrrell et al., 1974; Peak and

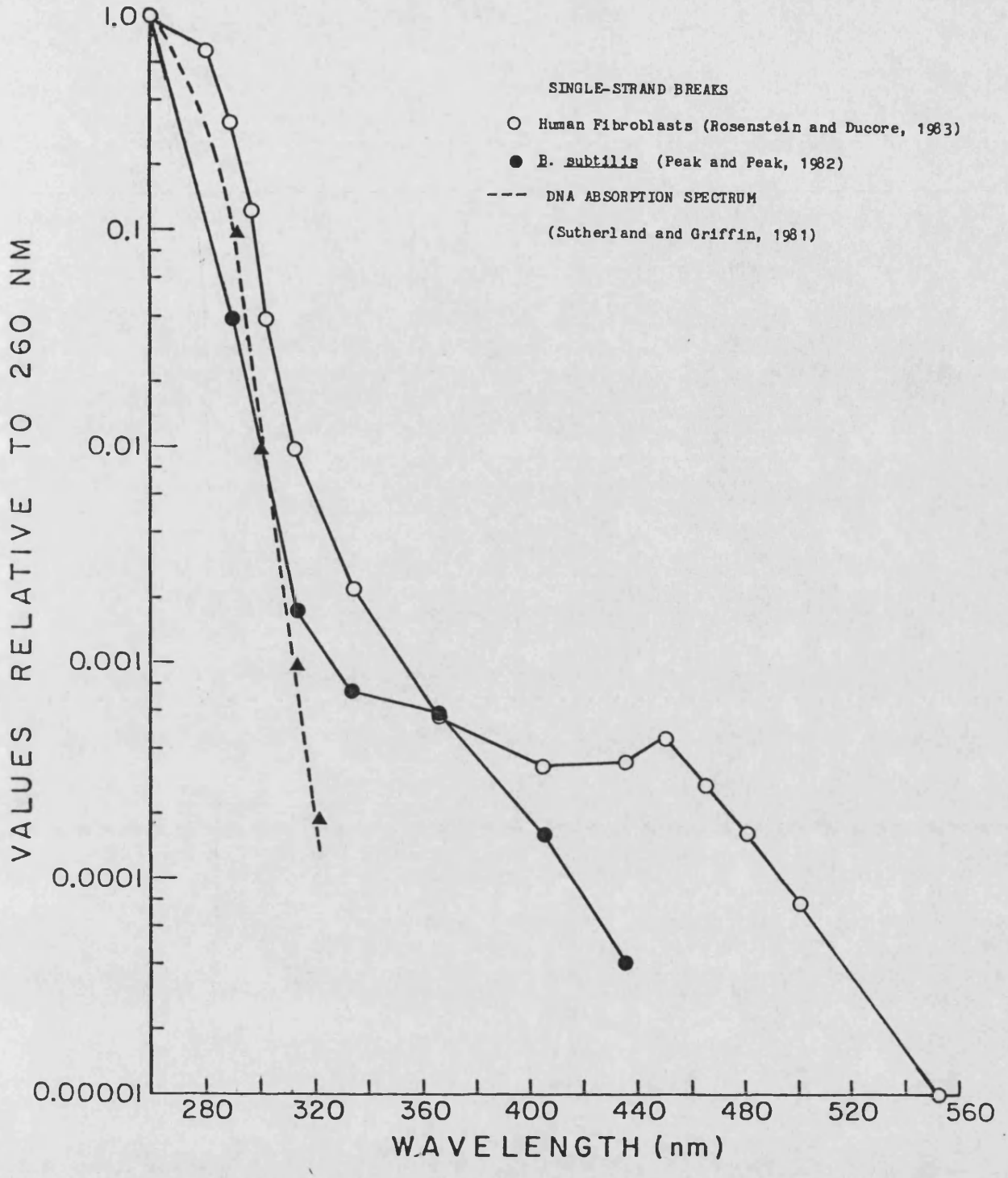

Figure 4. Action spectra for in vivo induction of single-strand breakage of DNA in human fibroblasts (O) and in Bacillus subtilis (●). Also shown is the absorption spectrum of purified mammalian DNA (dashed line).

Peak, 1982). Glycerol, DABCO, AET and histidine which protect against ssb induction by 365 nm (Peak and Peak, 1982; Tyrrell et al., 1974) also reduce the inactivation of whole bacterial cells and transforming DNA by near-UV irradiation (Peak and Peak, 1980 ; Peak et al., 1973; Peak and Peak, 1975; Peak et al., 1981) thus implicating ssb as a lethal lesion.

Not all studies, however, agree with these conclusions. Roza et al., (1985) in a comparative study of the lethal effects of far- and near-UV light on human skin fibroblasts and ssb induction, reported that 90 per cent of the ssb were repaired within 15 minutes. They proposed that ssb induction by near-UV irradiation was due to the formation of hydrogen peroxide which would be converted to highly reactive hydroxyl radicals and damage the DNA. In support of this idea, the presence of catalase during irradiation was found to greatly reduce the amount of ssb formed by near-UV irradiation but did not alter survival. This implies that ssb are not a critical lesion, unless a very small residual fraction of ssb, still present after prolonged repair periods, is responsible for cell death (both after irradiation in the presence and absence of catalase). Han et al. (1984) also observed that ssb induced in Chinese hamster cells by 365 and 405 nm were efficiently repaired. When expressed relative to killing efficiency, the efficiency of induction of ssb by these wavelengths is significantly lower than that attributed to ionizing radiation, for which DNA breaks are generally thought to be a biologically important lesion.

Thymine glycols

Thymine glycols, monomeric ring-saturated products of the 5,6-dihydroxydihydrothymine type have been detected in the DNA of human cells both *in vitro* and *in vivo* following far-UV irradiation (Hariharan and Cerutti, 1977). In HeLa S-3 cells, one thymine glycol was formed for 8.4 pyrimidine dimers at 240 nm and then, one thymine glycol for 20, 17, 1.4 pyrimidine dimers at 260, 280 and 313 nm, respectively. At 334 and 365 nm the thymine glycol yield was considerably less than that of pyrimidine dimers. The biological significance of thymine glycols has not yet been determined.

DNA-protein crosslinks

DNA-protein crosslinks caused by far-UV radiation were reported as early as 1964 by Smith but interest in this lesion has only recently revived. Han *et al.* (1984) reported the induction of DNA-protein crosslinks in Chinese Hamster cells by monochromatic 254, 365 and 405 nm irradiation, as measured by alkaline elution. The crosslinks were detected even after relatively low fluences that resulted in 60 per cent survival. An action spectrum for the induction of DNA-protein crosslinks in human cellular DNA, measured by the previous technique, was reported by Peak *et al.* (1985a, b) (Fig. 5). It has a component that is similar to the DNA absorption spectrum in the 254-313 nm region and a component with a second peak three orders of magnitude lower at 405 nm. At 405 nm the induction of the lesions depends upon the presence of oxygen whereas this is not the case for far-UV induction. The reduced yield of crosslinks under anaerobic conditions and the increased induction of crosslinks in a deuterium oxide environment is evidence that the mechanism of

action of 405 nm irradiation is via a reactive species of oxygen, such as singlet oxygen, since deuterium oxide slows the decay time of singlet oxygen by about one order of magnitude (Merkel et al., 1972). The nature of the proteins that are crosslinked to DNA and the sites on the DNA to which they are crosslinked, remain unclear.

2.2.4 Non-DNA lesions: Damage to repair systems

When examining the effects of solar UV both genetic and non-genetic lesions must be considered. As well as the lesions above, cellular systems that could be damaged with severe consequences for the cell survival include DNA repair systems. DNA repair has been extensively studied in bacterial cells due to the ease of their manipulation and the availability of mutants lacking in one or more repair processes. This work has gone into great biochemical detail but will only be discussed briefly since the enzymatic details may not be applicable to mammalian cells.

There are three modes of repair which can be classified into those which act on non-replicating DNA, e.g. photoreactivation and excision repair, and those which involve the interaction of damage and repair with replicating DNA, termed post-replication repair.

Photoreactivation

Photoreactivation involves the photoenzymatic repair of pyrimidine dimers which starts by the formation of an enzyme-dimer complex which, on subsequent absorption of near-UV or visible light, cleaves the dimer with dissociation of the enzyme from DNA thus repairing the damage. Photoreactivation is highly specific for pyrimidine dimers (Setlow and Setlow, 1972). Photoreactivating enzyme has been found in both bacterial and eukaryotic cells

although its activity in mammalian cells is uncertain (for review see Sutherland, 1977).

Excision repair

The process of excision repair involves the removal of a damaged section of DNA and its replacement with undamaged nucleotides thus restoring the normal function of DNA. The original model of excision repair proposed by Setlow and Carrier (1964) envisaged a four-step process. First, an incision step adjacent to the damage made by an endonuclease, now known as the uvrABC product, followed by a break in the phosphodiester backbone adjacent to the dimer, and new synthesis by a DNA polymerase using the complementary strand of DNA as a template. The process is completed by the joining of the new patch of nucleotides to the pre-existing DNA by DNA ligase. The net result is an error-free repair of the DNA, with no loss of genetic information, and the release of dimers into the medium. This is an oversimplification of the process for which considerable detail of the genetic and physiological controls is now known for bacterial cells (Smith, 1978; Lehmann and Bridges, 1977; Hanawalt et al., 1979).

Post-replication repair

Post-replication repair or dimer bypass mechanism is thought to involve discontinuous synthesis of DNA with gaps at damaged templates which are subsequently filled by recombinational events between homologous DNA strands (Rupp et al., 1971). This may be an error-prone pathway of DNA repair which results in mutations. The mechanisms and genetic control of these pathways in bacteria have been the subject of recent reviews (Hanawalt et al., 1979; Lehmann and Karran, 1981).

The above repair processes are very effective. Photoreactivation can increase the fluence required for a given effect by a factor of up to 10. Mutants of E. coli defective either in excision or post-replication repair are about 30 fold more sensitive to far-UV irradiation than the wild type, while the double mutant is approximately 1000 times more sensitive than the wild type. It can be expected that damage to these systems would have important consequences for cell survival.

It has been suggested that repair of many types of DNA lesions is disrupted by near-UV radiations within the same dose range as lesion induction and that the combination of the reduced repair ability together with the lethal potential of DNA lesions could result in cell death. The evidence supporting this model comes largely from bacterial work and is included in a review (Tyrrell, 1979).

2.2.5 Damage to membranes

The question of whether membrane damage is important for UV-induced cell inactivation has been re-addressed in the past few years. Several possible damaging effects that have been investigated include structural changes of membranes, differences in surface potential, changes in passive permeability or active transport, lipid peroxidation products, or the release of other membrane constituents.

The first study which suggested a membrane contribution to near-UV radiation-induced lethality was that of Hollaender in 1943 who observed a sensitivity of near-UV irradiated E. coli to physiological saline. There was no such effect following far-UV

irradiation. This observation received no further notice until Moss and Smith (1981) showed that the survival of a wild type E. coli K-12 strain JG139 after irradiation with broad-band near-UV radiation was significantly influenced by the concentration of inorganic salts present in the minimal plating medium. They found that an increase in the salt concentration or the addition of a low concentration of commercial detergent to the minimal plating medium caused an increase in cell lethality after near-UV but not far-UV irradiation. In an action spectrum subsequently described, this effect was shown to occur only at wavelengths above 310 nm (Kelland et al., 1983a). The same strain of E. coli was used to demonstrate more direct UV-membrane interactions by examining the release of $^{86}Rb^{+}$ from UV-irradiated cells (Kelland et al., 1984). When comparing the action spectrum for this effect with the action spectrum for lethality (Fig. 6), it can be noted that leakage of $^{86}Rb^{+}$ occurs at fluences equivalent to, or slightly less, than fluences causing inactivation, at wavelengths longer than 305 nm.

Similar results that suggest an involvement of membrane damage in near-UV-induced lethality come from a variety of other cell types. Some studies report membrane-related effects such as increased $^{86}Rb^{+}$ leakage from rose cells (Murphy and Wilson, 1982) or efflux of Na^{+}, K^{+} and Cl^{-} from Chara corallina cells (Doughty and Hope, 1973) following 254 nm irradiation but do not comment that the fluences required to produce such effects are quite large (1080, 2820 Jm^{-2}). Other studies, however, such as Bruce in 1958 demonstrated that far-UV irradiation required an approximate 16-fold higher fluence to affect K^{+} retention of yeast cells than to affect survival, whereas after near-UV irradiation K^{+} retention and

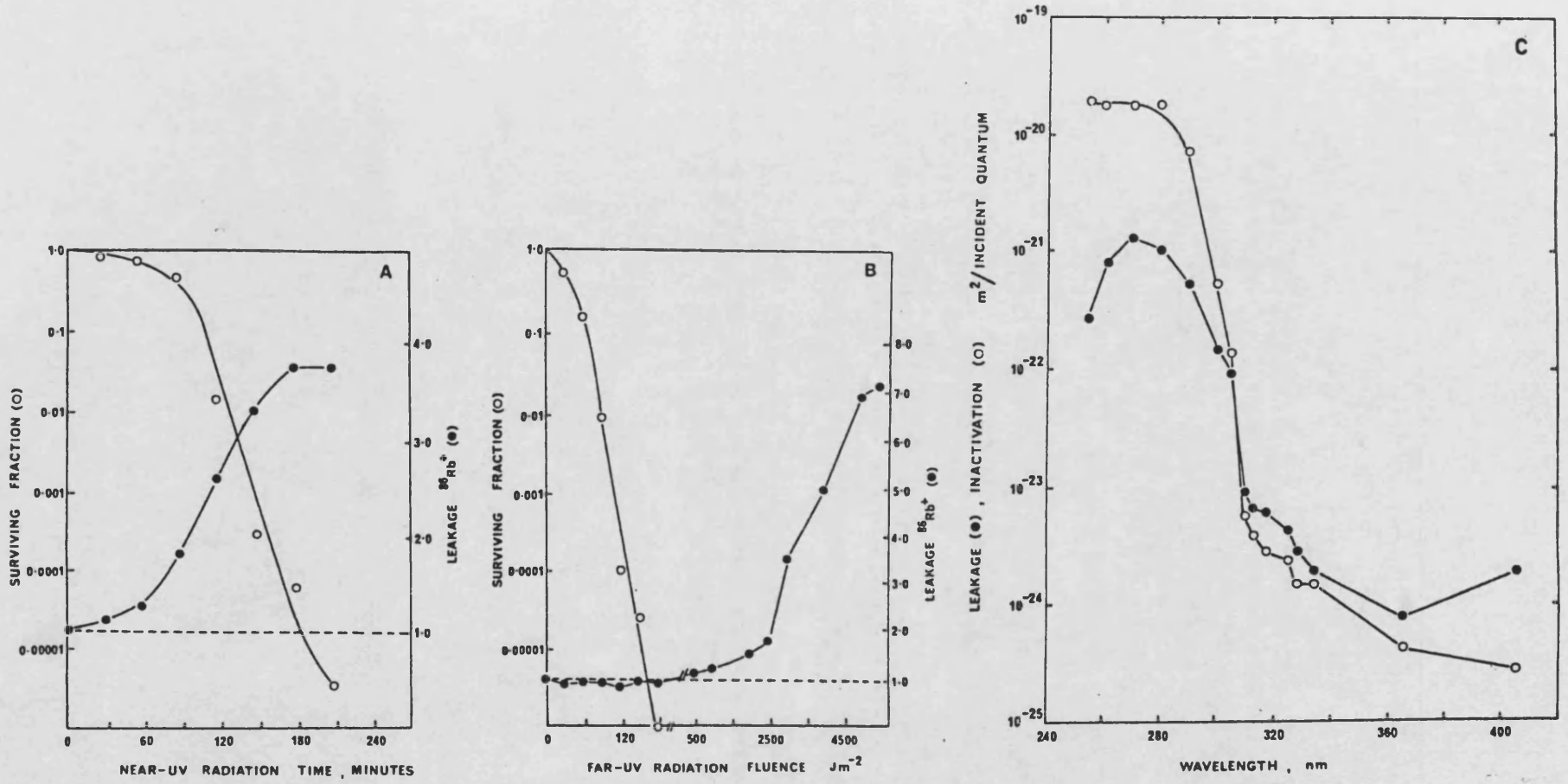

Figure 6. Survival (○) and leakage (●) of $^{86}Rb^+$ at 25°C from stationary phase E. coli K-12 (SR 385). Effects of broad-band near-UV (A), 254 nm far-UV (B) and complete action spectra (C) is shown. Viability was assessed on minimal medium and leakage of $^{86}Rb^+$ expressed as the ratio of disintegrations per minute for irradiated samples to unirradiated samples. Action spectra were based on $1/F_{37}$ values (from Kelland et al., 1984).

survival were influenced by similar fluences. In a more recent study, Ito and Ito (1983) observed an oxygen-dependent damaging effect on exponential-phase yeast cell membranes manifested as a disruption of the permeability barrier after broad-band (300-400 nm) but not after 254 nm irradiation.

Studies with mammalian cells are much rarer and the majority of these deal with the erythrocyte because it is uncomplicated by intracellular membranes. UV-radiation-induced effects on the red blood cell (RBC) membrane are apparent either as haemolysis or as lipid peroxidation products. Both far- and near-UV wavelengths have been shown to cause oxygen-dependent haemolysis related to lipid peroxidation (Roshchupkin et al., 1975). Again, very large doses of 254 nm (10^3 Jm^{-2}) were utilized to induce lipid peroxidation in this study, and it was later confirmed with erythrocyte membranes and liposomes that 365 nm irradiation is more efficient in inducing lipid peroxidation than 254 nm by a factor of 2 (Mandal et al., 1980).

Increased lipid peroxidation, measured as thiobarbituric acid reacting (TBA) materials has also been observed after broad-band 290-320 nm irradiation of mouse melanoma cells at doses where 90 per cent viability was retained (Sakanashi et al., 1986). However, lipid peroxidation did not induce a significant alteration of membrane fluidity immediately, but only after 6 hours, reflecting perhaps a delayed membrane injury during the metabolism of lipid peroxidation products or during repair processes.

Irradiation of mouse fibroblasts and human keratinocytes in culture with primarily mid-UV wavelengths (290-320 nm) induces the release of arachidonic acid from membrane phospholipids (DeLeo et

al., 1984, 1985). The almost immediate release of arachidonic acid (within 5 minutes of irradiation) suggests a direct action of UV radiation on cell membranes.

Scattered evidence, therefore, points to a damaging effect of mid- and near-UV wavelengths on the cellular membranes which under some circumstances may contribute to cell death. Proposed mechanisms for the near-UV induced damage include peroxidation of the membrane lipids initiated and propagated by active oxygen species which are thought to be involved in near-UV induced lethality.

3. BIOLOGICAL EFFECTS OF REACTIVE OXYGEN SPECIES

As previously discussed, oxygen is an important mediator of the biological effects of near-UV radiation. It both sensitizes cells to inactivation and increases the incidence of lesions such as single-strand breaks and protein crosslinks. The observation that oxygen alters specifically near-UV but not far-UV effects is taken as strong evidence of the existence of different mechanisms of action between the two spectral regions. However, the mechanisms by which oxygen exerts its effects remain largely undefined and are termed loosely as 'indirect photodynamic action by oxygen reactive species using endogenous sensitizers'. It is necessary to examine such reactive species, their formation, limited existence, and possible biological role as mediators of near-UV damage.

3.1. Generation of reactive oxygen species

Oxygen in its ground state contains two unpaired electrons with parallel spins. The parallel spins impose a restriction on electron transfer which makes oxygen relatively non-reactive with non-radicals. Therefore, the majority of oxygen's photodynamic effects are thought to arise through more reactive species generated either by photosensitized reactions or during the univalent reduction of oxygen to water which takes place in all respiring cells (Fridovich, 1975).

In a photosensitized reaction , certain molecules absorb light of a specific wavelength and the energy raises the molecule into an 'excited state'. The excitation energy can then be transferred to an adjacent oxygen molecule, converting it to the singlet state (Krinsky, 1984).

$$S + h \longrightarrow {}^1S \rightsquigarrow {}^3S + {}^3O_2 \longrightarrow S + {}^1O_2$$

(Type II Photosensitization)

Sensitizers which could produce singlet oxygen intracellularly include riboflavin and its derivatives, bilirubin and various porphyrins (Halliwell and Gutteridge, 1985). Such an effect is possible by energy absorption in the near-UV region and singlet oxygen has been investigated as a possible mediator of near-UV effects (Peak et al., 1981; Peak et al., 1985b).

While singlet oxygen is the primary species generated through photosensitized reactions, superoxide anion, hydrogen peroxide and hydroxyl radical formation are all possible by other enzymatic reactions depicted in Fig. 7. Scheme I shows the reduction of

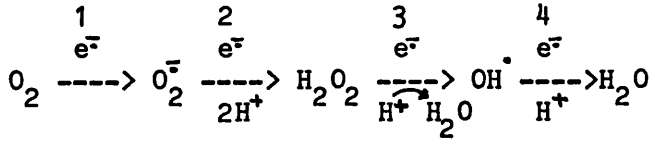

Scheme I. Univalent reduction of oxygen to water

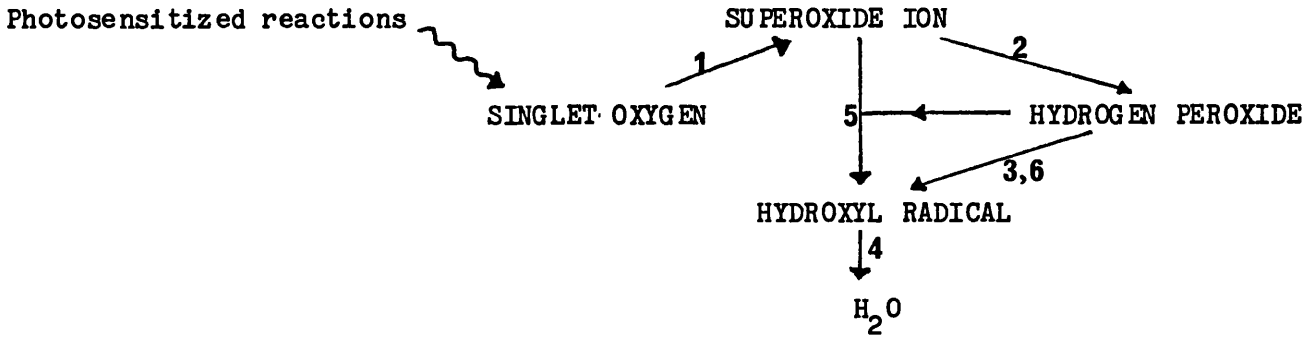

5:metal-catalysed Haber-Weiss reaction:

$$O_2^{\cdot-} + Me^{3+} \longrightarrow O_2 + Me^{2+}$$

$$Me^{2+} + H_2O_2 \longrightarrow Me^{3+} + OH^{\cdot} + OH^- \quad \text{(6:Fenton reaction)}$$

(overall)

$$O_2^{\cdot-} + H_2O_2 \xrightarrow{\text{metal catalyst}} O_2 + OH^{\cdot} + OH^-$$

Scheme II. Reactive oxygen species interconversion by reactions numbered as shown in scheme I. Depicted also the metal-catalysed Haber-Weiss and Fenton reactions.

Figure 7.

oxygen by acceptance of one electron to form the superoxide ion (which is also a radical, $O_2^{\bullet-}$), hydrogen peroxide (H_2O_2) and the hydroxyl radical ($OH^{\bullet}$), before being reduced to water.

The multiple reactions depicted in Scheme II are only some of the reactions thought to occur amongst these species whereby one leads to another. Hydrogen peroxide can also be produced by the dismutation reaction (see page 29) and the peroxide ion and hydrogen peroxide together can result in hydroxyl radical formation through the metal-catalysed Haber-Weiss reaction. There is some controversy over the production of singlet oxygen from the same reaction. The possible involvement of the superoxide ion, hydrogen peroxide, and the hydroxyl radical in near-UV induced lethality has been considered (Peak et al., 1985b; Hoffmann and Meneghini, 1979b; Ward et al., 1985) but in doing so, two related factors are important and should be properly evaluated for each species. One is the reactivity of each species with the probable biological target, and the other is its ability to diffuse from the site of its generation to the site of damage. The reactivity determines in part the diffusion distance since the hydroxyl radical which has a high and indiscriminate reactivity is not likely to diffuse away from its cellular site of production but will react nearby. Its half-life at $37^{\circ}C$ is in the order of of 10^{-10} sec (Pryor, 1984). The superoxide ion, which is much less reactive than the hydroxyl radical, could potentially diffuse further away but due to its charged nature it cannot diffuse through non-polar regions unless it becomes protonated. Hydrogen peroxide, even less reactive, has been shown to diffuse across membranes and is able to exert toxic effects at a distance from its site of generation.

Singlet oxygen can also be expected to diffuse for some distance in the order of nanometers (Ito, 1978) and its half-life, which depends very much on its environment, can vary from 2 μsec to 1000 μsec (Kearns, 1979).

3.2. Toxicity of reactive oxygen species

3.2.1. Singlet Oxygen ($^1O_2$)

In singlet oxygen, which is an excited state of oxygen, the spin restriction is removed and the oxidizing ability greatly increased. It can therefore react with many biologically important molecules such as nucleic acid components, proteins and lipids (Foote, 1976; Halliwell and Gutteridge, 1985). Its reactions with lipids are of particular interest since $^1O_2$ has a longer lifetime in a lipid environment and it has been shown that it can react chemically with conjugated double bonds present in the fatty-acid chains of membrane lipids initiating lipid peroxidation reactions (Halliwell and Gutteridge, 1985). Considerable evidence has been accumulating indicating a role for $^1O_2$ in photosensitized reactions, i.e. where the exogenous sensitizer, commonly a dye such as acridine orange or toluidine blue, is added to a biological system. Since at least part of near-UV damage is thought to occur through endogenous sensitization, the participation of $^1O_2$ in near-UV induced lethality has been extensively studied. Klamen and Tuveson (1982) proposed that near-UV generated $^1O_2$ may lead to generalized membrane destruction, but this should only be treated as a speculation as no evidence is presented in support of it. A variety of other important molecules amongst which are protein residues such as histidine, tryptophan and cysteine, and vitamin E (Halliwell and

Gutteridge, 1985) also react with singlet oxygen. Therefore, one can expect multiple biological actions as a result of singlet oxygen production. Unfortunately, direct experimental evidence is inadequate in the field and relies on two approaches which are not entirely specific to singlet oxygen and could be an indication of involvement of other active oxygen species as well.

One approach to determine the involvement of singlet oxygen in a biological effect is by the use of scavengers. Peak et al. in 1981 showed protection of transforming DNA against near-UV inactivation when 0.1 M DABCO was present during irradiation. The maximum dose modification factor obtained was 0.51 at 350 nm, while no protection occurred with wavelengths shorter than 313 nm. Similar results have been obtained by the same workers using histidine and AET as scavengers of singlet oxygen (Peak et al., 1973; Peak and Peak, 1975). However, it should be pointed out that all these compounds are capable of quenching other excited species as well (Foote, 1979).

An alternative approach to the study of the biological effects of $^1O_2$ is by the use of D_2O. The decay time of $^1O_2$ is about 10 times slower in a solution of D_2O compared to H_2O (Merkel et al., 1972) and enhanced biological damage in the former solvent is taken as evidence for the participation of active oxygen species in the damage (Merkel et al., 1972; Ito, 1978; Kearns, 1979; Peak et al., 1985b). In a 100 per cent D_2O environment, Peak et al. (1985) showed increased DNA-protein crosslinks induced by 405 nm radiation, measured in human cellular DNA by alkaline elution techniques. However, no direct evidence is available for the ability of $^1O_2$ to

break DNA or cause crosslinks, and it could be that another oxygen species might be responsible for the effect.

3.2.2 Superoxide ion ($O_2^{\cdot-}$)

The superoxide ion is generated by many spontaneous and enzymatic reactions during cellular metabolism, and its production is assumed in all respiring cells (Fridovich, 1975). Its steady state concentration in mitochondria is estimated to be about 10^{-11} μM (Freeman, 1984). It does not diffuse through non-polar microenvironments of a cell because of its charged nature and, although it is stable in organic solutions, in aqueous solutions it undergoes dismutation reactions to produce hydrogen peroxide and oxygen:

	Rate constants of reactions
$HO_2^{\cdot} + HO_2^{\cdot} \rightarrow H_2O_2 + O_2$	$7.6 \times 10^5\ M^{-1}s^{-1}$
$HO_2^{\cdot} + O_2^{\cdot-} + H^+ \rightarrow H_2O_2 + O_2$	$8.5 \times 10^7\ M^{-1}s^{-1}$

represented overall by:

$O_2^{\cdot-} + O_2^{\cdot-} + 2H^+ \rightarrow H_2O_2 + O_2$	$< 100\ M^{-1}s^{-1}$

There is great controversy over the biological importance of the superoxide ion since it is said to be too unreactive with the probable biological targets (Midden, 1985). However, it is an important mediator of toxicity through the production of hydroxyl radicals in the presence of metal catalysts (iron-catalysed Haber-Weiss reaction in Fig. 7) and possibly through the production of singlet oxygen by dismutation or other reactions (Midden, 1985).

Recently, a pathway for $O_2^{\cdot-}$ generation via a UV-type II photosensitization by intracellular NADH and NADPH was suggested by Cunningham *et al.* (1985), but even at the most energetic wavelength

examined (290 nm) the molar quantity of $O_2^{\cdot-}$ produced was low, producing only 4 x 10^{-8} molecules of $O_2^{\cdot-}$ per photon of incident light.

3.2.3 Hydrogen peroxide (H_2O_2)

Considerable interest has recently been focused on the toxic effects of hydrogen peroxide in relation to the mechanisms by which near-UV radiation can induce lethality. The interest originated after it was shown that near-UV irradiation of tissue culture medium leads to the formation of photoproducts toxic to mammalian cells (Stoien and Wang, 1974). The photoactive components of the medium responsible for this effect were identified as L-tryptophan, riboflavin and L-tyrosine (Stoien and Wang, 1974) and the toxic photoproduct formed was hydrogen peroxide (McCormick et al., 1976). When solutions of L-tryptophan and riboflavin in buffer were exposed to near-UV radiation in the presence of oxygen and subsequently added to bacterial (Yoakum and Eisenstark, 1972) or mammalian (Hoffmann and Meneghini, 1979a) cells, they resulted in cell inactivation, indicating that the toxic photoproduct (hydrogen peroxide) was stable and long-lived.

Although hydrogen peroxide is a normal metabolite in cells, maintained at a concentration of 10^{-7}-10^{-9} μM (Freeman, 1984), excess H_2O_2 has been shown to be toxic to a variety of mammalian cell lines including human fibroblasts (Hoffmann and Meneghini, 1979b). In this study, 20μM H_2O_2 was able to kill more than 95 per cent of the cells after a 30 minute incubation at 37 °C. Formation of single-strand breaks in the DNA of the cells was shown, the numbers increasing with increasing concentration of H_2O_2. However,

it is doubtful whether these were the lesions leading to lethality since effective repair of single-strand breakage was shown to take place. The observation by the same workers that no single-strand breaks were formed when purified DNA was treated with H_2O_2 led to the conclusion that it was not H_2O_2 itself but another species, generated intracellularly, that ultimately exerts the damage to the DNA. Ward et al. (1985) suggested that highly reactive hydroxyl radicals are formed as a result of treating mammalian cells with H_2O_2 by impurity metal ion reduction of the H_2O_2 (Fenton reaction). They noted that H_2O_2 and $OH^{\bullet}$, produced by ionizing radiation, result in a similar range of lesions in the DNA. To provide evidence for their suggestion, they exposed V-79 cells for 10 minutes to H_2O_2 at 0-4°C and measured single-strand break formation in cellular DNA. Based on the argument that H_2O_2 treatment could be related to ionizing radiation damage via the number of single-strand breaks each one induces, they claimed that the single-strand breaks produced by H_2O_2 were ineffective in causing cell death. In fact, concentrations of H_2O_2 three orders of magnitude higher had to be used to cause significant cell killing. They concluded that the mechanism by which higher concentrations of H_2O_2 kill cells at 0°C is unknown and may not even include DNA as the target. However, it should be noted that the concentration of H_2O_2 at which cell lethality became apparent in their experiments was ~ 8×10^4 μM, 5,400 times greater than that reported by Hoffmann and Meneghini, but the authors believed this was due to the temperature of their 10 minute treatment at 0°C as opposed to 37°C for 30 minutes, which was used in the other study. Bradley and Erickson (1981), also in search of a common active species generated by H_2O_2 and X-rays,

reported the efficient repair of the single-strand breaks formed in the DNA of Chinese Hamster V-79 cells. Their survival showed that an intermediary 500 μM H_2O_2 was required to kill 90 per cent of the cells, but interestingly, they did not observe a shoulder in the survival and suggested that lethality may occur through a non-DNA lesion. They also did not specify the details of their treatment procedure so it is difficult to draw further conclusions about the temperature dependency reported by Ward *et al.* (1985).

In summary, the above studies indicate that H_2O_2 generates intracellularly a more active species, possibly $OH^{\bullet}$, which results in lethality. The lesion measured, *i.e.*, single-strand break formation, does not appear to effect lethality and is efficiently repaired. Therefore, another DNA or non-DNA lesion appears to be responsible for lethality.

The above conclusions are consistent with what is already known about near-UV lethality, and it has been proposed that damage by the two agents may occur through a similar pathway. Evidence for this came when *E. coli* strains hypersensitive to H_2O_2 (Demple *et al.*, 1983) were found to be sensitive to broad-spectrum near UV as well (Sammartano and Tuveson, 1983). Pretreatment of *E. coli* with sublethal doses of H_2O_2 has been shown to induce resistance to broad-spectrum near-UV damage (Sammartano and Tuveson, 1985), to further H_2O_2 damage (Tyrrell, 1985) and to ionizing radiation (Demple and Halbrook, 1983). It is thought that either a specific pathway of repair of oxidative DNA damage is induced (Demple and Halbrook, 1983) or that transient enhancement of catalase induced by one of the agents allows scavenging of the H_2O_2 formed subsequently by the other agent (Tyrrell, 1985).

3.2.4 Hydroxyl radicals ($OH^{\bullet}$)

Hydroxyl radicals are extremely reactive with almost every type of molecule found in living cells (sugar, amino acids, phospholipids and nucleotides, amongst others) with rate constants of the order of 10^{8}-10^{10} $M^{-1}s^{-1}$. If they are formed, therefore, in living systems they react immediately with whatever biological molecule is in their vicinity and it has been proposed that they are the ultimate oxygen species which forms lethal lesions in the DNA after a variety of treatments.

3.3 Antioxidant defense mechanisms

Elaborate defense systems have evolved to avoid cellular damage from highly reactive oxygen species. The concentration of these species increases in response to environmental stresses such as exposure to ionizing and UV radiation, hyperoxia, or during drug metabolism. There is a mutually supportive group of enzymes such as superoxide dismutases (SOD), catalases and glutathione peroxidases/reductases which remove destructive oxygen species in the following way:

Superoxide dismutases catalytically scavenge the superoxide ion by enhancing the rate of the dismutation reaction:

$$O_2^{\bullet-} + O_2^{\bullet-} + 2H^{+} \longrightarrow H_2O_2 + O_2$$

The resultant hydrogen peroxide is then either removed by catalases which catalyse the reaction:

$$2\ H_2O_2 \longrightarrow 2\ H_2O + O_2$$

or by peroxidases which bring about the general reaction:

$$SH_2 + H_2O_2 \longrightarrow S + 2\ H_2O$$

in which SH_2 is a substance that becomes oxidized.

Additional protection is provided by conjugated diene systems such as those found in melanins, carotenoids and tocopherols that quench reactive species and stop destructive reactions. Finally, there are individual reducing molecules such as sulphydryl compounds, phenols, purines, selenium, ascorbic acid and others which have an antioxidant role in the cell.

Although each of the antioxidant enzymes is considered to perform vital protective reactions in the cell, when in a genetic disorder one enzyme is completely missing such as in glutathione-deficient patients or acatalasemic individuals, this is not detrimental for the cell's, and consequently, the individual's survival. It is considered that some compensatory induction of another defense system occurs but attempts to find increased levels of the remaining antioxidant enzymes have been unsuccessful (Marklund *et al.*, 1984a). Negative results have also been obtained when trying to correlate enzymatic activities with responses of human cells to environmental stresses *i.e.* ionizing radiation (Marklund *et al.* 1984b) which indicate that the mechanisms by which the cell responds to oxidative damage are largely unknown at present.

Exogenous addition of these enzymes has also yielded contradictory results depending on what biological system is investigated, what type of oxidative stress it is challenged with and what endpoint is followed. Exogenous SOD has been shown to protect mycoplasma cells from gamma- radiation-induced lethality (Petkau and Chelack, 1974) and bacterial cells from photosensitized UV- radiation (Lavelle *et al.*, 1973) but endogenous induction of an elevated enzyme level in *E. coli*, (Goskin and Fridovich, 1973) did

not lead to enhanced survival against ionizing radiation. Conflicting experimental evidence also exists for the effects of exogenous catalase addition. In a bacterial system (Sammartano and Tuveson, 1984), 10 μg/ml catalase in the post-irradiation medium provided protection for E. coli cells to inactivation by near-UV irradiation. However, when catalase was present during broad-band near-UV irradiation of human fibroblasts, it did not alter their sensitivity, even though it reduced the number of single-strand breaks detected in the DNA of the cells (Roza et al., 1985).

3.3.1 Vitamin E

A single molecule which has attracted considerable attention in its antioxidant role is vitamin E, or alpha-tocopherol. Due to its lipophilicity, it partitions into membranes where it is in close proximity to the unsaturated chains of lipids to exert both a structural stabilizing action and inhibition of lipid peroxidation (Figures 8,9).

Lipid peroxidation reactions may arise from both singlet oxygen and hydroxyl radicals directly attacking polyunsaturated fatty acids to give hydroperoxides or forming other free radicals which may initiate a chain of reactions leading again to hydroperoxides, as shown in Figure 9. Such changes are known to lead to membrane damage and are under investigation as a possible pathway of near-UV radiation induced damage.

Termination of lipid peroxidation reactions is the primary function ascribed to vitamin E, which does so, by reacting with the alkyl peroxy radicals formed (see Fig. 9) itself forming a tocopheryl radical. The rate constants of the reaction are of the

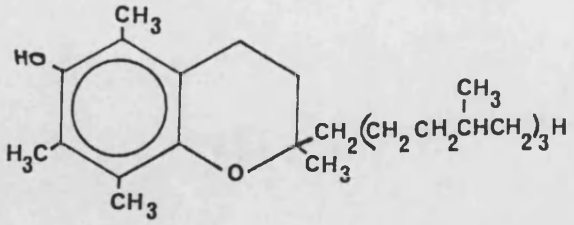

Structure of vitamin E

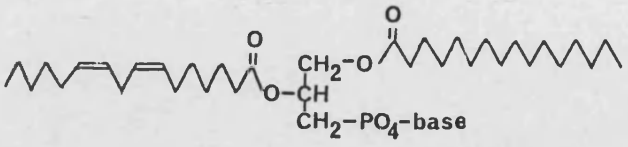

Structure of a phospholipid

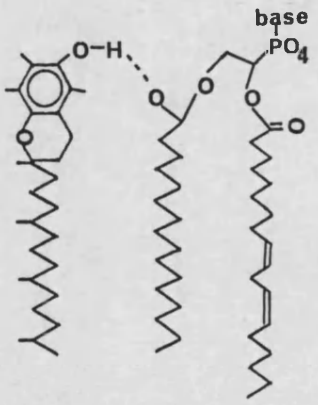

Possible interaction between vitamin E and membrane phospholipids through hydrophobic and hydrogen bondings

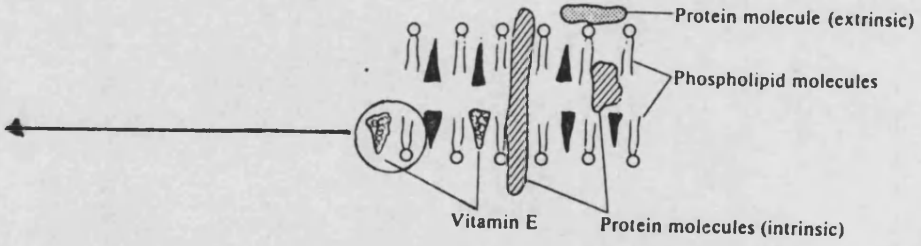

membrane

Figure 8. The structure of vitamin E, the structure of a phospholipid and their possible interaction in membranes.

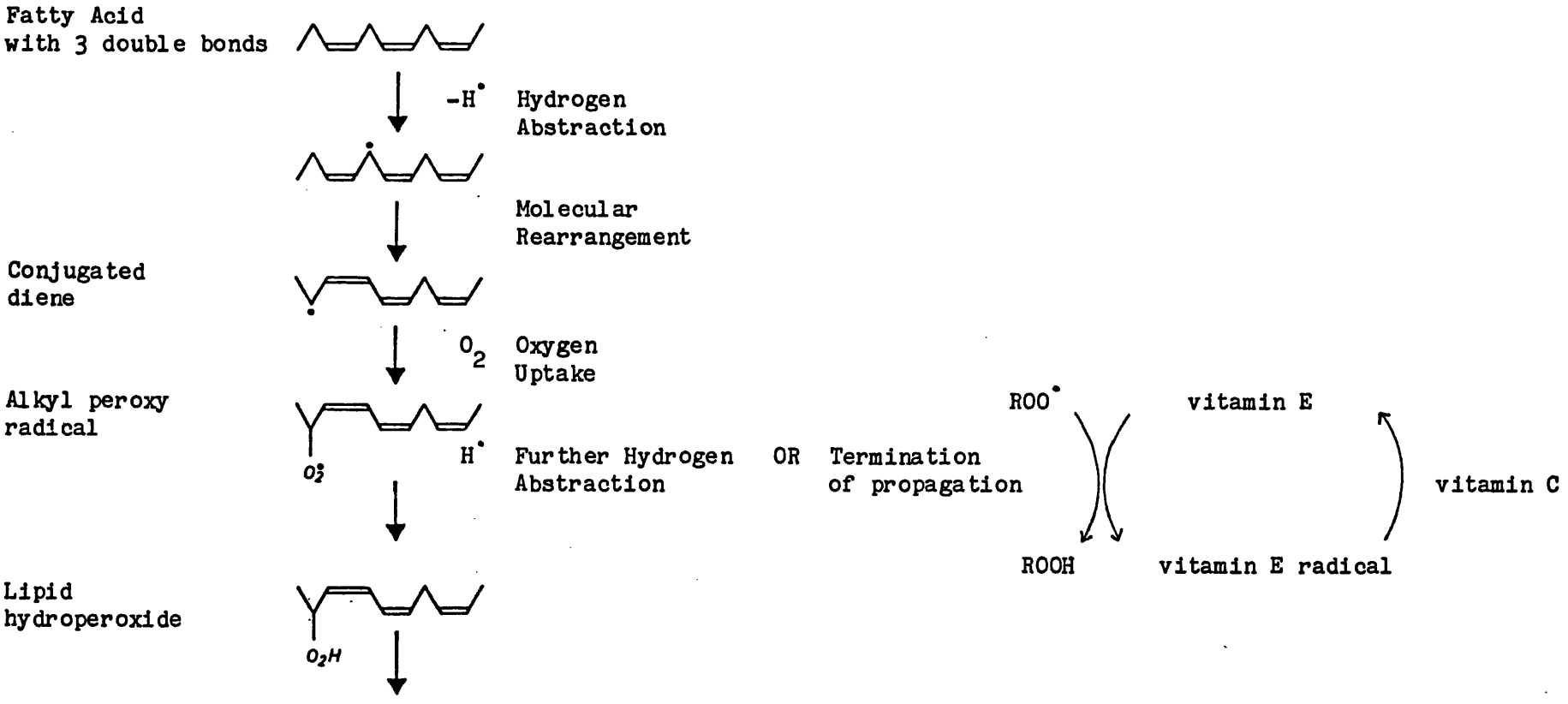

Figure 9. Initiation and propagation reactions of lipid peroxidation resulting to hydroperoxide formation. Vitamin E can stop the propagation step, by reacting with alkyl peroxyradicals, forming itself the tocopheryl radical which can be regenerated by vitamin C.

order of $10^7 M^{-1}s^{-1}$ (Bisby et al., 1984). The tocopheryl radical then reacts with vitamin C according to the original Tappel (1968) proposal and regenerates vitamin E. Direct evidence for this radical interaction has been provided in organic solvents by pulse radiolysis studies (Packer et al., 1979) and in model systems where vitamin E is in a lipid environment and vitamin C in an aqueous one (Scarpa et al., 1984; Doba et al., 1985).

Additional functions of vitamin E appear to be also the scavenging of radicals involved in the initiation of lipid peroxidation, such as singlet oxygen (Grams and Eskins, 1972; Foote, et al., 1974) and superoxide anion (Yagi et al., 1978; Ozawa and Hanaki, 1985) and the repair of free radical sites on membrane bound proteins oxidized by cellular free radical processes (Bisby et al., 1984).

Such a multiplicity of functions is thought to be due to the structure of vitamin E which allows it to assume a particular orientation within the membrane bilayer. Alpha-tocopherol would be expected to align its alkyl chain with the fatty-acid chains of the lipid molecules towards the hydrophobic bilayer interior keeping the hydroxyl group at the membrane aqueous interface. This alignment, assisted by specific interactions of alpha-tocopherol with the lipids through hydrophobic binding (Diplock and Lucy, 1973) and through hydrogen bonding (S rivastava et al., 1983) would result in physicochemical stabilization of the membrane which has been observed both in model (Ohyashiki et al., 1986) and natural membranes (lysosomal, sarcoplasmic reticulum, erythrocyte), (Jain, 1983; Erin et al., 1984). Therefore, the ability of vitamin E to alter the physical state of membranes, recently described as a

decrease of membrane fluidity (Ohyashiki et al., 1986), can be considered as an integral part of its antioxidant activity.

At the cellular level, vitamin E has been shown to allow cells to survive better under several environmental stress conditions which cause damage to the membrane lipids and disruption of the membrane organization. Cultured cells are quite deficient in vitamin E since their only source is an approximately 1μg/ml present in the foetal calf serum which supplements their growth medium i.e. ten times less than the normal vitamin E plasma concentration of 10 μg/ml. Due to this deficiency, when vitamin E was blended in the growth medium of WI-38 human cells at a concentration of 10 and 100 μg/ml, it increased their in vitro life span by almost two-fold. However, this effect proved to be associated with a particular batch of serum since change of serum made cell division cease and the observation could not be repeated with another batch of serum (Packer and Smith, 1974). In the same study, vitamin E supplementation in the medium was shown to effectively prevent the oxidation of WI-38 cell lipids as measured by malondialdehyde formation. When WI-38 cells were exposed to various oxygen tensions, partial protection was afforded by the presence of 100 μg/ml dl-alpha-tocopherol in the medium for oxygen tensions up to 50 per cent (Packer, 1978).

Complete protection from ribolavin photosensitized damage was obtained if 100 μg/ml of vitamin E was present during growth prior to exposure of the WI-38 cells to a visible light dose sufficient to kill about 50 per cent of the control cells (Pereira et al., 1976). However, lipid peroxidation products could not be detected as

thiobarbituric acid-reacting material, perhaps due to the short lifetime of measurable species.

4. SOLAR-UV EFFECTS ON HUMAN SKIN

It has been well established that a number of skin conditions (including skin cancer) are a consequence of exposure to the UV portion of the solar spectrum reaching the earth (see reviews by Blum, 1959; Black and Chan, 1977; Urbach et al., 1974). When trying to view the subject as a whole, there are tremendous difficulties related to the polychromatic nature of sunlight, the anatomical complexity of the skin and the multiplicity of effects arising from the interaction.

Physical and biological interactions may occur between different spectral regions of solar UV because light from one region may augment or inhibit, either directly or through a biological effect, an action from another region. Such wavelength interactions have attracted considerable interest recently and studies with very interesting results have emerged (Jagger, 1985).

When whole skin is considered as opposed to individual cells, difficulties concerning the absorption of energy at a specific site and the multiple environment of cells, arise. The skin is a very metabolically active organ consisting of an epidermis of about 60-100 μm thickness where the principal cell types found are keratinocytes and melanocytes, and an underlying dermis where the main cell type is the fibroblast. In this layer which ranges from 0.3-3.0 mm in thickness, fibroblast cells lie in ground substance composed of collagen and elastin, served by capillary blood supply.

Depending on the incident wavelength, only a portion of the radiation can penetrate to various depths through the epidermis to exert its effects, the least energetic wavelengths being the most penetrating. At the site of action, the absorbed photons may act on the DNA of the cells producing lesions such as those described previously. Wavelengths of 250-320 nm were shown to be effective in inducing dimer formation in mammalian skin (Pathak et al., 1972) and a recent action spectrum constructed by Freeman et al. (1986) exhibited a maximum at 296 nm. The absorbed photons may also act on different sites producing either direct damage to the target or inducing the production of substances that are detrimental to the cell. For example, some evidence suggested free-radical involvement in UV-mediated cutaneous damage through the formation of cholesterol epoxide which is UV-dose dependent (Black, 1986). DeLeo et al. (1984) reported the release of arachidonic acid metabolites from keratinocyte membranes in a dose-dependent fashion following broad-band 270-360 nm irradiation with 60 per cent of the output between 290 and 320 nm. The potential importance of lysosomes, which are organelles containing a wide range of lytic enzymes, has also been considered (Johnson and Daniels, 1969; Weissman and Dingle, 1961; Daniels, 1963) and products of lipid peroxidation (Malondialdehyde, Schiff's bases) have also been detected following broad-band (250-400 nm) irradiation of whole skin (Meffert et al., 1976). However, evidence is still inconclusive, and it would be very difficult to attempt to propose a single model for ultraviolet-induced cutaneous damage.

One possible approach to elucidate such mechanisms of damage might be to investigate a disease condition based on a cellular

sensitivity to UV-radiation. Research into the genetic condition xeroderma pigmentosum which shows extreme sensitivity to far-UV wavelengths, led to new discoveries in the field of DNA repair. Since the disease is characterized by a marked predisposition of patients to develop skin cancers after exposure to sunlight, it provided a link between a particular enzymatic defect in DNA repair and tumourigenicity (Cleaver and Bootsma, 1975). Considerable effort has been made to identify an analagous model to serve as a probe to near-UV mechanisms of damage.

4.1 Actinic Reticuloid (AR)

Actinic reticuloid is a photodermatosis, characterized by skin sensitivity to solar UV, and part of the visible spectrum. It principally affects exposed skin areas of middle aged or elderly men which acquire erythemato-papulo-vesicular lesions, sometimes with plaques resembling skin reticulosis (Ive et al., 1969).

Evidence for a cellular defect underlying the disease condition came from the studies by Giannelli et al. (1983) and Botcherby et al. (1984). They observed gross cytopathic changes and abnormal DNA fragmentation when actinic reticuloid cells were irradiated as a confluent monolayer with broad-band near-UV , at room temperature, in full medium. Since a striking feature of the histopathology of actinic reticuloid is an increased number of leukocytic infiltrates at the site of inflammation it was proposed that the sensitivity of AR cells might be due to a defect in their ability to deal with the action of radicals such as the superoxide anion which would be present in the leukocytic infiltrates.

5. SCOPE OF PRESENT WORK

This study was designed to investigate near-UV-induced damage using actinic reticuloid cells as a possible sensitive model. During studies to define this sensitivity to monochromatic light under controlled conditions of irradiation, it was found that temperature significantly alters the response of both normal and actinic reticuloid cells to irradiation. The first chapter deals with this effect on normal cells at specific monochromatic wavelengths. The second chapter then describes the actinic reticuloid sensitivity while the third and fourth examine the protective effect of a vitamin E analogue which acts as an antioxidant and the sensitizing effect of deuterium oxide which prolongs the lifetime of singlet oxygen and other oxygen species. Finally, the last chapter is concerned with the possible membrane damage induced by UV-radiation in both normal and AR cells.

MATERIALS AND METHODS

1. GROWTH OF HUMAN SKIN FIBROBLASTS IN CULTURE

1.1 Equipment

1.1.1 Laminar Flow Facilities

A 1.3 m, vertical displacement type, Class I biological safety cabinet, Microflow Model No. 20229 (MDH Ltd., Andover) was used for aseptic manipulations. All the surfaces of the hood were swabbed with 70 per cent alcohol before use.

1.1.2 Incubators

LEEC PF2 anhydric incubators with forced air circulation (Laboratory and Electrical Engineering Company, Nottingham) were used. The thermostatic controls were adjusted to maintain a temperature of $37^{o}C$.

1.1.4 Bench Centrifuge

Centrifugations were carried out in a MSE Minor, Model No. S-61 (MSE Scientific Instruments, Crawley) bench centrifuge.

1.1.4 Freezing Unit

Freezing of cells took place in a Union Carbide BF-6 biological freezer (Union Carbide UK Ltd., Cleveland), a plug type device, designed for use with the LR-33-10 freezer. This unit is capable of cooling up to eight 2 ml ampoules at between $0.5^{o}C$ and $7^{o}C\ min^{-1}$ to below $-70^{o}C$.

1.1.5 Liquid Nitrogen Freezer

Stock cultures of cells were stored in 2 ml ampoules in a Union Carbide model no. LR-40 (Union Carbide UK Ltd.) shelved in the vapour phase of the liquid N_2 at approximately -148 °C.

1.1.6 Haemocytometer

Standard double grid improved Neubauer-type blood cell haemocytometer, with coverslips (Fisons Ltd., Loughborough) were used for cell counting.

1.1.7 Microscope

For the examination of growing cell cultures under phase contrast and for haemocytometer counting an inverted biological microscope Wild M40 (Wild Heerbrugg Ltd., Heerbrugg, Switzerland) was employed. This instrument fitted with appropriate condensers and X10 and X20 objectives gives magnifications of X187 and X375, respectively.

1.1.8 Automatic Pipettes

Pipetman P50	1-50	µl
Pipetman P200	20-200	µl
Pipetman P1000	200-1000	µl
Pipetman P5000	1000-5000	µl

Pipetman pipettes with tips were obtained from Anachem Ltd., Luton. All pipettes were checked to ensure they were delivering accurately and reproducibly. A gravimetric method was used in which 10 replicates of a set volume of water at 20 °C were each weighed on an analytical balance. The coefficient of variation was less than

one per cent and the deviation from the nominal value was less than 0.5 per cent.

An automatic Pipetus (Flow Laboratories Ltd., Irvine, Scotland) with a sterile air filter in line was used in conjunction with 10 ml disposable pipettes (Sterilin, Ltd., Feltham) for quicker dispensing of media.

1.1.9 Glassware and Recycling of Glassware

125 ml and 500 ml bottles for the storage of solutions and media were obtained with caps, from Flow Laboratories Ltd. General laboratory glassware was obtained from Fisons Ltd.

Immediately after use all glassware was rinsed with tap water, and processed as follows:

(i) All articles were soaked in a hand-hot 2 per cent v/v solution of RBS 25 detergent (Fisons Ltd.) for 30 min.

(ii) Thoroughly cleaned, using a China brush on all surfaces under running water.

(iii) Rinsed in three changes of tap water, being left for 30 min in the last rinse.

(iv) Finally, all articles were rinsed and left for at least 30 min in a large volume of freshly collected glass distilled water.

After drying in a hot air oven, all items were foil capped and sterilized at 160° for a minimum of one hour.

1.1.10 Cell Culture Plasticware

Disposable 80 cm^2 and 175 cm^2 tissue culture flasks (Nunc, Gibco Ltd., Paisley, Scotland) and 90 mm x 15 mm petri dishes with triple vented lids (Sterilin Ltd.) were all of tissue culture grade

polystyrene and obtained ready sterilized. Polystyrene universal containers (30ml) with screw caps, plugged 10 ml pipettes and 2 ml polypropylene ampoules with silicone rubber-lined screw tops were also disposable and obtained ready sterilized from Sterilin Ltd.

Reusable centrifuge tubes (100 mm x 16 mm) with plastic screw tops were obtained from Nunc, Gibco Ltd. These were washed following the same procedures as the glassware, packed separately in D.H.S.S. specification bags (J. Dickenson and Sons Ltd.) before sterilization at 132°C for 5 minutes in a Drayton Castle high vacuum autoclave and assembled in the laminar flow hoods before use. The same washing and sterilizing procedures were used for the reusable pipette tips (Anachem Ltd.).

1.1.11 Gases and Gassing Procedures

(i) Cylinders of CO_2 and 5 per cent CO_2 in air mixture (5% CO_2 and 20% O_2 in N_2) were both obtained from British Oxygen Company, Bristol and were piped to each work station from a central holding reservoir.

(ii) Gas flowmeter, floating-needle type, 0.1-1.0 l min^{-1} (Rotameter Manufacturing Co. Ltd., Croydon), calibrated for use with CO_2.

(iii) Incubation boxes, rigid clear plastic boxes, 3.25 litre volume (A. Gallenkamp and Co. Ltd., London)

(iv) Gas-tight tape, British standard vinyl tape, 2.5 cm wide (Intech Tapes Ltd., Manchester).

All the cell culture media used contained a bicarbonate pH buffer system designed to equilibrate with 5 per cent CO_2 in air. To achieve this, all gas-tight culture bottles and flasks were

charged with such a mixture, introduced at a low flow rate through a sterilized Pasteur pipette plugged with non-absorbent cotton wool. Cell culture dishes were placed in incubator boxes which were flushed with 150 ml of CO_2 from a metered supply, through a plugged Pasteur pipette. The boxes were then sealed with gas-tight tape.

1.2. Cell Culture Materials

1.2.1 Water

Double glass distilled water (DDH_2O) was used in the preparation of all solutions and media. This was obtained from a 4-litre hr^{-1} bi-distillation Fistream still, model 2903 (Fisons Ltd.) fitted with a Fistream pre-deionizer (Fisons Ltd.) which was changed at regular intervals. DDH_2O was sterilized by autoclaving at 121°C in 100 ml and 500 ml quantities in glass bottles, for appropriate times. Sterile DDH_2O produced in this way had a pH of 4.5.

1.2.2 Media

Eagles Minimum Essential Medium with Earle's Salts, which was routinely used, was obtained as sterile 10x liquid concentrate with phenol red but without L-glutamine or sodium bicarbonate from Flow Laboratories Ltd. and stored at 4°C until use.

The Dulbecco's modification of Eagle's medium which was used in one set of experiments was obtained as a sterile 10x liquid concentrate without L-glutamine or sodium bicarbonate from Gibco Ltd.

1.2.3 Additives for Cell Culture Medium

(i) Antibiotic solution, penicillin (5,000 iu ml^{-1}) and streptomycin (5,000μg ml^{-1}) sterile solution was obtained from Flow Laboratories Ltd. in 100 ml unit quantities. This was subdivided into 15 ml volumes and stored frozen in plastic universals at -20°C, for a maximum of one year.

(ii) L-glutamine solution was obtained as a sterile 200 mM solution in 100 ml unit quantities from Flow Laboratories Ltd. This was subdivided into 15 ml volumes and stored frozen in plastic universals at -20°C, for a maximum of one year.

(iii) Sodium bicarbonate was obtained as a sterile 7.5 per cent w/v $NaHCO_3$ solution in 100 ml quantities from Flow Laboratories Ltd. This solution was stored at room temperature for a maximum of one year.

1.2.4 Sera

Foetal calf serum and newborn calf serum were both obtained from Flow Laboratories Ltd., the latter replacing, for reasons of economy, foetal calf serum as a supplement in the large volumes of medium used in plating experiments. Both sera types were tested before purchase for their ability to support growth of the cell lines and for their ability to form colonies after dilution plating. Three batches of foetal calf serum and three batches of newborn calf serum were utilized during the course of these studies. The batch number of the serum used in each experiment was recorded so that any possible effects of serum on the sensitivity of cells could be detected. All the sera were stored at -20°C until use.

1.2.5 Growth Media Preparation

The growth media used for the maintenance of the human fibroblasts and the assessment of their colony forming ability had the following formula, adopted from Flow Laboratories Catalogue. Unless otherwise specified, growth medium will refer to EMEM supplemented with the following additives and 15 per cent foetal calf serum.

10x liquid medium concentrate	EMEM	DMEM
(full formula in Appendix 1)	40.0 ml	40.0 ml
L-glutamine 200 mM	4.0 ml	8.0 ml
Penicillin 5000 iu/ml and Streptomycin 5000 µg/ml	4.5 ml	4.5 ml
Sodium Bicarbonate 7.5% Solution	12.8 ml	19.6 ml
Foetal or newborn calf serum	68.0 ml	68.0 ml
Sterile double glass distilled water	340.0 ml	329.2 ml

First, media components were thawed where necessary in a water bath at 30°C. Single strength medium was prepared by the aseptic additions of all media components to the appropriate volume of double glass distilled water previously sterilized by autoclaving at 121°C for 30 minutes in 500 ml Flow bottles.

Media containing foetal calf serum were decanted aseptically into sterile 125 ml Flow bottles.

All media thus prepared were stored in a darkened refrigerator at 4°C and used within one month of preparation.

1.2.6 Balanced Salt Solution

Dulbecco's phosphate buffered saline was routinely used, either with or without added calcium and magnesium ions, solutions designated PBS and PBS(A), respectively.

Composition:

Component	$gl^{-1}DDH_2O$
NaCl	8.0
KCl	0.2
Na_2HPO_4	1.15
KH_2PO_4	0.2
$CaCl_2 \cdot 2H_2O$	0.132
$MgCl_2 \cdot 6H_2O$	0.1

Sterile PBS(A) was prepared by dissolving one PBS(A) tablet (Oxoid Ltd., London) in 100 ml of freshly collected DDH_2O and autoclaving for 15 min at 121°C. PBS was prepared by the aseptic addition of 0.5 ml Dulbecco B solution (Oxoid Ltd.) to 100 ml of sterile PBS(A). Both PBS and PBS(A) were stored at room temperature for a maximum of one month.

1.2.7 Trypsin Solution

Trypsin (1:250) was obtained as a sterile 2.5 per cent w/v solution in Hanks balanced salt solution without calcium, magnesium and phenol red, in 100 ml unit quantities from Flow Laboratories Ltd. This was aseptically diluted to 0.25 per cent with PBS(A), stored as 15 ml volumes in plastic universals at -20°C and used within four weeks.

1.2.8 Chemicals

A list of chemical compounds used in this study is given below:

1. Trolox-C

6-hydroxy-2,5,7,8-tetramethyl-chroman-2-carboxylic acid (Trolox-C) was a gift from Hoffman-LaRoche Inc., New Jersey, U.S.A. It was in powder form and kept in tightly capped glass bottles, protected from light, at 4°C.

2. Deuterium oxide

D_2O of isotopic purity 99.8 per cent (Sigma Chemical Group Ltd., Dorset) was obtained in sterile form in 25 ml quantities and stored anhydrous, at room temperature, for a maximum of one month.

3. Hydrogen peroxide

H_2O_2 (Fluka, W. Germany) was obtained as a 30 per cent concentrate (8.82 M) and stored at room temperature.

4. Dimethylsulphoxide

DMSO, grade I (Sigma Ltd.) was obtained in 100 ml quantities and stored in tightly capped glass bottles at room temperature.

5. Methylene blue

Methylene blue was obtained in powdered form (BDH Chemicals Dorset) and stored at room temperature.

1.3. Cell Culture Methods

1.3.1 Cell Lines

The diploid human skin fibroblast strains used in this study were

GM730 - from a normal female donor (45-year old) kindly provided by the MRC Cell Mutation Unit, University of Sussex, Brighton. The cell line originated from the Human Genetic Mutant Cell Repository, Camden, New Jersey, USA

AR6LO - from an actinic reticuloid patient,(55-year old male, clinical details in Appendix 9) kindly provided by Dr. F. Giannelli, Guys Medical School, London

The maintenance of more than one cell line in the same laboratory presents a problem of cross contamination (Paul, 1975). Great care was therefore taken to maintain the purity of cultures throughout these studies. Simultaneous handling of different cell lines was never undertaken and bottles of medium were designated for use with only one particular cell line.

1.3.2 Maintenance of Cell Lines

The cell lines employed in these studies both grow as monolayers, therefore, stock cultures were routinely maintained in culture medium in 80 cm^2 or 175 cm^2 tissue culture flasks at 37^{o}C. Routine subculture protocols were designed to keep cells in a state of active growth.

1.3.3 Cell Storage

Cells were stored in the vapour state of a liquid nitrogen refrigerator at approximately -148 °C.

Existing stocks of cells were built up from the ones received in the following way:

First, the cells received were examined macroscopically and microscopically and, if the culture appeared healthy, the medium was decanted and the cells subcultured in the usual manner into one or two 80 cm^2 flasks. The cells were allowed to form a confluent layer and then subcultured twice more with a 1:3 split ratio so that at least eighteen 80 cm^2 flasks were obtained after the last subculture. Cells to be frozen were harvested in exponential growth. Six flasks at a time were trypsinized, the cells resuspended in whole medium and centrifuged. The cell pellets from each flask were pooled and resuspended in 8 ml of growth medium containing five per cent DMSO, which had been freshly prepared by the aseptic addition of 5 ml of filter sterilized DMSO (disposable Millex-FG units [Millipore] fitted with Fluorophore hydrophobic membrane filters of 0.2μm pore size were used to filter DMSO) to 95 ml of growth medium. The cell suspensions were aspirated using a sterile Pasteur pipette and one ml of suspension transferred into each of eight sterile 2 ml ampoules. All ampoules were clearly marked with the cell strain, the passage number, the date and a batch code. Subsequently, these were placed in the BF-6 biological freezer set to be cooled at a cooling rate of 1 °C $minute^{-1}$ and frozen to below -70 °C. The ampoules were then quickly transferred to the shelves of the liquid nitrogen refrigerator for long term storage at approximately -148 °C.

1.3.4 Recovery of Cells from Storage

Cells were recovered from liquid nitrogen storage in the following way:

Ampoules were removed from the refrigerator, thawed quickly in a water bath at 37°C and their contents transferred using a sterile Pasteur pipette to a 80 cm^2 tissue culture flask containing 15 ml growth medium. Flasks were then overgassed with 5 per cent CO_2 in air and incubated at 37°C.

1.3.5 Preparation of Cell Suspensions from Monolayer Cultures

The essential procedure in the maintenance of cells in culture is subculture, which involves the transfer of cells from one culture vessel to another. To effect this for monolayer cultures a suspension of cells must first be obtained. Once in suspension, cells can also be greatly diluted and plated so that colonies arise from single cells, a procedure important in many experiments. Prior to manipulation, the culture medium of the flask to be subcultured was examined by eye for the absence of floating cellular debris and to ensure it was not too acidic or basic, as indicated by the phenol red component. This was followed by closer examination of the cell cultures, under phase contrast microscopy, to ensure that cells had a normal appearance, with nonrefractile granules in their cytoplasm. If a particular culture failed to fulfill these requirements, it was discarded.

The medium was removed from the flask and the monolayer rinsed with 5 ml of ice-cold 0.25 per cent trypsin solution. This was discarded and replaced by another 5 ml of trypsin solution, which

was also discarded and the cells were allowed a 5 minute period with only a residual thin layer of trypsin covering them. Low temperature trypsinization was adopted as cells are reported to be more resistant to mechanical stresses (Wang et al., 1968), suffer less intracellular penetration of trypsin (Hodges et al., 1973) and show increased cell viability if all steps of subculturing are performed at temperatures below 15°C (McKeehan et al., 1981). At the end of the trypsinization period, single cells were released from the surface of the flask, resuspended in cold growth medium and transferred to a tissue culture centrifuge tube. After a 1 min centrifugation step at 1000 rpm the supernatant was discarded and the cells resuspended in a further 5 ml of EMEM. The suspension was then aspirated with a Pasteur pipette to obtain a suspension of single cells and the cell density determined using a haemocytometer. Routinely, 8 x 10^5 cells were added to 15 ml of EMEM containing 15 per cent foetal calf serum in 80 cm^2 tissue culture flasks. Flasks were then overgassed with a 5 per cent CO_2 in air mixture delivered at a low flow rate through a sterile Pasteur pipette plugged with non-absorbent cotton wool. All cell cultures were clearly marked with the cell strain, the passage number and the date and incubated at 37°C in the dark, as photoproducts toxic to mammalian cells are known to be formed from certain media components (Wang et al., 1974) when cultures are incubated in the light.

1.3.6 Determination of Cell Density

This was achieved by haemocytometer counting, a method which also allows visual examination of the cells prior to experiments. The haemocytometer was first prepared as follows: The surface of the

slide was cleaned with 70 per cent alcohol, taking care not to scratch the semi-silvered surface. The coverslip was also cleaned and, after wetting the edges slightly, it was pressed down over the grooves and semi-silvered counting area. The appearance of interference patterns ('Newton's rings') indicated that the coverslip was properly attached, thereby determining the depth of the counting chamber (0.1mm). Cells were throroughly mixed before a small volume was withdrawn from just below the surface of the suspension, and introduced into the haemocytometer chamber. A total cell count was performed on eight large squares ($1mm^2$ each) of the haemocytometer grid under phase contrast microscopy. If cell clumping was observed, the count was discarded, and the suspension aspirated to break up the clumps before a new sample was taken. If the cell density was greater than 150 cells per large square, at which point counting became impeded by crowding, the suspension was further diluted and sampling repeated.

Cell count per ml^{-1} is given by:

cell $ml^{-1} = 10^4 n$, where n is the average number of cells per large square.

1.3.7 Preparation of Cell Suspensions for Experimental Use

Cells to be irradiated in suspension were harvested in exponential growth according to the following set procedure. In order to standardize as far as possible the culture conditions, all cell strains were subcultured by inoculation of 8×10^5 cells into each of two 80 cm^2 tissue culture flasks containing 15 ml of growth medium and incubated at 37^oC for 48 hours, by which time cells had begun to grow. At the end of this period one of these flasks was

harvested to provide the cell suspension for irradiation while the other, after incubation for a further five days was subcultured again to provide the cells for the next experiment as described above. With each strain in use, a cycle was thus established such that cells were only subcultured once weekly and not subjected to a loss of division potential by routine subculturing. Cells to be irradiated were trypsinized in the usual manner but after cell detachment they were resuspended in 10 ml of complete phosphate buffered saline with calcium and magnesium. This served both to inhibit further tryptic action and to minimise the carry over of organic media components into the irradiation suspension. The cell suspension was then centrifuged at 1000 rpm for 1 minute, the supernatant liquid decanted and the cell pellet resuspended in 5 ml of complete PBS. The suspension was then aspirated using a sterile Pasteur pipette, the cell density determined by haemocytometer counting and adjusted to 10^5 cells ml^{-1} by further dilution in complete PBS.

1.3.8 Assessment of Viability

Cell survival was determined by relative colony forming ability using adaptations of the single cell plating techniques first developed by Puck et al. (1956), specifically the homologous feeder layer technique of plating human skin fibroblasts (Cox and Masson, 1974). Each 80 cm^2 culture flask of cells to be used in a UV-irradiation experiment was coupled with a 175 cm^2 culture flask of homologous cells. On the day prior to irradiation this culture was trypsinized and the cells resuspended in 20 ml of EMEM with 15 per cent foetal calf serum. The cell density was then determined by

haemocytometer count and sufficient medium then added to the suspension in the flask to give a cell concentration of 6.4×10^4 cells ml^{-1}. A quantity of this cell suspension, sufficient, when subsequently diluted 10-fold, to pour the number of plates required to conduct the experiment, was aseptically transferred into a sterile 125 ml Flow bottle and given an inactivating dose of 50 Gy of gamma radiation in a 2000 curie Caesium^{137} gamma source (Gravatom Industries Ltd.). After irradiation the cell suspension was diluted 10-fold to a final concentration of 6.4×10^3 cells ml^{-1} in EMEM supplemented with 15 per cent newborn calf serum. Ten ml of this suspension were then dispensed onto the appropriate number of 90 mm tissue culture dishes using an automatic Pipetus (Flow Labs., Ltd.) giving a cell density on each petri dish of 10^3 cells per cm^2, which had been found to be the optimal density for colony forming efficiency of human skin fibroblasts (Cox and Masson, 1974). Plates were then placed in clear polystyrene boxes previously swabbed with 70 per cent ethanol for disinfection and air dried, each box holding 18 plates. The boxes were then gassed with 150 ml of CO_2 delivered from a metered supply, sealed with gas tight tape and incubated overnight at 37°C.

Control and irradiated cell samples were diluted in whole medium at room temperature. The dilution employed depended on both the cloning efficiency of the cell strain and its expected sensitivity to the ultraviolet radiation treatment. Final colony counts of between 20 and 150 were considered desirable. The cells were added as 1 ml aliquots to each of three feeder layer plates per fluence point and spread by gentle agitation of the plates. Plates

were then replaced in the boxes, gassed, sealed and reincubated for 14 - 21 days at 37°C in the dark to allow colony formation.

At the end of the growth period plates were removed from the incubator, the medium was poured off and approximately 2 ml of 0.5 per cent methylene blue in 50 per cent methanol was added to each plate. After a 15 minute period to allow for fixing and staining of colonies this was poured off and the plates rinsed in tap water, and dried. Plates were coded and randomised before counting.

1.3.9 Preparation of Attached Cells for Experimental Use

Certain experiments required irradiation or other treatment of cells attached to plates. A modification of the methods described above was therefore used, in which the feeder layer was prepared first and plates containing gamma-inactivated 6.4×10^3 cells ml^{-1} in EMEM supplemented with 15 per cent newborn calf serum were incubated overnight at 37°C.

The following day, a 10^5 cell suspension of the cells to be irradiated or otherwise treated was prepared and appropriate dilutions were plated depending on the cloning efficiency of the cell line and the expected sensitivity to the treatment. Cells were irradiated 48 hours later so that the stage of growth of the cells in either way (suspension or attached) was similar. After irradiation, assessment of viability by colony formation counting was done as described previously.

2. IRRADIATION OF HUMAN SKIN FIBROBLASTS IN CULTURE

Human fibroblasts were irradiated in suspension with monochromatic wavelengths in the far-, mid- and near-UV regions for the purpose of determining their survival characteristics. For assessment of membrane damage irradiation of cells attached on plates was carried out, for reasons that will be discussed later. Monochromatic irradiation of attached cells was not feasible with the apparatus available so irradiations were restricted to broad-band far and near UV. Finally, determination of the gamma-radiation sensitivity of human fibroblasts and routine preparation of a feeder layer for UV experiments required the use of the ^{137}Cs-gamma-radiation source.

2.1. Equipment

2.1.1 Dark Room

All experiments involving irradiation with ultraviolet light or gamma-rays were carried out in a 'dark room' under illumination from red fluorescent tubes (Atlas Ltd. 80W), which emit only light of wavelengths longer than 500 nm.

2.1.2 Monochromatic Radiation Sources

Penray Lamp (Ultraviolet Products, Inc.)

A 5 cm low pressure mercury lamp fitted with an integral filter (G-275) was used. This was designed to isolate the 253.7 nm line of the mercury spectrum and about 92-97 per cent of lamp output is at this wavelength. The lamp was used in a vertical position on an optical bench as described later.

Bausch and Lomb SP 200 Lamp (Bausch and Lomb, Rochester, New York)

This was a 200W super pressure mercury vapour lamp with a fused silica envelope and an appropriate fused silica condensing lens system. Newly fitted lamps were allowed to burn off at least 2 hours before being used for irradiation and were replaced after 100 hours use. This light source was used in conjunction with a Bausch and Lomb high intensity grating monochromator, which was fitted with a UV-visible diffraction grating of 1350.0 lines per mm blazed for maximum efficiency at 300 nm. Operation was over a wavelength of 200 nm-800 nm with a stated reciprocal dispersion of 6.4 nm/mm. Matched fixed slit discs were used, the entrance and exit slits being 2.68 mm and 1.5 mm, respectively.

Arrangement of Optical Bench

The general arrangement of the apparatus for irradiation of cell suspensions is shown in Fig. 10. All optical components were arranged in a horizontal plane on an Ealing Beck optical bench and associated supports, allowing vertical and horizontal adjustment.

The shutter

This was an iris camera shutter (G. B. Kernshaw 630) with a 2 cm aperture, fitted with a cable release. Exposures were timed using a stopwatch.

The focusing lens

This was used only in conjunction with the Bausch and Lomb SP 200 source and was a 40 mm diameter Spectrosil biconvex lens having a focal length of 55 mm. This produced an inverted magnified image of the exit slit of the monochromator 3 cm high x 1 cm wide allowing full illumination of the irradiation cuvette.

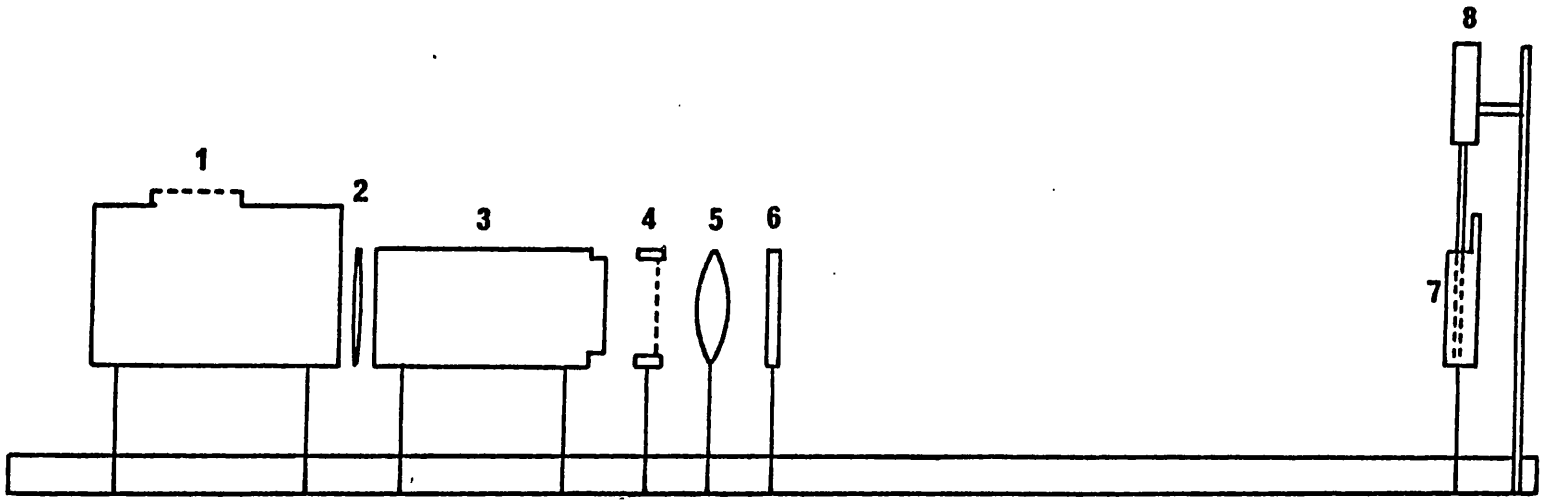

Figure 10. Diagram of apparatus for UV irradiation of cells in suspension.

1. Mercury UV Source (SP200)
2. Quartz Collective Lens
3. Monochromator
4. Shutter
5. Focusing Lens
6. Stray Light Filter
7. Irradiation Cuvette (See Fig. 12)
8. Stirrer

Stray light filters

During irradiation with wavelengths longer than 254 nm selected using a monochromator, it is essential that any stray light of shorter wavelength be removed from the radiation beam to prevent its contribution to inactivation and the introduction of a corresponding error in determination of the biological sensitivity. An appropriate UV-absorbing filter was thus positioned between the monochromator and the irradiation cuvette. Details of these filters are given in Table 1 and Figure 11. On receipt from the supplier all glass UV-absorbing filters were checked against specification by the determination of the UV-transmission spectrum relative to air using a Pye-Unicam SP1800 scanning spectrophotometer.

For irradiation at 313 nm a film of Mylar C 2.5 μm (DuPont Ltd.) was employed as a stray light filter. This material required a period of about 2 hours exposure to the 313 nm radiation before use to "age" it. During this time the transmission of the filter at 313 nm fell initially and then remained stable. The absorbance of Mylar C was typically 0.27 at 313 nm and 3.0 at 300 nm indicating that effective filtration of 300 nm and below was achieved.

The irradiation cuvette

A jacketed 10 mm internal width, 10 mm pathlength quartz cuvette was used (Thermal Syndicate, Ltd.). This is illustrated diagramatically in Fig. 12. Control of the temperature of the cell suspensions was achieved by circulation of water from a water bath through lagged rubber tubing by a peristaltic pump (Watson Marlow Ltd.).

Two water baths were routinely used. One, for irradiation at 0°C, contained a 50 per cent ethylene glycol solution which was cooled by a U-cool refrigeration unit (Neslab Instruments, Inc.).

TABLE 1

DETAILS OF STRAY LIGHT FILTERS, BAND WIDTHS AND FLUENCE RATES USED IN IRRADIATION EXPERIMENTS

WAVELENGTH	STRAY LIGHT FILTER	WAVELENGTH 1% TRANSMISSION ON LOW SIDE nm	%TRANSMISSION AT DESIGNATED WAVELENGTHS	BAND WIDTH AT 50% MAXIMUM nm	FLUENCE RATE $Jm^{-2}s^{-1}$
*254 nm	G275	---	---	---	$5.2 - 7.3 \times 10^{-2}$
*313 nm	Mylar C 2.5μm	301 nm	63	7.0 nm	$5.8 - 9.3 \times 10^{0}$
325 nm	Corning 0-54	298 nm	84	12.5 nm	$3.6 - 6.5 \times 10^{0}$
*334 nm	Oriel WG-335	311 nm	77	7.25 nm	$3.6 - 8.2 \times 10^{0}$
*365 nm	Corning 0-52 (1/2 thickness)	332 nm	85	7 nm	$1.9 - 4.2 \times 10^{1}$

*Mercury resonance lines.

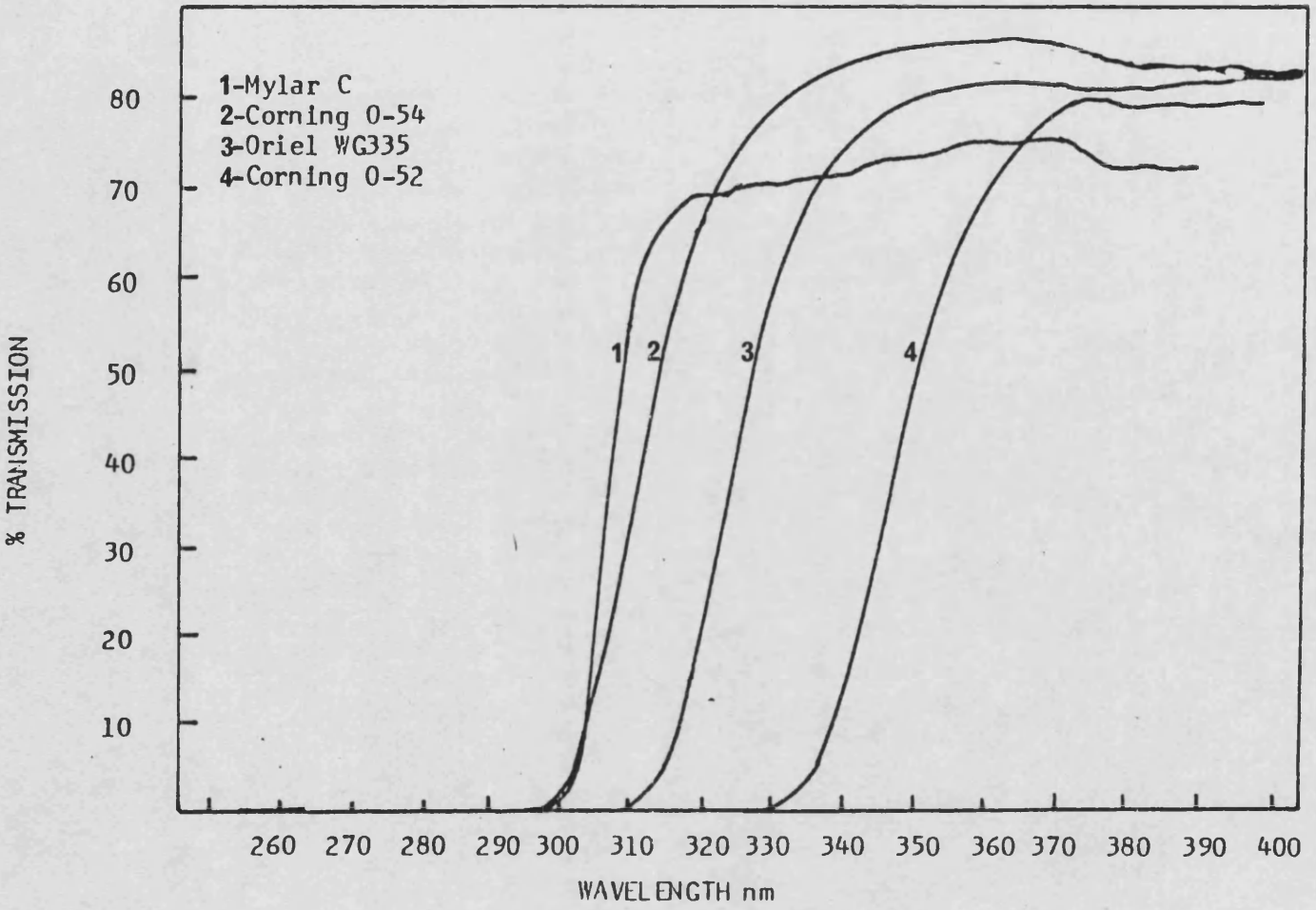

Figure 11. Transmission characteristics of stray light filters.

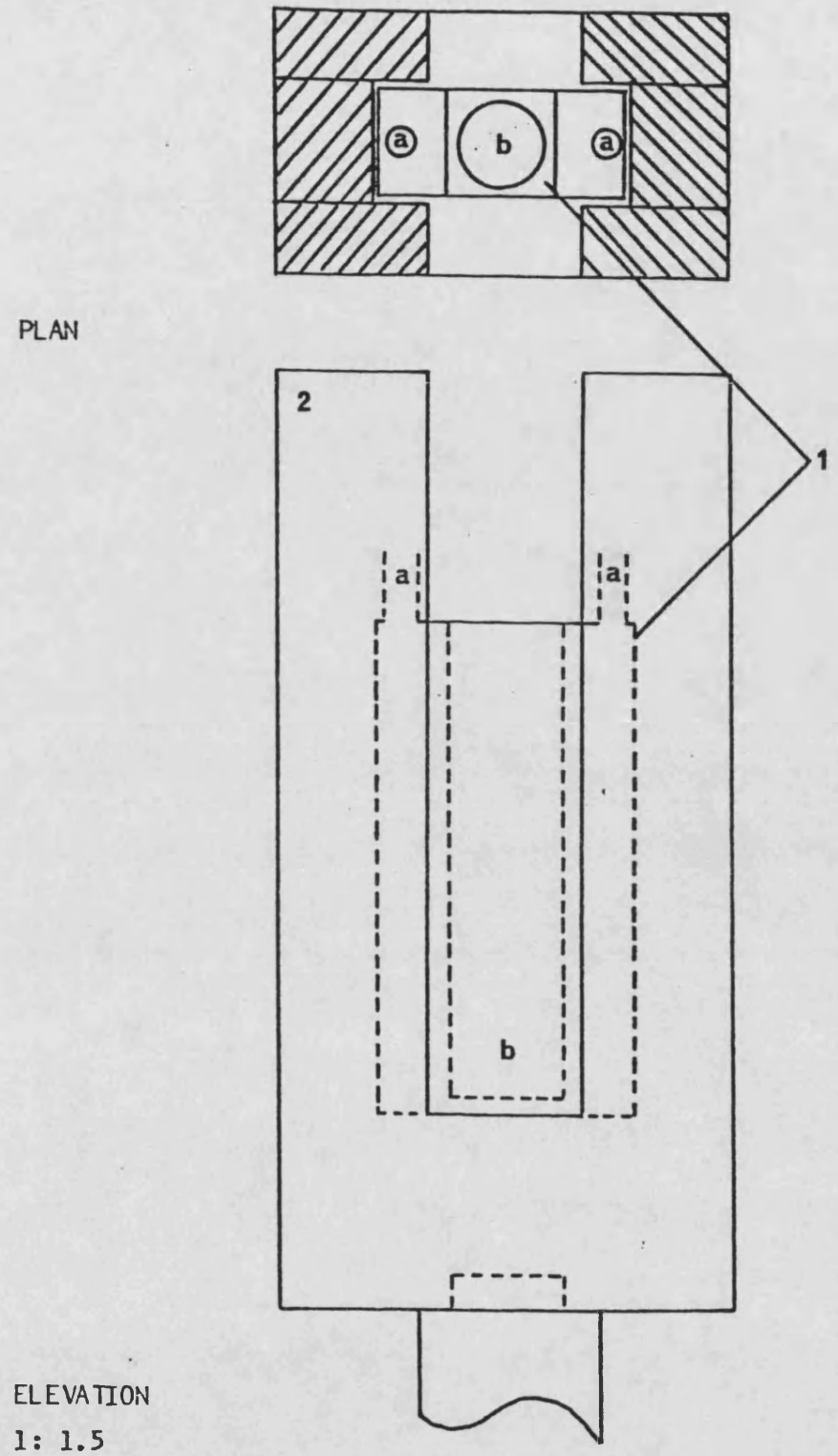

Figure 12. Diagram of the irradiation cuvette

1. Irradiation cuvette
   a. Entrance and exit ports for circulating fluid
   b. Position of suspension for irradiation
2. Perspex holder

The other, reserved for the other temperatures, contained distilled water and thermostatic regulation was by a heating coil pump (Grant Instruments Ltd.). Periodic monitoring of the cuvette temperature was achieved by a probe thermometer (Comark Ltd.). Before the start of each experiment, the water bath temperature which would allow the cuvette temperature to be at the desired level would be determined and maintained constant throughout the experiment. In this way, a +/- 0.5^{o}C of the desired temperature was always maintained.

The stirrer

Cell suspensions were stirred during irradiation by means of rotation of a quartz paddle in a laboratory stirrer (Stanhope Sera Ltd.) at approximately 600 r.p.m.

Fluence Rate Determination for Ultraviolet Radiations

The fluence rates of UV radiations received by cell suspensions were measured using an Oriel 7102 thermopile (Oriel Corp. of America) in conjunction wth chemical actinometry. The thermopile was mounted in a sliding bench saddle beside the cuvette such that the detector was coincident with the inside front face of the cuvette when moved across into the radiation beam. Output voltages were measured on a microvoltameter (Keithley Instruments Model 150B).

Normally, conversion of the incident energy from microvolts to Joules $m^{-2}s^{-1}$ are made with reference to the calibration factor of the thermopile obtained by chemical actinometry (Hatchard and Parker, 1956). However, this assumes a uniform fluence rate received on the whole area of the cuvette (observed as a uniform 'image') which could not always be obtained with the Bausch and Lomb monochromator. Furthermore, this image changed for different lamps or as a particular lamp aged. Regarding the 254 nm irradiation using

the penray lamps, the thermopile reading was so low that it was very difficult to obtain an accurate reading. The situation was rendered more complicated due to the radiant heat detected by the thermopile. Therefore, chemical actinometry was very much relied upon and always performed at the beginning of every experiment. The thermopile readings served to check whether the fluence had remained constant throughout an experiment.

Potassium ferrioxalate actinometry relies on the light catalysed production of Fe^{2+} ions in a solution of $K_3Fe(C_2O_4)_3$. The solution absorbs light completely in the UV region, the quantum yield of the reaction is practically constant throughout the UV region and the yield is independent of the fluence rate. Actinometry was performed under red light according to the method of Jagger (1967), as described in Appendix 2. A calibration curve of optical density at 510 nm against amount of ferrous ion (as determined by Kelland, 1984, Fig. A1) was used to ascertain the amount of ferrous ion formed by the radiation. From this, a fluence rate was calculated by application of the constants pertaining to the wavelength chosen. A number of fluences were obtained for different time exposures at a particular monochromatic wavelength and an average fluence rate for a particular experiment was calculated.

2.1.1 Broad-band Radiation Sources

For broad-band irradiation, the apparatus shown diagrammatically in Fig. 13, consisting of two 18" lamps mounted horizontally in a metal box, was used. For broad-band near-UV irradiation two F15TB 'Black-Light Blue' lamps (15W, General Electric, Ultraviolet Products) and for broad-band far-UV

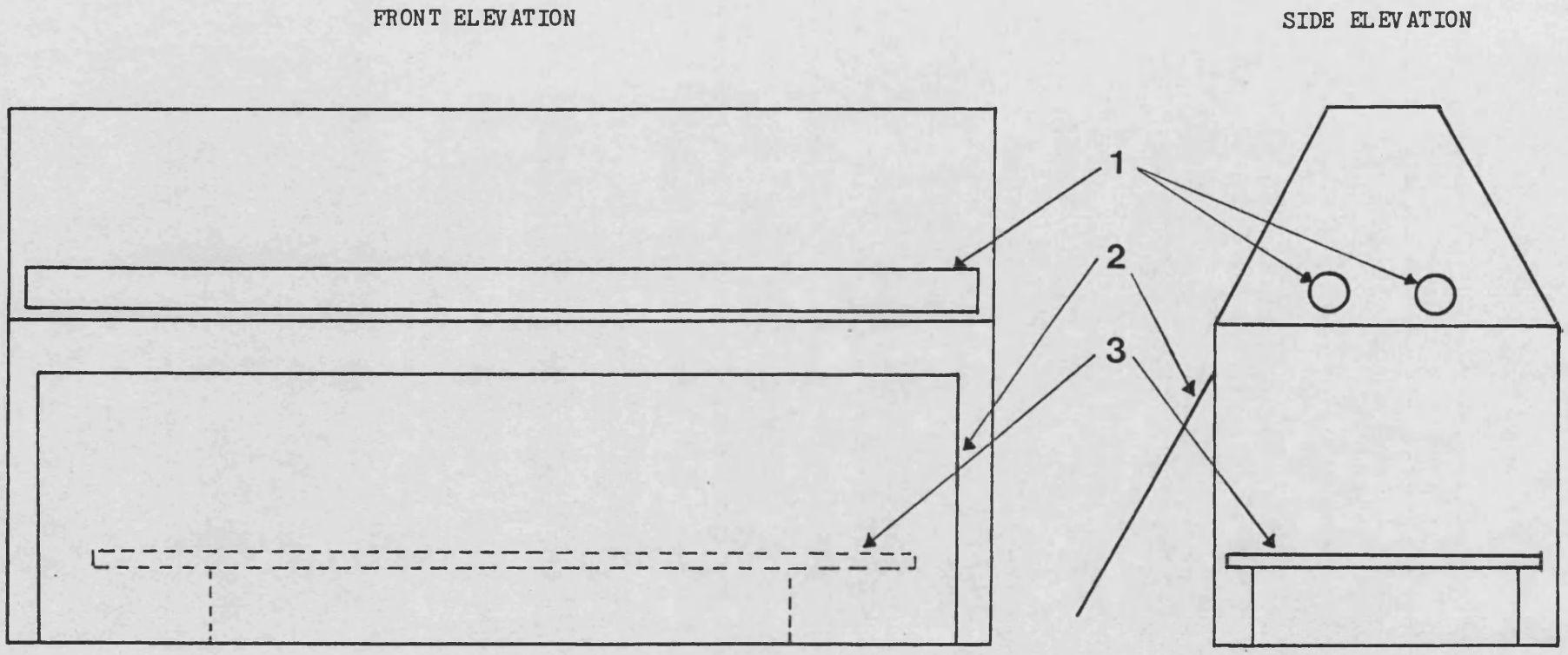

Figure 13. Diagram of the housing used for broad-band irradiation.

1. Position of lamps
2. Front opening
3. Support for plates

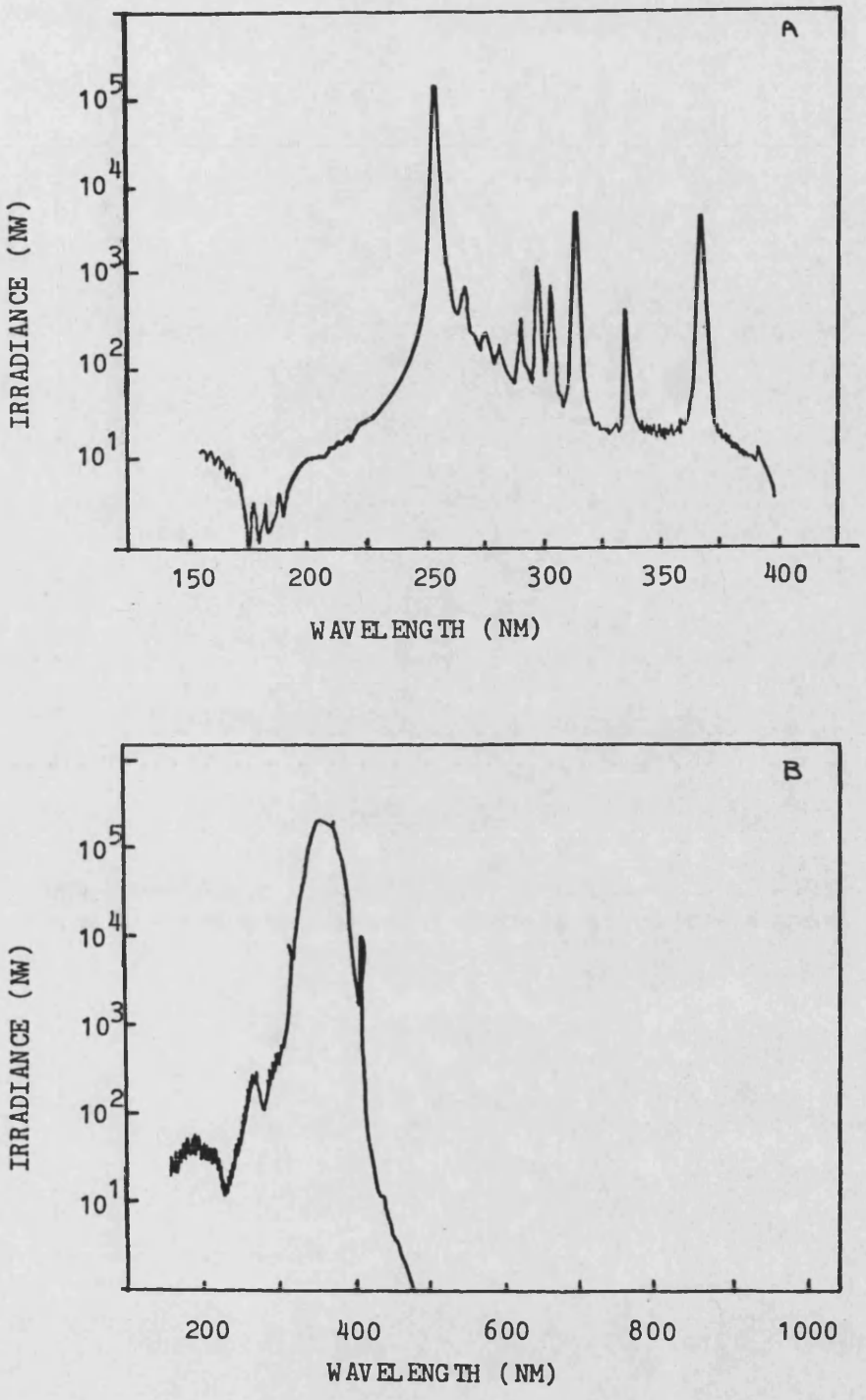

Figure 14. Emission spectra for (A) short wave G15T8 (15W)
(B) long wave F15T8 (15W) lamps.
(Instrumentation uncalibrated for wavelengths less than 200 nm or greater than 900nm).

irradiation two G15T8 (15W, Coast Wave, Ultraviolet Products) lamps were used. The emission spectra for both lamps as obtained from the manufacturers are shown in Fig. 14.

Plates were irradiated either at a distance of 8 cm from the lamps (near-UV) through their lids or at a distance of 16 cm from the lamps without lids (far-UV).

The fluence rate obtained by chemical actinometry assuming that 365 nm and 254 nm were mostly delivered was 30 $Jm^{-2}s^{-1}$ for broad-band near-UV irradiation and 18 $Jm^{-2}s^{-1}$ for far-UV irradiation. However, these fluences are only approximations, due to the assumptions made, and in the experimental section both membrane damage and lethality resulting from broad-band irradiations will be expressed relative to the duration of irradiation rather than the fluence received.

2.1.3 Gamma-Radiation Source

For routine preparation of feeder layers prior to experiments and for one set of survival experiments, a ^{137}Cs source (Gravatom Industries Ltd, England) of about 2000 Ci was used. This isotope has a physical half-life of 30 years and emits gamma rays of about 0.662 MeV. A schematic diagram of this source is shown in Fig. 15.

The irradiation unit had a vertical radiation beam with exposure chamber built from locking lead bricks. A lead door with a safety lock provided access to the chamber. The ^{137}Cs source was mounted such that it could be drawn horizontally into the exposure position by means of an electric drive. Exposure times could be controlled automatically using the preset time counter, or manually by using the 'exposure-return' buttons on the control panel.

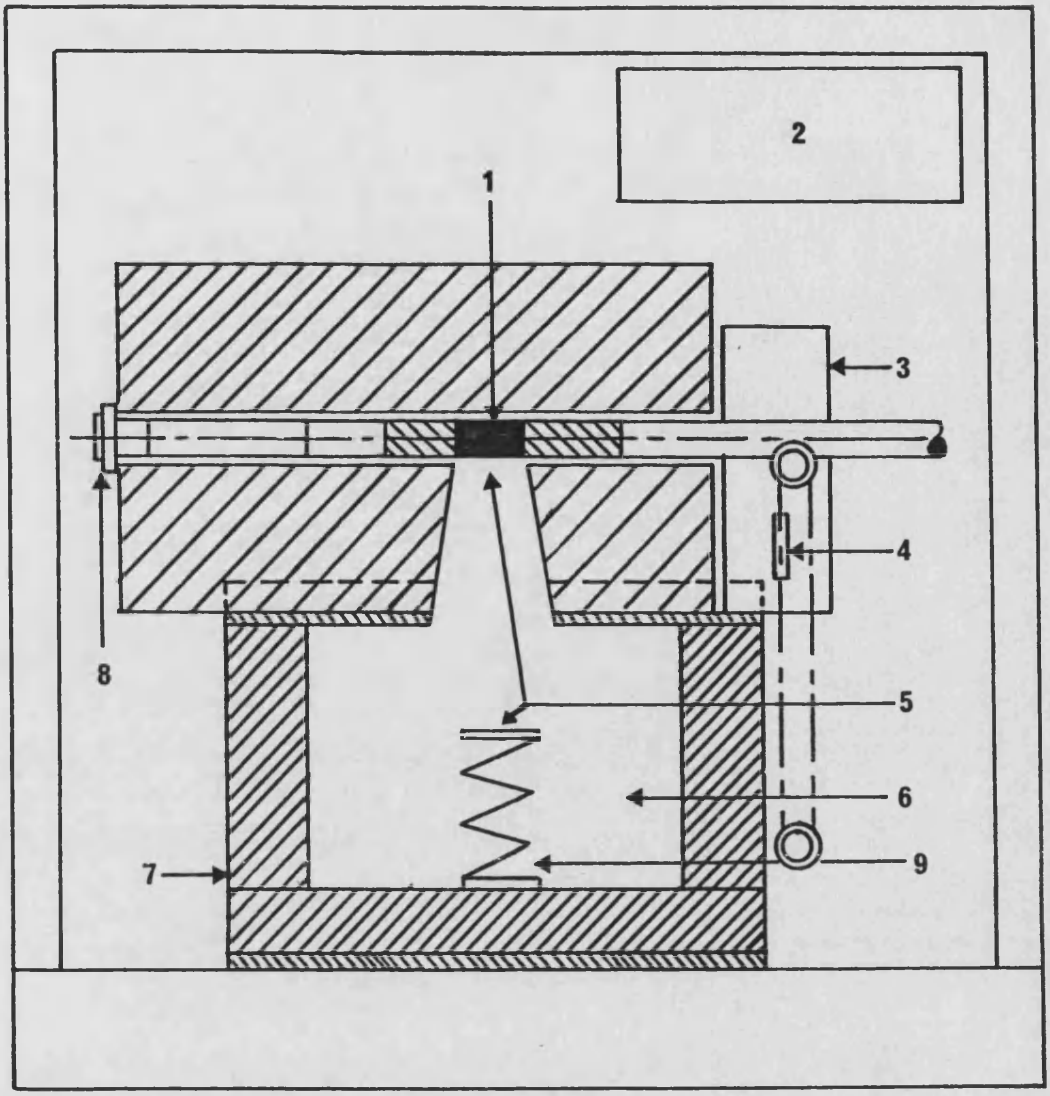

Figure 15. Vertical section of Gravatom ^{137}Cs source

1. ^{137}Cs source
2. Control panel
3. Drive unit
4. Failsafe weight
5. Position of irradiation vessel (see Fig. 16)
6. Irradiation chamber
7. Lead shield
8. Source lock
9. Lab jack

The irradiation vessel used for assessment of cell survival (shown in Fig. 16) consisted of a pyrex glass vessel of diameter 50 mm and depth 35 mm, fitted with a glass tubing for sampling. It was mounted on top of a metal cylinder at a distance of 23 cm from the bottom of the source. For the preparation of feeder layers, cells were irradiated in 125 ml Flow bottles mounted on top of the metal cylinder and elevated to the nearest point of the source by means of a lab jack as shown in Fig. 15.

Dosimetry

The ^{137}Cs dose rate was measured using the Fricke dosimetry system (see Appendix 3). In this method, the oxidation of ferrous ions to ferric ions in the presence of oxygen, determined by direct spectrophotometry of the dosimeter solution, provides a direct measure of the energy absorbed due to ionizing radiation.

At the position where irradiations in the vessel were carried out, the gamma dose rate was calculated as 103 rads min^{-1}, whereas at the nearest point to the source, the dose rate was calculated as 500 rads min^{-1}; therefore a standard time of 10 minutes was always used for the irradiation of cell suspensions to be used as a feeder layer.

2.2 Irradiation Procedures

2.2.1 Procedure for UV Irradiation of Cells in Suspension

The radiation sources were always allowed time to 'warm up', in the case of the penray lamp for 20 minutes and in the case of the super pressure mercury vapour lamp for at least 30-60 minutes. The irradiation cuvette was then positioned on the optical bench at a height and distance from the source such that the front face of the cuvette was within the field of illumination. The thermopile was

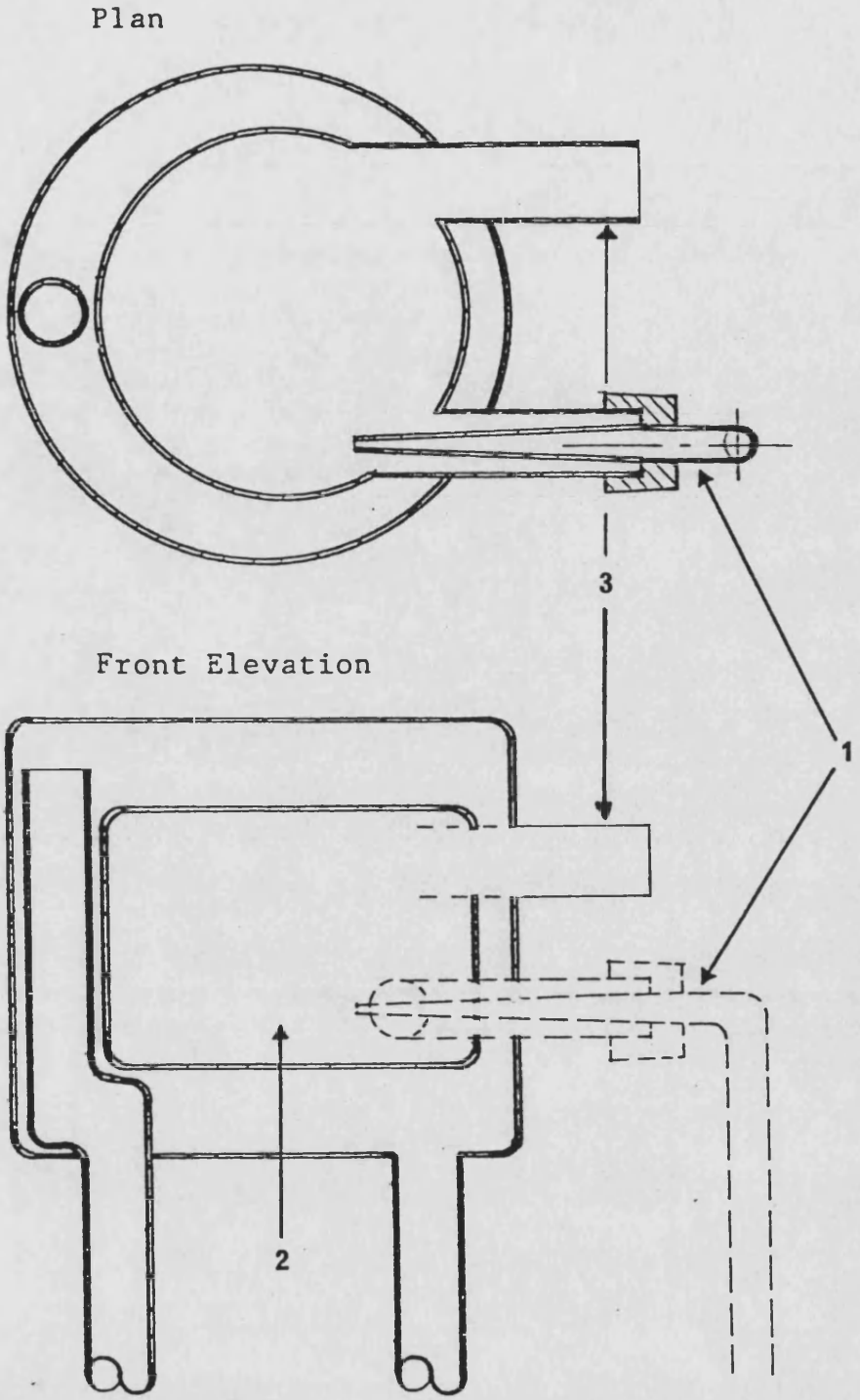

Figure 16. Diagram of irradiation vessel

1. Gassing tube
2. Position of suspension for irradiation
3. Outlet for sampling

temporarily moved into the radiation beam and a number of microvolt readings was taken to serve as a reference for the stability of the lamp throughout the experiment. With the irradiation cuvette moved into position again, chemical actinometry was performed on four different samples. The average of calculated fluences were used to calculate the incident fluence rate. After this determination, the cuvette was repeatedly rinsed with sterile distilled water, while sterile PBS was used for the last rinse. At this stage, determination of the temperature inside the cuvette was made and any adjustments, if needed, on the temperature of the water bath or the rate of circulation through the jacketed cuvette made. The stirring paddle was then moved into position and switched on. Sterilization of the cuvette was achieved by exposure to the 254 nm output of a penray lamp, mounted a few centimeters in front of the cuvette, for 20 minutes.

At the end of this period a 3 ml volume of the cell suspension was transferred to the sterile irradiation cuvette and allowed 5 minutes to equilibrate at the correct temperature. The cell suspension was then exposed to graded fluences of UV radiation and a sample removed from the cuvette both as a control and after each fluence for assessment of viability.

Correction of Fluence Due to Cell Concentration

In experimental work involving the irradiation of cells in suspension with UV radiation of wavelengths below 380 nm, part of the radiation becomes absorbed or scattered by the cells which results in cells near the rear surface of the cuvette receiving a smaller UV fluence than those at the front. Rapid stirring of the cells eliminates this non-uniformity but overall, the dose received by the cells is less than the one calculated by dosimetry.

Therefore, the fluence reduction resulting from 10^5 cells/ml, which was the concentration at which cells were irradiated in these studies was determined and a fluence correction applied.

The correction was based on an accurate determination of the optical densities of different cell concentrations (Morowitz, 1950). This corrects for the simple absorption of a photon by a cell, the passage of a photon through the cell suspension without encountering a cell (sieve effect) and the screening of cells at the rear of the sample by other cells (shielding effect). Normally determination of the optical density of the cell suspension is made using a spectrophotometer, but as Jagger et al.,(1975) pointed out, if the light is scattered appreciably by the sample, then a photon which has traversed most or all of the sample may be scattered sufficiently to miss the detector, due to the large sample-detector distance. This was shown experimentally by Keyse (1983). Therefore, determination of the optical density was made utilizing the Oriel 7201 thermopile positioned directly against the back of the cuvette, which reduced the sample-detector distance to about 3 mm. Using this arrangement, the optical densities of cell concentrations between 5 x 10^4 and 10^6 cells/ml were determined, using PBS alone as a blank, for the 3 different wavelengths used for cell irradiation (see Table A3 and Fig. A3 in Appendix 4). The reduction in transmission relative to the blank , could be related to a correction factor, by using the linear portion of the curve in Fig. A4 in which the data of Morowitz (1950) for rapidly stirred cells is depicted. The correction factors obtained at 254 nm, 313 nm and 365 nm were 0.945, 0.983, and 0.989, respectively. A larger reduction in transmission due to a larger cell absorption is observed at 254 nm since the nucleic acids and proteins in the cells

absorb the incident radiation more effectively. The correction factors obtained were used to calculate the appropriate time exposures to give the fluences required at a particular wavelength before each experiment.

2.2.2 Procedure for UV Irradiation of Cells Attached on Plates

Plates containing the appropriate number of cells which had been allowed to attach for 48 hours prior to irradiation were removed from the incubator. Their medium was collected and the plates washed twice with 5 ml sterile PBS. Then 10 ml of PBS was added and irradiation was carried out with the appropriate fluences. At the end of each irradiation, the PBS was replaced by 10 ml of 'conditioned' medium, i.e., the medium in which the cells were grown. Plates were gassed and returned in their boxes to the incubator at $37^{o}C$ where they were allowed 2-3 weeks for colony formation.

2.2.3 Procedure for Gamma Irradiation of Cells in Suspension

A 10 ml volume of a 10^{5} cells ml^{-1} concentration was pipetted into the sterile irradiation vessel. Oxygen, filtered through a series of cotton plugs was blown over the suspension in order to ensure mixing of the suspension throughout the experiment so that the cells received the same dose and provide fully oxygenated conditions which might affect sensitivity. As the experiments lasted only 8 minutes at the most, additional means of keeping the cells in suspension were not considered necessary. The suspension was exposed to graded doses of gamma rays and after each exposure time a sample was removed for the assessment of viability. These samples were transferred, covered in aluminium foil, to the laminar

flow cabinet where dilutions and plating were carried out in the normal way.

All manipulative procedures were carried out at room temperature under red light from Atlas fluorescent tubes.

3. TREATMENT OF DATA

The survival of irradiated human fibroblasts was expressed graphically by plotting the surviving fraction (N/N_0), on a logarithmic scale, against the amount of radiation received expressed as the fluence.

In most cases, the survival curves obtained consisted of an initial shoulder followed by an exponential portion and could be described by the expression

$$N/N_0 = ne^{-kD}$$

where N/N_0 is the surviving fraction

D is the UV fluence

k is a measure of the slope of the linear portion of the survivor curve

n is a measure of the extrapolation of the curve with the y-axis

Visual inspection of the curves showed that the basic shape, i.e. the width and extent of the shoulder varied with experimental conditions such as the wavelength of irradiation, the temperature during irradiation or the presence of other agents before, during or after irradiation. For each group of experiments, all the data points were plotted together and the width of the shoulder was estimated by eye, a subjective procedure. The remaining data points

were subjected to least squares linear regression analysis, each individual experiment being analysed separately.

In the tables constructed, each survival curve is represented by its slope and y-axis intercept with their associated errors. From these, three parameters were calculated and used to describe each curve, D_0, D_q and D_{10}. The D_0 value is the fluence required to reduce survival to 37 per cent in the exponential portion of the curve and is equivalent to the inverse of the slope of the straight-line portion of the curve multiplied by 2.303. The D_q value, determined by extrapolating the linear portion of the curve to 100 per cent survival is a measure of the width of the shoulder. The D_{10} value, the fluence required to reduce survival to 10 per cent, is a useful parameter since it reflects both the size of the shoulder and the slope of the exponential decline. These parameters were chosen so as to facilitate comparison with most published work. The statistical analyses applied to the survival parameters obtained are given in Appendix 5 and the surviving fractions for the experiments in the text are listed by experiment number in Appendix 8.

RESULTS AND DISCUSSION

PART 1

THE EFFECT OF THE IRRADIATION TEMPERATURE ON THE SENSITIVITY OF THE NORMAL SKIN FIBROBLAST STRAIN GM730 TO SPECIFIC MONOCHROMATIC WAVELENGTHS

A major concern throughout these studies, which are principally directed towards investigating the response of human fibroblasts to near-UV inactivating fluences, has been to identify and control factors which modify this response. The influence of any such factors was compared with the corresponding effect at shorter wavelengths, in particular 254 nm, since more is known about the mechanisms of inactivation by this wavelength.

A review of the literature concerning the UV sensitivity of human cells reveals that the temperature during the irradiation period has not always been strictly controlled, especially in studies where irradiation of attached cells was carried out. With the experimental facilities available for this study, irradiation of the cell suspension in a jacketed cuvette allowed control of the temperature to $\pm$ 0.5^{o}C. In the past, irradiations were routinely carried out at 0^{o}C to avoid concomitant repair during the irradiation period. However, this deviates from the *in vivo* situation where the cell would respond to UV damage while being at a temperature close to 37^{o}C. With this concern, and following the initial observation of Keyse (1983) that the survival response of 1BR fibroblasts to 365 nm at 25^{o}C shows increased resistance to inactivation, the effect of temperature during the irradiation of the normal GM730 cell line was studied.

The Effect of the Irradiation Temperature on the Near-UV (365 nm) Sensitivity of GM730 Cells

The response of GM730 cells following 365 nm irradiation at 0°C, 25°C and 37°C is shown in Figures 17, 18 and 19, respectively, where the data for all the individual experiments are presented. The survival parameters which describe the individual experiments at each temperature are listed in Table 2 while the data for these experiments and all experiments referred to in this work, are included in Appendix 8.

The results of seven experiments, covering a three year period, which show the inactivation of GM730 cells by 365 nm radiation at 0°C, are shown in Fig. 17. The survivor curves are characterized by an initial shoulder, followed by an exponential portion through two log cycles of inactivation. Throughout the experimental period, no effect of serum batch on the survival characteristics of GM730 was detected, although there was a difference in the plating efficiency of the cell line which ranged from 8 per cent to 33 per cent. Similarly, no effect of the cell passage number which was always between 10 and 20 could be seen.

Figure 18 shows the response of the same cell line under similar growth and irradiation conditions (stirring, fluence rates) but at the temperature of 25°C. It can be noted that there was a decrease of the shoulder region relative to the result obtained at 0°C and a significant decrease in the rate of inactivation. The wider range of response obtained may reflect a very delicate balance of cellular activities at this temperature, as will be discussed later.

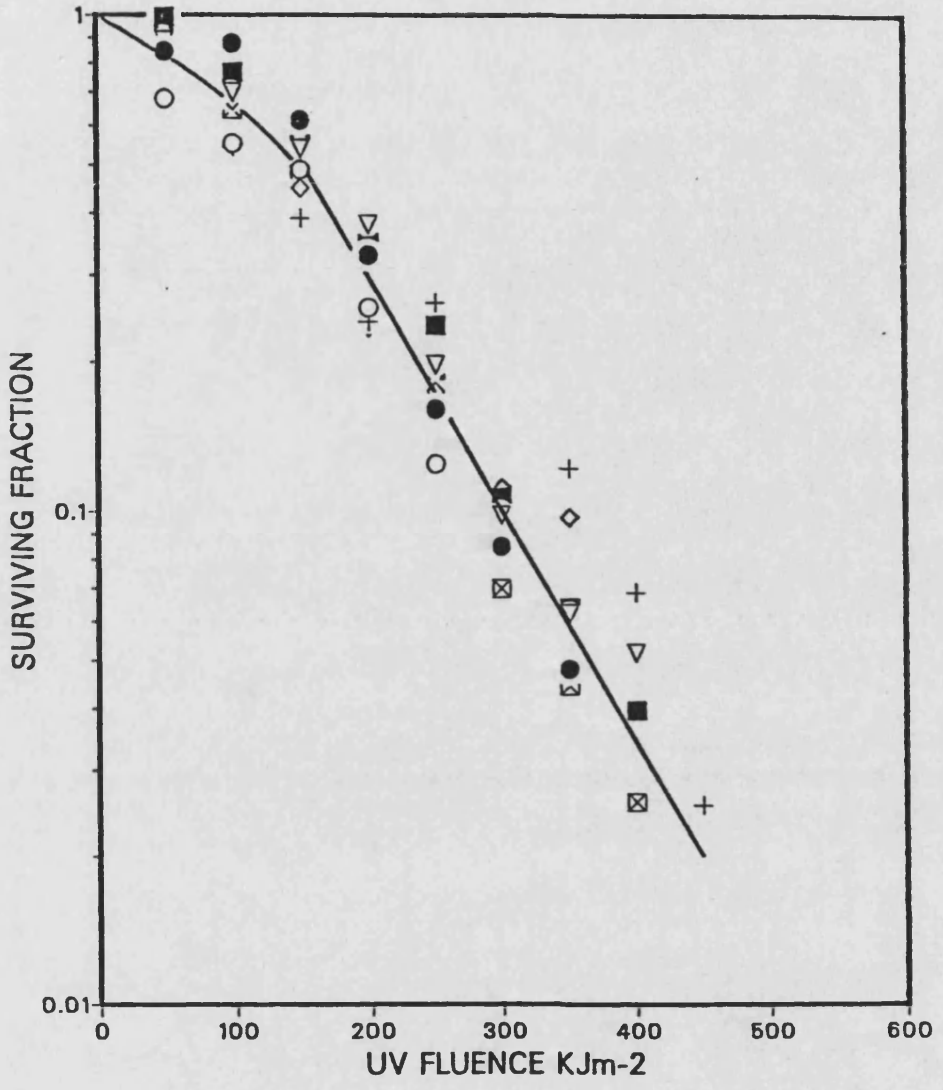

Figure 17. The inactivation of GM730 normal skin fibroblasts by 365nm, irradiated at 0°C. The different sets of symbols represent the results of replicate experiments.

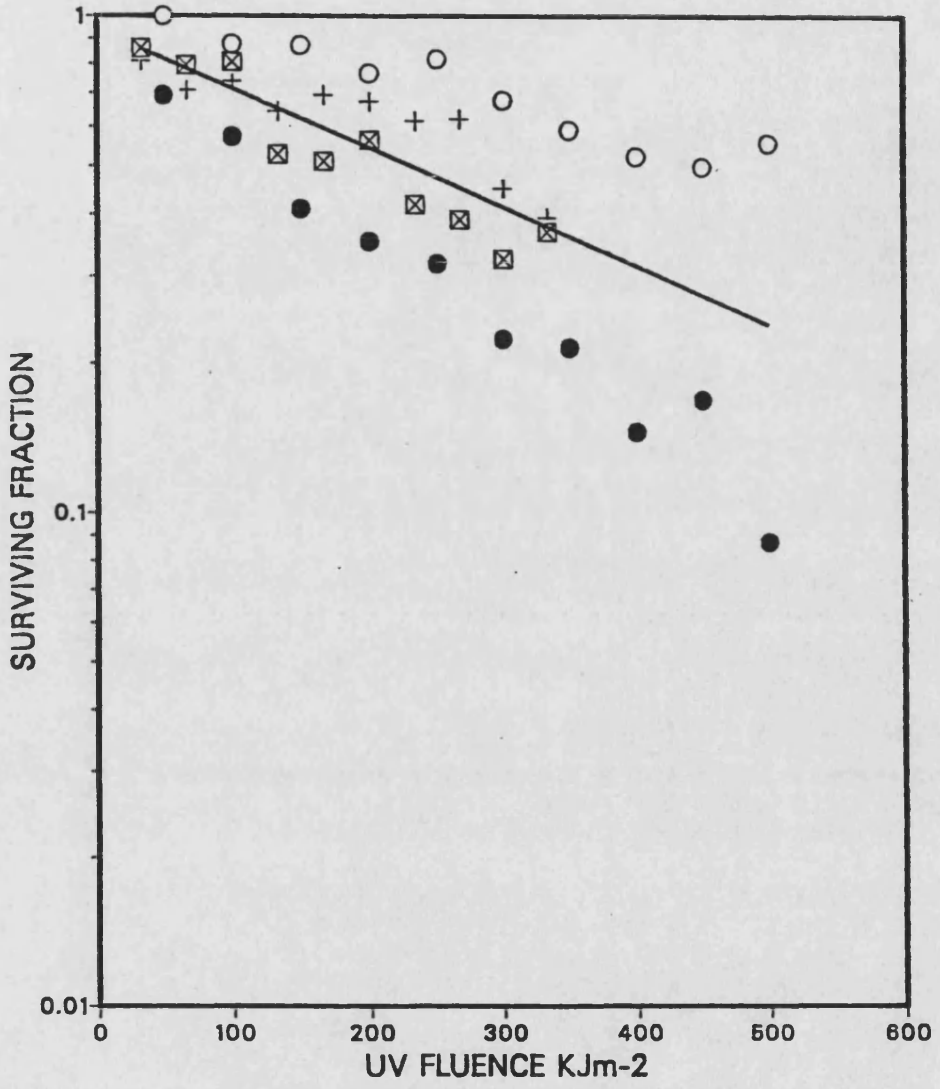

Figure 18. The inactivation of GM730 normal skin fibroblasts by 365nm, irradiated at 25°C. The different sets of symbols represent the results of replicate experiments.

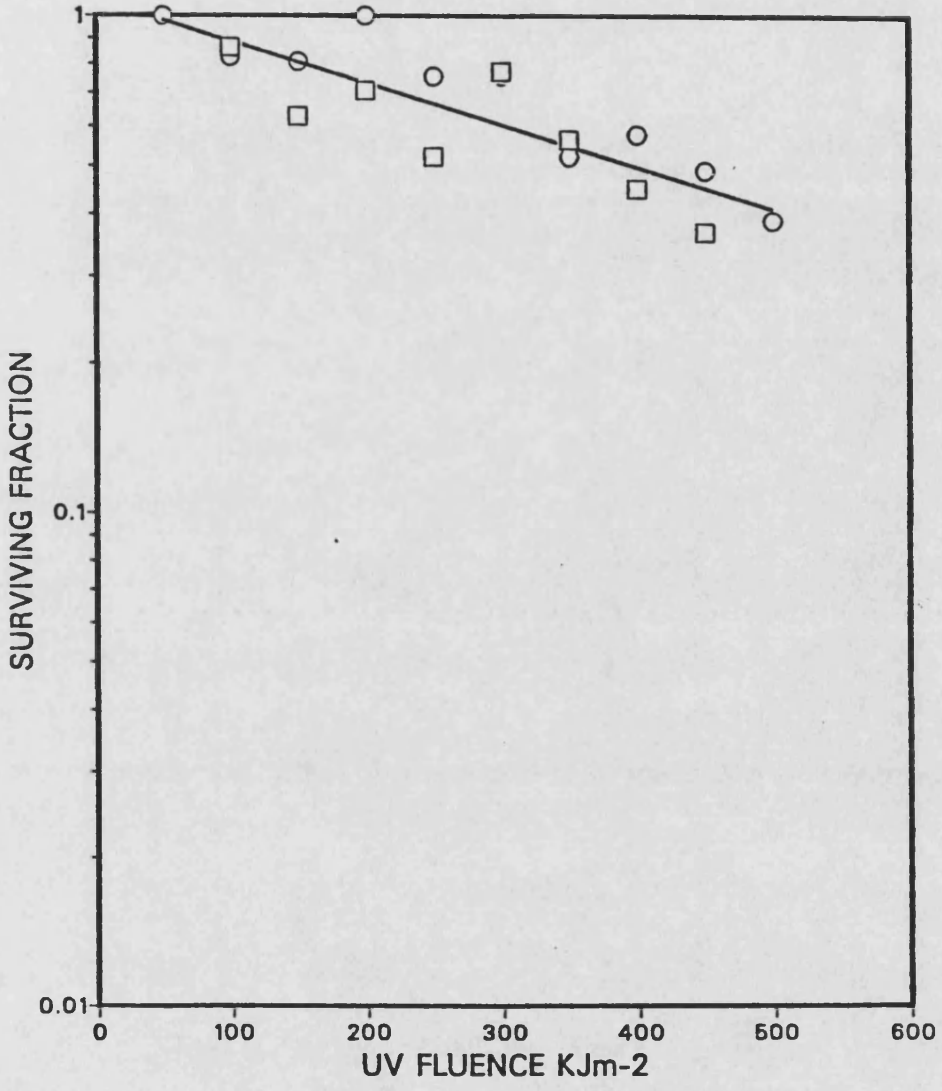

Figure 19. The inactivation of GM730 normal skin fibroblasts by 365nm, irradiated at 37°C. The different sets of symbols represent the results of replicate experiments.

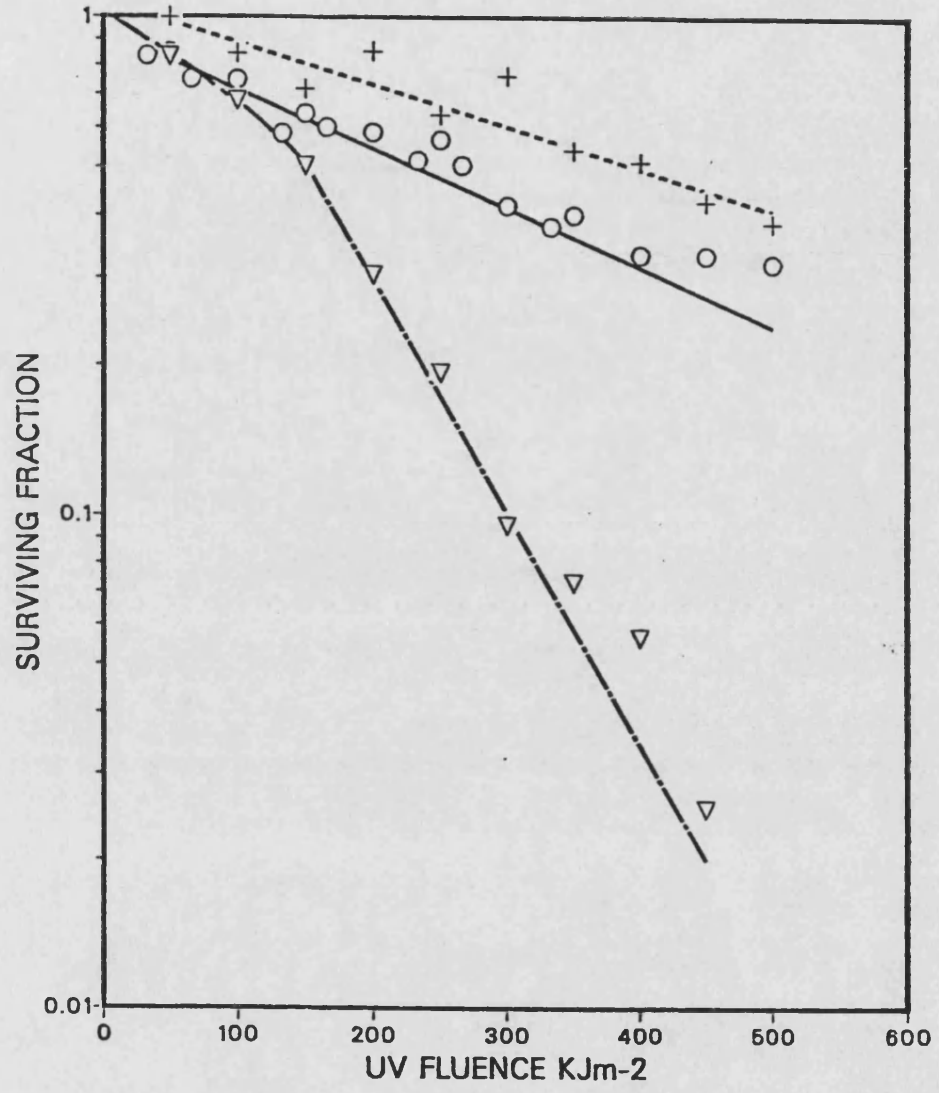

Figure 20. The comparative response of GM730 cells to 365nm irradiation at 0°C (▽ , —·—), 25°C (o , ———) and 37°C (+ , - - - - -).

TABLE 2

SURVIVAL PARAMETERS FOR THE INACTIVATION OF GM730 CELLS BY 365 NM IRRADIATED AT DIFFERENT TEMPERATURES

Temperature	Expt. No.	Slope $(Jm^{-2})^{-1}$	Standard Deviation	Intercept y-axis	Standard Deviation	$D0_2$ Jm^{-2}	Dq_2 Jm^{-2}	$D10$ Jm^{-2}
0°C	1	5.60×10^{-6}	1.19×10^{-7}	6.25×10^{-1}	3.19×10^{-2}	7.75×10^{4}	1.12×10^{5}	2.90×10^{5}
	2	5.93×10^{-6}	2.09×10^{-7}	5.86×10^{-1}	4.26×10^{-2}	7.32×10^{4}	9.88×10^{4}	2.67×10^{5}
	3	4.42×10^{-6}	3.46×10^{-7}	4.01×10^{-1}	1.05×10^{-1}	9.82×10^{4}	9.07×10^{4}	3.17×10^{5}
	4	4.77×10^{-6}	2.15×10^{-7}	4.97×10^{-1}	6.22×10^{-2}	9.10×10^{4}	1.04×10^{5}	3.14×10^{5}
	5	3.56×10^{-6}	5.33×10^{-7}	1.71×10^{-1}	1.69×10^{-1}	1.22×10^{5}	4.80×10^{4}	3.29×10^{5}
	6	5.35×10^{-6}	3.43×10^{-7}	5.35×10^{-1}	9.87×10^{-2}	8.12×10^{4}	1.00×10^{5}	2.87×10^{5}
	7	3.32×10^{-6}	4.09×10^{-7}	8.90×10^{-2}	1.06×10^{-1}	1.31×10^{5}	2.69×10^{4}	3.28×10^{5}
	Mean	$\mathbf{4.71\times10^{-6}}$		$\mathbf{4.15\times10^{-1}}$		$\mathbf{9.63\times10^{4}}$	$\mathbf{8.29\times10^{4}}$	$\mathbf{3.05\times10^{5}}$
25°C	8	1.80×10^{-6}	1.29×10^{-7}	-7.78×10^{-2}	3.99×10^{-2}	2.41×10^{5}	-4.33×10^{4}	5.12×10^{5}
	9	6.77×10^{-7}	7.52×10^{-8}	3.15×10^{-2}	2.32×10^{-2}	6.41×10^{5}	4.65×10^{4}	1.52×10^{6}
	10	1.43×10^{-6}	1.64×10^{-7}	-1.58×10^{-2}	3.30×10^{-2}	3.04×10^{5}	-1.11×10^{4}	6.88×10^{5}
	11	8.42×10^{-7}	1.62×10^{-7}	-5.21×10^{-2}	3.35×10^{-2}	5.16×10^{5}	-6.19×10^{4}	1.13×10^{6}
	Mean	$\mathbf{1.19\times10^{-6}}$		$\mathbf{-2.86\times10^{-2}}$		$\mathbf{4.26\times10^{5}}$	$\mathbf{-1.75\times10^{4}}$	$\mathbf{9.63\times10^{5}}$
37°C	12	8.21×10^{-7}	2.41×10^{-7}	-4.43×10^{-3}	7.17×10^{-2}	5.29×10^{5}	-5.40×10^{3}	1.21×10^{6}
	13	8.45×10^{-7}	1.49×10^{-7}	6.95×10^{-2}	4.61×10^{-2}	5.14×10^{5}	8.23×10^{4}	1.27×10^{6}
	Mean	$\mathbf{8.33\times10^{-7}}$		$\mathbf{3.25\times10^{-2}}$		$\mathbf{5.21\times10^{5}}$	$\mathbf{3.85\times10^{4}}$	$\mathbf{1.24\times10^{6}}$

Data in Appendix 8 (Tables A6, A7, A8)

The inactivation of GM730 cells by 365 nm radiation at 37°C is shown in Fig. 19. An absence of shoulder and a further decrease in the inactivation rate can be noted.

In Fig. 20, the comparison of the inactivation curves obtained at each temperature is shown. The points on the graph represent the mean values obtained at each fluence for a particular set of experiments and the parameters of the lines are calculated as the mean of the individually regressed experiments. This is the procedure which will be usually followed throughout this work for presenting the data. Comparison of the survivor curves at the three temperatures reveals a difference in the shape of the curves since the value of the shoulder present at 0°C ($D_q 0^\circ = 82.9 kJm^{-2}$) diminished at the higher temperatures of 25° and 37°C ($D_q 25^\circ = <1$, $D_q 37^\circ = 38.5\ kJm^{-2}$). In parallel, there was a marked increase in the resistance of the cells to inactivation as the irradiation temperature was increased. This is reflected by the D_0 values which are 96, 426 and 521 kJm^{-2} at 0°, 25° and 37°, respectively. These values represent approximate 4-fold and 5-fold increases of cellular resistance to 365 nm inactivation at 25° and 37°C, compared to 0°C, which are statistically significant (x^2 of 471.32 and 495.17 respectively, $p < 0.001$).

The Effect of the Irradiation Temperature on the Far-UV (254 nm) Sensitivity of GM730 Cells

Having observed a significant increase in the resistance of GM730 cells to 365 nm irradiation as the irradiation temperature was increased, the response to 254 nm irradiation was examined in a similar manner.

The inactivation curves obtained at the three different temperatures of 0°, 25° and $37^{\circ}C$ are shown in Figures 21, 22, 23 and the parameters describing the individual experiments are included in Table 3. Fig. 24 is the comparison of the mean response obtained at each temperature, each response being represented by the mean survival points at each fluence and by the mean line calculated from the individually regressed slopes.

When irradiation was carried out at $0^{\circ}C$, the response was characterized by an initial shoulder, followed by exponential inactivation with values of D_q=14.7 Jm^{-2} and D_0=17.7 Jm^{-2}, respectively. When the irradiation temperature was increased to 25° and $37^{\circ}C$ the following changes in the survival response could be observed: At $25^{\circ}C$ there was a small increase in the rate of inactivation as seen by comparison of the D_0 values of 17.7 Jm^{-2} at $0^{\circ}C$ and 14.9 Jm^{-2} at $25^{\circ}C$. This difference was not observed at $37^{\circ}C$ (D_0=18.4 Jm^{-2}), but at this temperature there was a decrease in the extent of the shoulder as seen by comparison of the D_q values of 14.7 Jm^{-2} at $0^{\circ}C$ and 4.51 Jm^{-2} at $37^{\circ}C$. These differences are small but show that in contrast to the result at 365 nm, there was no increase in the resistance of the cells with increase in irradiation temperature. On the contrary, there was a small but significant decrease in the resistance of the cells as the irradiation temperature was increased, observed either as an increased rate of inactivation (at $25^{\circ}C$) or as a decreased shoulder (at $37^{\circ}C$) relative to the response at $0^{\circ}C$. Both these differences were found to be statistically significant at the 5% probability level with an $x^2(1)$ equal to 5.73 and 16.56, respectively.

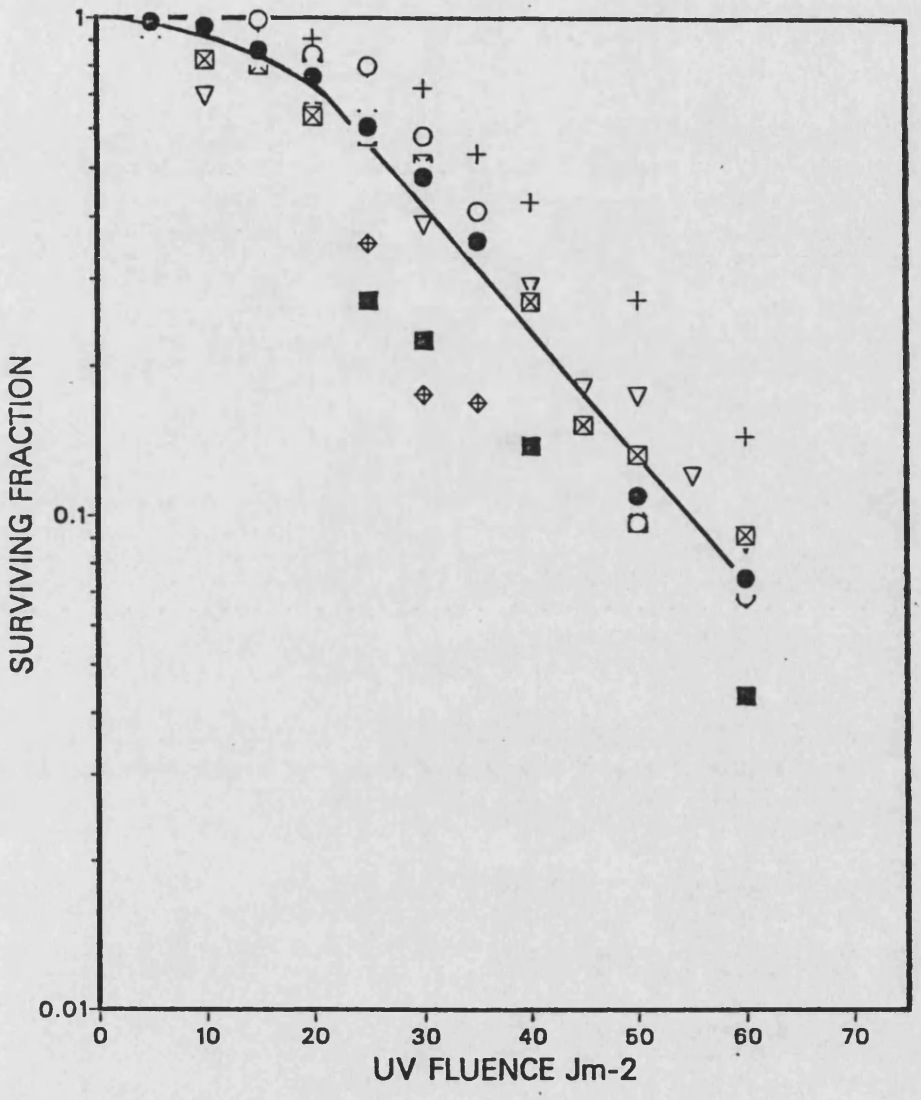

Figure 21. The inactivation of GM730 normal skin fibroblasts by 254nm, irradiated at 0 °C. The different sets of symbols represent the results of replicate experiments.

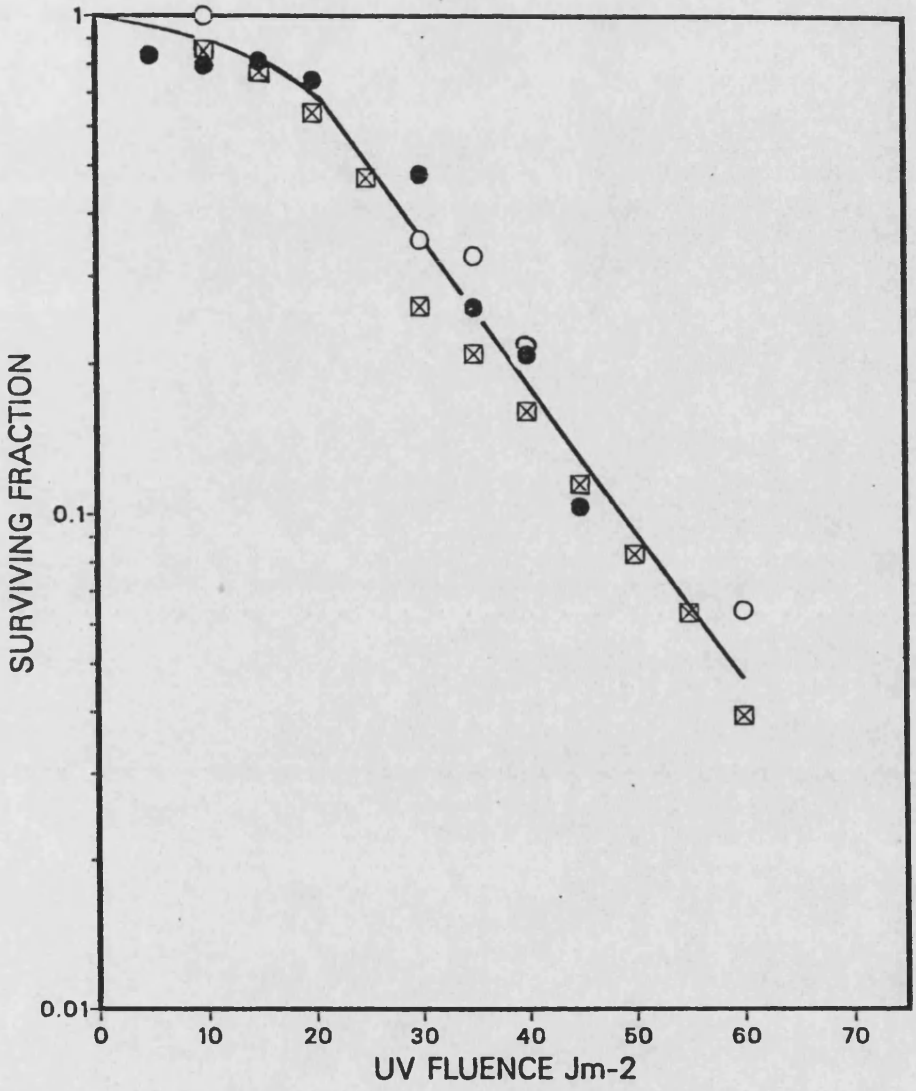

Figure 22. The inactivation of GM730 normal skin fibroblasts by 254nm, irradiated at 25°C. The different sets of symbols represent the results of replicate experiments.

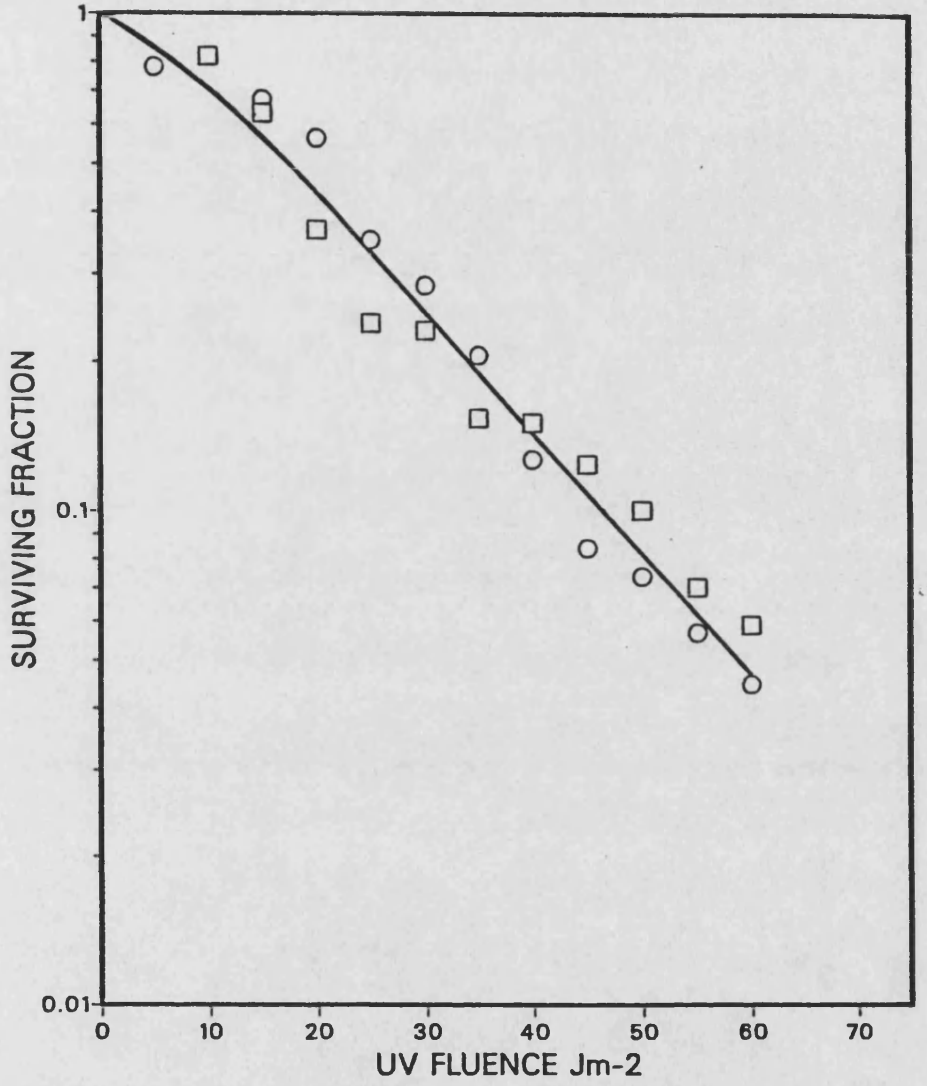

Figure 23. The inactivation of GM730 normal skin fibroblasts by 254nm, irradiated at 37°C. The different sets of symbols represent the results of replicate experiments.

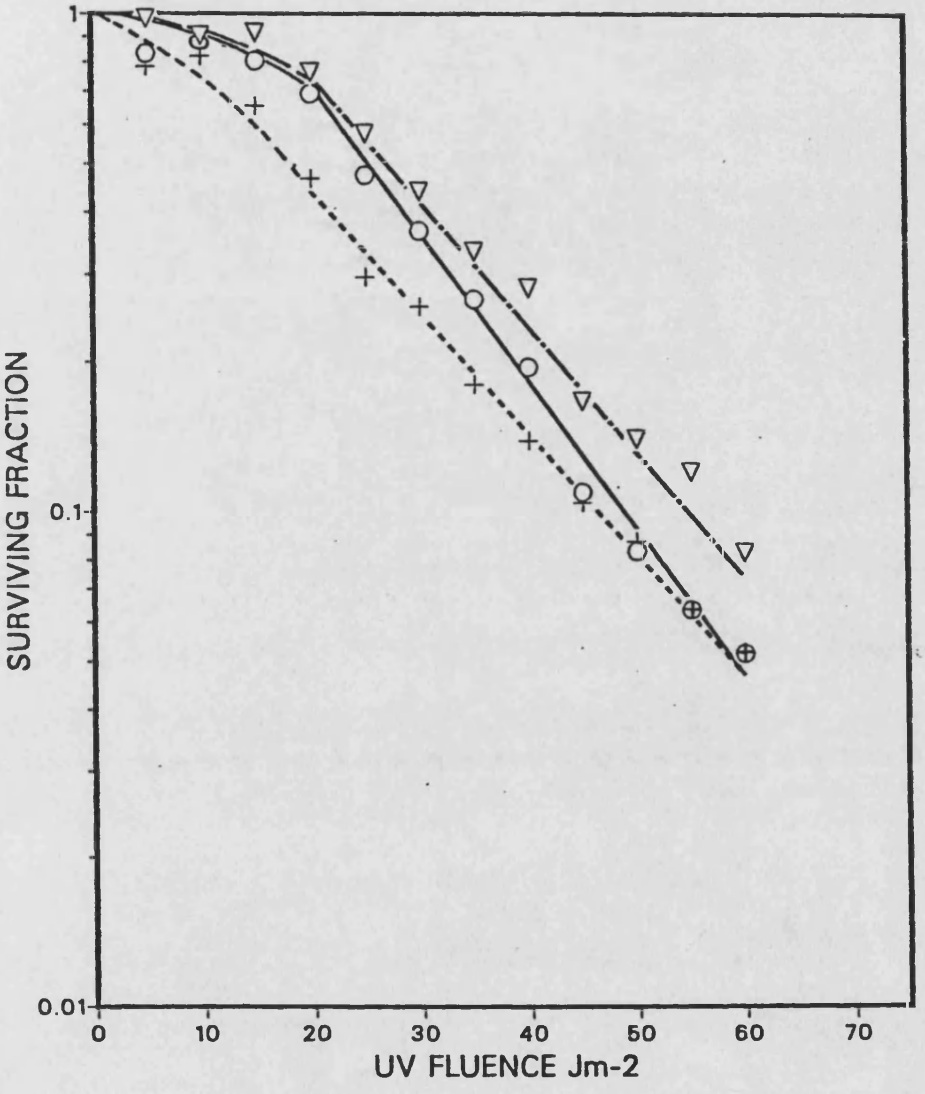

Figure 24. The comparative response of GM730 cells to 254nm irradiation at 0°C (▽ , ——--), 25°C (o , ———) and 37°C (+ , -----).

TABLE 3

SURVIVAL PARAMETERS FOR THE INACTIVATION OF GM730 CELLS BY 254 NM

IRRADIATED AT DIFFERENT TEMPERATURES

Temperature	Expt. No.	Slope $(Jm^{-2})^{-1}$	Standard Deviation	Intercept y-axis	Standard Deviation	$D0_2$ Jm^{-2}	Dq_2 Jm^{-2}	$D10$ Jm^{-2}
0°C	14	2.75×10^{-2}	1.77×10^{-3}	4.87×10^{-1}	7.41×10^{-2}	1.58×10^{1}	1.77×10^{1}	5.41×10^{1}
	15	3.25×10^{-2}	2.64×10^{-3}	7.20×10^{-1}	1.11×10^{-1}	1.34×10^{1}	2.22×10^{1}	5.29×10^{1}
	16	2.04×10^{-2}	1.17×10^{-3}	4.23×10^{-1}	4.62×10^{-2}	2.13×10^{1}	2.07×10^{1}	6.98×10^{1}
	17	2.36×10^{-2}	1.92×10^{-3}	3.43×10^{-1}	7.73×10^{-2}	1.84×10^{1}	1.45×10^{0}	5.69×10^{1}
	18	2.26×10^{-2}	4.48×10^{-3}	1.16×10^{-1}	1.76×10^{-1}	1.92×10^{1}	5.13×10^{0}	4.94×10^{1}
	19	2.70×10^{-2}	3.56×10^{-3}	2.49×10^{-1}	1.40×10^{-1}	1.61×10^{1}	9.23×10^{0}	4.63×10^{1}
	20	2.18×10^{-2}	1.27×10^{-3}	2.85×10^{-1}	5.42×10^{-2}	1.99×10^{1}	1.31×10^{1}	5.89×10^{1}
	Mean	$\mathbf{2.51\times10^{-2}}$		$\mathbf{3.75\times10^{-1}}$		$\mathbf{1.77\times10^{1}}$	$\mathbf{1.47\times10^{1}}$	$\mathbf{5.55\times10^{1}}$
25°C	21	3.35×10^{-2}	4.33×10^{-3}	5.99×10^{-1}	1.52×10^{-1}	1.30×10^{1}	1.79×10^{1}	4.77×10^{1}
	22	2.59×10^{-2}	2.17×10^{-3}	3.72×10^{-1}	9.34×10^{-2}	1.68×10^{1}	1.44×10^{1}	5.30×10^{1}
	23	2.90×10^{-2}	9.82×10^{-4}	3.62×10^{-1}	4.13×10^{-2}	1.50×10^{1}	1.25×10^{1}	4.70×10^{1}
	Mean	$\mathbf{2.95\times10^{-2}}$		$\mathbf{4.44\times10^{-1}}$		$\mathbf{1.49\times10^{1}}$	$\mathbf{1.49\times10^{1}}$	$\mathbf{4.92\times10^{1}}$
37°C	24	2.06×10^{-2}	1.43×10^{-3}	-8.79×10^{-3}	5.75×10^{-2}	2.11×10^{1}	-4.27×10^{-1}	4.81×10^{1}
	25	2.78×10^{-2}	1.27×10^{-3}	2.63×10^{-1}	5.43×10^{-2}	1.56×10^{1}	9.45×10^{0}	4.54×10^{1}
	Mean	$\mathbf{2.42\times10^{-2}}$		$\mathbf{1.27\times10^{-1}}$		$\mathbf{1.84\times10^{1}}$	$\mathbf{4.51\times10^{0}}$	$\mathbf{4.68\times10^{1}}$

Data in Appendix 8 (Tables A9, A10)

The Effect of the Irradiation Temperature on the Mid-UV (313 nm) Sensitivity of GM730 Cells

Further investigations involved 313 nm irradiation of GM730 fibroblasts at 0°, 25° and $37^{\circ}C$. The inactivation curves obtained at the three different temperatures are shown in Figures 25, 26 and 27 while the parameters describing the individual experiments are included in Table 4. Fig. 28 depicts the comparative responses calculated from the individual experiments.

The responses obtained at the three different temperatures in response to 313 nm irradiation again followed the reverse pattern of that observed at 365 nm, in that the sensitivity of the cells was progressively increased as the irradiation temperature was increased. This is reflected clearly in the comparison of the parameters D_0, D_q and D_{10} in Table 4. The D_0 values, 14.2 kJm^{-2} and 14.4 kJm^{-2} at 0° and $25^{\circ}C$, respectively, decrease to 9.3 kJm^{-2} at 37° whereas the D_q value, shows the diminution of the shoulder at both 25° and $37^{\circ}C$ (D_q at 0°=14.2 kJm^{-2}, at 25°=4.2 kJm^{-2} and at $37^{\circ}C$=3.3 kJm^{-2}). The D_{10} values which reflect both the rate of inactivation and the extent of the shoulder show a clear drop from 46.9 to 37.4 to 24.7 kJm^{-2} at 0°, 25° and 37°, respectively.

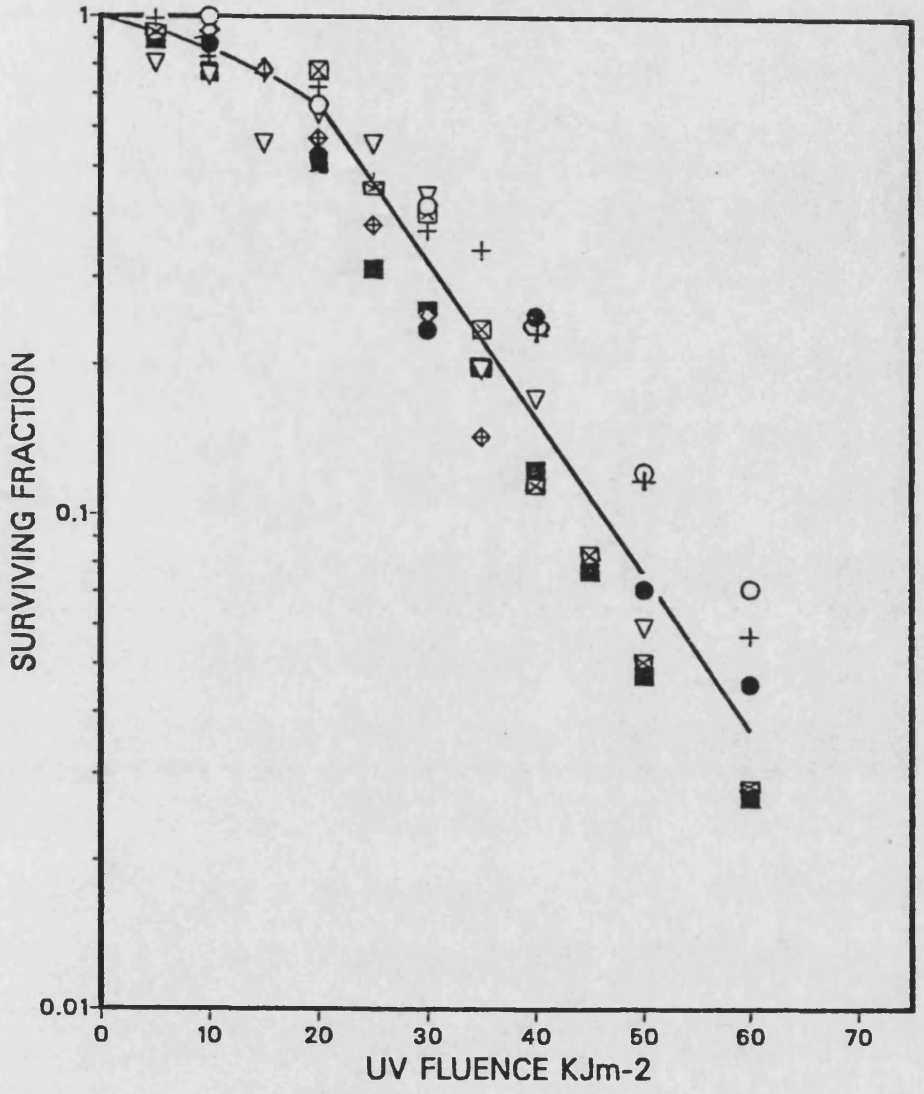

Figure 25. The inactivation of GM730 normal skin fibroblasts by 313nm, irradiated at 0°C. The different sets of symbols represent the results of replicate experiments.

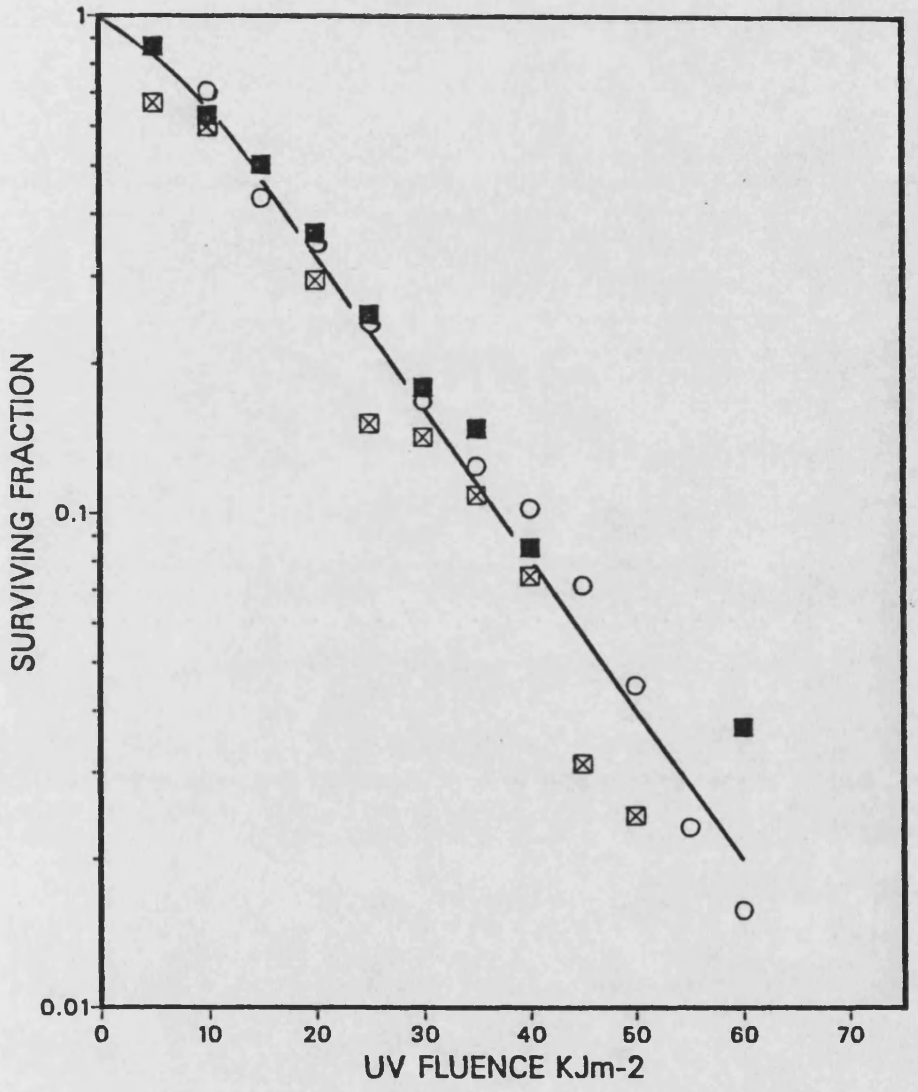

Figure 26. The inactivation of GM730 normal skin fibroblasts by 313nm, irradiated at 25°C. The different sets of symbols represent the results of replicate experiments.

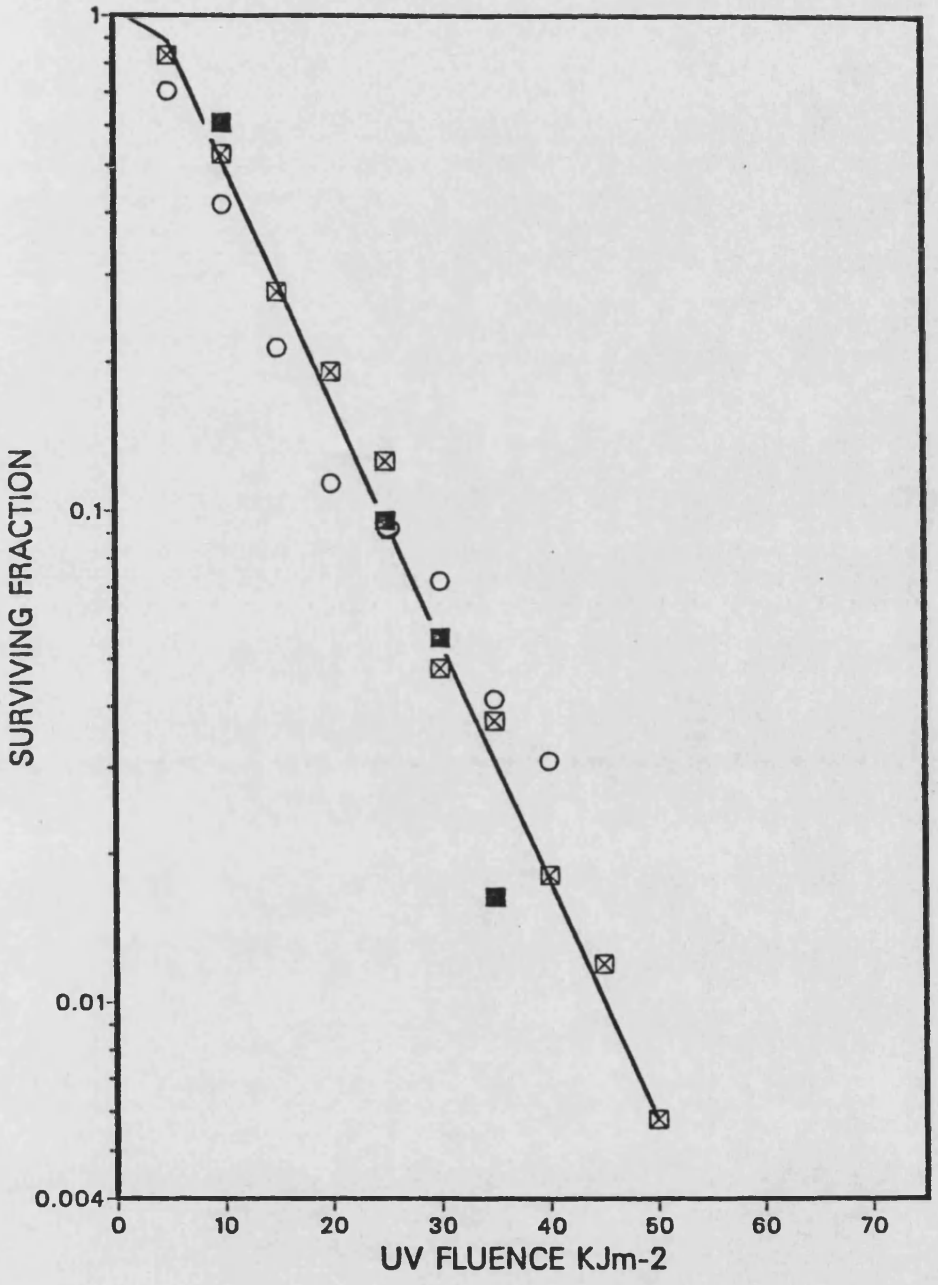

Figure 27. The inactivation of GM730 normal skin fibroblasts by 313nm, irradiated at 37°C .The different sets of symbols represent the results of replicate experiments.

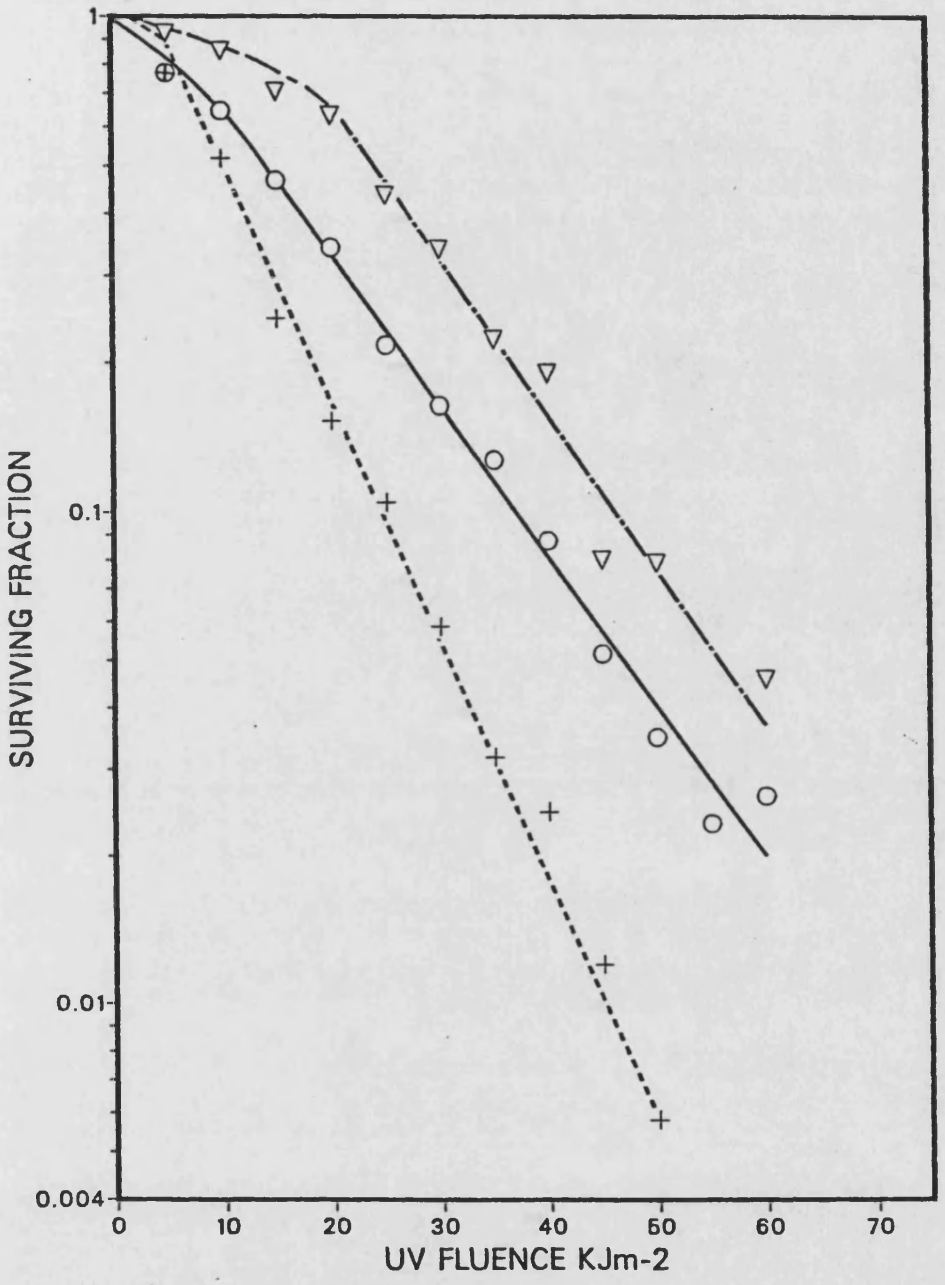

Figure 28. The comparative response of GM730 cells to 313nm irradiation at 0°C (▽ , ———), 25°C (○ , ———) and 37°C (+ , -----).

TABLE 4

SURVIVAL PARAMETERS FOR THE INACTIVATION OF GM730 CELLS BY 313 NM IRRADIATED AT DIFFERENT TEMPERATURES

Temperature	Expt. No.	Slope $(Jm^{-2})^{-1}$	Standard Deviation	Intercept y-axis	Standard Deviation	$D0_2$ Jm^{-2}	Dq_2 Jm^{-2}	$D10$ Jm^{-2}
0°C	26	2.64×10^{-5}	4.30×10^{-6}	2.59×10^{-1}	1.82×10^{-1}	1.64×10^{4}	9.78×10^{3}	4.77×10^{4}
	27	2.48×10^{-5}	8.67×10^{-6}	3.44×10^{-1}	3.63×10^{-2}	1.75×10^{4}	1.39×10^{4}	5.42×10^{4}
	28	3.57×10^{-5}	3.55×10^{-5}	6.05×10^{-1}	1.23×10^{-1}	1.22×10^{4}	1.70×10^{4}	4.50×10^{4}
	29	2.63×10^{-5}	1.55×10^{-5}	3.86×10^{-1}	6.08×10^{-2}	1.65×10^{4}	1.47×10^{4}	5.27×10^{4}
	30	3.99×10^{-5}	1.74×10^{-5}	5.88×10^{-1}	4.89×10^{-2}	1.09×10^{4}	1.48×10^{4}	3.98×10^{4}
	31	3.19×10^{-5}	1.33×10^{-6}	3.62×10^{-1}	5.42×10^{-2}	1.36×10^{4}	1.13×10^{4}	4.27×10^{4}
	32	3.57×10^{-5}	1.75×10^{-6}	6.48×10^{-1}	7.44×10^{-2}	1.22×10^{4}	1.82×10^{4}	4.62×10^{4}
	Mean	$\mathbf{3.15\times10^{-5}}$		$\mathbf{4.56\times10^{-1}}$		$\mathbf{1.42\times10^{4}}$	$\mathbf{1.42\times10^{4}}$	$\mathbf{4.69\times10^{4}}$
25°C	33	2.55×10^{-5}	1.51×10^{-6}	5.02×10^{-2}	5.26×10^{-2}	1.70×10^{4}	1.97×10^{3}	4.12×10^{4}
	34	3.17×10^{-5}	1.57×10^{-6}	1.90×10^{-1}	6.29×10^{-2}	1.37×10^{4}	5.99×10^{3}	3.75×10^{4}
	35	3.49×10^{-5}	3.60×10^{-6}	1.66×10^{-1}	1.29×10^{-1}	1.24×10^{4}	4.74×10^{3}	3.34×10^{4}
	Mean	$\mathbf{3.07\times10^{-5}}$		$\mathbf{1.35\times10^{-1}}$		$\mathbf{1.44\times10^{4}}$	$\mathbf{4.23\times10^{3}}$	$\mathbf{3.74\times10^{4}}$
37°C	36	5.97×10^{-5}	6.65×10^{-6}	4.25×10^{-1}	1.78×10^{-1}	7.27×10^{3}	7.12×10^{3}	2.39×10^{4}
	37	3.81×10^{-5}	2.47×10^{-6}	-4.42×10^{-2}	6.20×10^{-2}	1.14×10^{4}	-1.16×10^{3}	2.51×10^{4}
	38	4.77×10^{-5}	1.29×10^{-6}	1.94×10^{-1}	3.99×10^{-2}	9.10×10^{3}	4.07×10^{3}	2.50×10^{4}
	Mean	$\mathbf{4.85\times10^{-5}}$		$\mathbf{1.92\times10^{-1}}$		$\mathbf{9.26\times10^{3}}$	$\mathbf{3.34\times10^{3}}$	$\mathbf{2.47\times10^{4}}$

Data in Appendix 8 (Tables A11, A12)

The Effect of the Irradiation Temperature on the Sensitivity of GM730 Cells to 325 and 334 nm Radiation

The effect of the temperature during the irradiation period on two additional wavelengths was studied in order to determine whether the response of cells to wavelengths between 313 and 365 nm followed one or the other pattern. The inactivation curves at 0° and $25^{\circ}C$ following 325 and 334 nm irradiation are shown in Figs. 29A and B and the calculated parameters for the individual experiments are found in Table 5. It can be seen that the response to both wavelengths is similar in pattern to the response obtained using 365 nm since cells showed increased resistance at $25^{\circ}C$ relative to $0^{\circ}C$ by a factor of 4.7 at 325 and 6.7 at 334 when comparing the D_0 values.

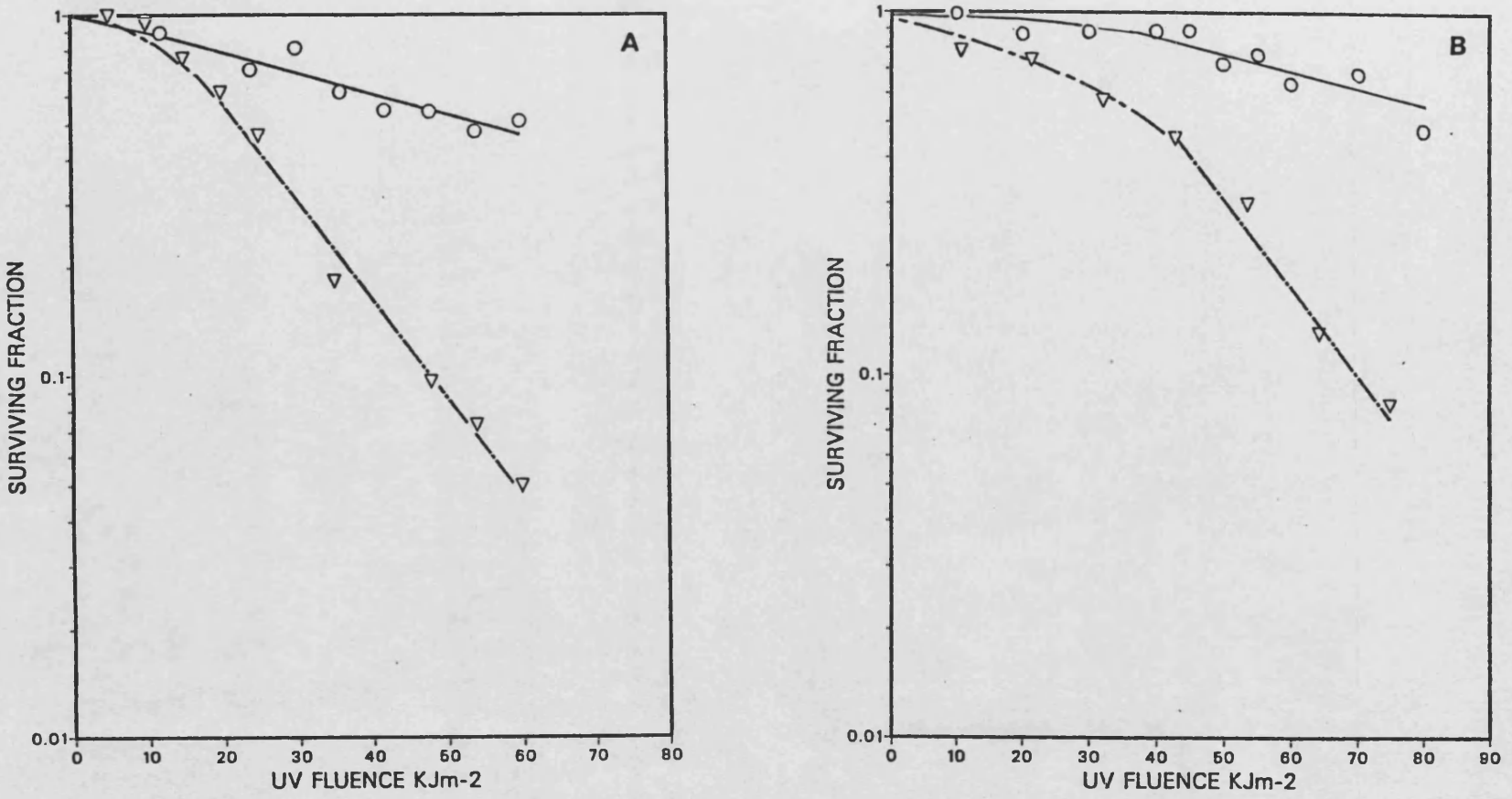

Figure 29. The comparative response of GM730 cells to (A) 325 nm irradiation (B) 334 nm irradiation at 0°C (▽ , —·—) and 25°C (○ , ——). Single experiment depicted in panel (A), mean experimental points and calculated mean lines of duplicate experiments depicted in panel (B).

TABLE 5

SURVIVAL PARAMETERS FOR THE INACTIVATION OF GM730 CELLS BY 325 NM AND 334 NM IRRADIATED AT DIFFERENT TEMPERATURES

Temperature	Expt. No.	Slope $(Jm^{-2})^{-1}$	Standard Deviation	Intercept y-axis	Standard Deviation	$D0_2$ Jm^{-2}	Dq_2 Jm^{-2}	$D10$ Jm^{-2}
325 nm								
0°C	39	2.72×10^{-5}	1.54×10^{-6}	3.07×10^{-1}	6.60×10^{-2}	1.60×10^{4}	1.13×10^{4}	4.81×10^{4}
25°C	40	5.75×10^{-6}	9.12×10^{-7}	1.55×10^{-2}	3.75×10^{-2}	7.55×10^{4}	2.70×10^{3}	1.77×10^{5}
334 nm								
0°C	41	2.20×10^{-5}	1.08×10^{-6}	6.35×10^{-1}	6.52×10^{-2}	1.97×10^{4}	2.88×10^{4}	7.43×10^{4}
	42	2.65×10^{-5}	3.27×10^{-6}	7.83×10^{-1}	2.03×10^{-2}	1.64×10^{4}	2.96×10^{4}	6.73×10^{4}
	Mean	$\mathbf{2.43\times10^{-5}}$		$\mathbf{7.09\times10^{-1}}$		$\mathbf{1.81\times10^{4}}$	$\mathbf{2.92\times10^{4}}$	$\mathbf{7.08\times10^{4}}$
25°C	43	5.87×10^{-6}	9.12×10^{-7}	1.89×10^{-1}	5.31×10^{-2}	7.40×10^{4}	3.22×10^{4}	2.03×10^{5}
	44	2.62×10^{-6}	2.85×10^{-6}	-2.14×10^{-2}	1.32×10^{-3}	1.66×10^{5}	-8.03×10^{3}	3.77×10^{5}
	Mean	$\mathbf{4.25\times10^{-6}}$		$\mathbf{8.38\times10^{-2}}$		$\mathbf{1.20\times10^{5}}$	$\mathbf{1.21\times10^{4}}$	$\mathbf{2.90\times10^{5}}$

Data in Appendix 8 (Tables A13, A14)

Discussion

Comparison of the above survival data at the five monochromatic wavelengths studied, with other published data, is only possible at 0°C. Table 6 includes published D_0, D_q and D_{10} values for normal human fibroblasts irradiated in suspension. It can be seen that if we exclude the results for 1MR-91 which are very different and perhaps specific to that strain (it is a lung fibroblast instead of a skin fibroblast), there is relatively good agreement with other results. Previous comparisons of GM730 cell response to short and long wavelength radiation with other normal human skin fibroblast strains 1BR and 48BR (Keyse et al.,1985) found no difference, so GM730 strain was considered as a typical normal strain. At 254 nm, comparison to Keyse et al. (1985) shows an apparent two-fold difference in the sensitivity of GM730 cells. Since there is better agreement between the corresponding results at 313 and 365 nm, the discrepancy could be attributed to the determination of the fluence rate, which was performed in a different manner. In the first study the fluence rate was calculated by thermopile measurement with allowance for the heat ommitted (Keyse et al., 1985) whereas in this study fluence determination was based on chemical actinometry readings which were repeated several times. Other published values of D_0 for human fibroblasts irradiated by 254 nm are between 2.5-9 Jm^{-2} (Smith and Paterson, 1982; Kraemer et al., 1976; Zamansky et al., 1985; Fujiwara and Tatsumi, 1976; Wells and Han, 1985) but refer to fibroblasts irradiated by broad-band far-UV sources while attached on plates (see Table 29). The increased sensitivity of attached cells is expected since cells are flattened and the distance of the cell surface to the nucleus

and to the centre of the nucleus is much smaller. As an example, measurements for African green monkey kidney cells (CV-1) as obtained by Coohill et al. (1979) are shown below:

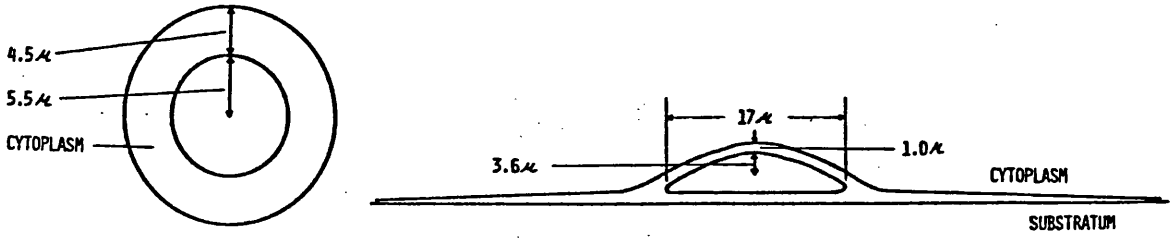

spherical cell attached cell

In Table 6 it can also be seen that amongst the three fibroblast strains used in this establishment, each strain has its inherent sensitivity. 1BR cells are more sensitive than GM730 which in turn are more sensitive than 48BR in response to any wavelength used. This makes comparisons between different normal cells from different laboratories very difficult even before starting to consider other important factors such as purity of wavelength, fluence rate, growth conditions and irradiation conditions which may differ.

The effect of the temperature during irradiation was studied in detail and results showed that, following 254 and 313 nm irradiation, cells exhibited a decreased resistance when irradiated at higher temperature, whereas following 325, 334 and 365 nm irradiation, the opposite effect was observed.

The interpretation of these results in relation to the actions of UV radiation on human cells can only be speculative since the mechanisms of inactivation, especially at the longer wavelengths, remain unclear.

TABLE 6

SURVIVAL PARAMETERS OBTAINED FOR HUMAN FIBROBLASTS IRRADIATED IN SUSPENSION AT 0°C

Wavelength	Cell Line	D_0 Jm^{-2}	D_q Jm^{-2}	D_{10} Jm^{-2}
254 nm	GM730[a]	17.7± 0.3	14.7± 6.1	55.5± 7.1
	GM730[b]	13.0	16.5	57.0
	GM730[c]	8.8± 1.7	9.6± 1.8	29.7± 4.0
	1BR[c,d]	8.1± 0.7	10.4± 2.5	28.9± 1.5
	48BR[c]	9.6± 0.7	7.9± 4.0	31.1± 3.5
		D_0 kJm^{-2}	D_q kJm^{-2}	D_{10} kJm^{-2}
313 nm	GM730[a]	14.2± 0.3	14.2± 3.0	46.9± 5.2
	GM730[c]	14.7± 2.9	13.9± 2.6	47.8± 6.0
	1BR[c]	12.4± 0.2	10.8± 1.8	37.3± 3.5
	48BR[c]	16.6± 3.7	11.4± 4.7	55.5±14.0
	1MR-91[e]	3.2	4.8	---
	GM38[g]	13 ± 1	---	40 ± 2
	GM498[g]	15 ± 1	---	32 ± 2
	CRL1141[g]	13 ± 1	---	33 ± 2
325 nm	GM730[a]	16.0	11.3	48.1
	1BR[d]	9.49± 0.45	12.2± 2.26	34.1± 3.46
334 nm	GM730[a]	18.1 ± 2.3	29.2± 0.6	70.8± 4.9
	1BR[d]	14.7 ± 0.4	19.1± 2.5	53.0± 1.4
	1MR-91[e]	126	160	---
365 nm	GM730[a]	96.3±22.4	82.9±32.3	305 ± 23
	GM730[b]	83	100	295
	GM730[c]	84.9±11.6	101.2± 8.9	297 ± 23
	1BR[c,d]	83.5±14.1	97.5± 12.6	289 ± 28
	48BR[c]	150 ±31	63.0± 46.4	408 ± 38
	1MR-91[e]	325	1640	---
	GM38[f]	200 ±20	210 ±30	---

[a] this thesis
[b] McAleer *et al.*, 1987
[c] Keyse *et al.*, 1985
[d] Keyse, 1983 (thesis)
[e] Wells and Han, 1985
[f] Smith and Paterson, 1982
[g] Smith and Paterson, 1981

Lethality following 254 nm radiation is generally considered to be due to pyrimidine dimer formation which is a photochemical event and as such not dependent upon temperature. Observations in the past with bacterial cells have confirmed little difference in response between irradiation at 0°C and 37°C (Jagger, 1967). The repair of the damage, being due to enzymatic processes, is dependent upon temperature but during a short time of irradiation (<15 minutes), in the dark, the amount is insignificant and does not modify the response. It is not known what causes the small decrease in the resistance of the cells if the induction of the lesion as such is not dependent upon temperature. An altered DNA conformation could be put forward as a cause for further investigations. However, the observation that the cellular response to 254 and 365 nm irradiation is influenced by temperature in a different way, suggests that lethal mechanisms are not common to both treatments.

The response of GM730 cells to 313 nm irradiation shows a more definite increase in sensitivity as the irradiation temperature is increased which suggests that the production of the lethal lesion is more pronounced at higher temperatures and is not repaired during the irradiation period of 3 hours. Amongst possible lethal lesions induced by 313 nm irradiation are pyrimidine dimers, thymine glycols and single-strand breaks. An observation by Niggli and Cerutti (1983) that induction of thymine-containing pyrimidine dimers in human fibroblasts is more efficient at 37° than at 0° is consistent with our results and supports a role for pyrimidine dimers being the lethal lesion following 313 nm irradiation. This was the first report of a dependence of pyrimidine dimer formation upon temperature. The role of temperature in pyrimidine dimer formation

is not known, nor is it known to what extent 254nm-induced pyrimidine dimers are influenced by temperature, if at all. Single-strand break formation has been shown to be temperature-independent since 313 nm-irradiated human fibroblasts showed a very small increase in single-strand breakage frequency at 37°C relative to 0°C. In the four human skin fibroblast strains tested the number of breaks/10^{10}daltons was 1.3-1.9 at 0° and 1.7-2.0 at 37°C (Hirschi et al.,1981).

In response to irradiation by wavelengths greater than 325nm there is a clear increase of cellular resistance as the irradiation temperature is increased. Several suggestions regarding alterations in the production of lesions or their repair can be put forward. It is becoming accepted that near-UV radiation effects are mediated by oxygen reactive species. Increased production of any of these species following near-UV radiation in a biological system has not been conclusively shown as yet but experimental evidence from chemical systems suggests that this is possible. Singlet oxygen can be formed by endogenous type II photosensitization reactions (Krinsky,1984) but the nature of the sensitizer still remains unknown. The production of superoxide ion has also been recently demonstrated following mid- and near-UV irradiation of NADH and NADPH coenzymes via a similar type II photosensitization reaction (Cunningham et al., 1985). In addition, near-UV irradiation of L-tryptophan in buffer has been shown to result in H_2O_2 formation (McCormick et al., 1976). Once the concentration of one particular species becomes elevated as a result of near-UV irradiation, further reactions allow the formation of other oxygen species as well and it becomes difficult to distinguish between their effects. Therefore,

unless experimental evidence favours the involvement of one particular species, these will be referred to collectively as 'reactive oxygen species.'

Theoretically, it can be suggested that the production of reactive oxygen species will be reduced at higher temperatures because of the decreased solubility of O_2 in aqueous media, but no studies as yet have investigated the temperature dependence of the production of active oxygen species. On the contrary, it is well established that enzymatic action is very dependent upon temperature. Therefore, increased temperature during irradiation should allow better enzymatic scavenging of the surplus reactive species formed as a result of near-UV irradiation. Antioxidant defense enzymes such as superoxide dismutase, catalase and glutathione peroxidase would remove excess superoxide ions and hydrogen peroxide, thereby preventing lesion formation in the DNA and/or other cellular targets and result in increased resistance of the cells to inactivation. Experimental evidence to support this idea has been difficult to obtain since exogenous addition of the above enzymes does not result in increased intracellular levels because they do not cross the plasma membrane. However, their selective inhibition by diethyldithiocarbamate or 3-amino-1,2,4-triazole or buthionine sulphoximine which are known to respectively reduce superoxide dismutase, catalase and glutathione activities, in mammalian cells (Lesko et al., 1985) would perhaps clarify the importance of these enzymatic systems in near-UV induced lethality. Such studies in conjunction with different irradiation temperatures might also clarify the mechanisms underlying the increased resistance human fibroblasts exhibit as the temperature

during irradiation is increased. Indeed, a recent study by Tyrrell and Pidoux (1986), in which inhibition of de novo synthesis of glutathione by buthionine sulphoximine resulted in increased cellular sensitivity to 313, 334, 365 and 405 nm irradiation but no alteration of the response to 254 nm irradiation, indicates a role for endogenous glutathione in the protection of human fibroblasts from solar-UV wavelengths. The importance of the other enzymes remains to be examined.

The possibility that the target itself also changes at different temperatures should also be considered. DNA conformation is known to be dependent on several conditions, one of which is temperature (Niggli and Cerutti, 1983) but if this is important in relation to cell lethality we would expect its effect to be more pronounced following far-UV-induced lethality, which is believed to depend primarily upon a DNA lesion. However experimental data showed that cell sensitivity to far-UV radiation is influenced by the irradiation temperature to a lesser degree and in the opposite way to cell sensitivity to near-UV radiation.

Membrane composition and fluidity are also known to vary at different environmental temperatures, although it is not clear how quickly cells are expected to adapt to new conditions. Higher environmental growth temperatures produce a lower content of unsaturated fatty acids in mouse and human fibroblasts (Konings and Ruifrok, 1985; McAleer et al., 1987) and decreased membrane fluidity. Neither the unsaturated fatty-acid content of cells nor their membrane fluidity have clearly been correlated with the cellular response to near-UV inactivation but are under investigation.

Klamen and Tuveson (1982) used a strain of E. coli (K1060) which can neither synthesize nor degrade unsaturated fatty acids to test whether the degree of fatty-acid unsaturation can influence sensitivity to near-UV inactivation. They reported that the higher the unsaturation of the fatty acids incorporated in the membrane phospholipids, the more sensitive log-phase cells were to near-UV radiation. They explained this as a result of $^1O_2$ attack on double bonds leading to increased production of lipid peroxidation. Chamberlain and Moss (1987) extended this work using the same strain of E. coli by showing that near-UV induced membrane damage, measured as $^{86}Rb^+$ leakage, was also increased in cells containing fatty acids with a higher degree of unsaturation and was paralleled by increased lipid peroxidation products. Both lipid peroxidation products and $^{86}Rb^+$ leakage from the cells were increased when irradiation was carried out in the presence of D_2O which again supports a role for $^1O_2$ in the damaging process. However a study using photosensitized cells exposed to near-UV radiation reported the opposite effect, i.e., increased resistance to inactivation as the unsaturation of the fatty acids incorporated in E. coli K1060 was increased (Wagner et al., 1980). The authors suggested that a higher degree of unsaturation in the lipids resulted in increased membrane fluidity which would be less susceptible to disruption.

In mammalian cells, alteration of the lipid content is more complex and involves inner membranes such as nucleic, mitochondrial and lysosomal, as well as the outer cell membrane. To date studies have not indicated any correlation between the unsaturated fatty-acid content of the cells and their response to either UV or gamma irradiation (McAleer et al., 1987; Wolters and Konings, 1984).

Another group of enzymes whose activity would also increase as the temperature during irradiation increases are DNA repair enzymes. Concomitant repair of any DNA lesions during the irradiation period of 4 hours could be expected to result in increased cellular resistance to irradiation. Results showed that irradiation with 313 nm at 37°C which lasted for about 3 hours did not result in increased cellular resistance, but this could be a result of the rate of lesion formation exceeding the rate of repair at that particular wavelength. This might not be the case during 365 nm irradiation, so this point warrants more extensive investigation. An obvious method to carry out this investigation, such as to increase or decrease the irradiation fluence rate and follow its effect on survival, was not feasible in this study, since the fluence rate used was the maximum emitted by the monochromatic source and the irradiation time of 4-4.5 hours was also near the maximum time cells could be stirred in buffer without a decrease of viability (Keyse 1983, see also Table 8).

RESULTS AND DISCUSSION

PART 2

THE SENSITIVITY OF AN ACTINIC RETICULOID STRAIN, AR6LO, TO ULTRAVIOLET RADIATION, GAMMA RADIATION AND HYDROGEN PEROXIDE AND ITS COMPARISON TO THE RESPONSE OF NORMAL GM730 FIBROBLASTS

Investigations into the cellular responses of actinic reticuloid (AR) cells to near-UV light were prompted by reports that AR cells exhibited an abnormal response to broad-band near-UV radiation characterized by changes in the morphological appearance to the cells, decrease in RNA synthesis and increase in the incidence of DNA single-strand breaks (Giannelli *et al.*, 1983; Botcherby *et al.*, 1984). The initial objective of this work relating to AR cellular response was to determine the sensitivity of AR cells to specific monochromatic wavelengths under controlled conditions of irradiation. Inactivation studies of AR cells by gamma radiation and H_2O_2 are also included in this chapter since the responses obtained should be taken into account when formulating a hypothesis for the underlying cause of AR sensitivity.

Growth Characteristics of AR Fibroblasts

Cells were grown in EMEM medium supplemented with 15 per cent foetal calf serum as previously described for normal human fibroblast strains.

Growth curves for both cell lines were constructed (experimental details in Appendix 6) and shown in Fig. 30. There was a similarity of shape in the growth curves which were characterized by a lag-phase, an exponential or log-phase and a plateau phase. In this and other growth curves constructed in this study (Fig. 42), the lag-phase could be more accurately described as a drop from the number of cells initially inoculated on the plates due to their inability to attach and divide. The proportion of AR cells unable to multiply, as shown in this growth curve, was greater than that of normal GM730 cells. AR cells grew more slowly than GM730 cells (doubling time of 39 hrs compared to 26 hrs) and did not grow to as high numbers as normal cells did, under identical conditions. This could be (1) due to a smaller densing capacity of the AR cell line, (2) due to more rapid depletion of nutrients from the growth medium or (3) due to some other inhibitory factor. AR cells were often more ragged in appearance, as seen under the microscope after trypsinization, especially when older in passage (17-20) or when more than 5-6 days had passed since previous subculture. Their plating efficiency was also lower and ranged from 4 - 21 per cent throughout this work whereas for GM730 cells these values were 5 - 43 per cent. As mentioned previously, plating efficiencies depended partly on the serum used and were not correlated in any way to cellular sensitivity.

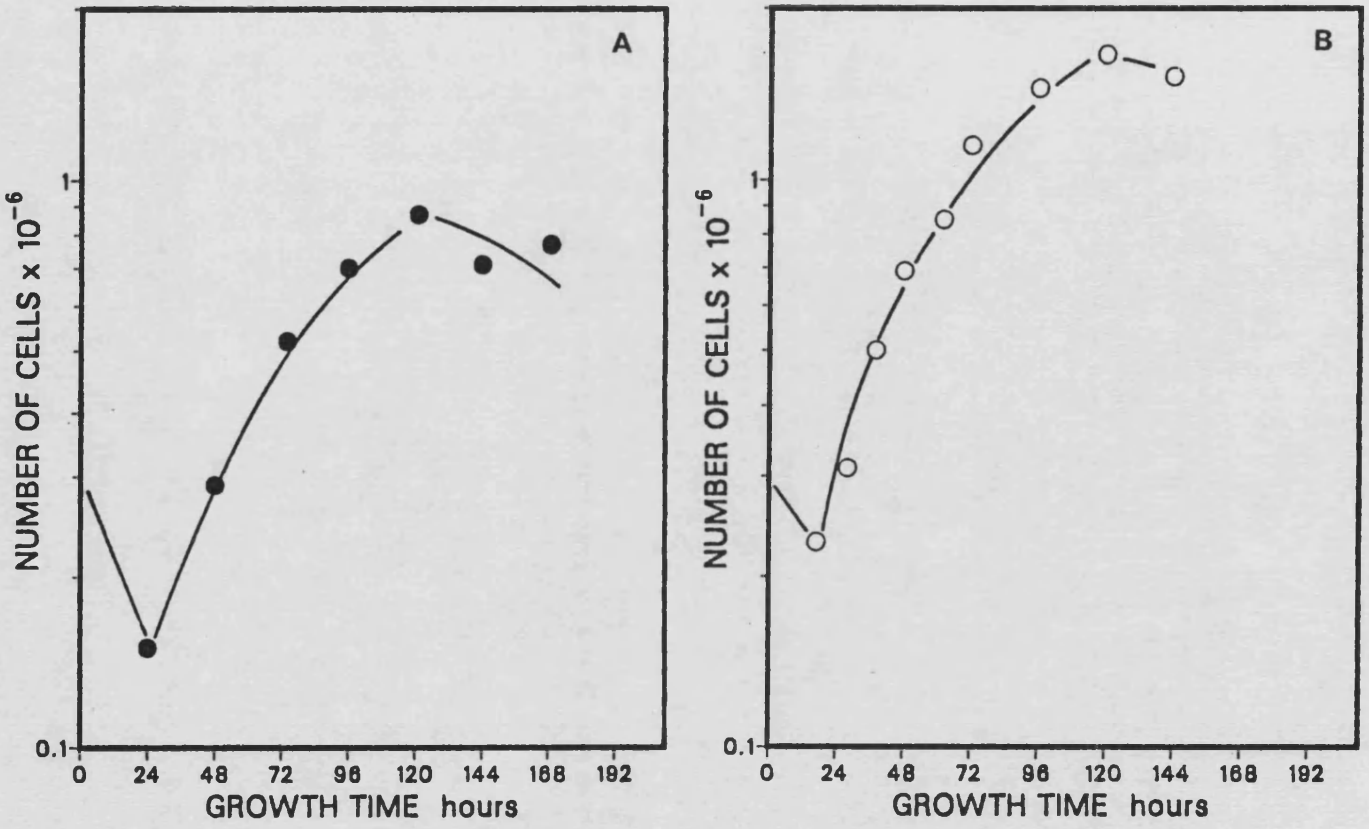

Figure 30. Growth curves for (A) AR6LO and (B) GM730 cells in EMEM supplemented with 15% foetal calf serum.

Sensitivity of AR Fibroblasts to Near-UV (365 nm) Radiation

The response of AR cells following irradiation with 365 nm wavelength was determined at 25°C since previously published results concerned irradiations performed at room temperature. Fig. 31 A includes the results of six replicate experiments and Table 7 the calculated parameters for each experiment. In Fig. 31 B the comparison of the mean response of AR and normal GM730 cells can be seen.

Although there was a variability in the response of AR cells to 365 nm at 25°C, the mean response of AR cells was found to be approximately 4 times more sensitive than the mean response of GM730 cells. The factors which influenced the sensitivity of both cell lines could not be detected but seemed to be related to the exact conditions of irradiation or medium in which cells were grown or irradiated, since, when matched experiments were performed on the same day, the same influence on sensitivity was apparent, i.e. a 'resistant' GM730 cell response was matched with a 'resistant' AR cell response. Therefore the difference in sensitivity remained around 4. When both sets of data were treated as a population, the difference between the two populations was found to be significant by statistical tests with an x^2 value of 10.33 for the intercept and 239 for the slope ($p<0.001$).

In order to exclude the possibility that some other factor related to the length of the irradiation time was responsible for the observed sensitivity, both normal and AR cells were kept stirred in the cuvette, at 25°C without receiving any irradiation, and their survival determined at 30 minute intervals. The results in Table 8

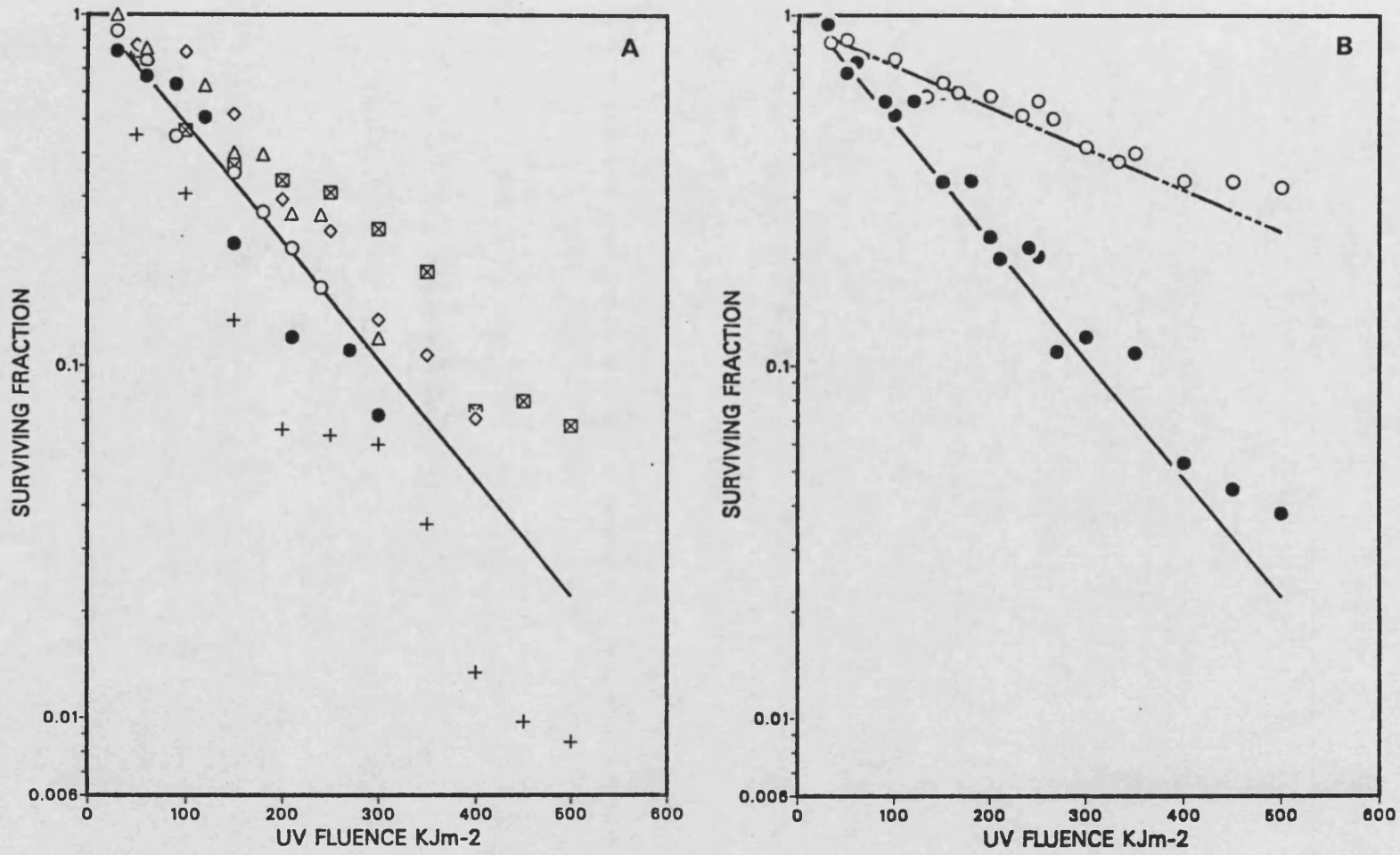

Figure 31. (A) The inactivation of AR6LO cells by 365nm irradiation at 25°C, in PBS. Different sets of symbols represent the results of replicate experiments.
(B) The inactivation of AR6LO (●, ———) and GM730 (○ , ------) cells by 365nm irradiation at 25°C. Mean experimental points at each fluence and calculated mean lines depicted.

TABLE 7

SURVIVAL PARAMETERS FOR THE INACTIVATION OF AR6LO CELLS BY 365 NM IRRADIATED AT 25°C IN DIFFERENT MEDIA

Irradiation Medium	Expt. No.	Slope $(Jm^{-2})^{-1}$	Standard Deviation	Intercept y-axis	Standard Deviation	$D0_2$ Jm^{-2}	Dq_2 Jm^{-2}	$D10$ Jm^{-2}
PBS	45	3.86×10^{-6}	2.62×10^{-7}	-2.13×10^{-1}	8.12×10^{-2}	1.12×10^{5}	5.49×10^{4}	2.04×10^{5}
	46	3.24×10^{-6}	1.68×10^{-7}	1.51×10^{-1}	4.24×10^{-2}	1.34×10^{5}	4.66×10^{4}	3.55×10^{5}
	47	2.34×10^{-6}	2.10×10^{-7}	-1.73×10^{-2}	6.52×10^{-2}	1.86×10^{5}	-7.41×10^{3}	4.20×10^{5}
	48	4.09×10^{-6}	4.01×10^{-7}	7.21×10^{-2}	7.17×10^{-2}	1.06×10^{5}	1.76×10^{4}	2.62×10^{5}
	49	3.39×10^{-6}	2.10×10^{-7}	3.66×10^{-2}	3.26×10^{-2}	1.28×10^{5}	1.08×10^{4}	3.06×10^{5}
	50	3.31×10^{-6}	2.33×10^{-7}	1.39×10^{-1}	4.06×10^{-2}	1.31×10^{5}	4.19×10^{4}	3.44×10^{5}
	Mean	$\mathbf{3.37\times10^{-6}}$		$\mathbf{2.81\times10^{-2}}$		$\mathbf{1.33\times10^{5}}$	$\mathbf{2.74\times10^{4}}$	$\mathbf{3.15\times10^{5}}$
EMEM	51	3.20×10^{-6}	2.50×10^{-7}	1.20×10^{-2}	6.31×10^{-2}	1.36×10^{5}	3.76×10^{3}	3.16×10^{5}
	52	2.49×10^{-6}	1.00×10^{-7}	3.30×10^{-2}	2.53×10^{-2}	1.74×10^{5}	1.32×10^{4}	4.15×10^{5}
	Mean	$\mathbf{2.85\times10^{-6}}$		$\mathbf{2.25\times10^{-2}}$		$\mathbf{1.55\times10^{5}}$	$\mathbf{8.48\times10^{3}}$	$\mathbf{3.66\times10^{5}}$
DMEM	53	3.66×10^{-6}	2.34×10^{-7}	7.80×10^{-2}	4.71×10^{-2}	1.19×10^{5}	2.14×10^{4}	2.95×10^{5}

Data in Appendix 8 (Tables A15, A16)

show that for up to 5 hours of stirring there was no significant decrease in the viability of either cell line.

TABLE 8
SURVIVING FRACTION OF AR6LO AND GM730 CELLS WITH TIME HELD IN BUFFER AT 25°C STIRRED AT 600 RPM

Holding time (mins)	Surviving fraction AR6LO	GM730
60	8.89×10^{-1}	1.04×10^{0}
90	9.67×10^{-1}	8.66×10^{-1}
135	1.15×10^{0}	9.26×10^{-1}
165	9.02×10^{-1}	1.01×10^{0}
195	9.02×10^{-1}	8.66×10^{-1}
240	8.63×10^{-1}	9.17×10^{-1}
300	8.17×10^{-1}	9.26×10^{-1}

Since published results on AR sensitivity concerned irradiations performed in full medium (Dulbecco's Modification of Eagle's Medium), it was decided to assess AR survival after irradiation in EMEM and DMEM supplemented with 15 per cent foetal calf serum as compared with irradiation in PBS. Figures 32 A, B show the response obtained when AR cells were irradiated with 365 nm at 25°C in EMEM and DMEM growth media. No further sensitization was observed relative to the response obtained when irradiation took place in PBS (Fig. 31). This result is perhaps surprising taking into account reports such as those of Wang *et al.* (1974) and Stoien and Wang (1974) who have shown the formation of toxic photoproducts in tissue culture medium by blacklight but perhaps AR cells are

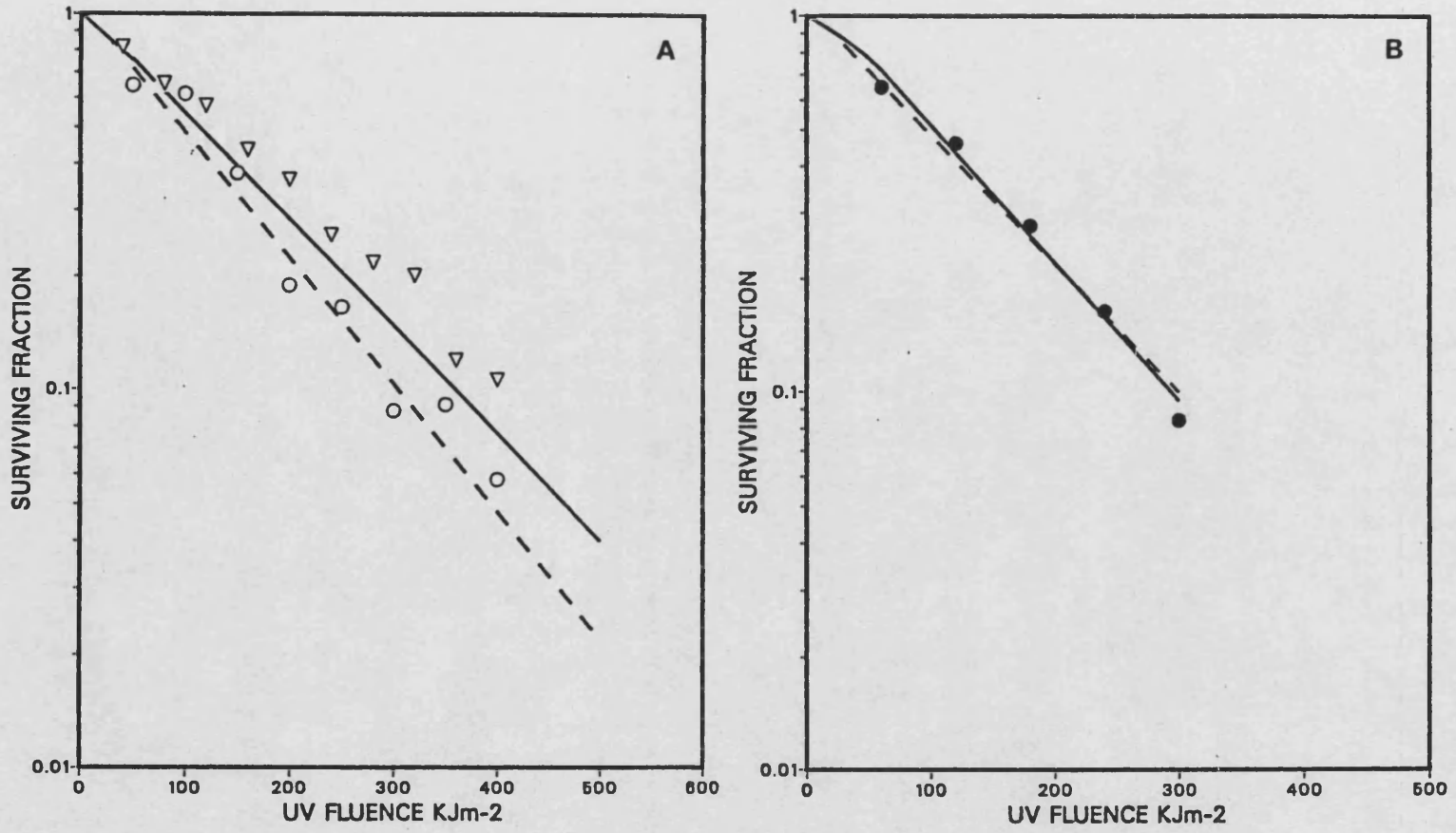

Figure 32. The inactivation of AR6L0 cells by 365nm irradiation at 25°C in (A) EMEM (B) DMEM medium. The different sets of symbols represent the results of replicate experiments. The dashed line represents the response obtained in PBS (see Fig.31)

already maximally sensitized to irradiation under the stated conditions.

The inactivation of AR cells by 365 nm was also determined at the temperatures of 0° and $37^{\circ}C$ in order to form further comparisons with normal cell strain GM730. The inactivation curves obtained are shown in Figs. 33 A, B and 34 A, B while the calculated parameters for the individual experiments are included in Table 9. No difference in the sensitivity of AR and normal cells could be seen when irradiation took place at those temperatures, and the same factors which increased the resistance of normal cells when the irradiation temperature was raised to $37^{\circ}C$ seemed to increase the resistance of AR cells as well. However, at the intermediate temperature of $25^{\circ}C$, as seen in Fig. 31 B, a difference in sensitivity was apparent. One interpretation of this observation at $25^{\circ}C$ could be that there is a partial enzymatic defect in AR cells. This could be either in the scavenging enzymes which would reduce the load of reactive oxygen species and prevent lesion formation or in the repair enzymes which would operate to repair lesions formed. From these initial experiments it is not possible to draw any further deductions as to which group of enzymes would most likely be affected. An alternative explanation could again be that the target(s) of near-UV radiation is altered in a different manner in the two cell lines as the temperature is increased.

Sensitivity of AR Fibroblasts to Far-UV (254 nm) Radiation

The inactivation of AR cells by 254 nm irradiation at 0°, 25° and $37^{\circ}C$ is shown in Panel A of Figures 35, 36, 37 and compared to the normal GM730 cell response in panel B of the same figure.

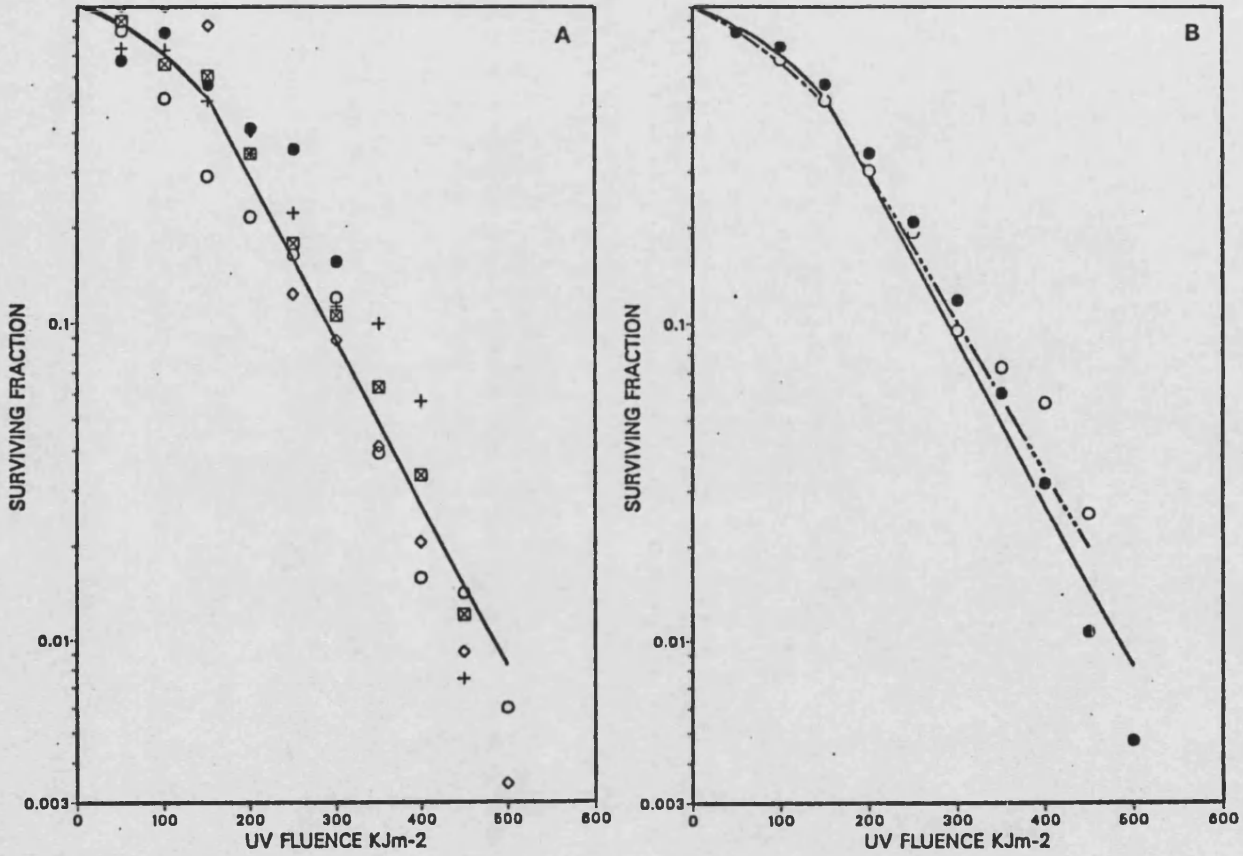

Figure 33. (A) The inactivation of AR6LO cells by 365 nm irradiation at 0°C. Different sets of symbols represent the results of replicate experiments.
(B) The inactivation of AR6LO (● , ——) and GM730 (○ , - - - -) cells by 365 nm irradiation at 0°C. Mean experimental points at each fluence and calculated mean lines depicted. non-irradiated)

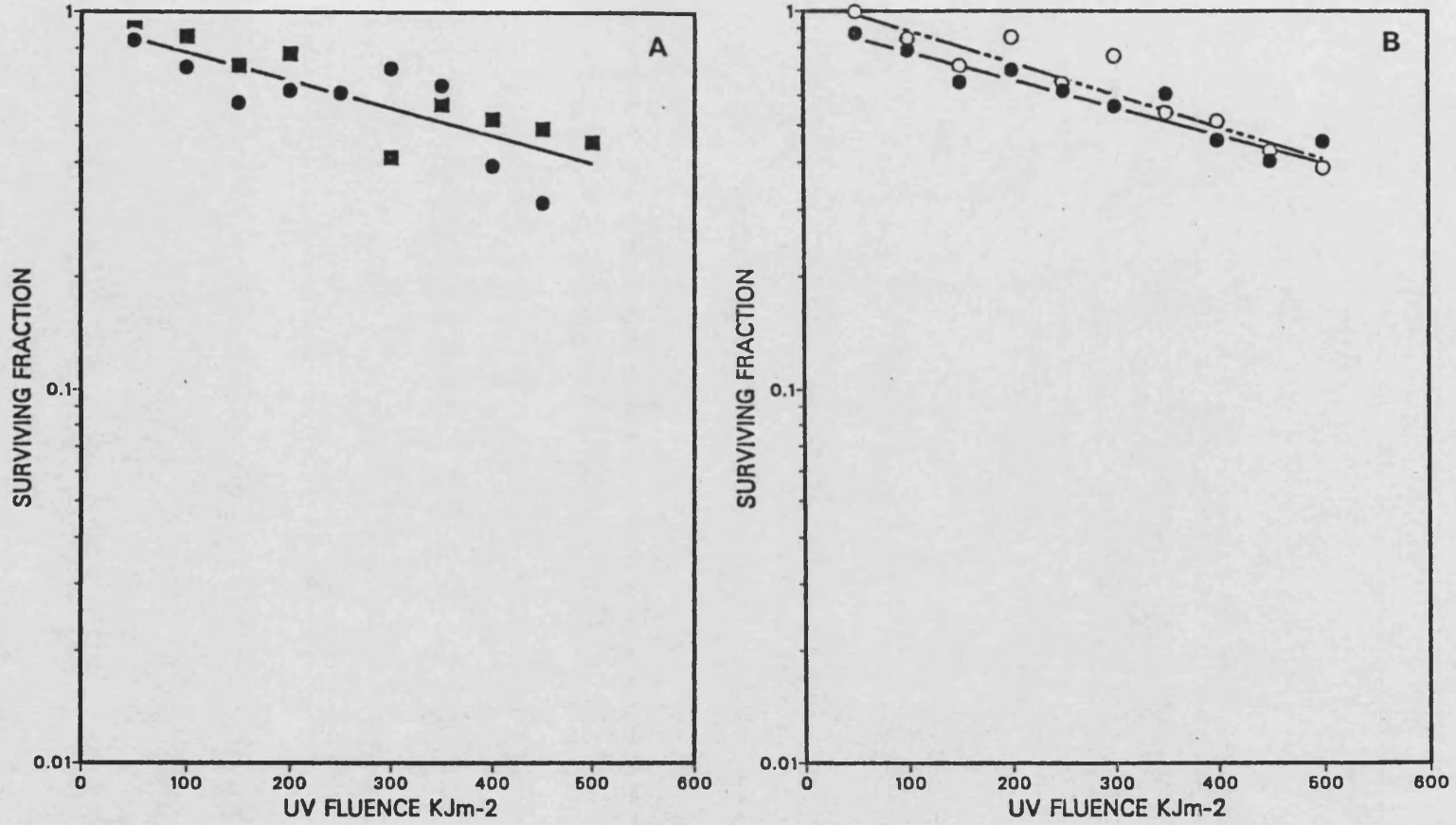

Figure 34. (A) The inactivation of AR6LO cells by 365nm irradiation at 37°C. Different sets of symbols represent the results of replicate experiments.
(B) The inactivation of AR6LO (● , ———) and GM730 (○ , —------) cells by 365nm irradiation at 37°C. Mean experimental points at each fluence and calculated mean lines depicted.

TABLE 9

SURVIVAL PARAMETERS FOR THE INACTIVATION OF AR6LO CELLS BY 365 NM

IRRADIATED AT 0°C AND 37°C

Temperature	Expt. No.	Slope $(Jm^{-2})^{-1}$	Standard Deviation	Intercept y-axis	Standard Deviation	$D0_2$ Jm^{-2}	Dq_2 Jm^{-2}	$D10$ Jm^{-2}
0°C	54	3.48×10^{-6}	8.60×10^{-7}	3.11×10^{-1}	1.99×10^{-1}	1.25×10^{5}	8.95×10^{4}	3.77×10^{5}
	55	5.06×10^{-6}	4.27×10^{-7}	3.72×10^{-1}	1.47×10^{-1}	8.58×10^{4}	7.35×10^{4}	2.71×10^{5}
	56	5.41×10^{-6}	2.53×10^{-7}	6.22×10^{-1}	8.01×10^{-2}	8.03×10^{4}	1.15×10^{5}	3.00×10^{5}
	57	5.28×10^{-6}	8.77×10^{-7}	6.23×10^{-1}	2.77×10^{-1}	8.22×10^{4}	1.18×10^{5}	3.07×10^{5}
	58	6.50×10^{-6}	3.11×10^{-7}	5.33×10^{-1}	9.83×10^{-2}	6.68×10^{4}	8.20×10^{4}	2.36×10^{5}
	Mean	$\mathbf{5.15\times10^{-6}}$		$\mathbf{4.92\times10^{-1}}$		$\mathbf{8.80\times10^{5}}$	$\mathbf{9.56\times10^{4}}$	$\mathbf{2.98\times10^{5}}$
37°C	59	7.79×10^{-7}	2.27×10^{-7}	-4.16×10^{-2}	6.43×10^{-2}	5.57×10^{5}	-5.34×10^{4}	1.23×10^{6}
	60	6.87×10^{-7}	1.34×10^{-7}	-2.29×10^{-2}	4.14×10^{-2}	6.32×10^{5}	-3.33×10^{4}	1.42×10^{6}
	Mean	$\mathbf{7.33\times10^{-7}}$		$\mathbf{-3.23\times10^{-2}}$		$\mathbf{5.95\times10^{5}}$	$\mathbf{-4.34\times10^{4}}$	$\mathbf{1.33\times10^{6}}$

Data in Appendix 8 (Table A17)

Calculated parameters for the individual experiments are found in Table 10. The survivor curves obtained for AR cells at the three temperatures did not show any significant differences from the normal GM730 response. They also followed the same pattern of response as the normal cells to an alteration of the irradiation temperature in that the resistance of AR cells was progressively decreased as the irradiation temperature was increased. This result confirms that AR sensitivity to far-UV radiation is normal and determined by similar mechanisms of lethality to those of normal GM730 cells.

Sensitivity of AR Fibroblasts to Mid-UV (313 nm) Radiation

The response of AR cells to 313 nm irradiation at 0^{o} and $25^{o}C$ was determined (Figs. 38 A, 39 A) and compared to normal GM730 response in Fig. 38 B, 39 B. Again, as seen in the graphs and by comparing the calculated parameters of Table 11 and Table 4 for AR and GM730 cells, respectively, there was no difference in the response of the two cell lines to this wavelength.

Normal and AR Human Fibroblast Response to Gamma Radiation

The question of whether there is any cross-sensitivity between cells showing increased sensitivity to gamma-irradiation and cells showing increased sensitivity to a specific section of UV light is a possibility that has been the subject of a number of investigations. It has been suggested that an AT strain (AT4BI) abnormally sensitive to gamma radiation is also sensitive to 313nm radiation, (Smith and Paterson, 1981; Keyse *et al.*,1985) but the most typical representative of far-UV sensitivity *i.e.* XP cell strains fall into

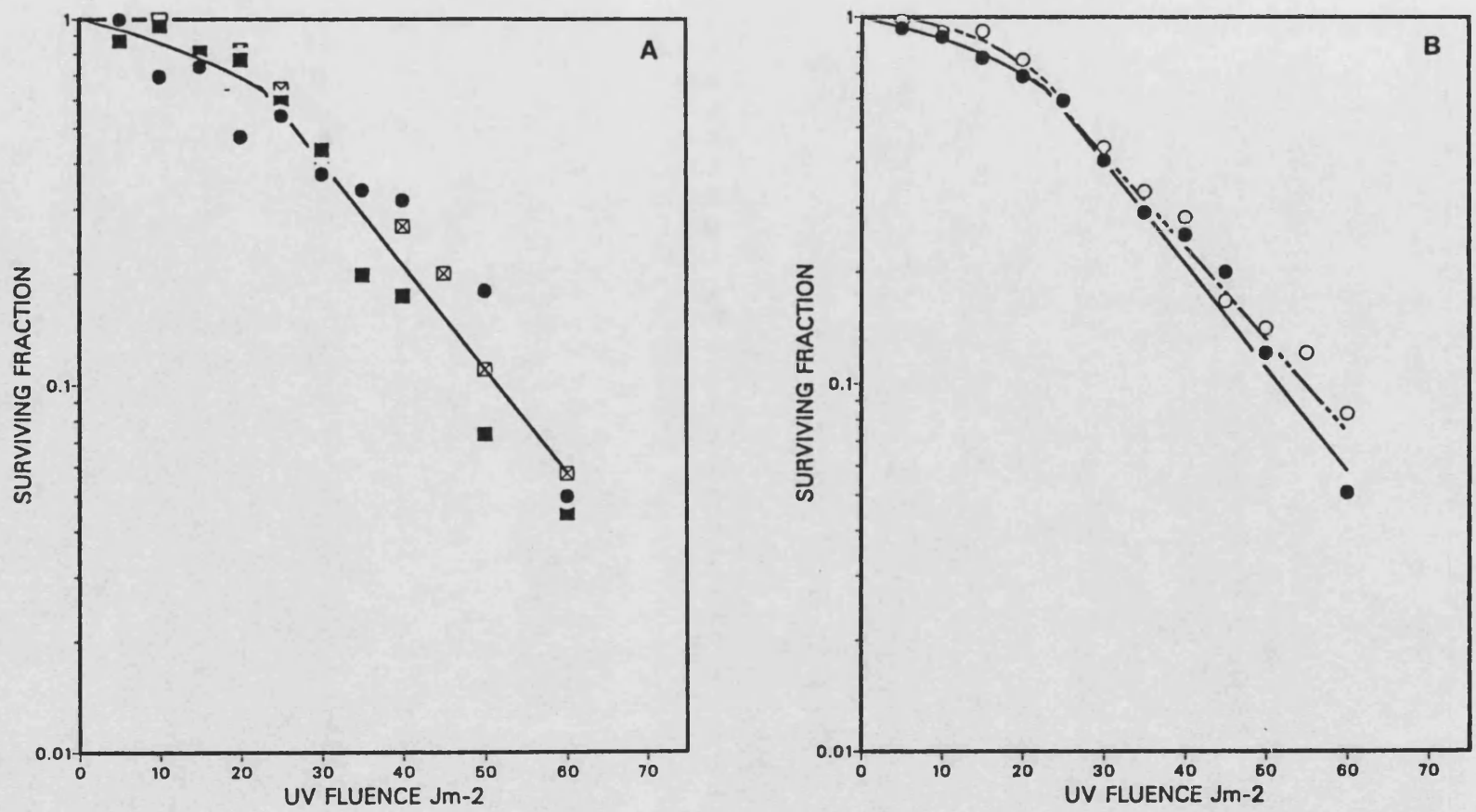

Figure 35. (A) The inactivation of AR6LO cells by 254nm irradiation at 0°C. Different sets of symbols represent the results of replicate experiments.
(B) The inactivation of AR6LO (● , ———) and GM730 (○ , —·····—) cells by 254nm irradiation at 0°C. Mean experimental points at each fluence and calculated mean lines depicted.

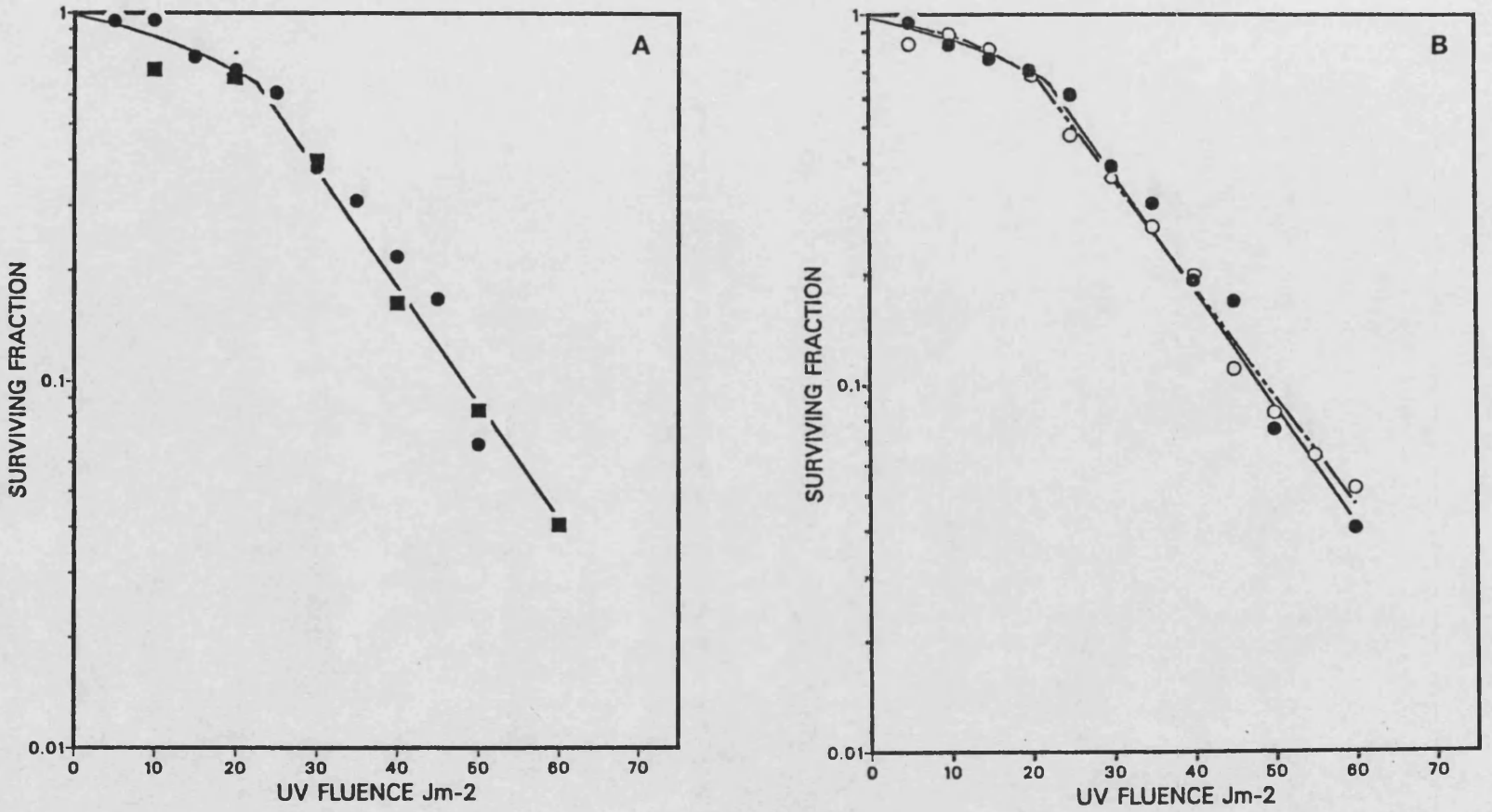

Figure 36. (A) The inactivation of AR6LO cells by 254nm irradiation at 25°C. Different sets of symbols represent the results of replicate experiments.
(B) The inactivation of AR6LO (● , ———) and GM730 (○ , —·····—) cells by 254nm irradiation at 25°C. Mean experimental points at each fluence and calculated mean lines depicted.

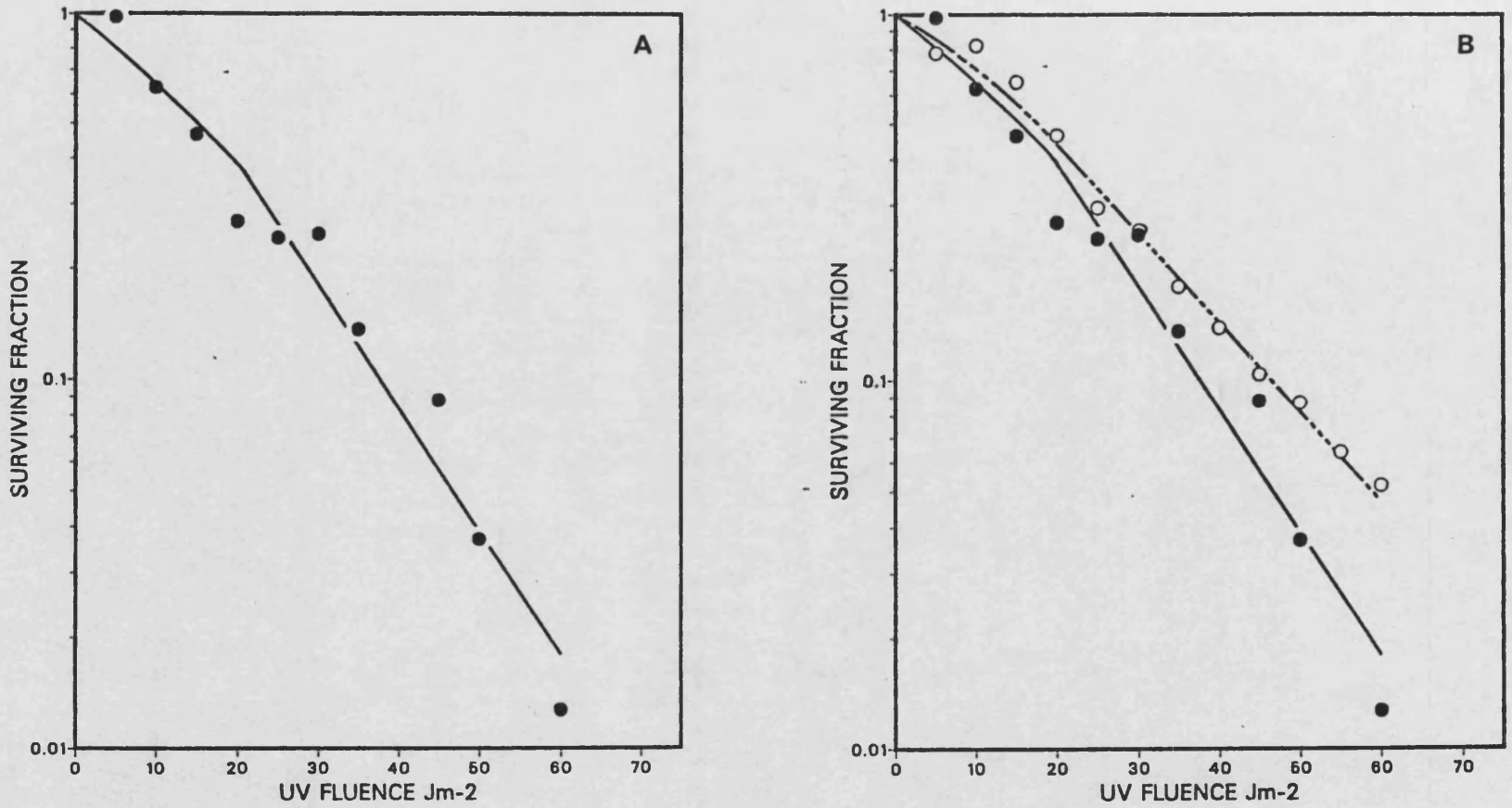

Figure 37. (A) The inactivation of AR6L0 cells by 254nm irradiation at 37°C. One experiment shown. (B) The inactivation of AR6L0 (●, ——) and GM730 cells (○, —·····—) cells by 254nm irradiation at 37°C. Single experiment for AR6L0 and mean response of GM730 cells depicted.

TABLE 10

SURVIVAL PARAMETERS FOR THE INACTIVATION OF AR6LO CELLS BY 254 NM IRRADIATED AT 0°C, 25°C, AND 37°C

Temperature	Expt. No.	Slope $(Jm^{-2})^{-1}$	Standard Deviation	Intercept y-axis	Standard Deviation	$D0_{-2}$ Jm^{-2}	Dq_{-2} Jm^{-2}	$D10_{-2}$ Jm^{-2}
0°C	61	2.34×10^{-2}	4.11×10^{-3}	2.94×10^{-1}	1.62×10^{-1}	1.86×10^{1}	1.26×10^{1}	5.53×10^{1}
	62	3.26×10^{-2}	2.04×10^{-3}	5.45×10^{-1}	8.02×10^{-2}	1.33×10^{1}	1.67×10^{1}	4.74×10^{1}
	63	2.86×10^{-2}	1.43×10^{-3}	5.16×10^{-1}	5.81×10^{-2}	1.52×10^{1}	1.81×10^{1}	5.30×10^{1}
	Mean	$\mathbf{2.82\times10^{-2}}$		$\mathbf{4.52\times10^{-1}}$		$\mathbf{1.57\times10^{1}}$	$\mathbf{1.58\times10^{1}}$	$\mathbf{5.19\times10^{1}}$
25°C	64	3.16×10^{-2}	3.42×10^{-3}	5.47×10^{-1}	1.25×10^{-1}	1.37×10^{1}	1.73×10^{1}	4.90×10^{1}
	65	3.17×10^{-2}	1.02×10^{-3}	5.07×10^{-1}	4.31×10^{-2}	1.37×10^{1}	1.60×10^{1}	4.75×10^{1}
	Mean	$\mathbf{3.17\times10^{-2}}$		$\mathbf{5.27\times10^{-1}}$		$\mathbf{1.37\times10^{1}}$	$\mathbf{1.67\times10^{1}}$	$\mathbf{4.83\times10^{1}}$
37°C	66	3.35×10^{-2}	4.15×10^{-3}	2.61×10^{-1}	1.67×10^{-2}	1.30×10^{1}	7.81×10^{0}	3.76×10^{1}

Data in Appendix 8 (Table A18)

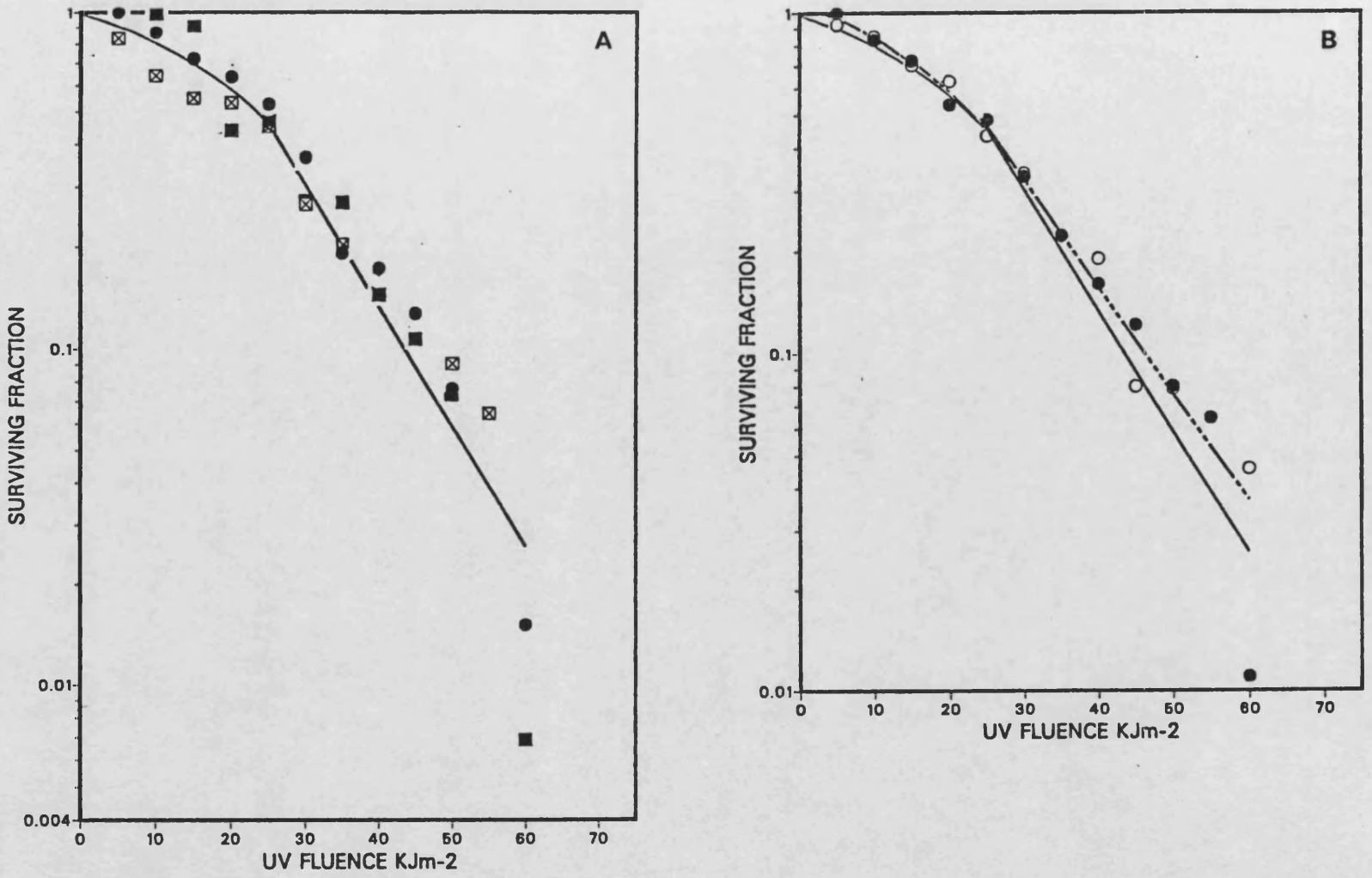

Figure 38. (A) The inactivation of AR6LO cells by 313nm irradiation at 0°C. Different sets of symbols represent the results of replicate experiments.
(B) The inactivation of AR6LO (●, ——) and GM730 (○, ·····—) cells by 313nm irradiation at 0°C. Mean experimental points at each fluence and calculated mean lines depicted.

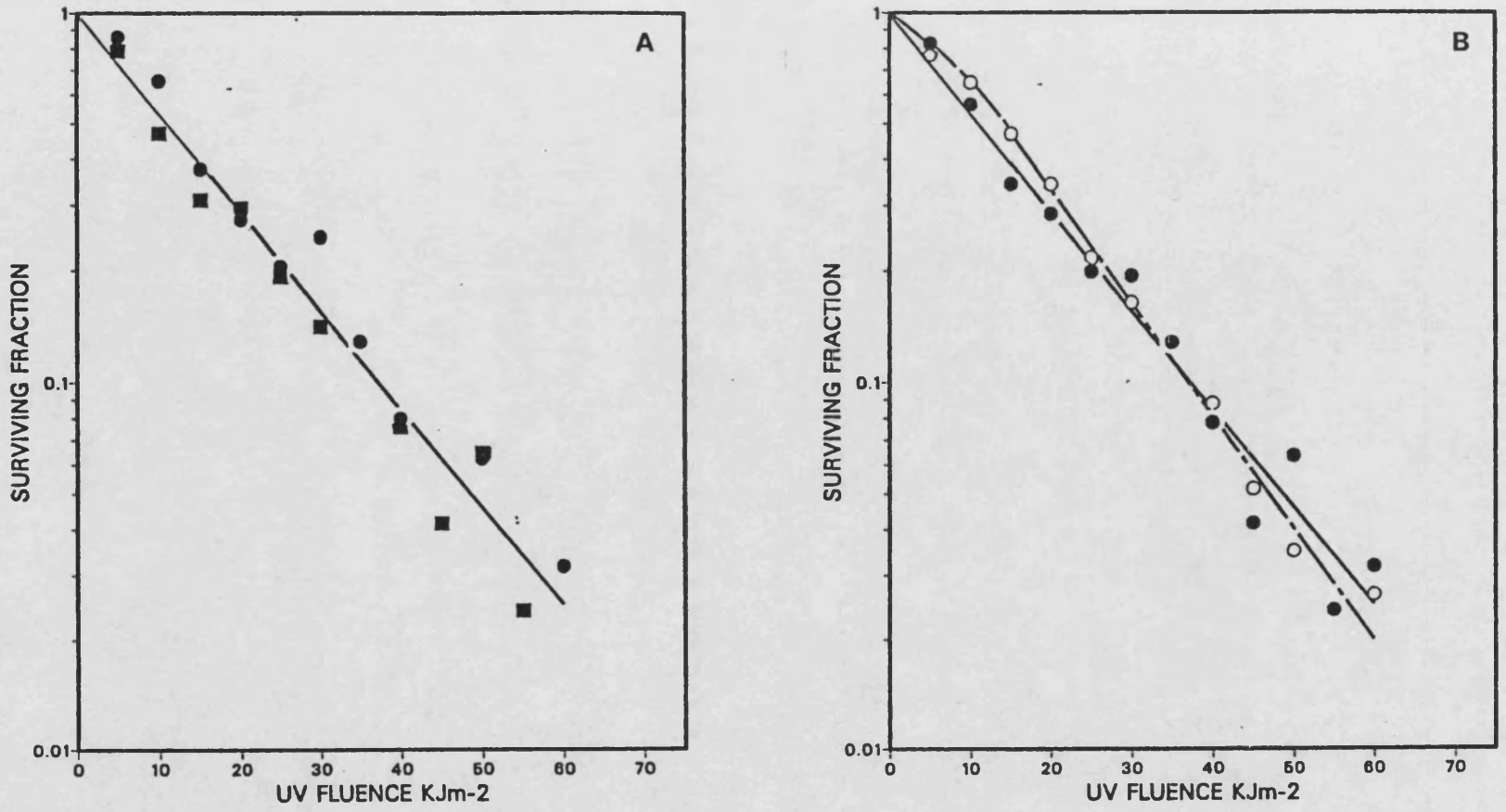

Figure 39. (A) The inactivation of AR6LO cells by 313 nm irradiation at 25°C. Different sets of symbols represent the results of replicate experiments.
(B) The inactivation of AR6LO (● , ———) and GM730 (○ , -----) cells by 313 nm irradiation at 25°C. Mean experimental points at each fluence and calculated mean lines depicted.

TABLE 11

SURVIVAL PARAMETERS FOR THE INACTIVATION OF AR6LO CELLS BY 313 NM IRRADIATED AT 0° AND 25°C

Temperature	Expt. No.	Slope $(Jm^{-2})^{-1}$	Standard Deviation	Intercept y-axis	Standard Deviation	$D0_{-2}$ Jm^{-2}	Dq_{-2} Jm^{-2}	$D10_{-2}$ Jm^{-2}
0°C	67	3.82×10^{-5}	3.71×10^{-6}	6.81×10^{-1}	1.49×10^{-1}	1.14×10^{4}	1.78×10^{4}	4.40×10^{4}
	68	4.24×10^{-5}	6.72×10^{-6}	7.70×10^{-1}	2.70×10^{-1}	1.02×10^{4}	1.81×10^{4}	4.17×10^{4}
	69	2.60×10^{-5}	1.10×10^{-6}	2.53×10^{-1}	4.31×10^{-2}	1.67×10^{4}	9.73×10^{3}	4.82×10^{4}
	Mean	**3.55×10^{-5}**		**5.68×10^{-1}**		**1.28×10^{4}**	**1.52×10^{4}**	**4.46×10^{4}**
25°C	70	2.38×10^{-5}	1.98×10^{-6}	-5.56×10^{-2}	7.38×10^{-2}	1.82×10^{4}	2.33×10^{3}	4.44×10^{4}
	71	2.67×10^{-5}	2.74×10^{-6}	-4.30×10^{-2}	1.02×10^{-1}	1.63×10^{4}	-1.61×10^{2}	3.58×10^{4}
	Mean	**2.53×10^{-5}**		**-4.93×10^{-2}**		**1.73×10^{4}**	**1.09×10^{3}**	**4.01×10^{4}**

Data in Appendix 8 (Table A19)

the normal range of radiosensitivity (Arlett and Harcourt, 1980; Dritschilo et al., 1984).

Gamma-irradiation experiments were performed with cells in suspension, bubbled with oxygen, at room temperature (20°C), as described in the Materials and Methods section. The dose rate was 10^3 rads min^{-1}. The results of 4 experiments with AR cells and 2 with GM730 cells are shown in panels A, B of Fig. 40, respectively. The mean responses obtained, which were calculated from the individual parameters for each experiment shown in Table 12, showed that the two cell lines did not exhibit a significant difference in their response to gamma radiation, although GM730 cells showed a small shoulder followed by a slightly steeper slope (D_0 of 95.7 rads for GM730 compared to 121 rads for AR). The steeper slope of GM730 was not reflected in the D_{10} values which were 369 rads for GM730 and 283 rads for AR, i.e. by comparison of D_{10} values AR cells were more sensitive. Comparison to other published values on the radiosensitivity of human fibroblasts shows both responses to be within the normal range since in a survey of radiosensitivity by Arlett and Harcourt (1980) where 54 human cell strains were assayed, the normal sensitivity was described by D_0 values of 97 to 180 rads. It should be noted that there is good agreement between the two experimental methods used since in the above study, log-phase cells were irradiated in suspension, in air, at ambient temperature. However, the dose-rate used by Arlett and Harcourt was 1.8-3.2 rads min^{-1}, approximately 30-60 times lower than the dose-rate used in the experiments presented above and, according to Dritschilo et al. (1984), human fibroblasts respond with an enhancement in survival when the dose rate is reduced. In their study they reported a D_0

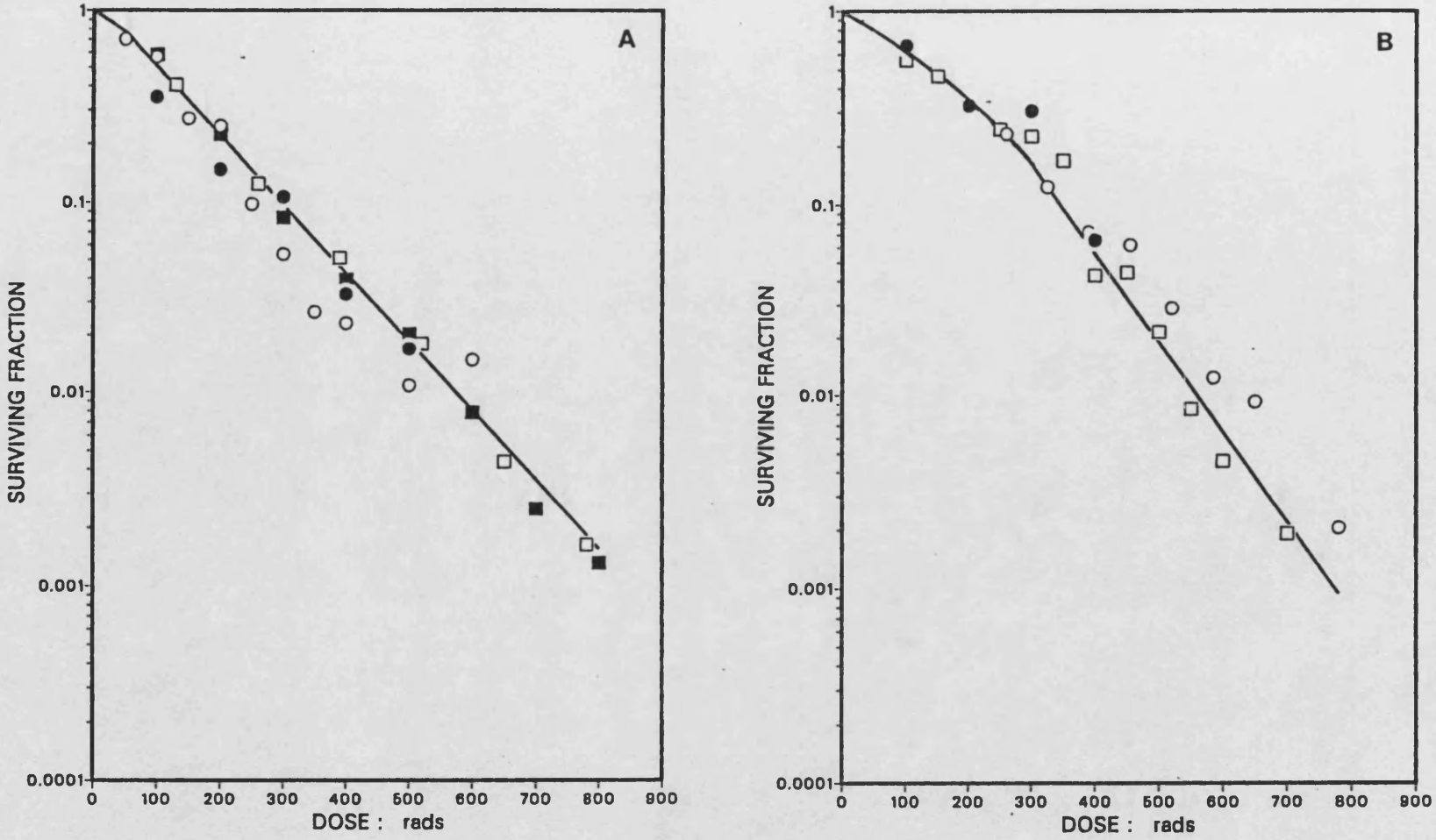

Figure 40. The inactivation of (A) AR6LO and (B) GM730 cells by gamma irradiation at room temperature (20 °C). The different sets of symbols represent the results of replicate experiments.

TABLE 12

SURVIVAL PARAMETERS FOR THE INACTIVATION OF AR6LO and GM730 CELLS

BY GAMMA-IRRADIATION

Cell Line	Expt. No.	Slope $(Rads)^{-1}$	Standard Deviation	Intercept y-axis	Standard Deviation	D0 Rads	Dq Rads	D10 Rads
AR6LO	72	3.28×10^{-3}	2.81×10^{-4}	-1.16×10^{-1}	9.33×10^{-2}	1.32×10^{2}	-3.53×10^{1}	2.70×10^{2}
AR6LO	73	3.61×10^{-3}	3.86×10^{-4}	-3.70×10^{-2}	1.29×10^{-1}	1.20×10^{2}	-1.02×10^{1}	2.67×10^{2}
AR6LO	74	3.77×10^{-3}	8.82×10^{-5}	1.16×10^{-1}	4.46×10^{-2}	1.15×10^{2}	3.07×10^{1}	2.96×10^{2}
AR6LO	75	3.69×10^{-3}	1.08×10^{-4}	1.01×10^{-1}	5.46×10^{-2}	1.18×10^{2}	2.74×10^{1}	2.98×10^{2}
	Mean	$\mathbf{3.59 \times 10^{-3}}$		$\mathbf{1.60 \times 10^{-2}}$		$\mathbf{1.21 \times 10^{2}}$	$\mathbf{3.15 \times 10^{0}}$	$\mathbf{2.83 \times 10^{2}}$
GM730	76	5.40×10^{-3}	3.40×10^{-4}	9.85×10^{-1}	1.69×10^{-1}	8.04×10^{1}	1.82×10^{2}	3.68×10^{2}
GM730	77	3.91×10^{-3}	2.42×10^{-4}	4.44×10^{-1}	1.33×10^{-1}	1.11×10^{2}	1.14×10^{2}	3.69×10^{6}
	Mean	$\mathbf{4.66 \times 10^{-3}}$		$\mathbf{7.15 \times 10^{-1}}$		$\mathbf{9.57 \times 10^{1}}$	$\mathbf{1.48 \times 10^{2}}$	$\mathbf{3.69 \times 10^{2}}$

Data in Appendix 8 (Tables A20, A21)

value of 160 rads when the dose rate was 160 rads/min and a D_0 value of 270 rads when the dose rate was 3 rads/min. These values were obtained for gamma irradiation of prepared dilutions of human fibroblasts attached on a flask, at room temperature. The discrepancy between their results and those of Arlett and Harcourt (1980) remains to be explained but is perhaps related to the stage of growth of cells and to their physical state during irradiation.

Normal and AR Human Fibroblast Response to Hydrogen Peroxide

Since it has been suggested that the AR sensitivity is related to an increased load of reactive oxygen species, the AR cellular response to H_2O_2 was determined.

The experiments were designed so that the appropriate concentrations of H_2O_2 were added to attached cells, prepared as described previously, 48 hrs after plating. H_2O_2 was added in the full growth medium of the cells in the dark. The plates were placed in boxes, gassed and kept in the dark at room temperature for a 24 hr period at the end of which the medium was discarded and fresh medium added. Boxes were regassed and incubated as normal.

The mean result of 2 replicate experments for each cell line is shown in Fig. 41. Both curves were characterized by a shoulder followed by exponential inactivation which proceeded at approximately double the rate in AR cells (D_0 for AR=3.77 μM, D_0 for GM=6.65 μM). These results can be compared with other published data such as that of Hoffmann and Meneghini (1979b) who found the average H_2O_2 concentration that corresponds to 37 per cent survival to be 9.6 $\pm$ 2.5 μM for an SV40 transformed WI-38 cell line, VA13. Our corresponding values would be 15.4 μM for AR cells and 21.1 μM

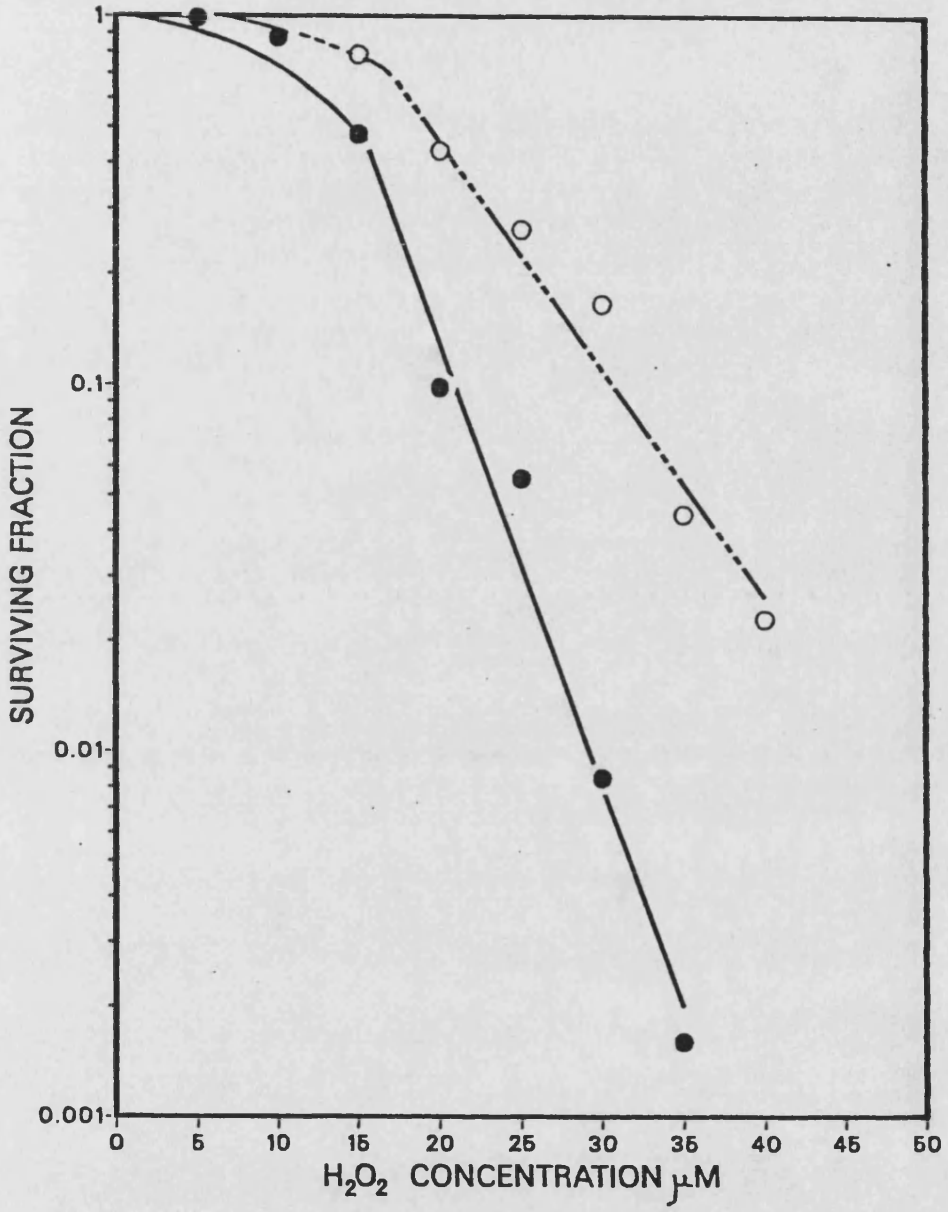

Figure 41. The inactivation of AR6LO (●,——) and GM730 (○,- - - - - -) cells by hydrogen peroxide treatment for 24 hours, at room temperature (20°C), in the dark. Mean experimental points at each concentration and calculated mean lines from duplicate experiments depicted.

TABLE 13

SURVIVAL PARAMETERS FOR THE INACTIVATION OF AR6LO AND GM730 CELLS BY H_2O_2

Cell Line	Expt.	Slope μM^{-1}	Standard Deviation	Intercept y-axis	Standard Deviation	D0 μM	Dq μM	D10 μM
AR6LO	78	1.11×10^{-1}	3.06×10^{-2}	1.46×10^{0}	7.40×10^{-1}	3.91×10^{0}	1.31×10^{1}	2.22×10^{1}
	79	1.20×10^{-1}	3.90×10^{-2}	1.43×10^{0}	1.00×10^{-1}	3.62×10^{0}	1.19×10^{1}	2.03×10^{1}
	Mean	$\mathbf{1.16 \times 10^{-1}}$		$\mathbf{1.45 \times 10^{0}}$		$\mathbf{3.77 \times 10^{0}}$	$\mathbf{1.25 \times 10^{1}}$	$\mathbf{2.13 \times 10^{1}}$
GM730	80	5.59×10^{-2}	7.98×10^{-3}	9.06×10^{-1}	2.30×10^{-1}	7.77×10^{0}	1.62×10^{1}	3.41×10^{1}
	81	7.86×10^{-2}	1.92×10^{-3}	9.98×10^{-1}	5.52×10^{-1}	5.52×10^{0}	1.27×10^{1}	2.54×10^{1}
	Mean	$\mathbf{6.73 \times 10^{-2}}$		$\mathbf{9.52 \times 10^{-1}}$		$\mathbf{6.65 \times 10^{0}}$	$\mathbf{1.45 \times 10^{1}}$	$\mathbf{2.98 \times 10^{1}}$

Data in Appendix 8 (Table A22)

for GM730 cells. This difference is not very large, considering the differences in methodology, their cells being incubated with H_2O_2 for 30 minutes at 37°C. Ward et al. (1985) claim that cells are more resistant at 0° than at 37°C, which is consistent with our results, obtained at 20°C, which showed an increased cellular resistance relative to that reported by Hoffmann and Meneghini (1979b).

The mechanism of damage by H_2O_2 has not yet been elucidated. H_2O_2 has been shown to produce single-strand breaks in cellular DNA of V-79 cells and human fibroblasts (Ward et al., 1985; Hoffmann and Meneghini, 1979b) but not in purified DNA (Hoffmann and Meneghini, 1979b). This has led to the conclusion that another, intracellularly generated, species exerts this damage and $OH^{\bullet}$ is the most probable candidate. However, the importance of these single-strand breaks in inducing lethality is not known since they are effectively repaired, 90 per cent of the original single-strand breaks induced by 0.1 mM H_2O_2 in human fibroblasts being repaired within 10 hours (Hoffmann and Meneghini, 1979b). A similar conclusion is reached by Ward et al. (1985) who suggest that single-strand breaks are ineffectual in causing cell death.

Therefore, another DNA or possibly non-DNA lesion could lead to lethality but there have been no speculations regarding its identity. The AR cells show a sensitivity to this agent which is consistent with the previous proposal that they may have an inability to scavenge reactive oxygen species. H_2O_2 addition to a biological system can be considered to increase the load of several other oxygen species. The generation of $OH^{\bullet}$ at a particular site would be possible via a metal-catalyzed Haber-Weiss reaction, and

could be expected to have important consequences for cell survival. If this site happened to be a membrane site, as $OH^{\bullet}$ is known to be a very good hydrogen abstractor, it would be able to start a chain of lipid peroxidation reactions. In vitro sudies have shown hydrogen peroxide and superoxide anions to be able to cause peroxidation of fatty acids via the generation of hydroxyl radicals and singlet oxygen which directly oxidize the unsaturated fatty acids (Kellogg and Fridovich, 1975). It is not clear whether lipid peroxidation can lead to cell lethality directly but it would severely damage membranes. Alternatively, lethal damage may occur in cellular DNA where $OH^{\bullet}$ is thought to cause single-strand breaks. Botcherby et al. (1984) have already reported an increased incidence of single-strand breaks in actinic reticuloid (relative to normal) cellular DNA following broad-band near-UV irradiation, at room temperature, in DMEM growth medium. Under these irradiation conditions toxic photoproducts such as hydrogen peroxide and at particular sites, $OH^{\bullet}$, would be expected to be formed. Whether near-UV induced single-strand breaks are more effective in causing cell death in AR cells than normal cells is a point that needs further examination.

It might be postulated that normal cells do not suffer damage to the same extent since they might be more able to remove both H_2O_2 and other resulting species before lesion formation. An alternative proposal would be that lesion formation takes place in both cell lines but, whereas normal cells are able to repair it to a certain extent, AR cells may have a defect in a repair process and hence show an increased sensitivity.

RESULTS AND DISCUSSION

PART 3

THE EFFECT OF A VITAMIN E ANALOGUE, TROLOX-C, ON THE SENSITIVITY OF NORMAL AND ACTINIC RETICULOID FIBROBLASTS TO NEAR-UV RADIATION

In order to test the hypothesis that AR cells have a reduced ability to cope with an excess of reactive oxygen species and possible other free radicals formed during near-UV irradiation, the effect of an antioxidant on the inactivation of AR cells by UV-light was examined. The choice of vitamin E was made due to its lipid soluble character which allows it to concentrate in cellular membranes, a possible target for near-UV-induced lethality. Embedded in the membranes, it is thought both to scavenge singlet oxygen (Grams and Eskins, 1972; Foote et al., 1974) and superoxide radicals (Yagi et al., 1978; Ozawa and Hanaki, 1985) and also to terminate lipid peroxidation reactions (Witting, 1980). Additionally, it can provide structural support to membranes by interacting with the fatty acids of membrane phospholipids (Diplock and Lucy, 1973; Srivastava et al., 1983).

Practical problems of handling lipid soluble forms of vitamin E made the use of the water-soluble analogue, Trolox-C, in which the long hydrocarbon chain is substituted by a -COOH group, preferable. Although this hydrocarbon chain was originally thought to assist in the interaction of vitamin E and the fatty acids of membrane lipids it has recently been shown that the interaction takes place via the methyl and hydroxyl groups of the chromanol nucleus (Erin et al., 1985) which are retained in the Trolox-C analogue as seen below. The

structure of alpha-tocopherol acetate is also included for future reference.

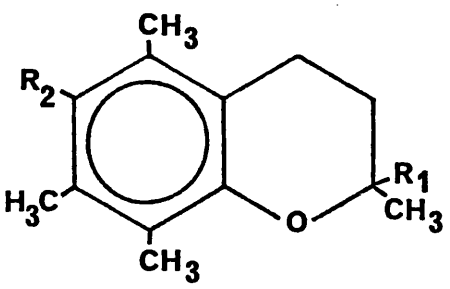

R1	R2	
$-CH_2(CH_2CH_2\underset{\displaystyle CH_3}{\underset{\vert}{C}}HCH_2)_3H$	-OH	Vitamin E
$-CH_2(CH_2CH_2\underset{\displaystyle CH_3}{\underset{\vert}{C}}HCH_2)_3H$	$-O\overset{\displaystyle O}{\overset{\Vert}{C}}CH_3$	Alpha-tocopherol acetate
-COOH	-OH	Trolox-C

The Use of Trolox-C in the Pre- or Post Irradiation Medium

For use in the experiments described, 1 mg/ml solutions of Trolox-C were prepared by the aseptic addition of the powdered form in sterile double distilled water. Since vitamin E can become oxidized, the solutions were only kept for use during the same day. Photooxidation of vitamin E also precluded its use during irradiation, so it was only used before and after irradiation.

When Trolox-C was incorporated in the post-irradiation medium 0.6 ml of the 1 mg/ml solution was added to the plates with the equivalent volume of double distilled water added to the controls. For this set of experiments the plates were prepared with 9 ml of medium to which 1 ml of cells were added so that approximately 60 µg/ml Trolox-C was present in the post-irradiation medium, during the incubation period. This concentration was chosen from a preliminary plating experiment in which out of the 1, 5, 10, 30 and 60 µg/ml Trolox-C concentrations used, 60 µg/ml was shown to increase the plating efficiency most.

An alternative method for using Trolox-C was to include it in the growth medium of the cells during the last subculture, 48 hours before the experiment. A 1.5 ml volume of the 1 mg/ml solution was added to 13.5 ml of the growth medium to give a 100 µg/ml concentration of Trolox-C. Trypsinization and washing of cells took place as normal before the experiment, so any effect seen could be attributed to the vitamin being actively taken up during the growth of the cells.

The Effect of Trolox-C on the Growth Characteristics of Normal and AR Fibroblasts

The effect of Trolox-C on the growth characteristics of the cells was determined in order to exclude the possibility of any adverse toxicity. Growth curves in the presence and absence of 30 μg/ml Trolox-C in the medium were constructed and are shown in Fig. 42 for AR (Panel A) and GM730 cells (Panel B). Experimental details are included in Appendix 6. It can be seen that at the concentration used, Trolox-C did not significantly alter the growth characteristics of either cell line but it markedly reduced the initial fall in cell number observed during the first 48 hours following subculture. Therefore this loss of cells, which was more pronounced for AR cells, may be due to some damage which can be partially alleviated by Trolox-C.

The Effect of Trolox-C and Alpha-Tocopherol Acetate on the Near-UV (365 nm) Inactivation of Normal and AR Fibroblasts

The effect of the vitamin E analogue, Trolox-C, on the sensitivity of AR cells to 365 nm, at 25°C, was investigated. These irradiation conditions were chosen as they show a difference in sensitivity between AR and normal cells. The Trolox-C was included in the post-irradiation medium, at a concentration of 60 μg/ml, as in this way a direct comparison could be made with the same cell suspension plated in medium with and without Trolox-C.

The results obtained are shown in Fig. 43. The points represent the mean of 3 matched experiments for AR cells (Panel A) and of 2 experiments for GM730 cells (Panel B). The calculated

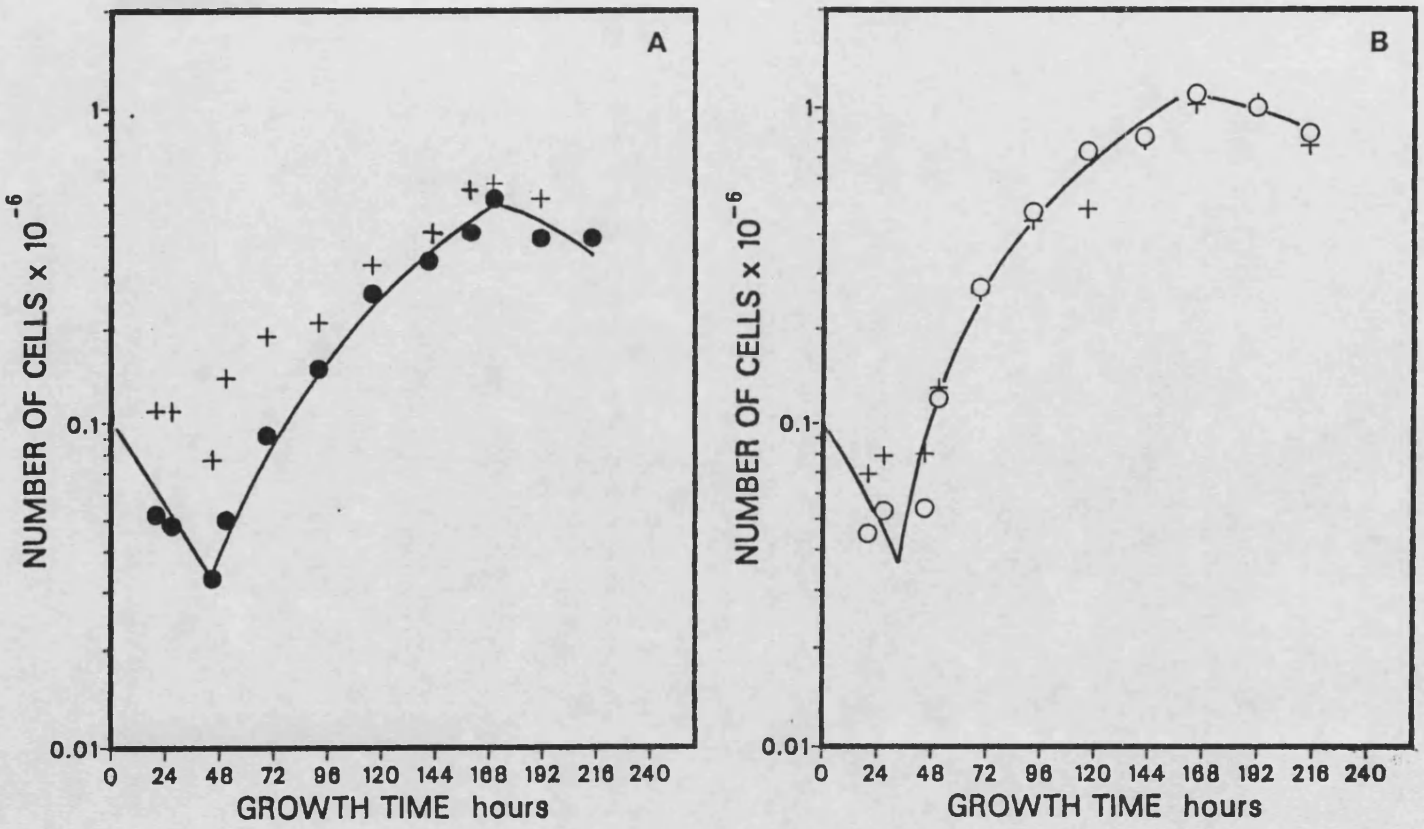

Figure 42. Growth curves for (A) AR6LO and (B) GM730 cells in EMEM in the absence (● , ○) and presence (+ , +) of 30 μg/ml Trolox-C.

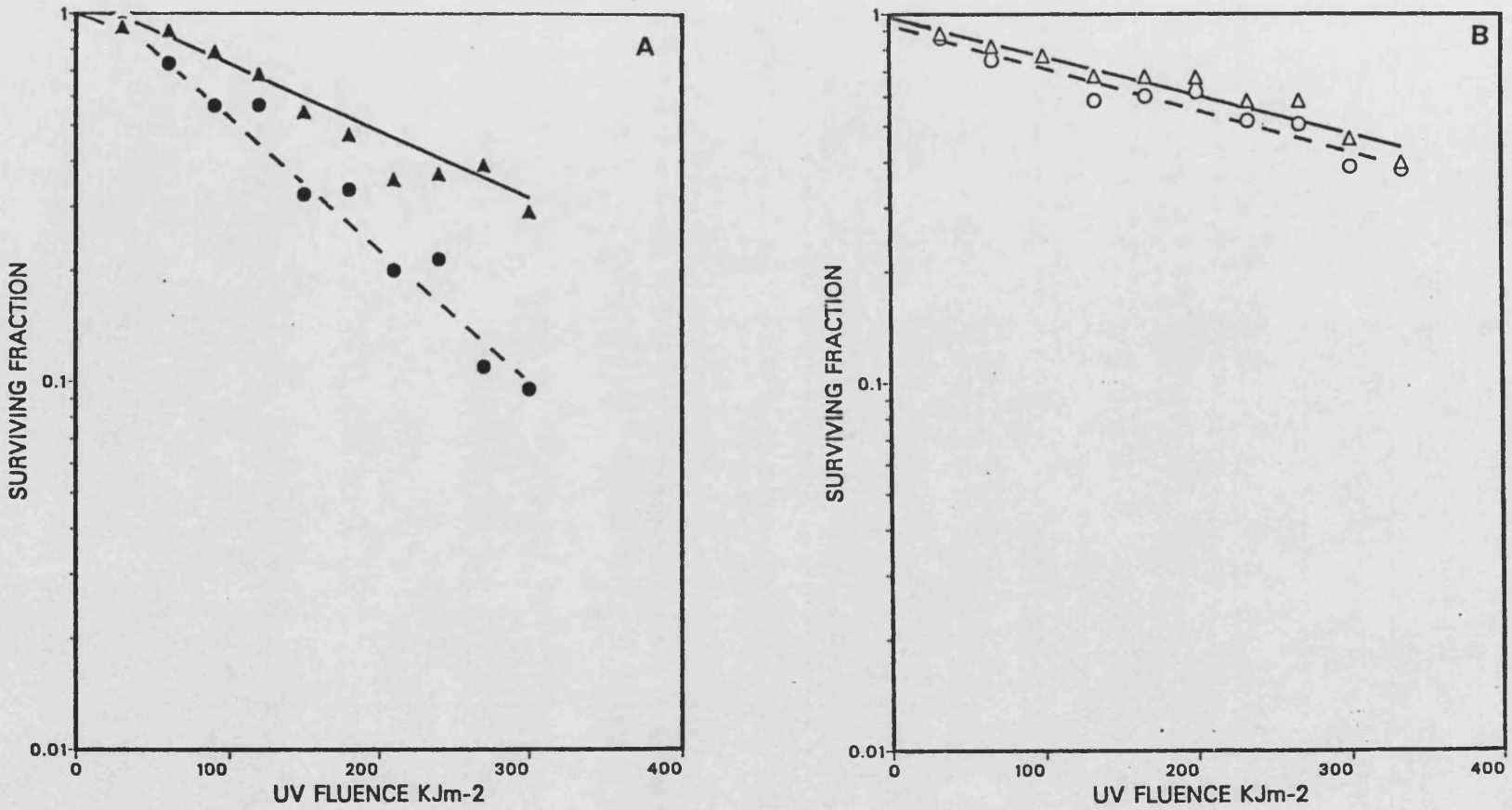

Figure 43. The inactivation of (A) AR6LO and (B) GM730 cells by 365 nm irradiation at 25°C, in the absence (● , ○ , dashed line) and the presence (▲ , △ , solid line) of 60 μg/ml Trolox-C in the plating medium. Mean experimental points at each fluence and calculated mean lines from individual experiments depicted.

TABLE 14

SURVIVAL PARAMETERS FOR THE INACTIVATION OF AR6LO AND GM730 CELLS BY 365 NM AT 25°C, IN THE PRESENCE AND ABSENCE OF 60 μg/ml TROLOX-C IN THE PLATING MEDIUM

Cell Line	Trolox C	Expt. No.	Slope $(Jm^{-2})^{-1}$	Standard Deviation	Intercept y-axis	Standard Deviation	$D0_2$ Jm^{-2}	Dq_2 Jm^{-2}	$D10$ Jm^{-2}
AR6LO	+	82	2.68×10^{-6}	2.74×10^{-7}	8.40×10^{-2}	5.10×10^{-2}	1.62×10^{5}	3.13×10^{4}	4.04×10^{5}
	+	83	1.47×10^{-6}	2.46×10^{-7}	5.51×10^{-3}	4.59×10^{-2}	2.96×10^{5}	3.75×10^{3}	6.84×10^{5}
	+	84	1.80×10^{-6}	1.34×10^{-7}	4.60×10^{-2}	2.26×10^{-2}	2.42×10^{5}	2.56×10^{4}	5.81×10^{5}
		Mean	$\mathbf{1.98\times10^{-6}}$		$\mathbf{4.52\times10^{-2}}$		$\mathbf{2.33\times10^{5}}$	$\mathbf{2.02\times10^{4}}$	$\mathbf{5.56\times10^{5}}$
AR6LO	-	48	4.09×10^{-6}	4.01×10^{-7}	7.21×10^{-2}	7.17×10^{-2}	1.06×10^{5}	1.76×10^{4}	2.62×10^{5}
	-	49	3.39×10^{-6}	2.10×10^{-7}	3.66×10^{-2}	3.26×10^{-2}	1.28×10^{5}	1.08×10^{4}	3.06×10^{5}
	-	50	3.31×10^{-6}	2.33×10^{-7}	1.39×10^{-1}	4.06×10^{-2}	1.31×10^{5}	4.19×10^{4}	3.44×10^{5}
		Mean	$\mathbf{3.60\times10^{-6}}$		$\mathbf{3.45\times10^{-2}}$		$\mathbf{1.22\times10^{5}}$	$\mathbf{2.34\times10^{4}}$	$\mathbf{3.04\times10^{5}}$
GM730	+	85	1.30×10^{-6}	1.60×10^{-7}	-2.35×10^{-2}	3.31×10^{-2}	3.34×10^{5}	-1.81×10^{4}	7.51×10^{5}
	+	86	7.96×10^{-7}	1.66×10^{-7}	4.65×10^{-3}	3.24×10^{-2}	5.45×10^{5}	5.84×10^{3}	1.26×10^{6}
		Mean	$\mathbf{1.05\times10^{-6}}$		$\mathbf{-9.43\times10^{-3}}$		$\mathbf{4.40\times10^{5}}$	$\mathbf{-6.13\times10^{3}}$	$\mathbf{1.01\times10^{6}}$
GM730	-	10	1.43×10^{-6}	1.64×10^{-7}	-1.58×10^{-2}	3.30×10^{-2}	3.04×10^{5}	-1.11×10^{4}	6.88×10^{5}
	-	11	8.42×10^{-7}	1.62×10^{-7}	-5.21×10^{-2}	3.35×10^{-2}	5.16×10^{5}	-6.19×10^{4}	1.13×10^{6}
		Mean	$\mathbf{1.14\times10^{-6}}$		$\mathbf{-3.40\times10^{-2}}$		$\mathbf{4.10\times10^{5}}$	$\mathbf{-3.65\times10^{4}}$	$\mathbf{9.09\times10^{5}}$

Data in Appendix 8 (Table A23)

parameters for the individual experiments are included in Table 14. The results clearly showed that the presence of Trolox-C protected the AR but not the normal cells. The protection of the AR cells by Trolox-C was such that their resistance was increased two-fold (Do=233 kJm^{-2} or 122 kJm^{-2} in the presence and absence of Trolox-C in the plating medium, respectively). An attempt was made to determine whether delay of addition of Trolox-C for different time periods would still result in measurable protection. The conclusion from two experiments, the results of which are shown in Table 15, was that Trolox-C added up to several hours after irradiation could still protect AR cells. This is consistent with the idea that Trolox-C may stop lipid peroxidation reactions which would be expected to be a slow process, but more experimental data are needed to clarify the length of this post-irradiation time period during which Trolox-C addition in the plating medium continues to be effective.

An alternative approach to the incorporation of Trolox-C was to include it in the pre-irradiation growth medium. Figure 44 A shows the results of two replicate experiments of AR cells grown in the presence of 100 µg/ml Trolox-C and irradiated with monochromatic 365 nm at 25°C. It can be seen that Trolox-C supplemented cells showed increased resistance to inactivation relative to the response in the absence of Trolox-C, shown as a dotted line, taken from the data in Fig. 31 A. As seen in Table 16 a fluence of 1300 kJm^{-2} was required to kill 90 per cent of the cells compared to 315 kJm^{-2} required for normally grown AR cells (Table 7).

In order to investigate whether a lipid-soluble form of vitamin E might afford greater protection to AR cells,

TABLE 15

SURVIVING FRACTION OF AR6LO CELLS TO A DOSE OF 365 NM RADIATION, IN THE PRESENCE OF 60 μg/ml TROLOX-C ADDED TO THE PLATING MEDIUM AT DIFFERENT TIMES FOLLOWING IRRADIATION

	Post-Irradiation Time Elapsed Before Trolox-C Addition (Hours)	Surviving Fraction$_2$ (UV Fluence:125 kJm^{-2})	Surviving Fraction$_2$ (UV Fluence:350 kJm^{-2})
Experiment 1	0	8.21×10^{-1}	6.67×10^{-1}
	2	8.25×10^{-1}	6.79×10^{-1}
	4	8.17×10^{-1}	6.43×10^{-1}
	8	7.14×10^{-1}	6.01×10^{-1}
	16	7.58×10^{-1}	5.87×10^{-1}
	30	8.45×10^{-1}	6.94×10^{-1}
	no Trolox-C	5.49×10^{-1}	3.22×10^{-1}
Experiment 2	0	7.09×10^{-1}	5.03×10^{-1}
	7	6.82×10^{-1}	5.23×10^{-1}
	21	6.70×10^{-1}	4.57×10^{-1}
	31	7.75×10^{-1}	4.70×10^{-1}
	45	7.29×10^{-1}	4.27×10^{-1}
	54	6.89×10^{-1}	3.84×10^{-1}
	70	5.70×10^{-1}	3.72×10^{-1}
	no Trolox-C	5.11×10^{-1}	3.75×10^{-1}

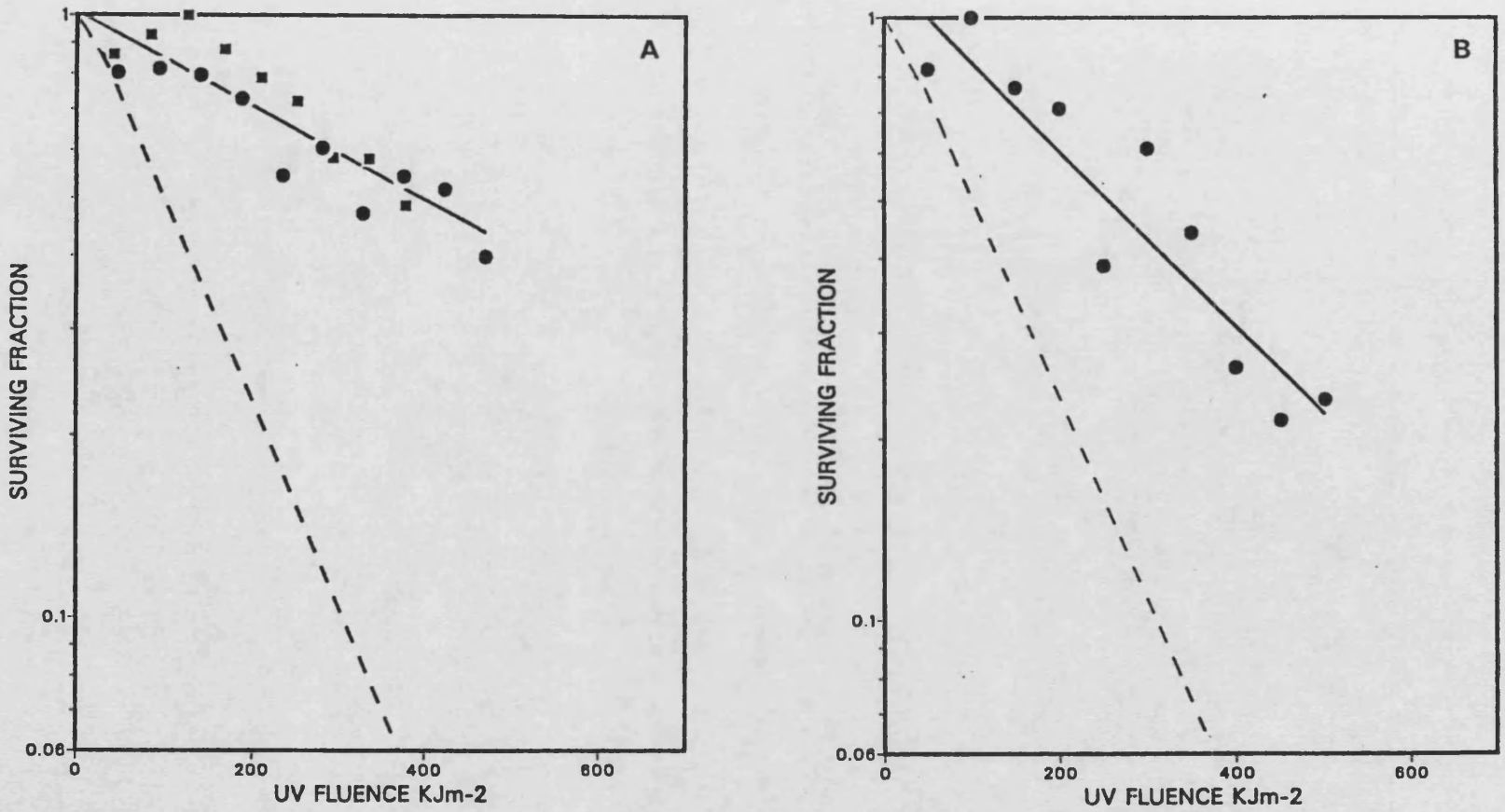

Figure 44. The inactivation of AR6LO grown (A) in the presence of 100 μg/ml Trolox-C or (B) 100 μg/ml alpha-tocopherol acetate, by 365 nm irradiation at 25°C. The different sets of symbols represent the results of replicate experiments. The dashed line represents the standard response of AR6LO as shown in Fig. 31.

TABLE 16

SURVIVAL PARAMETERS FOR THE INACTIVATION OF AR6LO CELLS GROWN IN THE PRESENCE OF 100 μg/ml TROLOX-C AND 100μg/ml ALPHA-TOCOPHEROL ACETATE BY 365 NM, AT 25°C

Grown in	Expt. No.	Slope $(Jm^{-2})^{-1}$	Standard Deviation	Intercept y-axis	Standard Deviation	$D0_2$ Jm^{-2}	Dq_2 Jm^{-2}	$D10$ Jm^{-2}
Trolox-C	87	7.05×10^{-7}	1.03×10^{-7}	-3.55×10^{-2}	2.29×10^{-2}	6.16×10^{5}	-5.04×10^{4}	1.37×10^{6}
	88	8.62×10^{-7}	1.42×10^{-7}	4.89×10^{-2}	3.34×10^{-2}	5.04×10^{5}	5.68×10^{4}	1.22×10^{6}
	Mean	$\mathbf{7.84\times10^{-7}}$		$\mathbf{6.70\times10^{-3}}$		$\mathbf{5.60\times10^{5}}$	$\mathbf{3.20\times10^{3}}$	$\mathbf{1.30\times10^{6}}$
alpha-Toc-acet.	89	1.50×10^{-7}	2.11×10^{-7}	9.10×10^{-2}	6.55×10^{-2}	2.90×10^{5}	4.37×10^{4}	7.10×10^{5}

Data in Appendix 8 (Table A24)

alpha-tocopherol acetate was included in the growth medium of the cells. Fig. 44 B shows the survivor curve obtained for AR cells grown in the presence of 100 µg/ml alpha-tocopherol acetate and irradiated with 365 nm at 25°C. The increase in resistance afforded by this form of vitamin E was less than that afforded by Trolox-C (D_{10}=710 kJm^{-2}) but it was still more than a two-fold increase. The reason for the acetate form providing only a partial protection could be either due to unsatisfactory blending of the vitamin in the medium, resulting in decreased availability to the cells, or due to a decreased interaction with lipids as a consequence of the presence of an acetate group instead of a hydroxyl group. This could prevent hydrogen bond formation between vitamin E and one of the oxygen atoms of the lipid. Such a difference between alpha-tocopherol and the corresponding acetate in binding with lipids has been shown by magnetic resonance studies (Srivastava et al., 1983).

The Effect of Trolox-C on the Far-UV (254 nm) Sensitivity of Normal and AR Fibroblasts

The effect of incorporating Trolox-C in the post-irradiation medium was also examined after 254 nm irradiation at 25°C. Fig. 45 shows the survivor curves obtained for AR (Panel A) and normal (Panel B) cells in which meaned results of two matched experiments are presented. The individual parameters for these experiments are included in Table 17. AR cells showed a small increase in D_0 when Trolox-C was present (17.5 compared to 13.7 Jm^{-2}) but this result should be treated with caution until a larger number of experiments is performed. The response of normal cells was not altered by the presence of Trolox-C in the plating medium.

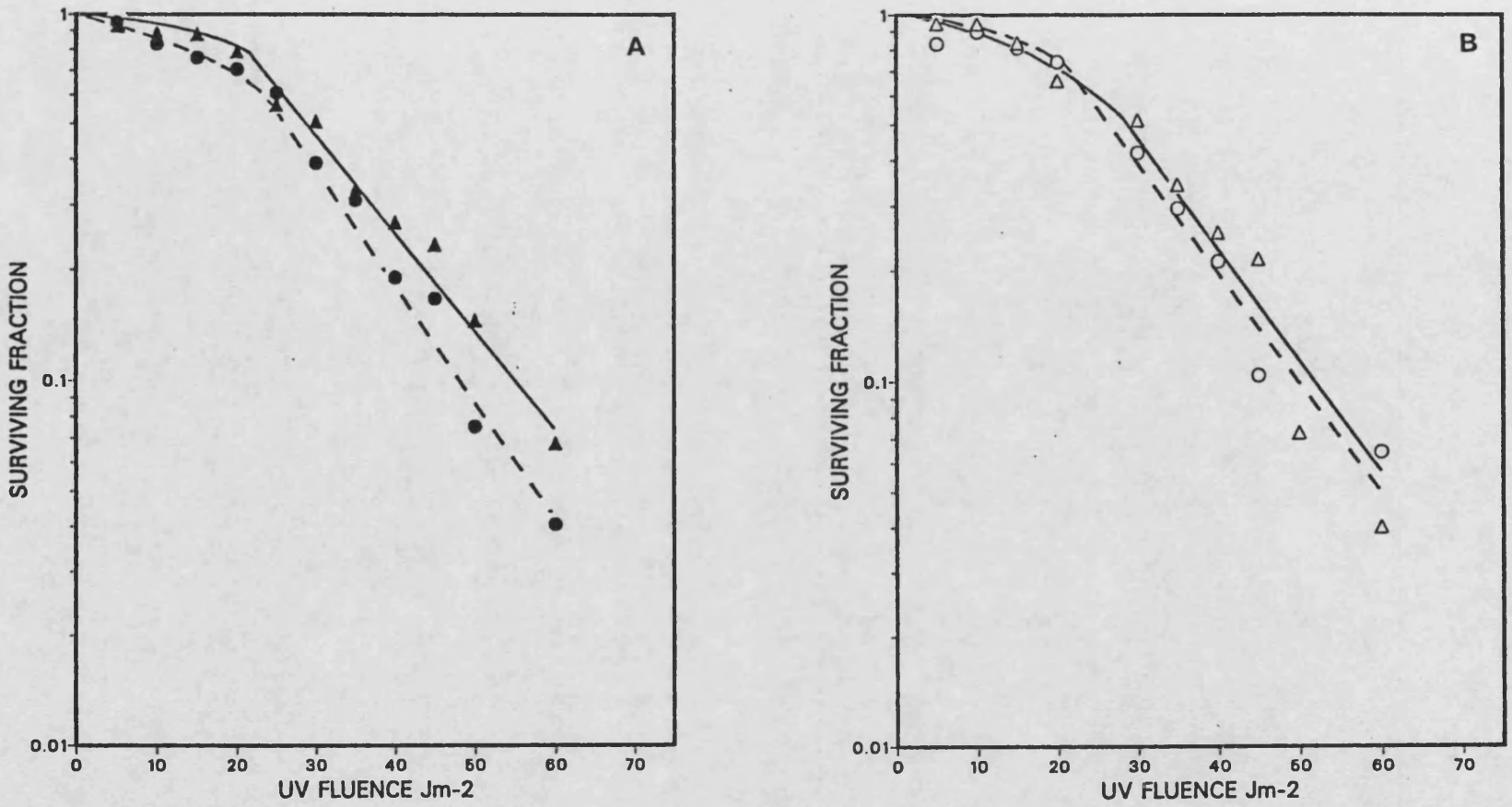

Figure 45. The inactivation of (A) AR6LO and (B) GM730 cells by 254 nm irradiation at 25°C, in the absence (● , ○ , dashed line) and in the presence (▲ , △ , solid line) of 60 μg/ml Trolox-C in the plating medium. Mean experimental points at each fluence and calculated mean lines depicted.

TABLE 17

SURVIVAL PARAMETERS FOR THE INACTIVATION OF AR6LO AND GM730 CELLS BY 254 NM AT 25°C IN THE PRESENCE AND ABSENCE OF 60 μg/ML TROLOX-C IN THE PLATING MEDIUM

Cell Line	Trolox C	Expt. No.	Slope $(Jm^{-2})^{-1}$	Standard Deviation	Intercept y-axis	Standard Deviation	$D0_2$ Jm^{-2}	Dq_2 Jm^{-2}	$D10$ Jm^{-2}
AR6LO	+	90	2.44×10^{-2}	2.45×10^{-3}	4.11×10^{-1}	8.94×10^{-2}	1.78×10^{1}	1.68×10^{1}	5.78×10^{1}
	+	91	2.54×10^{-2}	1.58×10^{-3}	4.01×10^{-1}	6.71×10^{-2}	1.71×10^{1}	1.58×10^{1}	5.52×10^{1}
		Mean	$\mathbf{2.49\times10^{-2}}$		$\mathbf{4.06\times10^{-1}}$		$\mathbf{1.75\times10^{1}}$	$\mathbf{1.63\times10^{1}}$	$\mathbf{5.65\times10^{1}}$
AR6LO	-	64	3.16×10^{-2}	3.42×10^{-3}	5.47×10^{-1}	1.25×10^{-1}	1.37×10^{1}	1.73×10^{1}	4.90×10^{1}
	-	65	3.17×10^{-2}	1.02×10^{-3}	5.07×10^{-1}	4.31×10^{-1}	1.37×10^{1}	1.60×10^{1}	4.75×10^{1}
		Mean	$\mathbf{3.17\times10^{-2}}$		$\mathbf{5.27\times10^{-1}}$		$\mathbf{1.37\times10^{1}}$	$\mathbf{1.67\times10^{1}}$	$\mathbf{4.83\times10^{1}}$
GM730	+	92	2.85×10^{-2}	7.01×10^{-3}	6.05×10^{-1}	2.66×10^{-1}	1.52×10^{1}	2.12×10^{1}	5.63×10^{1}
	+	93	3.19×10^{-2}	3.08×10^{-3}	5.34×10^{-1}	1.27×10^{-1}	1.36×10^{1}	1.67×10^{1}	4.81×10^{1}
		Mean	$\mathbf{3.02\times10^{-2}}$		$\mathbf{5.70\times10^{-1}}$		$\mathbf{1.44\times10^{1}}$	$\mathbf{1.90\times10^{1}}$	$\mathbf{5.22\times10^{1}}$
GM730	-	22	2.59×10^{-2}	2.17×10^{-3}	3.72×10^{-1}	9.34×10^{-2}	1.68×10^{1}	1.44×10^{1}	5.30×10^{1}
	-	21	3.35×10^{-2}	4.33×10^{-3}	5.99×10^{-1}	1.52×10^{-1}	1.30×10^{1}	1.79×10^{1}	4.77×10^{1}
		Mean	$\mathbf{2.97\times10^{-2}}$		$\mathbf{4.86\times10^{-1}}$		$\mathbf{1.49\times10^{1}}$	$\mathbf{1.62\times10^{1}}$	$\mathbf{5.04\times10^{1}}$

Data in Appendix 8 (Table A25)

Discussion

The results obtained when Trolox-C was used before and after the irradiation period show a clear protection of AR cells to inactivation by 365 nm wavelength. Possible lesion formation by near-UV wavelengths might be expected to be affected by the presence of Trolox-C in a multiplicity of ways.

At least part of near-UV damage is thought to occur through the formation of reactive oxygen species, the production of which as a consequence of near-UV radiation has been discussed previously. Trolox-C would be able to reduce the load of species such as $^1O_2$ and superoxide radical. To achieve this effect, the presence of Trolox-C would be necessary during the irradiation period as these species are short lived. Vitamin E is an excellent $^1O_2$ scavenger, one molecule of alpha-tocopherol has been shown to scavenge approximately 120 molecules of $^1O_2$ before itself becoming oxidized (Fahrenholtz et al., 1974). It is also the major lipid soluble scavenger of the superoxide radical. By this action, Trolox-C would prevent formation of lesions by these species and also prevent the formation of more reactive species such as $OH^{\cdot}$. Both $^1O_2$ and $OH^{\cdot}$ are known to react with unsaturated double bonds of fatty acids to start peroxidation of lipids which may lead to general disruption of membranes and cell death (Kellogg and Fridovich, 1975, 1977). The two separate issues of whether lipid peroxidation is a near-UV effect and whether lipid peroxidation leads to lethality, are yet to be resolved.

Trolox-C is able to terminate such reactions and this action could probably take place even if added in the plating medium, since lipid peroxidation reactions proceed slowly.

A physicochemical stability could also be provided by Trolox-C if present during the growth of cells and may contribute to an increased resistance of cells to near-UV irradiation, if membrane stability is an important factor.

This multiplicity of possible protective actions by Trolox-C makes the experimental observations more difficult to interpret. Some part of its action seems to be beneficial to all cells, whether irradiated or not, since its presence in the plating medium increases the plating efficiency of AR and to a lesser extent, GM730, as seen in Table 18 which summarizes the plating efficiencies of the matched experiments shown in Tables 14 and 17. A protective action to both cell lines, but more pronounced for AR cells, was also observed during the first two days following subculture (see Fig. 42).

TABLE 18
PLATING EFFICIENCIES OF AR AND GM730 CELLS IN THE PRESENCE AND ABSENCE OF 60 μg/ml TROLOX-C IN THE POST-IRRADIATION MEDIUM

	PLATING EFFICIENCY (%)			
	AR6LO		GM730	
	+Trolox-C	-Trolox-C	+Trolox-C	-Trolox-C
365 nm	25	21	48	41
	18	11	40	38
	33	20		
254 nm	21	15	27	24
	14	9	37	38

In summary, although part of the protective action by Trolox-C requires its presence intracellularly during irradiation, there is also some protective effect if Trolox-C is added after irradiation. If the AR sensitivity to 365 nm irradiation at 25°C is due to an enzymatic defect to deal with reactive oxygen species, then Trolox-C could be envisaged to exert a beneficial action by reducing the load of these reactive species. The presence of increased levels of reactive species in AR fibroblasts could possibly initiate lipid peroxidation reactions in cellular membranes and Trolox-C, by stopping these reactions, could provide cellular protection. Normal cells either do not suffer such damage due to efficient enzymatic mechanisms that keep the levels of reactive oxygen species under control with the result that addition of Trolox-C is of no further benefit, or alternatively normal cells are able to efficiently repair lesions produced both in the DNA of cells and in membranes.

RESULTS AND DISCUSSION

PART 4

THE EFFECT OF A PARTIALLY DEUTERATED IRRADIATION MEDIUM ON THE SENSITIVITY OF NORMAL AND ACTINIC RETICULOID FIBROBLASTS TO NEAR-UV RADIATION

The use of a deuterated solvent system during the irradiation procedure was designed to investigate the participation of reactive oxygen species in near-UV-induced lethality and in particular , the sensitivity of AR cells. In D_2O the lifetime of singlet oxygen is enhanced by up to a factor of 10 (Merkel et al., 1972) and this provides a diagnostic tool for the involvement of singlet oxygen in a variety of photochemical and photobiological processes (Kearns, 1979). More specifically, absence of potentiation of a reaction in D_2O implies non-involvement of singlet oxygen but potentiation does not necessarily prove a role for singlet oxygen since the concentration of other reactive species might also be increased in D_2O (Foote, 1979).

However, great care should be taken in interpreting results in a biological system since there is a multiplicity of other effects occurring when using D_2O. Deuterium is a stable isotope of hydrogen with an extra proton. It is represented by $^2H_2$ and can be exchanged with hydrogen in a molecule. This has important consequences on the reactivity of that molecule as deuterium bonds to carbon, nitrogen, oxygen, etc. are more stable than hydrogen bonds (primary isotope effect). Additionally, the presence of deuterium in a molecule may affect the reactivity even if the deuterium bond is not broken (secondary isotope effect). The

isotope effects coupled with the solvent effects of D_2O, *i.e.* differences in viscosity, conductivity, pH, solubility of gases, etc., can be expected to alter biological systems in a very complex way. In particular, a solvent effect that may be of considerable importance is its influence on the configuration of proteins in solution which can change from a helix to a random-coil form and *vice versa* (Thompson, 1963). Another aspect of the solvent effect of D_2O is its relationship to cellular and intracellular interfaces such as mitochondrial and nuclear membranes. Water at such interfaces is considered to resemble the structure of ice and this ice structure is thought to persist at a higher temperature in D_2O than in H_2O since there is a difference of $7^{\circ}C$ between their temperatures of maximum density (Thompson, 1963). Therefore, although the extension of the lifetime of singlet oxygen in D_2O medium is straightforward in a chemical system, it may not be the sole effect of such a change in the medium of living cells. Bearing in mind its limitations, the use of D_2O has been successfully employed in studies of photosensitization. Examples of such studies include the photosensitization of DNA by acridine in yeast cells (Kobayashi and Ito, 1976, 1977; Ito and Kobayashi, 1977) and the photosensitization of excitable cell membranes by various sensitizers (Pooler and Valenzeno, 1979).

Regarding near-UV-induced damage without exogenous addition of photosensitizers, by the use of D_2O, Peak *et al.* (1985b) have implicated $^1O_2$ involvement in the induction of DNA-protein crosslinks in human P3 teratocarcinoma cells in response to near-UV wavelengths (see Introduction, pages 18, 28 and Fig. 5).

The use of D_2O has also been studied in relation to its short and long term effects in the culture of bacterial and mammalian cells (Rothstein et al., 1960; DeGiovanni, 1960; Pollard, 1961; Joënje, et al., 1983). In this study it was decided to use D_2O during the irradiation period in order to investigate its effect on the sensitivity of human fibroblasts to specific monochromatic wavelengths under controlled conditions of irradiation.

The Use of Deuterium Oxide in the Irradiation Medium

PBS containing 3 parts double-distilled water and 7 parts D_2O was prepared as described in Materials and Methods (page 49). This solution, referred to as '70 per cent D_2O', was prepared in 10 ml quantities, in glass bottles, and kept for a maximum of 1 week at $4^{\circ}C$.

For use in an experiment, a 48 hour grown flask was trypsinized as normal and the cells were resuspended in 2 ml of 70 per cent D_2O. Following a 1 min centrifugation step as described previously, the cell pellet was resuspended in 70 per cent D_2O and diluted to 10^5 cells/ml. The cell suspension was then kept for 1 hour before irradiation so that equilibration in D_2O could take place. The samples which were removed during irradiation for the assessment of viability, remained undiluted for a further 20 min period, to allow any further effects to develop. Dilution in normal PBS and plating for the assessment of viability, followed as normal.

Toxicity of 70 per cent Deuterium Oxide to Normal and AR Fibroblasts

Toxic effects of D_2O are well documented depending on the concentration of D_2O, the cell type studied and the duration of the exposure (DeGiovanni, 1960; Ben-Hur and Riklis, 1980; Joënje et al., 1983). Investigations on the toxicity of a 70 per cent and a 45 per cent concentration of D_2O on both GM730 and AR cells under normal experimental conditions, i.e. stirring in the cuvette at 25°C, were first carried out. The results of the experiments included in Table 19 show that there was no significant loss of cell viability for up to 5 hours in either concentration of D_2O, so the higher concentration of D_2O was used in the following experiments.

TABLE 19
SURVIVING FRACTION OF AR6LO CELLS, STIRRED AT 25°C IN PBS CONTAINING 45% AND 70% D_2O

Time (min)	Surviving Fraction 45%D_2O	70% D_2O
30	1.01×10^{0}	8.51×10^{-1}
60	7.60×10^{-1}	8.24×10^{-1}
90	9.05×10^{-1}	8.65×10^{-1}
120	9.52×10^{-1}	8.92×10^{-1}
150	1.06×10^{0}	8.65×10^{-1}
180	1.05×10^{0}	9.32×10^{-1}
210	8.15×10^{-1}	7.30×10^{-1}
240	1.02×10^{0}	7.16×10^{-1}
270	8.05×10^{-1}	6.49×10^{-1}
300	7.45×10^{-1}	7.03×10^{-1}

Near-UV Inactivation of Normal and AR Fibroblasts in the Presence of 70 per cent Deuterium Oxide in the Irradiation Medium

The inactivation of AR and GM730 cells by 365 nm irradiation at 25°C in PBS containing 70 per cent D_2O was determined and the results are shown in Figures 46 and 47. The calculated parameters for the individual experiments are included in Table 20.

The sensitization observed in the presence of D_2O was large for both cell lines. Comparison of D_{10} values showed AR cells to be 2.4 times more sensitive in the presence of D_2O and GM730 cells to be 2.3 times more sensitive. However, it should be noted that the sensitization of GM730 cells became apparent only at doses greater than 200 kJm^{-2} and that the survivor curve depicted a large shoulder (D_q = 114 kJm^{-2}).

The same experiment was repeated at 0°C since there have been reports showing no effect of D_2O in the UV-sensitivity of mammalian cells (Ben-Hur and Riklis, 1980; Tyrrell, 1986). Indeed, as shown in Fig. 48 there was no alteration in the sensitivity of either cell line to 365 nm when irradiation was carried out at 0°C.

The Effect of the Incorporation of Trolox-C in the Post-Irradiation Medium

Trolox-C was incorporated in the plating medium to examine whether it would have a protective action following 365 nm irradiation as observed in the absence of D_2O (see Fig. 43). Fig. 49 shows that in two replicate experiments there was no protection offered by the presence of Trolox-C in the post-irradiation medium. This suggests that the presence of D_2O during the irradiation influences a mechanism of lethality that is completed quickly and

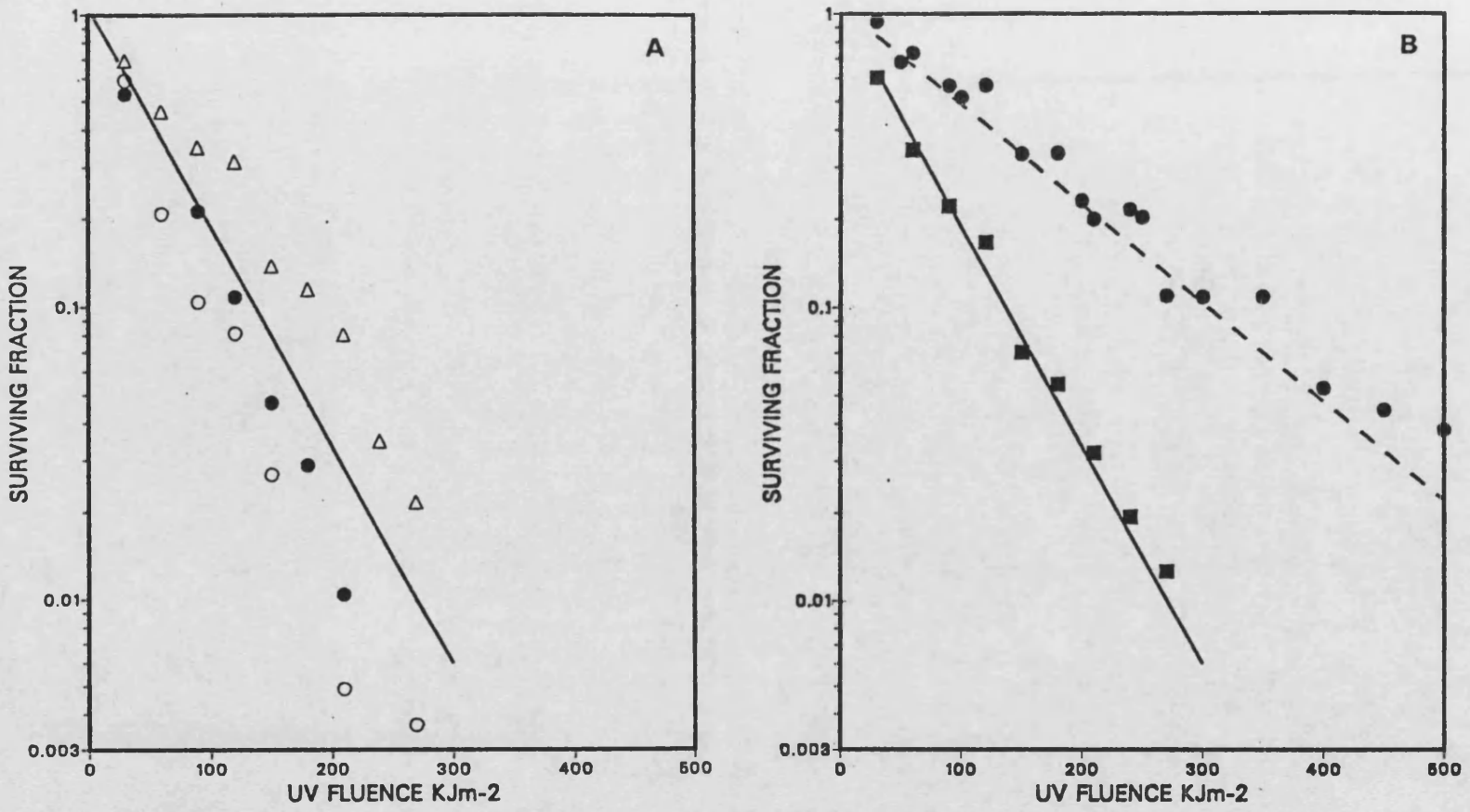

Figure 46. (A) The inactivation of AR6LO cells by 365 nm irradiation at 25°C in the presence of 70% D_2O in the irradiation medium. Different sets of symbols represent the results of replicate experiments.
(B) The inactivation of AR6LO cells by 365 nm irradiation at 25°C in the absence (●,---) and the presence (■,——) of 70% D_2O in the irradiation medium. Mean experimental points at each fluence and calculated mean lines from individual experiments are shown.

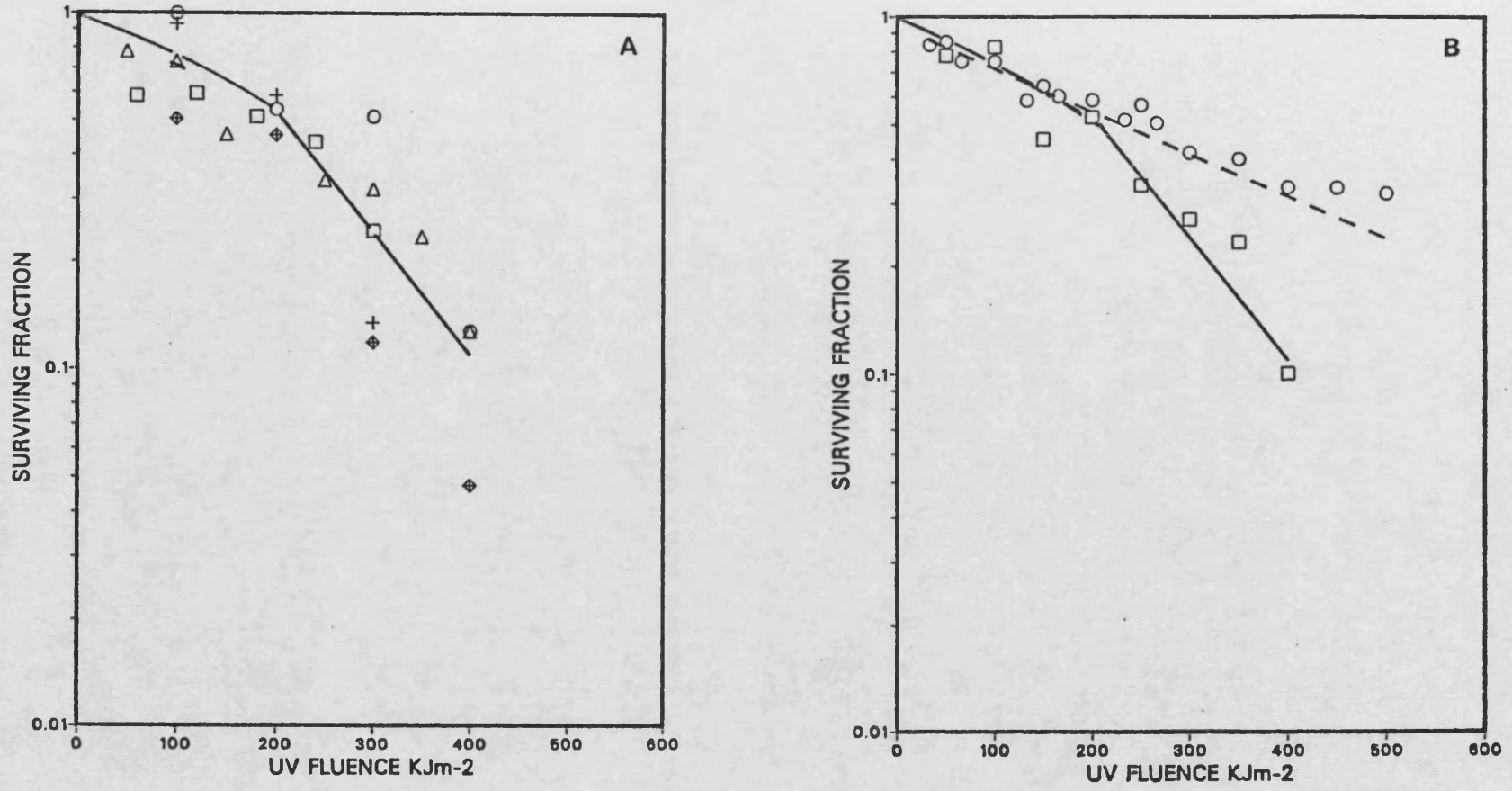

Figure 47. (A) The inactivation of GM730 cells by 365 nm irradiation at 25°C in the presence of 70% D_2O in the irradiation medium. Different sets of symbols represent the results of replicate experiments.
(B) The inactivation of GM730 cells by 365 nm irradiation at 25°C in the absence (○, ----) and the presence (□, ——) of 70% D_2O in the irradiation medium. Mean experimental points at each fluence and calculated mean lines from individual experiments are shown.

TABLE 20

SURVIVAL PARAMETERS FOR THE INACTIVATION OF AR6LO AND GM730 CELLS BY 365 NM AT 25°C IN THE PRESENCE OF 70% D_2O IN THE IRRADIATION MEDIUM

Cell Line	D_2O	Expt. No.	Slope $(Jm^{-2})^{-1}$	Standard Deviation	Intercept y-axis	Standard Deviation	$D0_{-2}$ Jm^{-2}	Dq_{-2} Jm^{-2}	$D10_{-2}$ Jm^{-2}
AR6LO	+	94	9.56×10^{-6}	6.31×10^{-7}	-5.32×10^{-2}	1.07×10^{-1}	4.54×10^{4}	-5.56×10^{3}	9.90×10^{4}
	+	95	9.48×10^{-6}	5.10×10^{-7}	1.07×10^{-1}	6.92×10^{-2}	4.58×10^{4}	1.13×10^{4}	1.17×10^{5}
	+	96	6.16×10^{-6}	4.02×10^{-7}	9.43×10^{-2}	6.78×10^{-2}	7.05×10^{4}	1.53×10^{4}	1.78×10^{5}
		Mean	$\mathbf{8.40\times10^{-6}}$		$\mathbf{4.94\times10^{-2}}$		$\mathbf{5.39\times10^{4}}$	$\mathbf{7.01\times10^{4}}$	$\mathbf{1.31\times10^{5}}$
AR6LO (Table 7)	-	**Mean**	$\mathbf{3.37\times10^{-6}}$		$\mathbf{2.81\times10^{-2}}$		$\mathbf{1.33\times10^{5}}$	$\mathbf{2.74\times10^{4}}$	$\mathbf{3.15\times10^{5}}$
AR6LO (+Trolox 60 µg/ml)	+	97	8.26×10^{-6}	7.13×10^{-7}	1.99×10^{-1}	7.10×10^{-2}	5.26×10^{4}	2.41×10^{4}	1.45×10^{5}
	+	98	9.45×10^{-6}	3.82×10^{-7}	1.61×10^{-1}	6.51×10^{-2}	4.59×10^{4}	1.70×10^{4}	1.23×10^{5}
		Mean	$\mathbf{8.86\times10^{-6}}$		$\mathbf{1.80\times10^{-1}}$		$\mathbf{4.93\times10^{4}}$	$\mathbf{2.06\times10^{4}}$	$\mathbf{1.34\times10^{5}}$
GM730	+	99	2.81×10^{-6}	7.56×10^{-7}	2.90×10^{-1}	2.49×10^{-2}	1.55×10^{5}	1.04×10^{5}	4.59×10^{5}
		100	4.91×10^{-6}	5.30×10^{-7}	6.08×10^{-1}	1.65×10^{-2}	8.84×10^{4}	1.24×10^{5}	3.27×10^{5}
		101	3.12×10^{-6}	1.68×10^{-6}	4.51×10^{-1}	5.23×10^{-2}	1.39×10^{5}	1.44×10^{5}	4.65×10^{5}
		102	2.69×10^{-6}	8.63×10^{-7}	2.24×10^{-1}	2.11×10^{-2}	1.61×10^{5}	8.31×10^{4}	4.55×10^{5}
		Mean	$\mathbf{3.38\times10^{-6}}$		$\mathbf{3.93\times10^{-1}}$		$\mathbf{1.36\times10^{5}}$	$\mathbf{1.14\times10^{5}}$	$\mathbf{4.27\times10^{5}}$
GM730 (Table 2)	-	**Mean**	$\mathbf{1.19\times10^{-6}}$		$\mathbf{-2.86\times10^{-2}}$		$\mathbf{4.26\times10^{5}}$	$\mathbf{-1.75\times10^{4}}$	$\mathbf{9.63\times10^{5}}$

Data in Appendix 8 (Tables A26, A27)

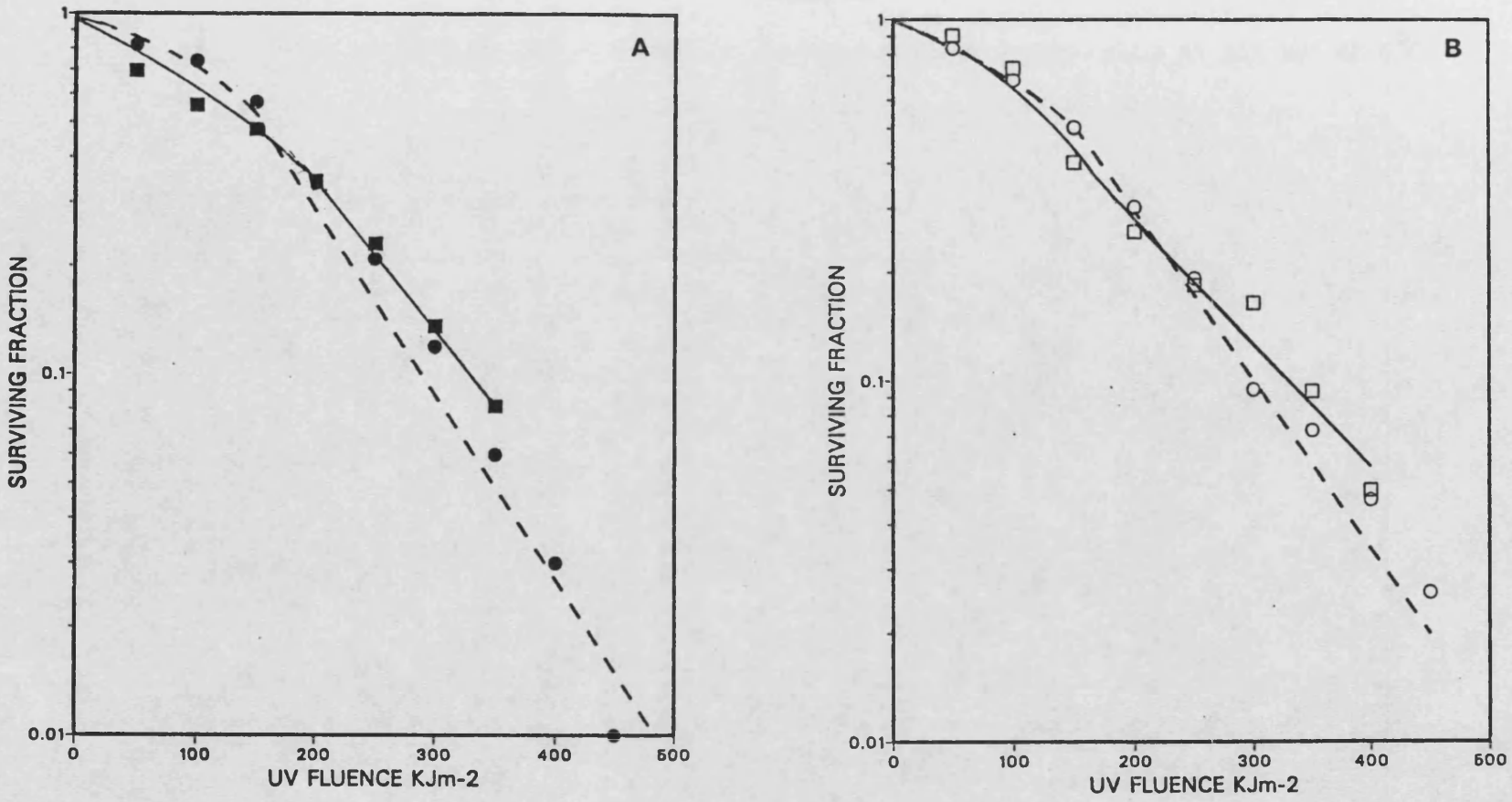

Figure 48. The inactivation of (A) AR6L0 and (B) GM730 cells by 365 nm irradiation at 0°C, in the absence (● , ○ , dashed line) and the presence (■ , □ , solid line) of 70% D_2O in the irradiation medium. Mean experimental points at each fluence and calculated mean lines from duplicate experiments shown.

TABLE 21

SURVIVAL PARAMETERS FOR THE INACTIVATION OF AR6LO AND GM730 CELLS BY 365 NM AT 0°C

IN THE PRESENCE OF 70% D_2O IN THE IRRADIATION MEDIUM

Cell Line	D_2O	Expt. No.	Slope $(Jm^{-2})^{-1}$	Standard Deviation	Intercept y-axis	Standard Deviation	D0 Jm^{-2}	Dq Jm^{-2}	D10 Jm^{-2}
AR6LO	+	103	3.49×10^{-6}	4.80×10^{-7}	2.31×10^{-1}	1.25×10^{-1}	1.24×10^{5}	6.60×10^{4}	3.53×10^{5}
		104	4.38×10^{-6}	6.33×10^{-7}	3.74×10^{-1}	1.63×10^{-1}	9.91×10^{4}	8.54×10^{4}	3.14×10^{5}
		Mean	$\mathbf{3.94\times10^{-6}}$		$\mathbf{3.03\times10^{-1}}$		$\mathbf{1.12\times10^{5}}$	$\mathbf{7.57\times10^{4}}$	$\mathbf{3.34\times10^{5}}$
AR6LO (Table 9)	-	**Mean**	$\mathbf{5.15\times10^{-6}}$		$\mathbf{4.92\times10^{-1}}$		$\mathbf{8.80\times10^{4}}$	$\mathbf{9.56\times10^{4}}$	$\mathbf{2.98\times10^{5}}$
GM730	+	105	3.62×10^{-6}	5.42×10^{-7}	2.41×10^{-1}	1.54×10^{-1}	1.20×10^{5}	6.66×10^{4}	3.43×10^{5}
		106	3.18×10^{-6}	3.71×10^{-7}	6.21×10^{-3}	1.07×10^{-1}	1.37×10^{5}	1.96×10^{3}	3.16×10^{5}
		Mean	$\mathbf{3.40\times10^{-6}}$		$\mathbf{1.23\times10^{-1}}$		$\mathbf{1.29\times10^{5}}$	$\mathbf{3.43\times10^{4}}$	$\mathbf{3.30\times10^{5}}$
GM730 (Table 2)	-	**Mean**	$\mathbf{4.71\times10^{-6}}$		$\mathbf{4.15\times10^{-1}}$		$\mathbf{9.63\times10^{4}}$	$\mathbf{8.29\times10^{4}}$	$\mathbf{3.05\times10^{5}}$

Data in Appendix 8 (Table A28)

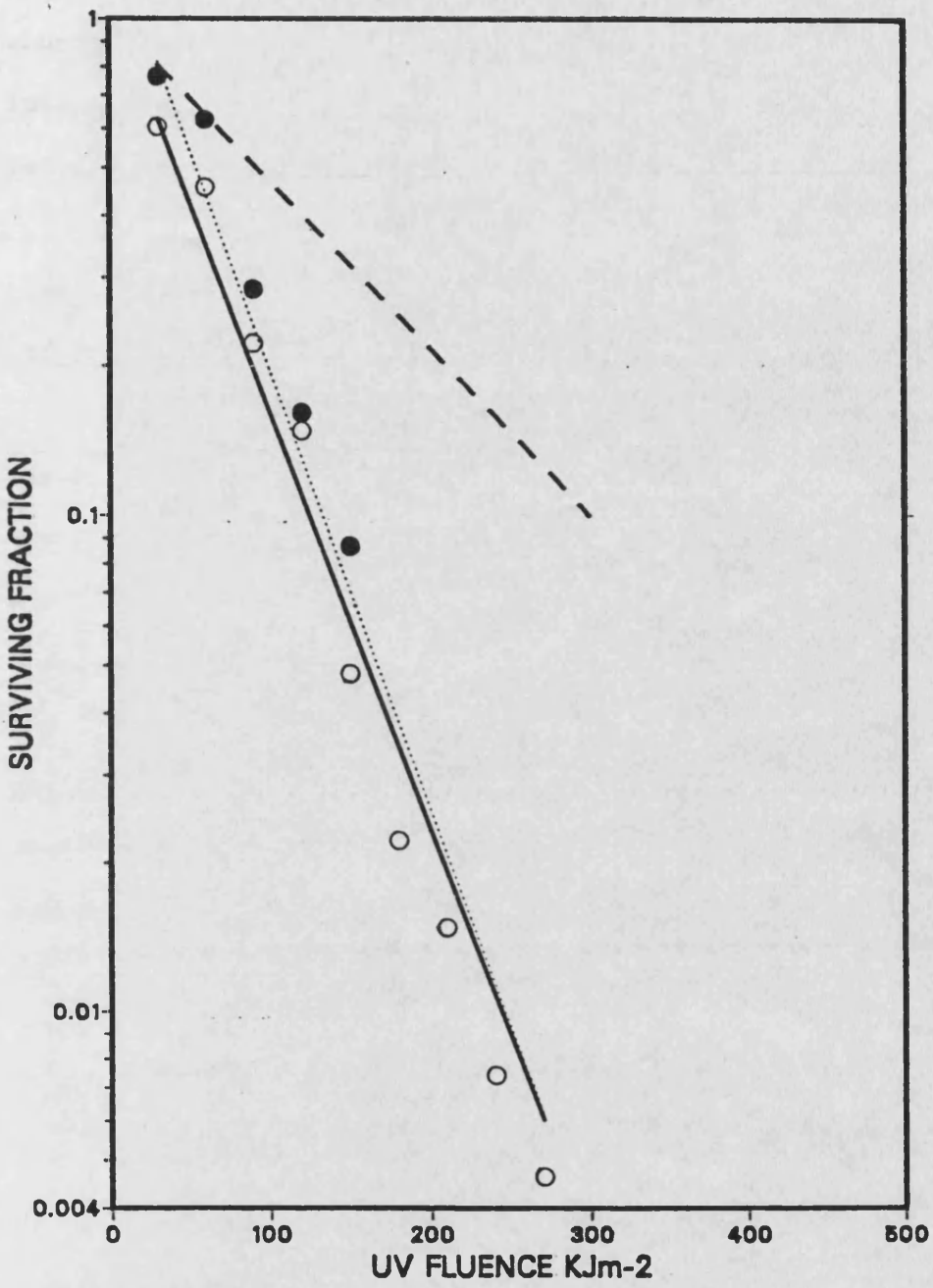

Figure 49. The inactivation of AR6L0 cells by 365 nm irradiation at 25°C, in the the presence of 70% D_2O and the presence of 60 μg/ml Trolox-C in the plating medium. The different sets of symbols represent the results of replicate experiments. The dotted line represents the response in the absence of Trolox-C (Fig. 46A) and the dashed line represents the standard response of AR6L0 to 365 nm, at 25°C (Fig. 31A)

cannot be reversed during post-irradiation incubation. It would be interesting to examine whether cells grown in Trolox-C would be better protected.

Far-UV Inactivation of Normal and AR Fibroblasts in the Presence of 70 per cent Deuterium Oxide in the Irradiation Medium

As with other results, examination of the cellular response to far-UV irradiation was essential before formulating any ideas as to the mechanisms underlying the observed effects. The response of AR and GM730 cells to 254 nm irradiation at 25°C, in the presence and absence of 70 per cent D_2O in the irradiation medium, was obtained and the results are shown in Fig. 50. Comparison of the calculated parameters for the individual experiments, included in Table 22, shows no alteration of the sensitivity of the cells by D_2O. This result indicates that there is no significant alteration in the DNA molecule by the use of the deuterated solvent, otherwise pyrimidine dimer formation would be expected to be altered and lead to an altered survival response as well.

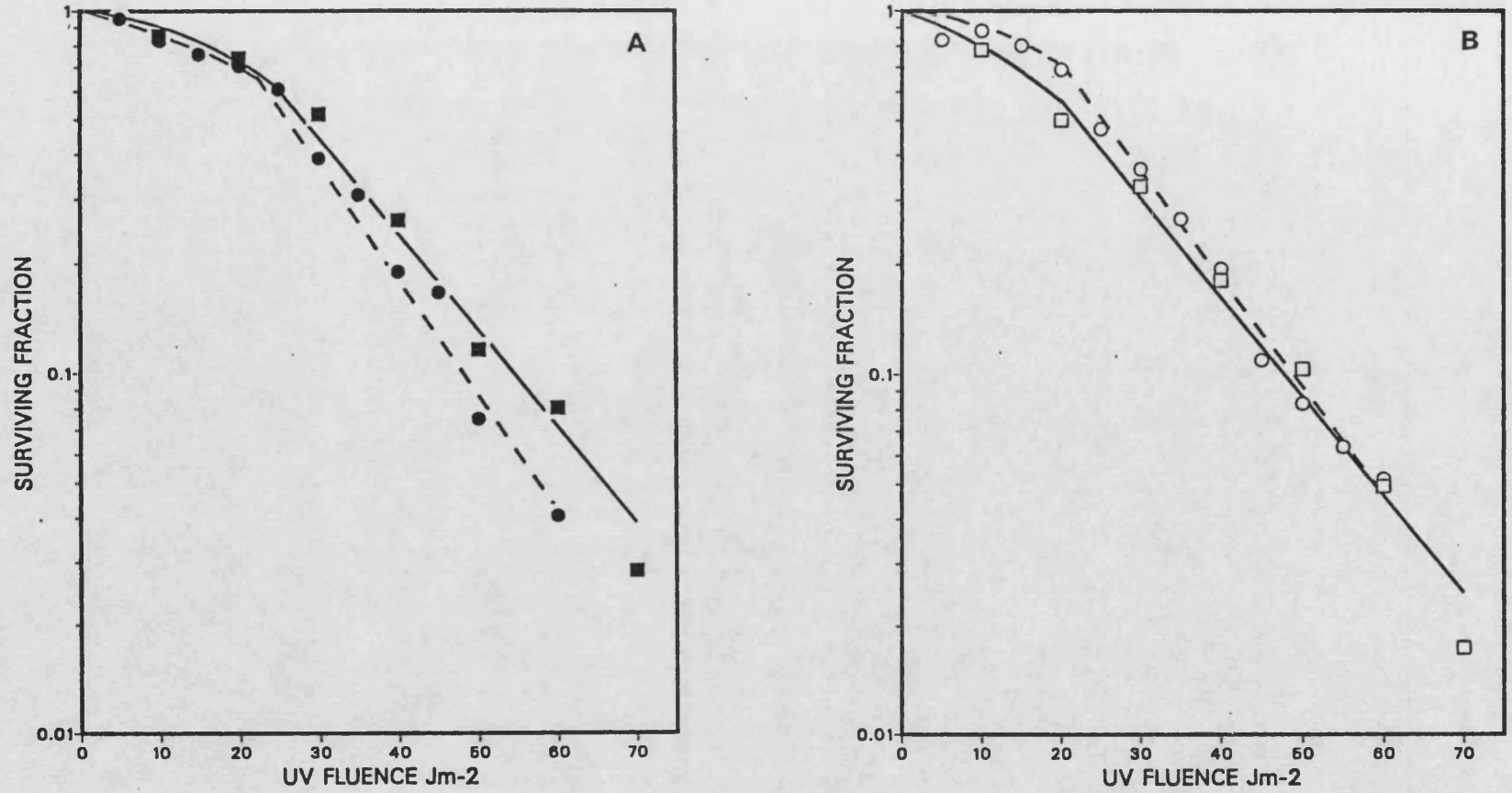

Figure 50. The inactivation of (A) AR6L0 and (B) GM730 cells by 254 nm irradiation at 25°C, in the absence (● , ○ , dashed line) and the presence (■ , □ , solid line) of 70% D_2O in the irradiation medium. Mean experimental points at each fluence and calculated mean lines from duplicate experiments shown.

TABLE 22

SURVIVAL PARAMETERS FOR THE INACTIVATION OF AR6LO AND GM730 CELLS BY 254 NM AT 25°C

IN THE PRESENCE OF 70% D_2O IN THE IRRADIATION MEDIUM

Cell Line	D_2O	Expt. No.	Slope $(Jm^{-2})^{-1}$	Standard Deviation	Intercept y-axis	Standard Deviation	D0 Jm^{-2}	Dq Jm^{-2}	D10 Jm^{-2}
AR6LO	+	107	2.47×10^{-2}	2.97×10^{-3}	4.30×10^{-1}	1.26×10^{-1}	1.76×10^{1}	1.74×10^{1}	5.79×10^{1}
		108	2.80×10^{-2}	1.19×10^{-3}	4.51×10^{-1}	5.71×10^{-2}	1.55×10^{1}	1.61×10^{1}	5.18×10^{1}
		Mean	$\mathbf{2.64\times10^{-2}}$		$\mathbf{4.41\times10^{-1}}$		$\mathbf{1.66\times10^{1}}$	$\mathbf{1.68\times10^{1}}$	$\mathbf{5.49\times10^{1}}$
AR6LO (Table 10)	-	**Mean**	$\mathbf{3.17\times10^{-2}}$		$\mathbf{5.27\times10^{-1}}$		$\mathbf{1.37\times10^{1}}$	$\mathbf{1.67\times10^{1}}$	$\mathbf{4.83\times10^{1}}$
GM730	+	109	2.37×10^{-2}	1.22×10^{-3}	9.51×10^{-2}	5.18×10^{-2}	1.83×10^{1}	4.01×10^{0}	4.62×10^{1}
		110	3.02×10^{-2}	2.78×10^{-3}	4.89×10^{-1}	1.34×10^{-1}	1.44×10^{1}	1.62×10^{1}	4.93×10^{1}
		Mean	$\mathbf{2.70\times10^{-2}}$		$\mathbf{2.92\times10^{-1}}$		$\mathbf{1.64\times10^{1}}$	$\mathbf{1.01\times10^{1}}$	$\mathbf{4.78\times10^{1}}$
GM730 (Table 3)	-	**Mean**	$\mathbf{2.95\times10^{-2}}$		$\mathbf{4.44\times10^{-1}}$		$\mathbf{1.49\times10^{1}}$	$\mathbf{1.49\times10^{1}}$	$\mathbf{4.92\times10^{1}}$

Data in Appendix 8 (Table A29)

Discussion

The presence of 70 per cent D_2O in the irradiation medium resulted in sensitization of both normal and AR cells to 365 but not 254 nm irradiation. The sensitization became apparent, for both cell lines, when irradiation took place at 25°C but not 0°C. Several explanations could be put forward for this effect.

It is known that singlet oxygen can lead to the formation of other reactive oxygen species through various enzymatic reactions as discussed in the introduction (page 25, Fig. 7). So if the production of the lethal lesion by 365 nm does not depend upon singlet oxygen itself, but on another species formed in the presence of singlet oxygen, then one interpretation of the observed sensitivity could be that it becomes apparent only at temperatures which allow an enzymatically controlled reaction, to convert singlet oxygen to another reactive species to take place, such as 25°C. An increased load of reactive oxygen species formed in this way could result in increased lesion formation and increased lethality for both cell lines.

Another aspect that should be examined is whether the D_2O solvent induces an alteration in the target of the radiation, either cellular DNA or membranes. D_2O would be expected to change the DNA conformation and short term exposure to D_2O has been shown to induce chromosomal aberrations in human lymphocyte cultures (Joenje *et al.*, 1983). However, such a change would also be expected to alter far-UV sensitivity, which was not found to be the case. Solvent effects could also result in altered membrane interphases. Again, such an alteration might be expected to take place at 0°C and thus

affect the sensitivity of cells at that temperature. However, this is not supported by the above results.

DNA repair enzymes are thought to offer concomitant repair of lesions during irradiation. D_2O has been suggested to inhibit repair of gamma-irradiated mammalian cells (Ben-Hur and Riklis, 1980; Ben-Hur *et al.*, 1980; Ueno *et al.*, 1984; Furuno-Fukushi and Matsudaira, 1985). This conclusion was reached because D_2O inhibits the fluence-rate effect of gamma rays (when the fluence rate is lowered and the exposure time extended, the biological effect of a given fluence is reduced) which is considered to involve among other events the repair of sublethal damage taking place during the irradiation of L5178Y cells at 37°C (Ueno *et al.*, 1984). In another study, split dose experiments of Ben-Hur and Riklis (1980) showed a reduced capacity of Chinese Hamster cells to repair gamma radiation-induced sublethal damage in the present of 90 per cent D_2O. They also showed that the enhancement of the sensitivity in the presence of D_2O in the medium after irradiation, depended on the cells being metabolically active *i.e.*, it was smaller when incubation was in buffer instead of growth medium and was reduced as the temperature was lowered from 37°C. Whether an analogy from the above gamma-irradiation studies can be drawn regarding the repair of DNA from UV-induced damage, is not known.

RESULTS AND DISCUSSION

PART 5

LEAKAGE STUDIES AFTER BROAD-BAND NEAR-UV IRRADIATION OF NORMAL AND ACTINIC RETICULOID FIBROBLASTS

One method of assessing membrane damage following stress conditions such as hyperthermia, gamma and UV irradiation, is by examining changes in the permeability of the cytoplasmic membrane. Under normal conditions, ions such as Na^+ and K^+, amino acids, sugars and other small molecules are continuously going in or out of the cell either by active processes such as the Na^+/K^+ pump or by passive diffusion. Any disturbance to these mechanisms can be considered to have important consequences for the cell.

Radioactive labelling of one of the above mentioned electrolytes or molecules allows the study of a specific membrane function which could be affected by radiation. Rb^+ is often used as a K^+ analogue since its radioactive isotope $^{86}Rb^+$ has a relatively short half-life (18.7 days) and is easier to handle than a K^+ isotope.

A previous study in E. coli cells showed $^{86}Rb^+$ leakage following broad-band near-UV radiation at doses comparable to those inducing lethality (Kelland et al., 1984). The initial objective of this section of experimental work was to repeat similar investigations using human skin fibroblasts and to examine the effect of Trolox-C on the leakage process.

Initial experiments involved monochromatic wavelength irradiation of cells in suspension, using an adaptation of the method of Kelland (1984). Results showed that the $^{86}Rb^+$ from both

control and irradiated cells leaked within the first 30 minutes after the collection of cells by trypsinization and centrifuging. It was presumed that prelabelled cells with ^{86}RbCl were suffering significant damage caused by the trypsinization step to make all the $^{86}Rb^{+}$ leak out of the cell whether irradiated or not. Therefore, a method by which cells would be irradiated as a monolayer had to be used. Since irradiation of a monolayer was not possible with the available monochromator system, it was decided that broad-band near-UV irradiation would be performed using the housing described in the Materials and Methods section (page 63, Fig. 13).

Radioactive Labelling of Fibroblasts

Three x 10^5 cells were inoculated into 90 mm^2 plates containing 9 ml of EMEM supplemented with 15 per cent foetal calf serum. The plates were placed in boxes, gassed so that 5 per cent CO_2 in air was present and incubated at 37°C. After 6 days of growth, the appropriate quantity of ^{86}RbCl, diluted in 1 ml of growth medium, was added to each plate aseptically, so that a final concentration of 1 μCi/ml $^{86}Rb^{+}$ was present. ^{86}RbCl was obtained as a sterile aqueous solution of concentration 1 mCi/ml, specific activity 108 mCi/mg, from Amersham International plc, Amersham. Since ^{86}RbCl has a radioactivity half-life of 18.7 days, the volume of ^{86}RbCl added was adjusted by calculating the amount of decay from the date when the activity was determined so that approximately 1 μCi/ml was always added.

Irradiation Procedures

Twenty-four hours after labelling the cells with $^{86}RbCl$, each plate was rinsed twice with 5 ml ice-cold PBS so that any $^{86}Rb^{+}$ in the extracellular medium was removed. The use of low temperature PBS minimized leakage of Rb^{+} from the cell interior during manipulations. Fifteen ml of PBS at room temperature were then added to each plate and both plates to be irradiated and controls were placed in the irradiation box, the control plates being covered in black tape and aluminium foil. This was to avoid any temperature difference between irradiated and non-irradiated plates which might affect the leakage process. The temperature of the PBS in the plates was found to rise to 25-29^{o}C during the irradiation. Cells to be near-UV irradiated were placed at a distance of 8 cm from the lamps where they received 30 $Jm^{-2}s^{-1}$ through their plastic lids while cells for far-UV irradiation were placed at a distance of 16 cm from the lamps and irradiated with 18 $Jm^{-2}s^{-1}$ without lids (see page 64 for assumptions underlying fluence determinations). Only the two central positions under the horizontal lamps, which were found to receive the same fluence, were used for irradiation, while the covered control plates were set at either side.

Measurement of Leakage

Samples of 0.3 ml were removed from each plate immediately after the addition of the 15 ml PBS and at specific time intervals for assessing the leakage of $^{86}Rb^{+}$ from the interior of the cells to the surrounding medium. Each sample was added to 4 ml of a xylene-based liquid scintillant, Optiphase 'Safe' (LKB, Liquid

Scintillation Products) in plastic scintillation vials and shaken well.

The amount of radioactive isotope in the medium was then determined using the 1215 Rackbeta liquid scintillation counter (LKB Wallac, Turku, Finland). This counter is able to count beta emissions and some gamma-emissions over the energy range of 1 KeV to 2.8 MeV. From the specifications given for Rackbeta 1215 counter, counting window settings of 110-212 were used. Counting of the samples was for 1 minute. Liquid scintillation counting involves placing the radioactive sample in an appropriate medium which converts radioactive energy into a pulse of light energy. This pulse of light energy is detected by means of a synchronized photocathode and is converted to an electrical pulse by a photomultiplier. During liquid scintillation counting the following energy steps occur between the radioactive sample (Rs) and the constituents of the scintillation cocktail:

```
          1          2          3
Rs---->solvent------>solute-------->photocathode.
```

At each of the three energy transfer steps there is a probability that an incomplete energy transfer will occur due to the nature of the scintillation cocktail. Interference may arise from photon quenching, chemical quenching and colour quenching. Therefore, the quantification of any radioactive sample depends upon the extent of this interference, termed 'quenching', and the ablity of the photocathode to detect the light pulses. The resultant quantification is expressed in counts per minute (cpm) which is a characteristic of a particular liquid scintillation counter and scintillation cocktail. Identical quantities of radioactive

material may produce different cpms in the same liquid scintillation counter and scintillation cocktail due to the presence of quenching agents. To convert cpm to an absolute quantity of radioactivity, a quench curve must be constructed so that the efficiency of the counting process may be estimated, hence taking into account interferences in energy transfer. From the efficiency measurement the absolute value of disintegrations per minute (dpm) may be determined. Therefore, dpm=cpm x efficiency.

Four methods exist for quench curve construction, those being internal standard, external standard, channels ratio and external standard channels ratio. Quench curves were constructed by the external standard channels ratio method which involved adding 4 ml of Optiphase to a series of 7 plastic mini-vials each containing a capsule of known radioactivity. To each sample, 0.3 ml of distilled water was added to simulate the emulsion system found in the experimental conditions. Increasing amounts from 0 to 40 µl of carbon tetrachloride were then added to provide quenching. The samples were then loaded into the counter, which had been programmed to count the samples and automatically construct a quench curve. The resultant quench curve for $^{86}Rb^{+}$ is shown in Appendix 7. This curve was then stored in the counter's memory so that dpms for all subsequent samples were calculated automatically.

Treatment of Results

The disintegrations per minute which were calculated by the scintillation counter represented the radioactivity present in the 0.3 ml sample. This value was then be multiplied with the total volume of PBS present in the plate at the time the measurement was

taken, so as to represent the total radioactivity present in the medium above the monolayer of cells. In order that comparisons between different experiments could be made, this value was then divided by the total number of cells present on that plate, which was estimated from an extra plate inoculated and grown under exactly similar conditions as the irradiated and control plates for each cell line.

Disintegrations per minute per cell were therefore plotted against time in the graphs presented in the following section.

Leakage of $^{86}Rb^{+}$ after Broad-Band Near-UV Irradiation of Normal and Actinic Reticuloid Fibroblasts

The results of experiments showing the amount of $^{86}Rb^{+}$ leaking out from human skin fibroblasts, expressed as disintegrations per minute, per cell, versus irradiation time can be seen in Figure 51 and Table 23. Each panel represents a matched experiment in which both AR and GM cells were irradiated simultaneously. Table 24 includes the ratio of $^{86}Rb^{+}$ leaked from irradiated versus non-irradiated cells.

All leakage curves obtained showed an increase in the leakage of $^{86}Rb^{+}$ with time until a plateau was reached. The exact shape of the curve and the time at which the plateau was reached differed between the two cell lines and depended on whether they were irradiated or not. Normal cells showed a gradual increase in the leakage of $^{86}Rb^{+}$ with time which reached a maximum between 3 and 4 hours after the beginning of the experiment. In panels B, C, and D it can be noted that there was hardly any effect of near-UV radiation on the $^{86}Rb^{+}$ leakage from normal cells, whereas in panel A

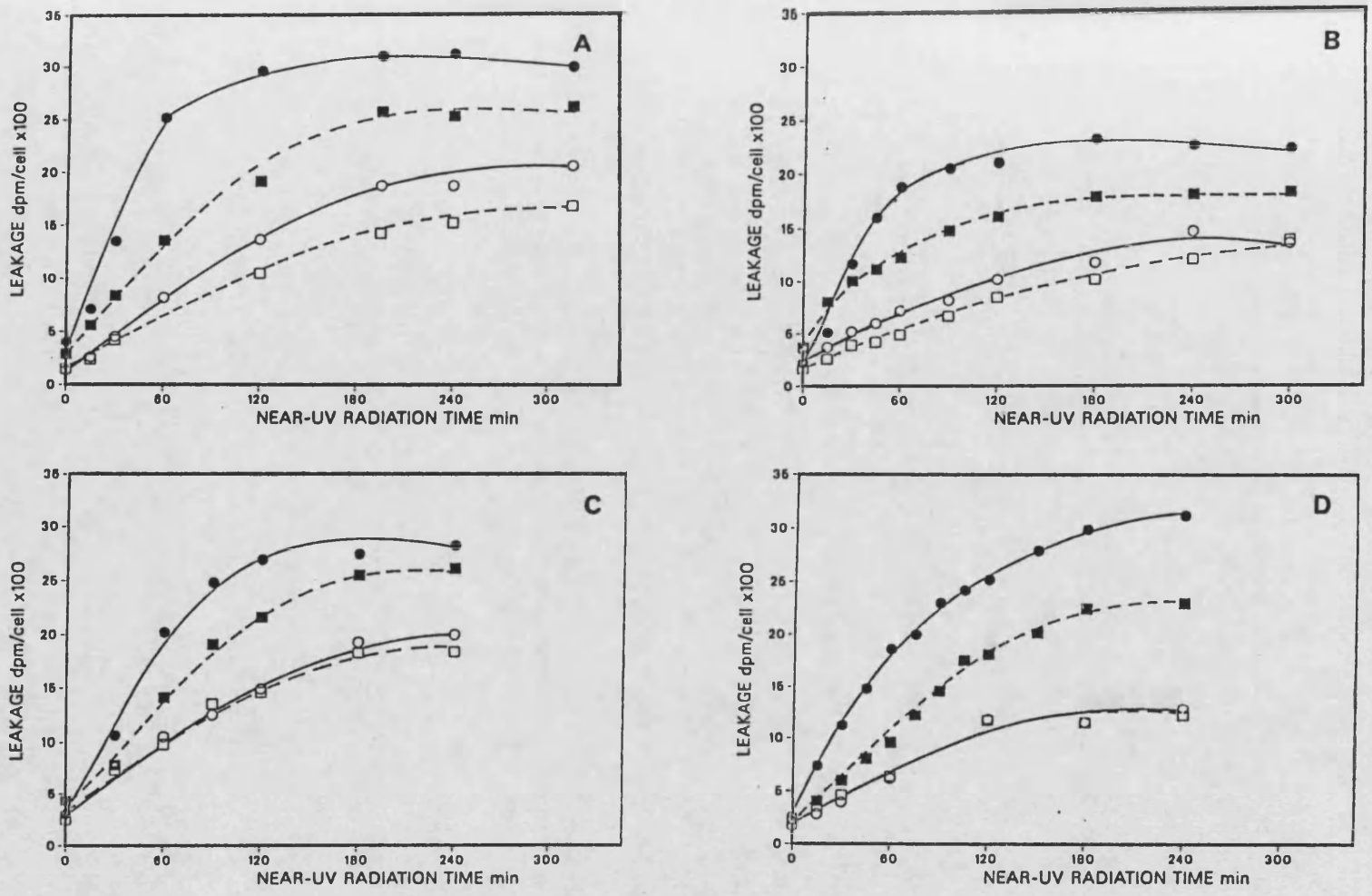

Figure 51. The leakage of $^{86}Rb^{+}$ from stationary AR6LO (● , ■) and GM730 cells (○ , □) expressed as disintegrations per minute per cell as a function of irradiation time with broad-band near-UV radiation (circles = irradiated, squares = non-irradiated). Panels A, B, C, and D represent the results of replicate experiments.

TABLE 23

THE LEAKAGE OF $^{86}RB^{+}$ FROM AR6LO AND GM730 CELLS IN RESPONSE TO BROAD-BAND NEAR-UV RADIATION

	51A				51B			
Time(min)	Disintegrations Per Minute Per Cell x 10^2							
	AR6LO		GM730		AR6LO		GM730	
	Control	Irrad	Control	Irrad	Control	Irrad	Control	Irrad
	($8.1x10^5$)*		($15.1x10^5$)*		($9.2x10^5$)*		($15.9x10^5$)*	
0	2.9	4.0	1.5	1.3	3.7	2.2	1.7	3.5
15	5.6	7.1	2.4	2.6	8.1	5.1	2.6	3.7
30	8.4	13.5	4.2	4.5	10.1	11.7	3.9	5.2
45	--	--	--	--	11.2	16.0	4.2	6.0
60	13.6	25.2	6.9	8.2	12.3	18.8	4.9	7.2
90	--	--	--	--	14.8	20.5	6.7	8.2
120	19.2	29.6	10.5	13.7	16.1	21.0	8.5	10.2
180	--	--	--	--	17.9	23.2	10.2	11.8
195	25.8	31.0	14.3	18.8	--	--	--	--
240	25.4	31.2	15.3	18.8	18.1	22.6	12.1	14.7
300	--	--	--	--	18.3	22.3	13.9	13.6
315	26.3	30.0	16.9	20.7	--	--	--	--

	51C				51D			
Time(min)	Disintegrations Per Minute Per Cell x 10^2							
	AR6LO		GM730		AR6LO		GM730	
	Control	Irrad	Control	Irrad	Control	Irrad	Control	Irrad
	($6.8x10^5$)*		($11.6x10^5$)*		($15.8x10^5$)*		($22.2x10^5$)*	
0	4.3	3.0	2.5	2.4	2.3	2.6	2.3	1.7
15	--	--	--	--	4.0	7.4	3.5	2.8
30	7.8	10.6	7.3	7.8	6.0	11.2	4.6	3.9
45	--	--	--	--	8.1	14.8	--	--
60	14.1	20.2	9.8	10.5	9.6	18.6	6.4	6.2
75	--	--	--	--	12.2	20.0	--	--
90	19.1	24.8	13.5	12.5	14.6	23.0	--	--
105	--	--	--	--	17.5	24.2	--	--
120	21.6	26.9	14.6	14.9	18.1	25.2	11.7	11.8
150	--	--	--	--	20.2	27.9	--	--
180	25.5	27.4	18.3	19.3	22.5	29.9	11.5	11.5
240	26.1	28.2	18.4	20.0	23.0	31.2	12.2	12.9

*cell concentration

TABLE 24

THE LEAKAGE OF $^{86}RB^{+}$ FROM AR6LO AND GM730 CELLS IN RESPONSE TO BROAD-BAND NEAR-UV RADIATION, EXPRESSED AS RATIO OF IRRADIATED:NON-IRRADIATED CELLS (DATA FROM TABLE 23)

Time	AR				GM			
min	51A	51B	51C	51D	51A	51B	51C	51D
0	1.38	0.59	0.70	1.13	0.87	2.06	0.96	0.74
15	1.27	0.63	--	1.85	1.03	1.42	--	0.80
30	1.61	1.15	1.36	1.87	1.07	1.33	1.07	0.85
45	--	1.43	--	1.83	--	1.43	--	--
60	1.85	1.53	1.43	1.94	1.19	1.47	1.07	0.97
75	--	--	--	1.64	--	--	--	--
90	--	1.39	1.30	1.58	--	1.22	0.93	--
105	--	--	1.38	--	--	--	--	--
120	1.54	1.30	1.25	1.39	1.30	1.20	1.02	1.01
150	--	--	--	1.38	--	--	--	--
180	--	1.30	1.07	1.33	--	1.16	1.05	1.00
195	1.20	--	--	--	--	--	--	--
240	1.23	1.25	1.08	1.36	1.31	1.21	1.09	1.06
300	--	1.22	--	--	1.22	0.98	--	--
315	1.14	--	--	--	--	--	--	--

there was a small increase in the total amount of $^{86}Rb^{+}$ leaked from the cells at times longer than 60 min of irradiation. In contrast, irradiated AR cells showed a larger increase in the rate of $^{86}Rb^{+}$ leakage initially and then reached a higher maximum leakage. The maximum difference between irradiated and non-irradiated AR cells in these experiments was seen after about 60 minutes of irradiation when 1.43-1.85 more $^{86}Rb^{+}$ was leaking from irradiated versus non-irradiated cells (Table 24). Panels C and D represent experiments which were done as part of subsequent investigations on the $^{86}Rb^{+}$ leakage from Trolox-C supplemented cells. In the experiment shown in Fig. 51 Panel D, a change of medium on alternate days brought about an increase of cell number but with no noticeable effect on the leakage process.

In order to attempt to answer any questions arising from these experimental observations such as :

1) Why did irradiated AR cells leak more than non-irradiated AR cells and why wasn't this observed with normal cells?

2) Why did irradiated AR cells reach a higher maximum leakage than non-irradiated AR cells and what does this represent?

3) Why did non-irradiated AR cells leak more than GM non-irradiated cells?,

there was a need to understand what this leakage represented. Most importantly, whether it was a result of severe damage to the cell and followed DNA-induced lethality, or whether it occurred at doses comparable to those producing lethality and could be inducing or influencing such a process by upsetting the electrolyte content of the cell. Therefore, an assessment of cell survival using broad-band near-UV radiation under experimental conditions similar

to those used for measurement of $^{86}Rb^{+}$ leakage was necessitated. Two methods exist for assessing the survival of fibroblasts attached in petri dishes. One involves irradiation of confluent or near-confluent monolayers and subsequent detachment of the fibroblasts using trypsin, followed by counting, diluting and adding the appropriate number of cells for colony formation to plates. The other method involves irradiation of prepared dilutions of cells and was prefered in this study because in this way the trypsinization step after irradiation could be avoided. Therefore, assessment of viability following near-UV irradiation was performed using appropriate dilutions of cells as described in the Materials and Method section (pages 58, 68) but otherwise under similar irradiation conditions to the ones used in the leakage experiments.

Three experiments were performed for each cell line but because some of these had less experimental points than the other two (Tables A30, A31), it was decided not to follow the normal procedure of regressing each experiment, but to regress the calculated mean points. The mean survival curve obtained for AR and normal cells is shown in Fig. 52 and the calculated parameters for each curve are included in Table 25. It can be seen that 47 and 60 minutes of broad-band near-UV irradiation resulted in 90 per cent lethality (D_{10}) of AR and GM730 cells respectively, which in the corresponding leakage experiments also resulted in measurable $^{86}Rb^{+}$ leakage. Assuming 365 nm was mostly emitted from the lamp, the corresponding D_{10} value was 142 kJm^{-2} and 180 kJm^{-2} for AR and GM730 cells, respectively. This value is considerably lower than the monochromatic 365 nm fluence resulting in 90 per cent lethality of cells irradiated in suspension, which is probably explained by the

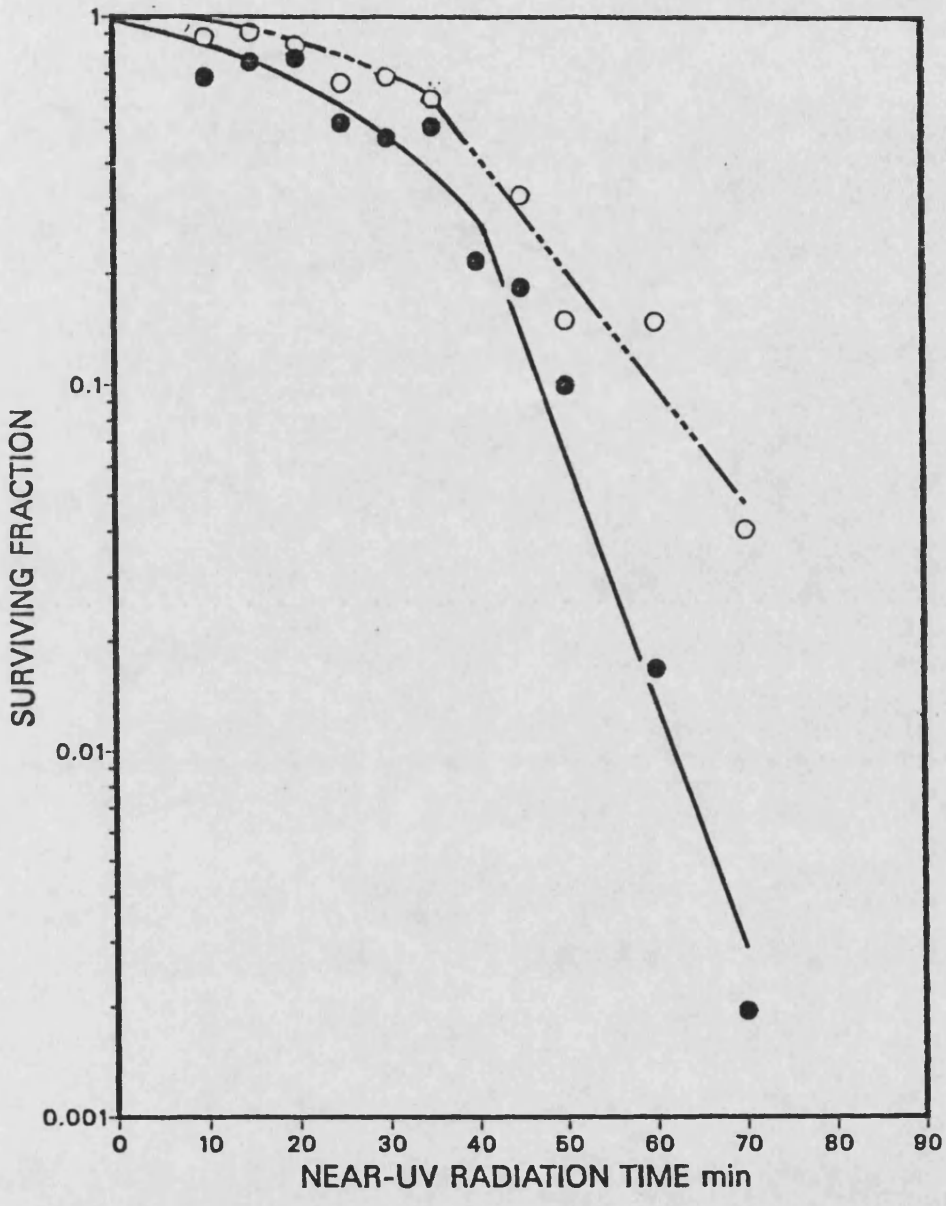

Figure 52. The inactivation of AR6LO (●) and GM730 (O) cells as a function of irradiation time with near-UV radiation. The points represent the mean of 3 experiments.

fact that shorter, more energetic wavelengths were present in the radiation beam (see Fig. 14). Since irradiation took place at ~25°C, the difference in the response of AR and normal cells to near UV irradiation was also apparent. Comparison of D_0 values in Table 25 shows AR cells to be two times more sensitive than normal GM730 cells to broad-band near-UV radiation.

TABLE 25
SURVIVAL OF AR6LO (1) AND GM730 (2) CELLS TO BROAD BAND NEAR-UV RADIATION

Slope min-1	Standard Deviation	Intercept	Standard Deviation	D_0 min	D_q min	D_{10} min
(1) 6.72×10^{-2}	6.0×10^{-3}	2.17×10^{0}	3.1×10^{-1}	6.46×10^{0}	3.23×10^{1}	4.72×10^{1}
(2) 3.13×10^{-2}	5.1×10^{-3}	8.80×10^{-1}	2.7×10^{-1}	1.39×10^{1}	2.82×10^{1}	6.01×10^{1}

Published results of similar studies are also included in Table 26 for comparative purposes, bearing in mind the use of different lamps with different emission spectra and intensities, as well as the use of different experimental procedures.

The conclusions that can be reached from these experiments are that AR^{6LO}cells are more sensitive to broad-band near-UV irradiation both in terms of clonogenic ability and in terms of a particular membrane function examined i.e. the leakage of $^{86}Rb^+$ from irradiated cells. It cannot be deduced from this work whether $^{86}Rb^+$ leakage (which is a K^+ analogue) is due to specific damage to the Na^+/K^+ pump or whether it is the result of generalized membrane damage, but the use of ouabain, a metabolic inhibitor of active

TABLE 26

SURVIVAL PARAMETERS OBTAINED FOR HUMAN FIBROBLASTS IRRADIATED ATTACHED ON PLATES WITH BROAD-BAND NEAR-UV RADIATION

Cell Line	Source	Fluence Rate $Jm^{-2}s^{-1}$	D_0 kJm^{-2}	D_q kJm^{-2}	D_{10} kJm^{-2}	Method of irradiation	Reference
AG1522	Sylvania	20.9	47.8±3.7	47.4±5.9	157.5±4.8	dilutions	Zamansky et al.,
GM3652	FR40T12		40.0±3.6	40.2±3.5	132.4±5.7	16-20 hours	1985
GM730	310-410nm max 350-355		39.2±4.2	45.2±4.7	135.5±5.6	after plating at 0-4°C	
GM730	Coast-Wave	30	41.7	84.6	180.3	at ~25°C	results presented
AR6LO	15 W		19.4	96.9	141.6		in Table 25
82MB2	1200 W type Sellas	165			320	confluent 1 day after plating below 14°C	Roza et al., 1985

transport, could perhaps clarify this point in the future. Similar changes in permeability of mammalian cells in response to ionizing radiation are generally considered to be a result of alterations in passive rather than active transport (Patrick, 1977).

Underlying causes that could result in generalized membrane damage include lipid peroxidation and oxidation of protein thiol groups, amongst others. Since AR6\O but not normal cells, are susceptible to this damage, it could be proposed that an inability of AR cells to maintain reactive oxygen species under control is responsible for the observed membrane alterations. The generation of reactive oxygen species in response to near-UV radiation has already been discussed and the ability of these species to initiate and propagate lipid peroxidation reactions has been broadly mentioned in the Introduction. In particular , the hydroxyl ion and singlet oxygen have been shown to initiate lipid peroxidation reactions in a variety of chemical and biological systems (Kellogg and Fridovich, 1975, 1977; Halliwell and Gutteridge, 1985).

It can be further suggested that AR cells suffer this membrane damage due to an inability to stop and/or repair the destructive oxidative reactions taking place in their membranes due to an enzymatic defect or due to a decreased concentration of an antioxidant such as vitamin E.

In AR$^{6\O}$cells, membrane damage occurs at doses comparable to lethality and could, therefore, contribute to it. On the contrary, normal cells do not suffer this membrane damage under normal circumstances. However, it would be interesting to examine what effect an induced enzyme depletion such as superoxide dismutase or glutathione or catalase would have on $^{86}Rb^{+}$ leakage. In a study

where K^+ leakage from X-irradiated mouse fibroblasts was measured by flame photometry cellular membranes were rendered more susceptible to lipid peroxidation when they contained increased levels of polyunsaturated fatty acids. Indeed, this alteration resulted in increased K^+ leakage which could be prevented by supplementation of vitamin E (Wolters and Konings, 1985).

Effect of Trolox-C on Near-UV Induced $^{86}Rb^+$ Leakage

Trolox-C incorporated in the growth medium was shown to protect AR cells against 365 nm-induced inactivation at 25°C (see Fig. 43 Panel A). An investigation of its effect on $^{86}Rb^+$ leakage, under similar conditions of irradiation to those previously described, was carried out.

Trolox-C was added at a concentration of 100 μg/ml in the plates during subculture which was designated as Day 0 and then on days 2, 4 and 6, the medium was changed and fresh Trolox-C was added. $^{86}RbCl$ was also added on day 6 and irradiation tok place on day 7 as previously described. The results of 2 leakage experiments for each cell line are shown in Figures 53, 54, where panel A represents results for AR cells and panel B for GM730 cells. The data for these experiments is included in Table 27. The results of the control experiments have already been presented in Figure 51 Panels C, D. In the experiment presented in Fig. 51C the medium of the non-supplemented cells was not changed and it can be noted that the cell concentration present on the plates was lower than that of the Trolox-C supplemented cells. However, this increase in cell numbers should not be attributed to the presence of Trolox-C since in the experiment presented in Fig. 51D where the medium of

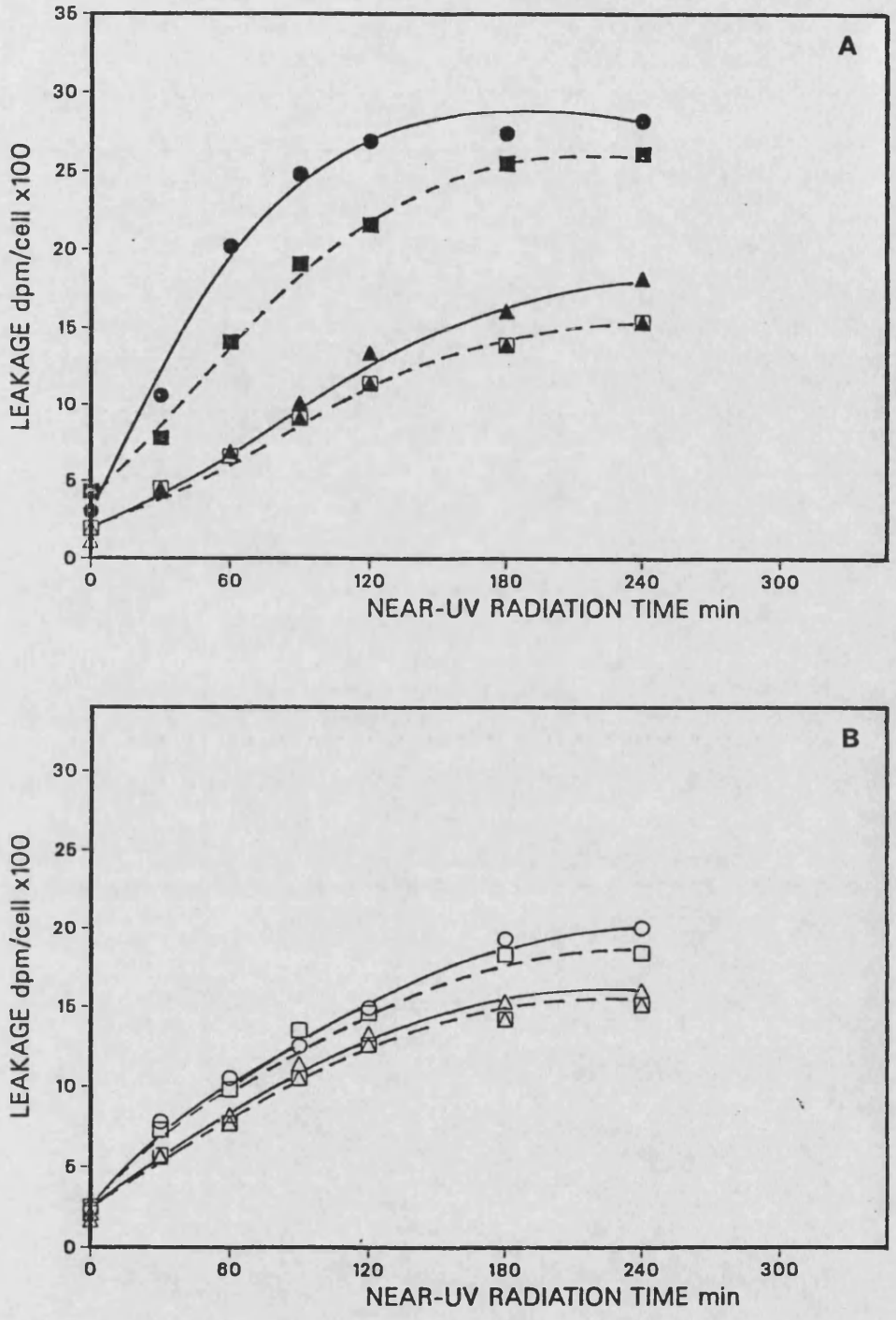

Figure 53. The leakage of $^{86}Rb^{+}$ from stationary AR6LO (Panel A) and GM730 (Panel B) cells expressed as disintegrations per minute, per cell, as a function of irradiation time with broad-band near-UV radiation.

● ○ = -trolox-C, irradiated
■ □ = -trolox-C, non-irradiated also Fig. 51C
▲ △ = +trolox-C, irradiated
◪ ⊠ = +trolox-C, non-irradiated

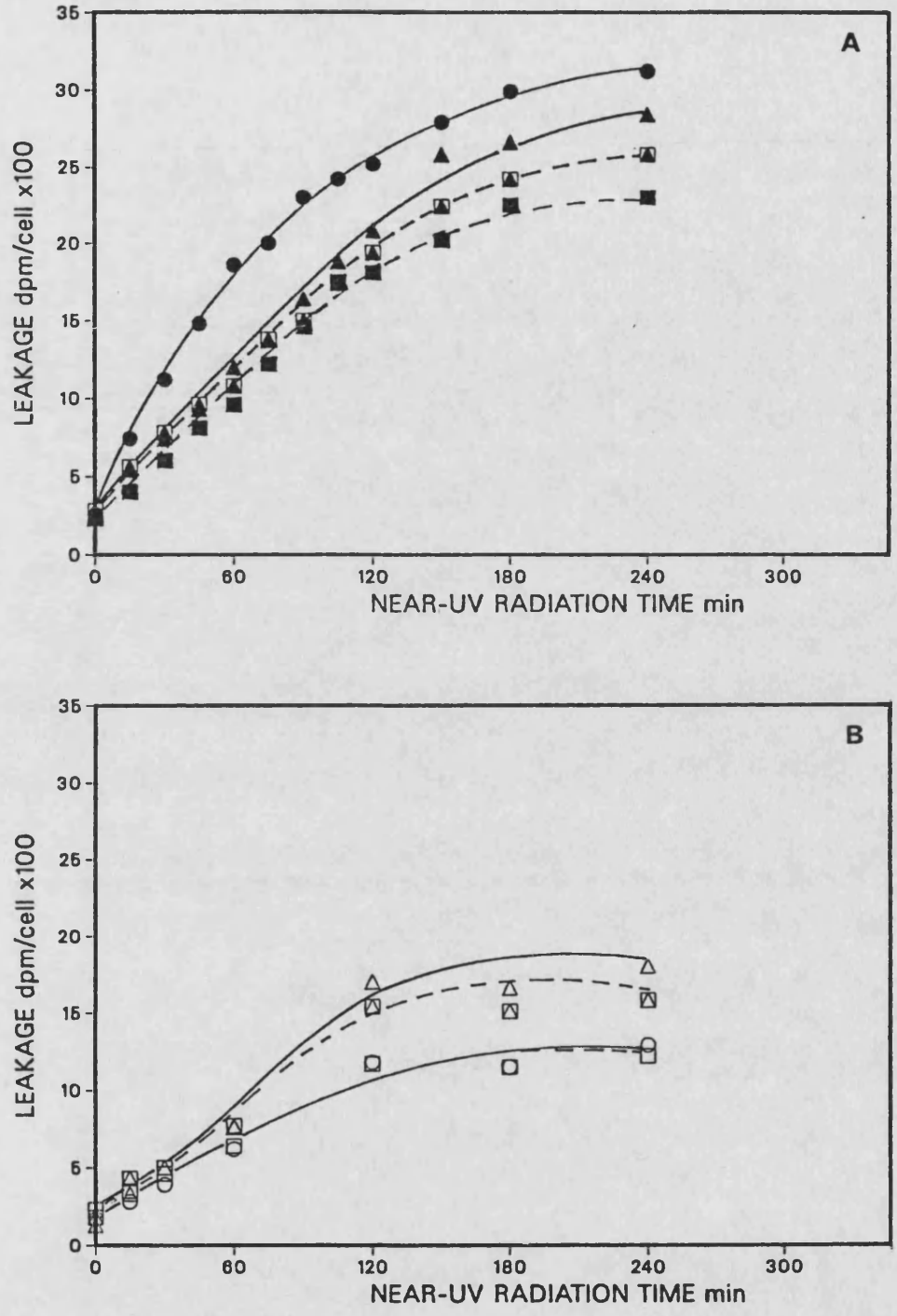

Figure 54. The leakage of $^{86}Rb^{+}$ from stationary AR6LO (Panel A) and GM730 (Panel B) cells expressed as disintegrations per minute, per cell, as a function of irradiation time with broad-band near-UV radiation.

● ○ = -trolox-C, irradiated
■ □ = -trolox-C, non-irradiated also Fig. 51D
▲ △ = +trolox-C, irradiated
▣ □ = +trolox-C, non-irradiated

TABLE 27

THE LEAKAGE OF $^{86}Rb^{+}$ FROM AR6LO AND GM730 CELLS GROWN IN THE PRESENCE OR ABSENCE OF 100 μg/ml TROLOX-C, IN RESPONSE TO BROAD-BAND NEAR-UV RADIATION

	53A				53B			
Time(min)	Disintegrations Per Minute Per Cell x 10^2							
	AR		AR + Trolox-C		GM		GM + Trolox-C	
	Control	Irrad	Control	Irrad	Control	Irrad	Control	Irrad
	(6.8×10^5)*		(16.8×10^5)*		(11.6×10^5)*		(21.4×10^5)*	
0	4.3	3.0	1.9	1.1	2.5	2.4	2.1	1.7
30	7.8	10.6	4.5	4.3	7.3	7.8	5.7	5.6
60	14.1	20.2	6.6	6.9	9.8	10.5	7.7	8.2
90	19.1	24.8	9.1	10.1	13.5	12.5	10.5	11.4
120	21.6	26.9	11.4	13.4	14.6	14.9	12.6	13.3
180	25.5	27.4	13.9	16.1	18.3	19.3	14.2	15.3
240	26.1	28.2	15.4	18.2	18.4	20.0	15.1	16.0

	54A				54B			
Time(min)	Disintegrations Per Minute Per Cell x 10^2							
	AR		AR + Trolox-C		GM		GM + Trolox-C	
	Control	Irrad	Control	Irrad	Control	Irrad	Control	Irrad
	(15.8×10^5)*		(17.2×10^5)*		(22.2×10^5)*		(20.8×10^5)*	
0	2.3	2.6	2.8	2.4	2.3	1.7	1.8	1.3
15	4.0	7.4	5.6	5.4	3.5	2.8	4.3	3.3
30	6.0	11.2	7.8	7.4	4.6	3.9	5.0	5.0
45	8.1	14.8	9.6	9.3	--	--	--	--
60	9.6	18.6	10.8	12.0	6.4	6.2	7.7	7.6
75	12.2	20.0	13.8	13.7	--	--	--	--
90	14.6	23.0	15.0	16.4	--	--	--	--
105	17.5	24.2	17.4	18.8	--	--	--	--
120	18.1	25.2	19.4	20.8	11.7	11.8	15.4	17.0
150	20.2	27.9	22.4	25.8	--	--	--	--
180	22.5	29.9	24.2	26.6	11.5	11.5	15.1	16.6
240	23.0	31.2	25.8	28.4	12.2	12.9	15.8	18.0

*cell concentration

non-supplemented cells was changed as well, the cell number was also increased to the same extent as for Trolox-C supplemented cells. It should be pointed out again that changes in cell number did not alter the rate of $^{86}Rb^{+}$ leakage. As previously discussed, for cells not supplemented with Trolox-C, near-UV irradiation induced $^{86}Rb^{+}$ leakage only in AR and not normal cells. The presence of Trolox-C clearly protected irradiated AR cells and there was no radiation-induced leakage in Trolox-C supplemented cells. It should be noted that for this protective effect to occur it was necessary that Trolox-C was added to the cells relatively near the irradiation time, since in an initial experiment where it was added during subculture, 7 days prior to irradiation, it did not offer any protection. In the case of normal cells, neither Trolox-C supplemented nor unsupplemented cells leaked in response to near-UV radiation.

It has already been discussed that Trolox-C may become associated with cellular membranes. A possible way by which Trolox-C might protect near-UV irradiated AR cells and prevent leakage of $^{86}Rb^{+}$, might be by prevention of lipid peroxidation reactions which could lead to generalized membrane damage. If it is hypothesized that AR cellular sensitivity is due to an inability to effectively scavenge reactive oxygen species which can start lipid peroxidation reactions and lead to generalized membrane damage (which would become apparent as an increase of $^{86}Rb^{+}$ leakage) then Trolox-C would be expected to offer some protection.

Leakage of $^{86}Rb^{+}$ after Broad-Band Far-UV Irradiation of Normal and AR Fibroblasts

Similar leakage experiments were performed using far-UV irradiation and the results of two replicate experiments for AR and GM730 cells are shown in Figure 55 and Table 28. Non-irradiated cells show no significant leakage during the total period examined (8 minutes), while irradiated cells show no leakage for the first 4 min of irradiation. Since the fluence rate given was approximately 18 $Jm^{-2}s^{-1}$, 4 minutes of irradiation correspond to a dose of 4320 Jm^{-2} which is 2-3 orders of magnitude larger than 254 nm doses that produce lethality. This is concluded both from our study of monochromatic 254 nm inactivation of fibroblasts in suspension at 25°C where D_0 was 14.9 and 13.7 Jm^{-2} and D_{10} was 49.3 and 48.3 Jm^{-2} for GM730 and AR cells, respectively and from other published data on the response of attached human fibroblasts to broad-band far-UV radiation (Table 29). Perhaps the response of human fibroblasts irradiated at different stages of growth is not strictly comparable (Griego *et al.*, 1981), but the dose resulting to 90 per cent lethality seems to be between 7 - 15 Jm^{-2} which corresponds to 0.45 - 0.9 seconds of irradiation. Therefore at inactivation fluences orders of magnitude larger than those producing lethality, irradiated cells do not leak $^{86}Rb^{+}$ into their surrounding medium. Then, either when a certain dose is reached or when a certain time elapses following the induction of damage, a sharp increase of $^{86}Rb^{+}$ leakage is observed.

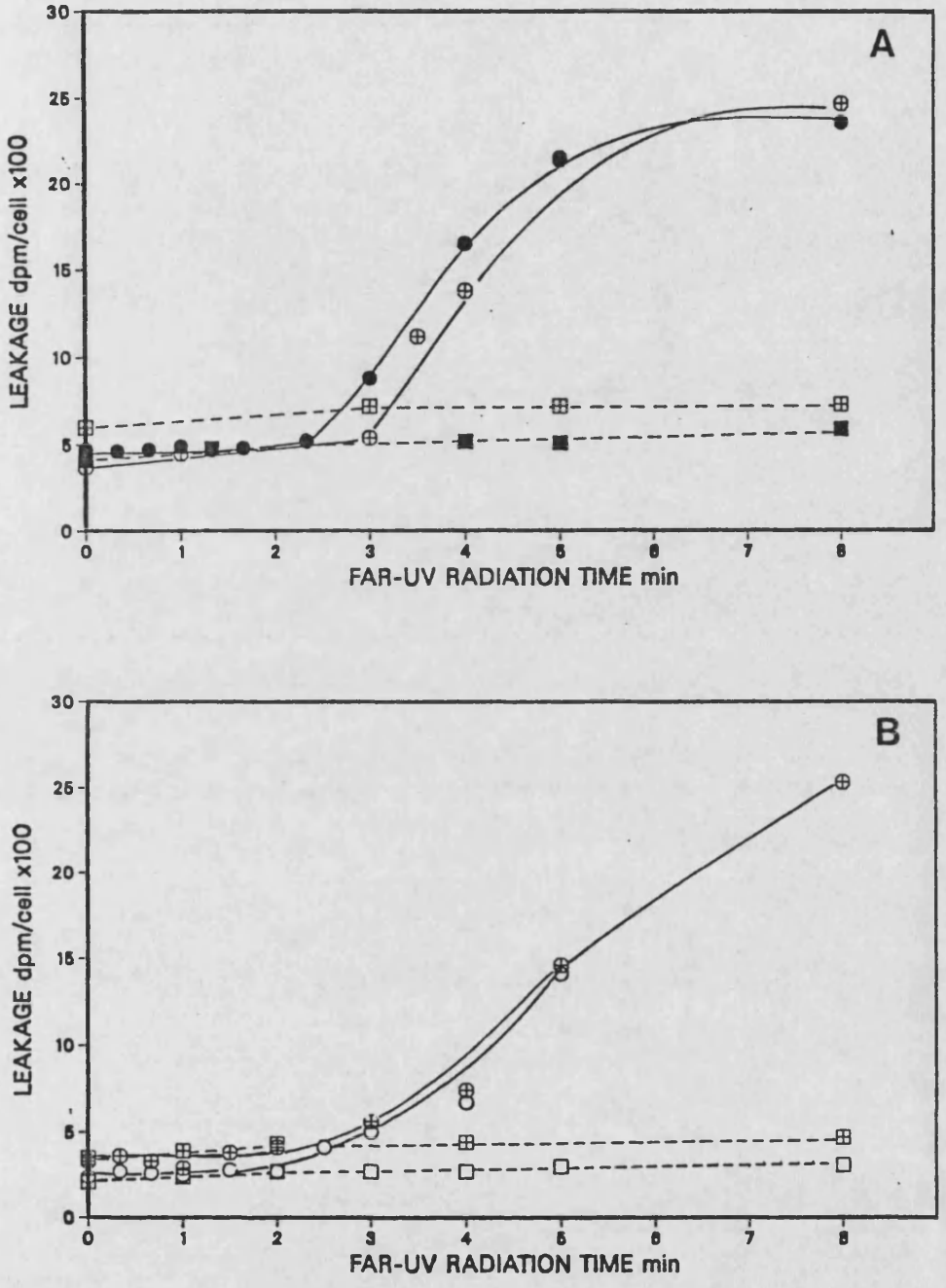

Figure 55. The leakage of $^{86}Rb^{+}$ from stationary AR6LO (Panel A) and GM730 (Panel B) cells expressed as disintegrations per minute per cell, as a function of irradiation time with broad-band far-UV radiation. The two sets of data represent the results of replicate experiments. (■ , □ , ⊞ = non-irradiated)
(● , ○ , ⊕ = irradiated)

TABLE 28

THE LEAKAGE OF $^{86}RB^{+}$ FROM AR6LO AND GM730 CELLS IN RESPONSE TO FAR-UV RADIATION

	55A				55B			
Time(sec)	Disintegrations Per Minute Per Cell x 10^{-2}							
	AR6LO		GM730		AR6LO		GM730	
	Control	Irrad	Control	Irrad	Control	Irrad	Control	Irrad
	($6.3x10^5$)*		($15.6x10^5$)*		($6.3x10^5$)*		($15.6x10^5$)*	
0	6.0	3.7	4.1	4.7	3.5	3.3	2.1	2.4
20	--	--	--	4.6	--	3.6	--	2.7
40	--	--	--	4.7	--	3.3	--	2.6
60	--	4.7	--	4.9	3.9	2.9	2.4	2.5
80	--	--	4.8	4.7	--	--	--	--
90	--	--	--	--	--	3.8	--	2.8
100	--	--	--	4.8	--	--	--	--
120	--	--	--	--	4.3	4.1	2.7	2.7
140	--	--	--	5.2	--	--	--	--
150	--	--	--	--	--	--	--	4.1
180	7.2	5.4	--	8.8	--	5.6	2.7	5.0
210	--	11.2	--	--	--	--	--	--
240	--	13.8	5.2	16.5	4.4	7.4	2.7	6.7
300	7.2	21.4	5.1	21.5	--	14.6	3.0	14.1
480	7.3	24.7	5.9	23.6	4.7	25.3	3.1	--

* cell concentration

TABLE 29

SURVIVAL PARAMETERS OBTAINED FOR HUMAN FIBROBLASTS IRRADIATED ATTACHED ON PLATES WITH BROAD-BAND FAR-UV RADIATION

Cell Line	Source	Fluence Rate $Jm^{-2}s^{-1}$	D_0 Jm^{-2}	D_q Jm^{-2}	D_{10} Jm^{-2}	Method of irradiation	Reference
AG1522 GM3652 GM730	General Electric G8T5	0.4	2.6±0.1 2.7±0.1 2.6±0.1	1.8±0.2 2.0±0.2 2.1±0.2	7.6±0.2 8.3±0.2 8.1±0.4	dilutions 16-20 hours after plating	Zamansky et al., 1985
NHSF3 NHSF6 NHSF40	Toshiba Electric 15W	0.12-1.0	8.5 9.0 8.8			dilutions 4-8 hrs after plating	Fujiwara and Tatsumi, 1976
GM38	General Electric 25W	1.25	3.4±0.3	8.7±1.2		dilutions 'dry' 18 hrs after plating	Smith and Paterson, 1982
GM38 GM498 CRL1141	General Electric 15W	1.4	6.0±0.5 7.6±0.4 6.7±0.3		16.2±0.9 16.7±0.6 19.1±0.5	dilutions 'dry' 6 hrs after plating	Smith and Paterson, 1981
1MR-91	General Electric, G15T8	1.0	4.8	6.5	- -	dilutions at 4°C	Wells and Han, 1985
CRL1121 CRL1119	General Electric G15T8	0.08-0.2	4.67 2.99	- -		confluent 5-7 days after plating	Kraemer et al., 1976
1BR, 4BR 1BI, 2BI	Hanovia or Philips	0.15-0.9		Mean of 4 normals = ~11		confluent 1 day after plating	Lehmann et al., 1977
1BR, 4BR 19BR, 2BI	Hanovia 12555	1.65		Mean of 4 normals = ~15		same	Arlett et al., 1975
82MB2	Phillips 15WTUV	0.38			7.5	confluent 1 day after plating	Roza et al., 1985

Post-irradiation Radioactive Labelling of Fibroblasts

In the following set of experiments an alternative approach to assess membrane damage was used, in which $^{86}Rb^{+}$ was added to the cells immediately after the irradiation period. In this way, the ability of the cells to take up the label, rather than release it, could be studied, since the leakage conditions were similar for differently treated cells.

The experimental method involved inoculation of $3x10^{5}$ cells into 90 mm^{2} plates containing 10 ml of EMEM supplemented with 15% foetal calf serum. After 4 days of growth at 37°C in a 5 per cent CO_2 atmosphere, the plates were removed from the incubator, rinsed twice with 5 ml PBS and irradiated through their lids, in 10 ml PBS for 1, 2 or 3 hours. At the end of the irradiation period, 9 ml of fresh medium were added to the cells and 1 ml of the appropriate dilution of $^{86}RbCl$ in medium to result in a concentration of 1 μCi/ml $^{86}Rb^{+}$. After a 24 hour incubation at 37°C the leakage of $^{86}Rb^{+}$ was assessed as previously described, by measuring its increasing concentration in 15 ml PBS.

Figures 56, 57 and 58 show the leakage curves obtained from AR and normal GM730 cells if irradiated for 1, 2, 3 hours or not irradiated at all. It can be seen both from these graphs and more clearly in Figure 59, in which the mean calculated value of the ratio of irradiated to control cells from the 5 previous experiments is shown, that irradiation reduces the ability of the cells to take up the label in a dose-dependent manner. This effect is more pronounced in AR cells since after 2 hours of leakage, only 65%, 35% and 15% of the label which would have leaked from non-irradiated cells has leaked from AR cells irradiated for 1, 2 or 3 hours,

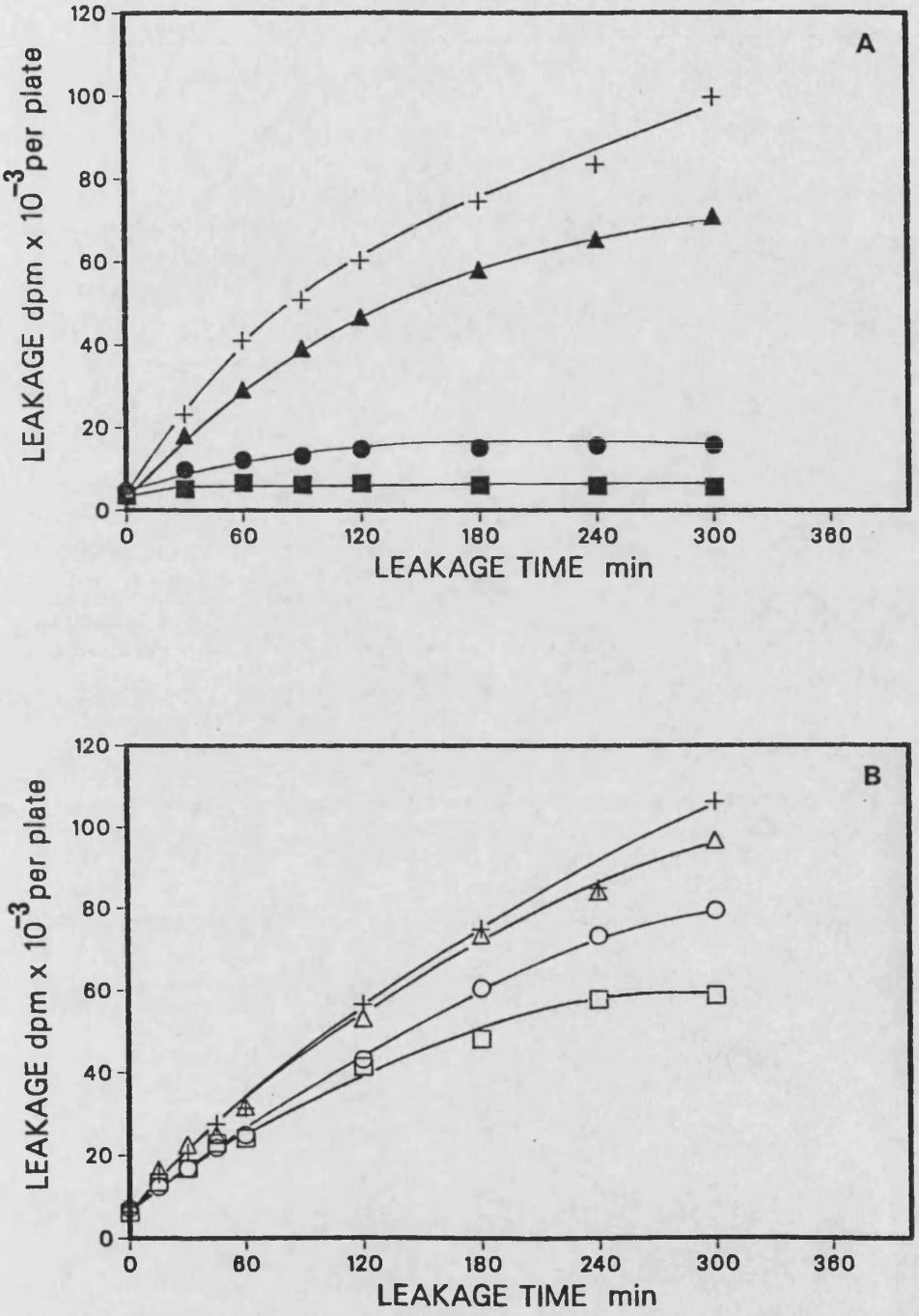

Figure 56. The leakage of $^{86}Rb^{+}$ from AR6LO (Panel A) and GM730 (Panel B) cells 24 hours after a + = 0 hour
▲ △ = 1 hour
● ○ = 2 hour
■ □ = 3 hour
irradiation with broad-band near-UV radiation.

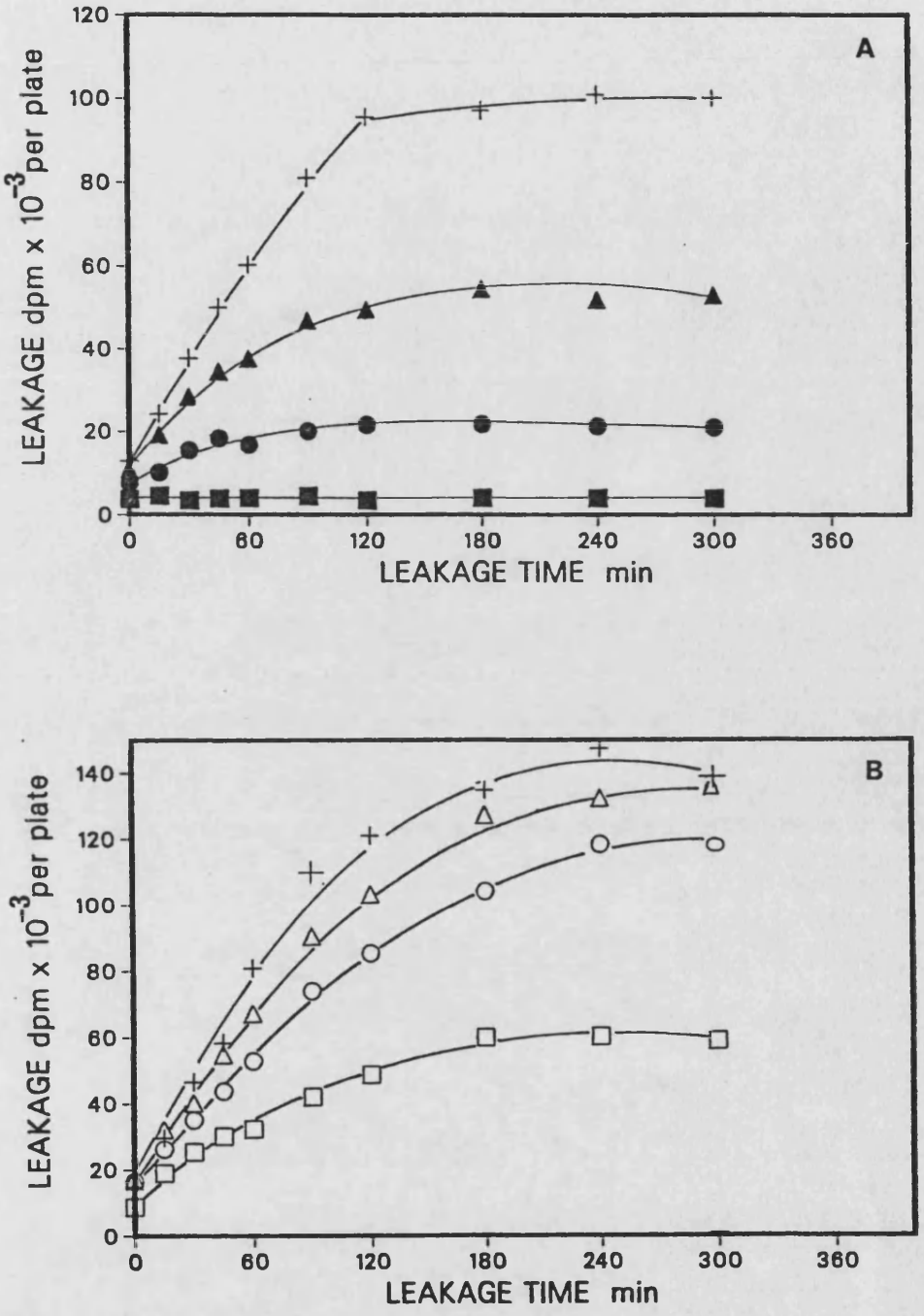

Figure 57. The leakage of $^{86}Rb^{+}$ from AR6LO (Panel A) and GM730 (Panel B) cells 24 hours after a + = 0 hour
▲ △ = 1 hour
● ○ = 2 hour
■ □ = 3 hour
irradiation with broad-band near-UV radiation.

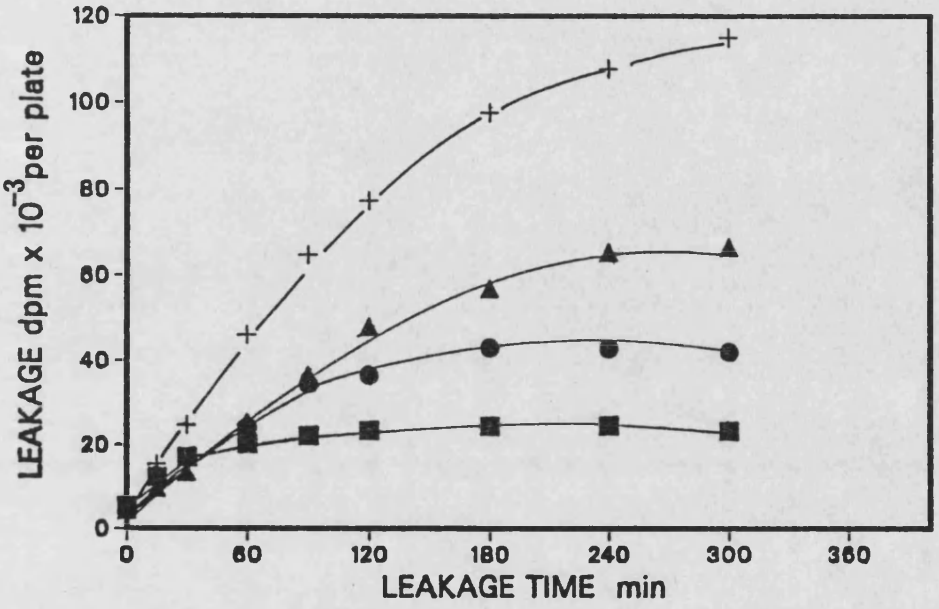

Figure 58. The leakage of $^{86}Rb^{+}$ from AR6LO cells 24 hours after a

+ = 0 hour
▲ △ = 1 hour
● ○ = 2 hour
■ □ = 3 hour

irradiation with broad-band near=UV radiation

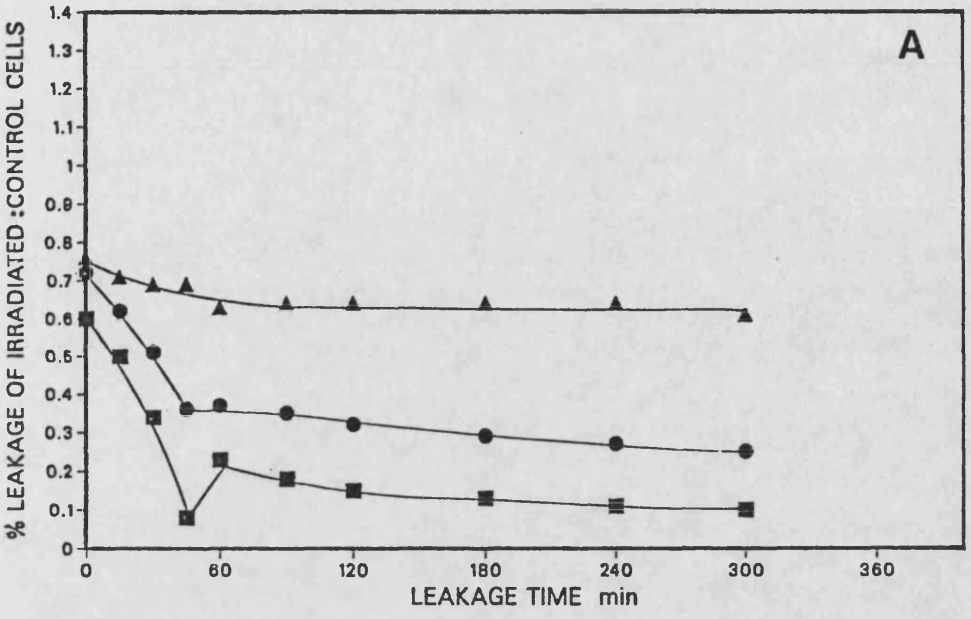

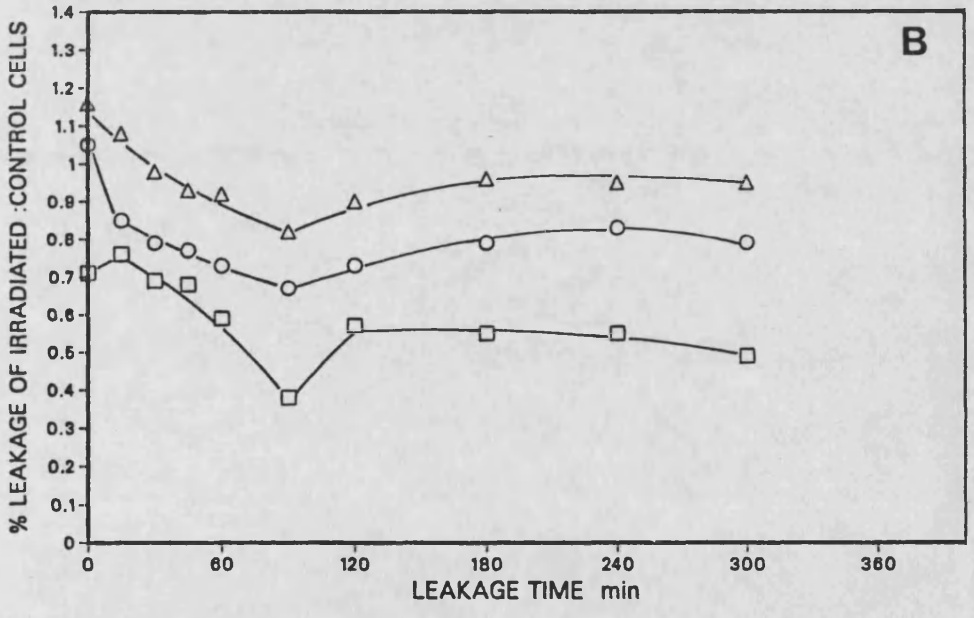

Figure 59. The leakage of $^{86}Rb^{+}$ from AR6L0 (Panel A) and GM730 (Panel B) cells 24 hours after a 1 hour (▲ , △), 2 hour (● , ○), 3 hour (■ , □), irradiation with broad-band near-UV radiation, expressed as a ratio of dpm of irradiated versus non-irradiated cells.

TABLE 30

THE LEAKAGE OF $^{86}RB^{+}$ FROM AR6LO CELLS WITH TIME 24 HOURS AFTER 1, 2 OR 3 HOURS OF BROAD-BAND NEAR-UV IRRADIATION. THE LEAKAGE IS EXPRESSED AS THE RATIO OF THE DISINTEGRATIONS PER MINUTE OF IRRADIATED:CONTROL CELLS

Time (min)	Experiment 1	Experiment 2	Experiment 3	Mean
	NEAR-UV IRRADIATION FOR ONE HOUR			
0	.84	.63	.82	.76
15	.79	.62	--	.71
30	.75	.54	1.79	.69
45	.69	--	--	.69
60	.62	.55	.71	.63
90	.58	.62	.77	.64
120	.52	.62	.78	.64
180	.56	.58	.78	.64
240	.51	.61	.79	.64
300	.54	.58	.72	.61
	NEAR-UV IRRADIATION FOR TWO HOURS			
0	.59	.68	.90	.72
15	.42	.81	--	.62
30	.41	.69	.42	.51
45	.36	--	--	.36
60	.28	.53	.30	.37
90	.25	.53	.26	.35
120	.23	.47	.25	.32
180	.22	.44	.20	.29
240	.21	.40	.19	.27
300	.21	.37	.16	.25
	NEAR-UV IRRADIATION FOR THREE HOURS			
0	.29	.79	.71	.60
15	.19	.80	--	.50
30	.09	.69	.23	.34
45	.08	--	--	.08
60	.07	.44	.17	.23
90	.06	.34	.13	.18
120	.04	.30	.11	.15
180	.04	.25	.09	.13
240	.04	.23	.07	.11
300	.04	.20	.06	.10

TABLE 31

THE LEAKAGE OF $^{86}RB^{+}$ FROM GM730 CELLS WITH TIME 24 HOURS AFTER 1, 2 OR 3 HOURS OF BROAD-BAND NEAR-UV IRRADIATION. THE LEAKAGE IS EXPRESSED AS THE RATIO OF THE DISINTEGRATIONS PER MINUTE OF IRRADIATED:CONTROL CELLS

Time (min)	Experiment 1	Experiment 2	Mean
	NEAR-UV IRRADIATION FOR ONE HOUR		
0	1.23	1.09	1.16
15	1.09	1.07	1.08
30	.86	1.10	.98
45	.94	.91	.93
60	.83	1.01	.92
90	.82	--	.82
120	.85	.94	.90
180	.94	.98	.96
240	.90	.99	.95
300	.98	.91	.95
	NEAR-UV IRRADIATION FOR TWO HOURS		
0	1.15	.95	1.05
15	.89	.81	.85
30	.75	.82	.79
45	.75	.79	.77
60	.65	.80	.73
90	.67	.--	.67
120	.70	.76	.73
180	.77	.81	.79
240	.80	.86	.83
300	.83	.75	.79
	NEAR-UV IRRADIATION TIME FOR THREE HOURS		
0	.61	.81	.71
15	.64	.88	.76
30	.55	.82	.69
45	.52	83	.68
60	.40	.77	.59
90	.38	.--	.38
120	.40	.73	.57
180	.45	.65	.55
240	.41	.68	.55
300	.43	.55	.49

respectively whereas the corresponding values for normal GM730 cells are 90%, 70% and 55%.

The decrease in the amount of $^{86}Rb^{+}$ released from the cells is a reflection of the $^{86}Rb^{+}$ which was taken up originally. The observation that irradiated cells have a reduced ability to actively take up $^{86}Rb^{+}$ can be a result of at least two different factors. First, it could reflect a decreased activity of the Na^{+}/K^{+} pump as a result of irradiation damage, or a decrease in the passive permeability of the cell. Alternatively, it could be a reflection of severely damaged cells which are no longer going to survive. Further experimental work is needed to clarify the mechanisms underlying these observations.

GENERAL CONCLUSIONS

The results presented in this work can be summarized as follows:

(1) The temperature during the irradiation of normal skin fibroblasts in suspension influenced their survival in a wavelength-dependent way. This may be taken as further evidence that irradiation with different sections of UV-light results in different cellular effects. Specif ically, an increase in the irradiation temperature resulted in sensitization to wavelengths 254 and 313 nm but in protection against lethality following 325, 334 and 365 nm irradiation.

(2) Actinic reticuloid (AR$\epsilon\omega$)cells were found to be approximately 4 times more sensitive than the normal human fibroblast strain GM730 to monochromatic 365 nm radiation at 25°C as well as to H_2O_2 treatment. No difference in their sensitivity to other monochromatic wavelengths (254 or 313 nm) or to gamma-radiation was found.

(3) Trolox-C, a vitamin E analogue, provided cellular protection to AR cells against 365 nm irradiation at 25°C. This protection was more pronounced when the cells had been grown in its presence prior to irradiation rather than when incubated in its presence after irradiation. Normal cell sensitivity and 254 nm sensitivity was not affected by the presence of Trolox-C in the plating medium after irradiation.

(4) The incorporation of 70 per cent D_2O in the buffer used for suspension of the cells during irradiation resulted in a sensitization of both cell lines to 365 nm irradiation at 25°C. No

alteration in sensitivity was observed when irradiation took place at 0°C or following 254 nm irradiation.

(5) Broad-band near-UV irradiation resulted in membrane damage evidenced as increased $^{86}Rb^{+}$ leakage in AR$^{6-9}$ but not normal cells at doses comparable to lethality. The presence of Trolox-C during the growth of cells prior to irradiation offered protection against $^{86}Rb^{+}$ leakage. Far-UV irradiation did not induce Rb^{+} leakage until doses 2-3 orders of magnitude greater than the lethal dose were reached.

The following ideas were developed regarding near-UV mechanisms of lethality and in particular AR$^{6-9}$ cellular sensitivity.

It is becoming accepted that reactive oxygen species are formed as a result of near-UV radiation and that it is a vital function of the cell to effectively scavenge these by antioxidant enzymes and antioxidant molecules. One hypothesis is that AR cells are defective in an enzymatic function related to this defense mechanism. The protective effect of Trolox-C can be envisaged as taking part in at least two steps. One part is related to the scavenging of these species, in particular singlet oxygen and superoxide anion, and the prevention of H_2O_2 and $OH^{\cdot}$ formation, and the other as the prevention of lipid peroxidation of cellular membranes. Near-UV induced lipid peroxidation could lead to generalized membrane damage which could result in $^{86}Rb^{+}$ leakage. This membrane damage due to inadequate scavenging of reactive oxygen species or due to other unidentified factors, was observed in AR cells but not normal cells.

The sensitization resulting from irradiation in D_2O occured in both cell lines and should be regarded separately. It could be

explained by the previous suggestion, i.e. D_2O enhances the lifetime of singlet oxygen which at temperatures allowing enzymatic action is in turn converted to other reactive oxygen species that present an extra load, both for AR cells which are already unable to scavenge all of them and to normal cells which are unable to scavenge the extra load. The non-scavenged reactive species could then lead to lethal lesions.

It cannot be excluded that AR^{6-4} cells may be deficient in another enzymatic function such as in enzymes which would normally repair near-UV induced damage and this possibility needs further investigation. Regarding the target of irradiation and the lethal lesions produced, as with normal cells, both DNA and membrane damage could be important and their relative contribution to lethality may depend on particular circumstances.

A P P E N D I C E S

APPENDIX 1

TABLE A1. CHEMICAL COMPOSITION OF MEDIA USED:

Ingredient	Minimum Essential Medium (Eagle) (Modified) with Earle's Salts (mg/litre)	Dulbecco's Modification of Eagle's Medium (mg/litre)
L-Arginine HCl	126.4	84.00
L-Cysteine disodium salt	28.42	56.78
L-Glutamine	292.3	584.0
Glycine	---	30.00
L-Histidine HCl H_2O	41.90	42.00
L-Isoleucine	52.50	104.8
L-Leucine	52.50	104.8
L-Lysine HCl	73.06	146.2
L-Methionine	14.90	30.00
L-Phenylalanine	33.02	66.00
L-Serine	---	42.00
L-Threonine	47.64	95.20
L-Tryptophan	10.20	16.00
L-Tyrosine disodium salt	45.02	89.50
L-Valine	46.90	93.60
D-Ca pantothenate	1.00	4.00
Choline chloride	1.00	4.00
Folic acid	1.00	4.00
i-Inositol	2.00	7.00
Nicotinamide	1.00	4.00
Pyridoxal HCl	1.00	4.00
Riboflavin	0.10	0.40
Thiamin HCl	1.00	4.00
$CaCl_2$ H_2O	264.9	264.9
$Fe(NO_3)_3 9H_2O$	---	0.10
KCl	400.00	400.0
$MgSO_4$ $7H_2O$	200.00	200.0
NaCl	6800	6400
$NaHCO_3$	2000	3700
NaH_2PO_4 $2H_2O$	158.3	141.3
D-Glucose	1000	4500
Phenol red sodium salt	17.00	15.00
Sodium pyruvate	---	110.0

APPENDIX 2: UV DOSIMETRY BY CHEMICAL ACTINOMETRY

a. Solutions Used

Actinometer solution:

0.006M of potassium ferrioxalate made up as follows:

800 ml of distilled water containing 2.947g of potassium ferrioxalate

+ 100 ml N H_2SO_4 (Volucon, M+B)

to 1000 ml with double distilled water

Calibration Solution

4×10^{-7} moles of Fe^{++} ions per ml made up as follows:

1 ml of 0.1 M solution of ferrous sulphate (AR)

to 250 ml with 0.1N H_2SO_4 (Volucon, M+B)

Phenanthroline Solution

1% Phenanthroline solution made up as follows:

1.00 g of 1:10 phenanthroline monohydrate (BDH)

to 1000 ml with double distilled water

Buffer

600 ml N sodium acetate solution (AR Solid)

+ 350 ml N H_2SO_4 (Volucon, M+B)

to 1000 ml with double distilled water

b. Calibration of the Actinometer Solution

Eleven x 25 ml stoppered volumetric flasks were used in which volumes of calibration solution from 0 to 5.0 ml were added in 0.5 ml steps. The necessary volume of 0.1 N H_2SO_4 was added to 12.5 ml followed by 2.0 ml of 1% phenanthroline solution and made up to 25 ml with buffer. The flasks were shaken and allowed to stand for 30 minutes to develop the colour, after which time an optical density

reading for each solution was taken at 510 nm, using the solution with no calibration solution as blank. A plot of optical density at 510 nm against moles of Fe^{++} ions was prepared and the slope of the line, calculated by regression analysis, was found to be 0.1121×10^{8} (Fig. A1).

c. Dosimetry for Ultraviolet Sources

Three ml of actinometer solution were placed in the quartz cuvette and exposed to monochromatic light for exposure times which would give appropriate optical density readings. After exposure, 2.5 ml of solution were removed from the cuvette and developed as previously described. The optical density at 510 nm and the slope of the calibration curve were used to calculate the fluence rate.

d. Calculation of Fluence Rate

Slope of calibration curve	=	0.1121×10^{8}
Volume irradiated	=	3.0 ml
Irradiation area	=	300 mm^2
Volume sampled and developed	=	2.5 ml

An exposure time of seconds gave an optical density at 510 nm

$$\frac{OD_{510\ nm}}{\text{Slope of calibration curve}} = \text{Moles per ml of } Fe^{++} \text{ ions}$$

This Fe^{++} ion concentration per ml was in 25 ml of developed solution originally from 2.5 ml sampled from a total of 3 ml of solution irradiated. Thus the above concentration of Fe^{++} ions, multiplied by 25 x 3/2.5 gives the total Fe^{++} concentration in moles in the 3 ml of irradiated solution. If the total moles of Fe^{++} ions

in 3 ml of irradiated solution is Y, then the fluence rate may be calculated as follows:

The quantum yield is 1.26 moles per Einstein.

Thus Y moles of Fe^{++} ions $= \frac{Y}{1.26}$ Einsteins

At a specific wavelength, ergs per Einstein = a

Therefore

$$\frac{Y}{1.26} \text{ Einsteins} = \frac{a \times Y}{1.26} \text{ ergs}$$

Since this is for 300 mm^2 irradiation area, the fluence is

$$\frac{a \times Y}{300 \times 1.26} \text{ ergs } mm^{-2}$$

Therefore, fluence rate $= \frac{a \times Y}{300 \times 1.26 \times t}$ ergs $mm^{-2} sec^{-1}$

$$= \frac{a \times Y}{300 \times 1.26 \times t \times 10} Jm^{-2} sec^{-1}$$

$$= \frac{a \times OD \times 25 \times 3}{300 \times 1.26 \times t \times 10 \times 2.5 \times \text{slope}} Jm^{-2} sec^{-1}$$

$$= \frac{a \times OD \times 7.0798 \times 10^{-10}}{t} Jm^{-2} sec^{-1}$$

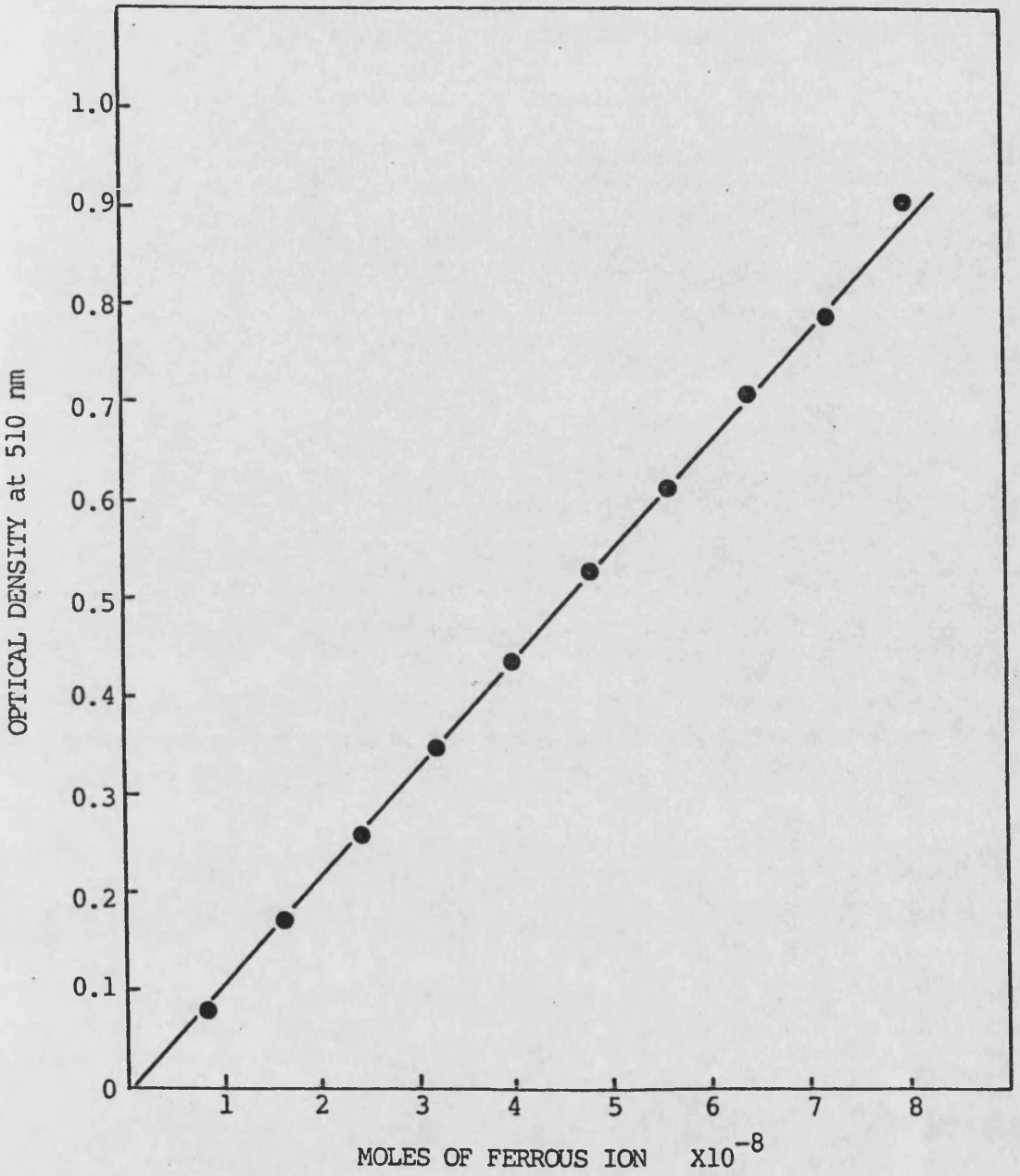

Figure A1: Calibration curve for the conversion of optical density to amount of ferrous ion.

APPENDIX 3: GAMMA-RADIATION DOSIMETRY BY FRICKE DOSIMETRY

a. Solutions Used

Dosimetric Solution

The dosimetric solution contained

10^{-3} M $Fe(NH_4)_2(SO_4)_2\ 6H_2O$

+ 10^{-3} M NaCl

dissolved in 0.8 N H_2SO_4

This was prepared freshly by using

0.985 g $Fe(NH_4)_2(SO_4)_2$ (BDH)

+ 25 ml 0.01 M NaCl (BDH)

+ 100 ml 2N H_2SO_4

to 250 ml with double distilled water

b. Dosimetry for ^{137}Cs source

10 ml of a freshly prepared dosimetric solution were transfered to the irradiation vessel positioned at 23 cm from the base of the chamber, and exposed to gamma irradiation for different time exposures. After each irradiation, the yield of ferric ions was measured spectrophotometrically at 305 nm at 22°C (Table A2). A plot of the absorbance of the dosimetric solution against irradiation time is shown in Fig. A2. The result demonstrates that within the irradiation time of 50 minutes, the absorbance increases linearly with dose.

c. Calculation of Fluence Rate

The absorbed radiation dose is calculated by an equation derived in the following manner:

The amount of Fe^{+++} liberated when the dosimetric solution is irradiated can be determined from Beer's Law.

$$C_{Fe^{+++}} \text{ (moles/litre)} = \frac{A}{\epsilon \times L}$$

where, A is the absorbance, ϵ is the absorbancy ($M^{-1}cm^{-1}$) at the wavelength used and L is the optical pathlength of the sample (in cm). If 1 cm cuvettes are used for the determination of the optical absorbance, then,

$$C_{Fe^{+++}} \text{ (moles/litre)} = \frac{A}{\epsilon}$$

$$C_{Fe^{+++}} \text{ (moles/ml)} = \frac{A}{10^3 \times \epsilon}$$

$$C_{Fe^{+++}} \text{ (moles/g)} = \frac{A}{10^3 \times \epsilon \times \rho}$$

Where ρ is the density of the solution.

Number of Fe^{+++} ions/g of solution

$$= \frac{A}{10^3 \times \epsilon \times \rho} \times \text{Avogadro's Number}$$

$$= \frac{A \times 6.023 \times 10^{20}}{\epsilon \times \rho}$$

Since the radiation chemical yield (G) represents the number of ions that are formed per 100 MeV absorbed, then:

$$E \text{ (in eV/g)} = \frac{A \times 6.023 \times 10^{20}}{\epsilon \times \rho \times G \times 10^{-2}}$$

Where E is the amount of energy absorbed.

1eV = 1.602×10^{-12} ergs. Therefore

$$E \text{ (in ergs/g)} = \frac{A \times 6.023 \times 10^{20} \times 1.602 \times 10^{-12}}{\epsilon \times \rho \times G \times 10^{-2}}$$

Since 1 rad = 100 ergs/g, then,

$$\text{Dose (in rads)} = \frac{A \times 6.023 \times 10^{8} \times 1.602}{\epsilon \times \rho \times G \times 10^{-2} \times 10^{2}}$$

$$= \frac{A \times 9.65 \times 10^{8}}{\epsilon \times \rho \times G}$$

ϵ at wavelength 305 nm, at 25°C, is 2196 $M^{-1}cm^{-1}$ and can be corrected for temperature differences by the factor $1+0.006(t_{25}-t)$, where t is the temperature at which the absorbance was read (22°C)

G-value for ^{137}Cs is 15.3 and ρ is 1.024.

Therefore when slope = 3.74×10^{-3} (see Table A2)

$$\text{Dose (in rads)} = \frac{3.74 \times 10^{-3} \times 9.65 \times 10^{8}}{2196 \times 15.3 \times 1.024 \; [(1 + 0.006 \; (25-22)]}$$

$$= 103.05 \text{ rads/min}$$

$$= 1.03 \text{ Gy/min}$$

TABLE A2. ABSORBANCE OF ^{137}Cs GAMMA IRRADIATED FERROUS SULPHATE SOLUTION, READ AT 305 NM, AT 22°C

Irradiation time (min)	Mean Absorbance (A)
0	
10	.033
15	.05
20	.075
25	.09
30	.11
35	.125
40	.145
45	.17
50	.18

By linear regression: Slope = 3.74×10^{-3}

I = -3.63×10^{-3}

Corr. Coeff. = .998

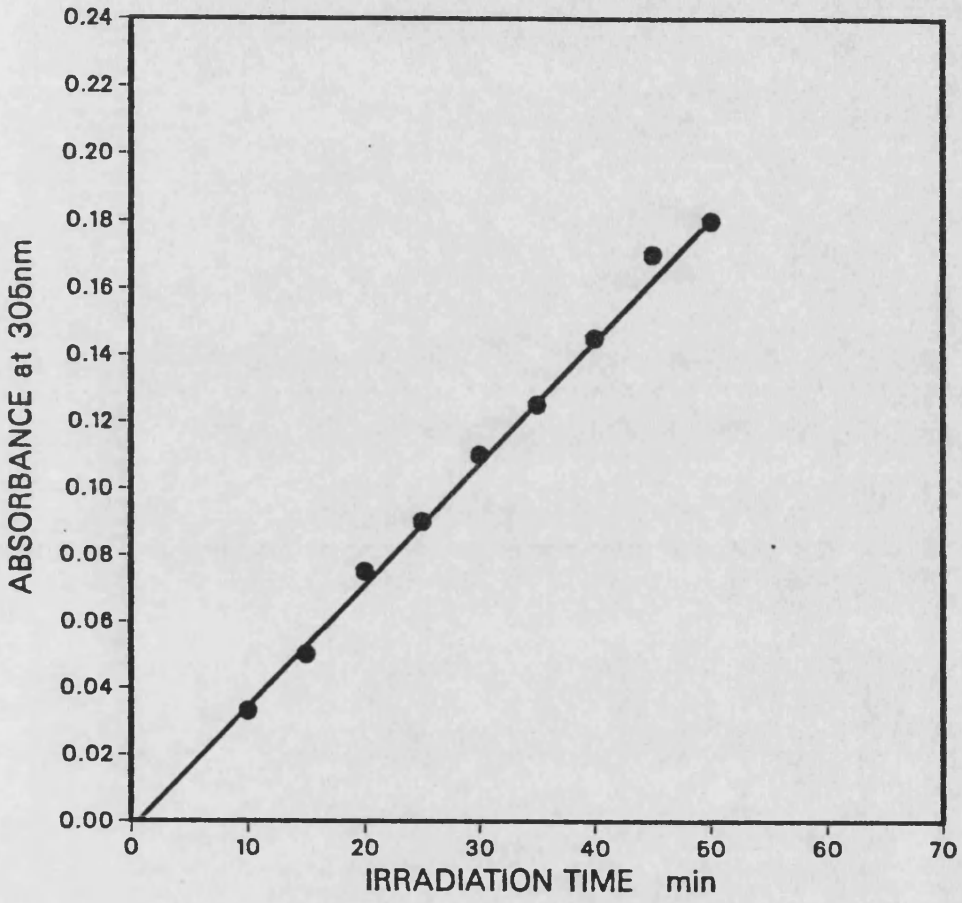

Figure A2: Absorbance of ferrous sulphate solution after ^{137}Cs gamma irradiation measured at 22 ^{o}C.

APPENDIX 4: CORRECTION OF UV-FLUENCE RATE BY THE MOROWITZ FACTOR

TABLE A3. REDUCTION IN OPTICAL DENSITY, MEASURED USING THE ORIEL 7102 THERMOPILE, WITH VARIOUS CONCENTRATIONS OF STIRRED CELLS AND THE CALCULATED MOROWITZ FACTOR AT 254, 313 AND 365 NM

Wavelength	Concentration (cells/ml)	Optical Density	%Transmission		Correction Factor
254 nm	blank	20.0	100		
	$5x10^4$	18.5	92.50		
	$1x10^5$	17.8	89.00	--->	0.945
	$2x10^5$	16.5	82.50		
	$4x10^5$	14.7	73.50		
	$6x10^5$	13.0	65.00		
	$8x10^5$	11.3	56.05		
	$1x10^6$	9.5	47.50		
313 nm	blank	235	100		
	$5x10^4$	230	97.87		
	$1x10^5$	227	96.60	--->	0.983
	$2x10^5$	212	90.21		
	$4x10^5$	190	80.85		
	$6x10^5$	170	72.34		
	$8x10^5$	158	67.23		
	$1x10^6$	135	57.45		
365 nm	blank	890	100		
	$5x10^4$	890	100		
	$1x10^5$	870	97.75	--->	0.989
	$2x10^5$	820	92.13		
	$4x10^5$	750	84.27		
	$6x10^5$	690	77.53		
	$8x10^5$	660	74.16		
	$1x10^6$	560	62.92		

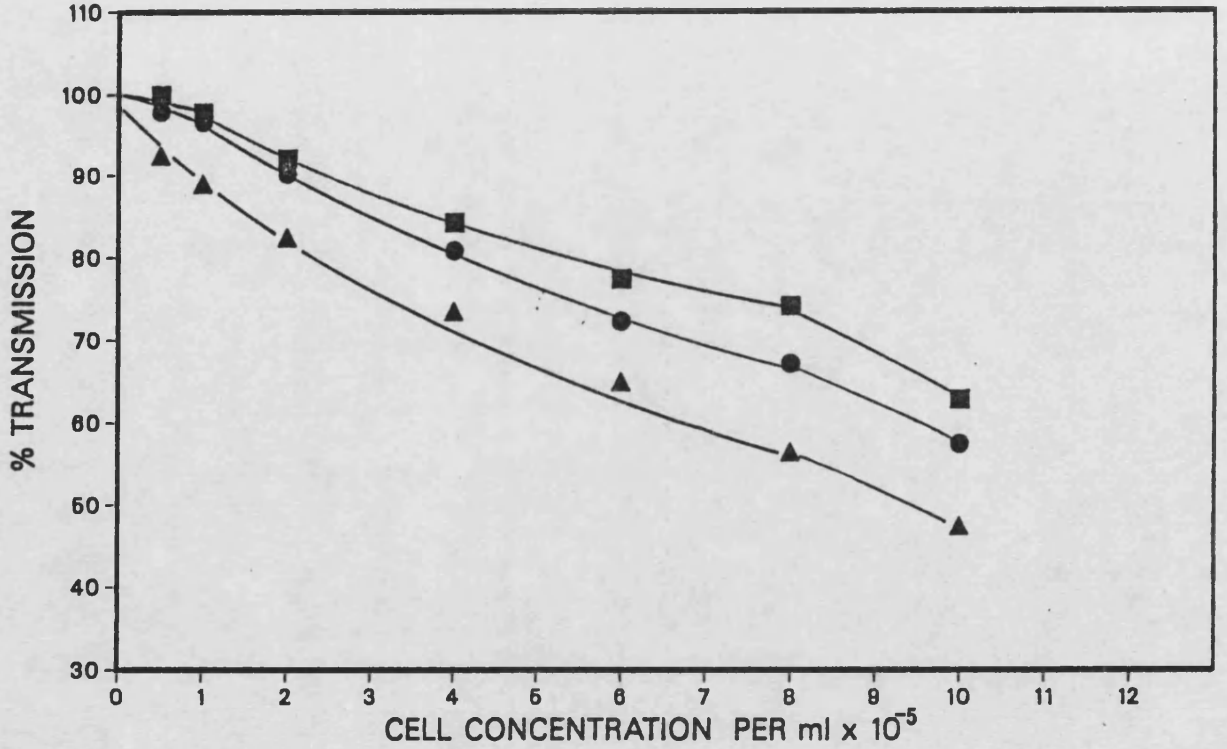

Figure A3: The reduction in transmission of 254 (▲), 313 (●) and 365 nm (■) radiation by cell suspensions of different cell concentration as measured by a thermopile.

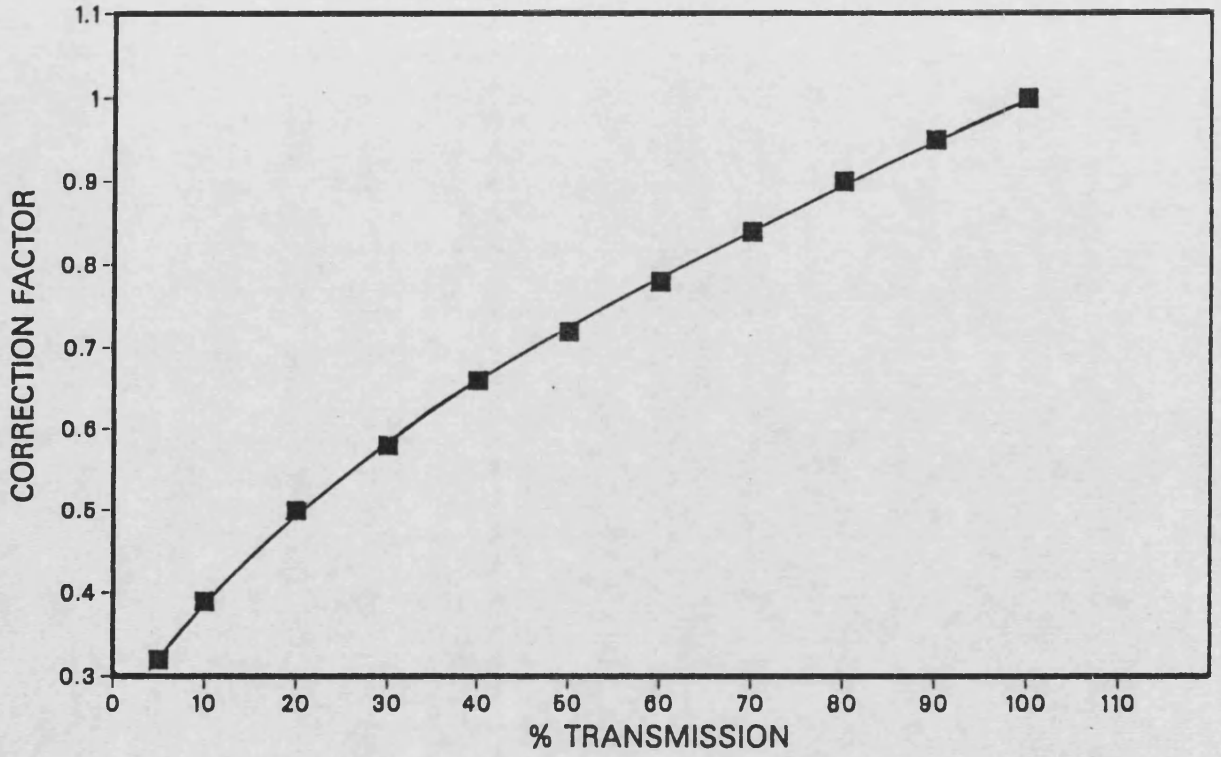

Figure A4: The correction factor curve as plotted using data from Morowitz, 1950.

APPENDIX 5: STATISTICAL ANALYSIS OF RESULTS

The (k) and (n) values from groups of survivor curves were analysed for homogeneity within groups and between groups by computing chi-squared (X^2) as follows. If $\Sigma(\bar{p}-p)^2$ is the sums of squares of n estimates of a parameter p computed from a normal distribution with variance σ^2, then the quantity

$$\Sigma \frac{(\bar{p}-p)^2}{\sigma^2}$$

follows a chi-squared distribution with n-1 degrees of freedom (Snedecar and Cochran, 1967) Thus

$$x^2(n-1) = \frac{\Sigma(\bar{b}-b)^2}{s^2}$$

where s^2 is a pooled estimate of the variance derived from the standard errors of the slopes (b) which can be used to test for significant heterogeneity amongst the n slopes. By subtracting the chi-squared for subsets from the chi-squared for the set, a between subset chi-squared can be derived.

APPENDIX 6: GROWTH CURVE CONSTRUCTION

Method

One ml of cells containing either 10^5 or 3×10^5 cells were added to 9 ml EMEM containing 15% foetal calf serum in 90 mm plates. Plates were placed in boxes, gassed with 5% CO_2 and incubated at $37^{\circ}C$. After appropriate time intervals, one plate at a time was trypsinized in the usual way and the number of cells counted using the haemocytometer.

If Trolox-C were to be used, the appropriate concentration was added during subculture.

Table A4: 3×10^5 cells inoculated

Table A5: 1×10^5 cells inoculated

TABLE A4. GROWTH OF AR6LO AND GM730 CELLS

AR6LO		GM730	
Time(hrs)	Cell counts x 10^{-5}	Time(hrs)	Cell counts x 10^{-5}
24	1.54	17	2.32
48	2.92	28	3.15
74	5.22	38	5.05
96	7.07	48	6.90
121	8.71	62	8.52
144	7.12	72	11.50
169	7.75	92	14.52
		120	16.65

TABLE A5. GROWTH OF AR6LO AND GM730 CELLS IN THE ABSENCE AND PRESENCE OF 30 μg/ml TROLOX-C IN THE GROWTH MEDIUM

Time(hrs)	Cell Counts x 10^{-5}			
	AR	AR+Trolox-C	GM	GM+Trolox-C
20	0.53	1.07	0.45	0.69
27	0.48	1.09	0.53	0.79
45	0.33	0.77	0.54	0.80
51	0.50	1.36	1.19	1.34
69	0.92	1.87	2.67	2.57
92	1.51	2.13	4.68	4.38
116	2.63	3.23	7.33	4.82
141	3.33	3.92	8.07	7.94
164	3.19	5.92	10.87	10.21
170	5.22	5.73	--	--
191	3.85	5.15	9.96	10.31
214	3.92	3.89	8.26	7.62

APPENDIX 7: $^{86}RB^{+}$ QUENCH CURVE

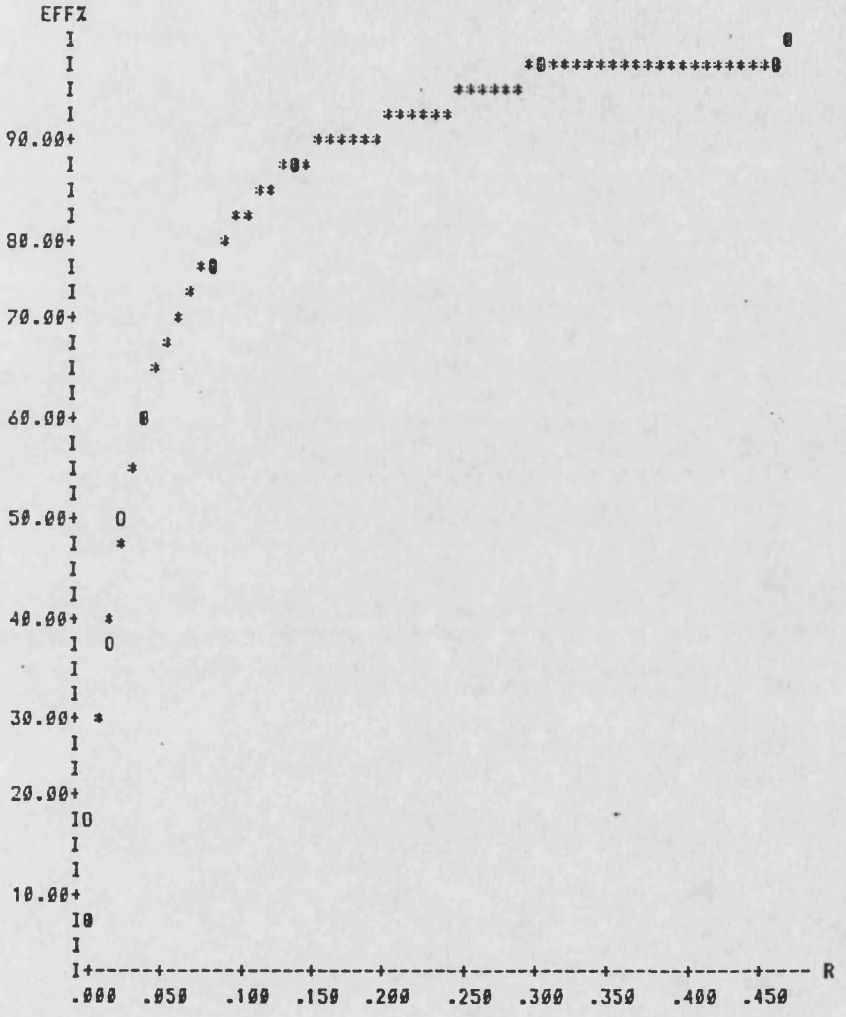

Figure A5. Quench curve for $^{86}Rb^{+}$ determined by the LKB Rackbeta 1215 liquid scintillation counter.

APPENDIX 8: E X P E R I M E N T A L D A T A

T A B L E S A 6 - A 31

TABLE A6. SURVIVAL OF GM730 CELLS TO 365 NM RADIATION AT 0°C (SEE FIG. 17)

Experiment Number	1	2	3	4	5	6	7
Passage Number	18	19	14	15	17	17	15
Plating Efficiency (%)	19	19	30	33	11	14	8
UV FLUENCE Jm^{-2}	S U R V I V I N G F R A C T I O N						
5.0×10^{4}	8.45×10^{-1}	6.79×10^{-1}	8.90×10^{-1}	9.94×10^{-1}	6.82×10^{-1}	9.04×10^{-1}	---
1.0×10^{5}	8.77×10^{-1}	5.53×10^{-1}	7.00×10^{-1}	7.68×10^{-1}	5.45×10^{-1}	6.47×10^{-1}	6.73×10^{-1}
1.5×10^{5}	6.15×10^{-1}	4.90×10^{-1}	5.40×10^{-1}	5.63×10^{-1}	3.91×10^{-1}	4.78×10^{-1}	4.50×10^{-1}
2.0×10^{5}	3.29×10^{-1}	2.58×10^{-1}	3.80×10^{-1}	3.58×10^{-1}	2.41×10^{-1}	3.25×10^{-1}	2.35×10^{-1}
2.5×10^{5}	1.61×10^{-1}	1.25×10^{-1}	1.98×10^{-1}	2.38×10^{-1}	2.64×10^{-1}	1.93×10^{-1}	1.75×10^{-1}
3.0×10^{5}	8.50×10^{-2}	---	9.85×10^{-2}	1.07×10^{-1}	1.00×10^{-1}	6.99×10^{-2}	1.12×10^{-1}
3.5×10^{5}	4.82×10^{-2}	---	6.25×10^{-2}	6.42×10^{-2}	1.23×10^{-1}	4.46×10^{-2}	9.67×10^{-2}
4.0×10^{5}	---	---	5.20×10^{-2}	3.98×10^{-2}	6.88×10^{-2}	2.59×10^{-2}	---
4.5×10^{5}	---	---	---	---	2.55×10^{-2}	---	---
5.0×10^{5}	---	---	---	---	---	---	---

TABLE A7. SURVIVAL OF GM730 CELLS TO 365 NM RADIATION AT 25°C (SEE FIG. 18)

Experiment Number	8	9	10	11
Passage Number	13	14	11	12
Plating Efficiency (%)	34	37	41	38
UV FLUENCE Jm^{-2}	SURVIVING FRACTION		UV FLUENCE Jm^{-2}	SURVIVING FRACTION
$5.0X10^{3}$	$6.92x10^{-1}$	$1.01x10^{0}$	$3.3x10^{3}$	$8.60x10^{-1}$ $8.10x10^{-1}$
$1.0x10^{4}$	$5.73x10^{-1}$	$8.79x10^{-1}$	$6.7x10^{3}$	$7.95x10^{-1}$ $7.07x10^{-1}$
$1.5x10^{4}$	$4.10x10^{-1}$	$8.74x10^{-1}$	$1.0x10^{4}$	$8.08x10^{-1}$ $7.39x10^{-1}$
$2.0x10^{4}$	$3.52x10^{-1}$	$7.66x10^{-1}$	$1.3x10^{4}$	$5.28x10^{-1}$ $6.43x10^{-1}$
$2.5x10^{4}$	$3.18x10^{-1}$	$8.20x10^{-1}$	$1.7x10^{4}$	$5.11x10^{-1}$ $6.93x10^{-1}$
$3.0x10^{4}$	$2.24x10^{-1}$	$6.77x10^{-1}$	$2.0x10^{4}$	$5.63x10^{-1}$ $6.72x10^{-1}$
$3.5x10^{4}$	$2.15x10^{-1}$	$5.91x10^{-1}$	$2.3x10^{4}$	$4.19x10^{-1}$ $6.15x10^{-1}$
$4.0x10^{4}$	$1.46x10^{-1}$	$5.24x10^{-1}$	$2.7x10^{4}$	$3.90x10^{-1}$ $6.21x10^{-1}$
$4.5x10^{4}$	$1.69x10^{-1}$	$4.99x10^{-1}$	$3.0x10^{4}$	$3.25x10^{-1}$ $4.51x10^{-1}$
$5.0x10^{4}$	$8.72x10^{-2}$	$5.57x10^{-1}$	$3.3x10^{4}$	$3.68x10^{-1}$ $3.94x10^{-1}$

TABLE A8. SURVIVAL OF GM730 CELLS TO 365 NM RADIATION AT 37°C (SEE FIG. 19)

Experiment Number	12	13
Passage Number	14	16
Plating Efficiency (%)	42	17
UV FLUENCE Jm^{-2}	S U R V I V I N G	F R A C T I O N
$5.0X10^{3}$	---	$9.98x10^{-1}$
$1.0x10^{4}$	$8.64x10^{-1}$	$8.26x10^{-1}$
$1.5x10^{4}$	$6.29x10^{-1}$	$8.09x10^{-1}$
$2.0x10^{4}$	$7.07x10^{-1}$	$1.08x10^{0}$
$2.5x10^{4}$	$5.21x10^{-1}$	$7.55x10^{-1}$
$3.0x10^{4}$	$7.71x10^{-1}$	$7.55x10^{-1}$
$3.5x10^{4}$	$5.64x10^{-1}$	$5.21x10^{-1}$
$4.0x10^{4}$	$4.50x10^{-1}$	$5.78x10^{-1}$
$4.5x10^{4}$	$3.68x10^{-1}$	$4.90x10^{-1}$
$5.0x10^{4}$	---	$3.88x10^{-1}$

TABLE A9. SURVIVAL OF GM730 CELLS TO 254 NM RADIATION AT 0°C (SEE FIG. 21)

Experiment Number	14	15	16	17	18	19	20
Passage Number	11	11	13	13	13	13	16
Plating Efficiency (%)	40	42	37	20	15	33	14
UV FLUENCE Jm^{-2}	S U R V I V I N G F R A C T I O N						
5.0×10^{0}	9.80×10^{-1}	1.00×10^{-1}	9.87×10^{-1}	9.50×10^{-1}	9.50×10^{-1}	1.17×10^{0}	---
1.0×10^{1}	9.60×10^{-1}	9.40×10^{-1}	1.07×10^{0}	8.23×10^{-1}	9.60×10^{-1}	9.46×10^{-1}	6.96×10^{-1}
1.5×10^{1}	8.60×10^{-1}	9.92×10^{-1}	9.76×10^{-1}	8.03×10^{-1}	9.90×10^{-1}	8.74×10^{-1}	---
2.0×10^{1}	7.60×10^{-1}	8.45×10^{-1}	9.08×10^{-1}	6.35×10^{-1}	7.40×10^{-1}	8.06×10^{-1}	6.47×10^{-1}
2.5×10^{1}	6.05×10^{-1}	8.00×10^{-1}	7.92×10^{-1}	5.79×10^{-1}	3.53×10^{-1}	2.71×10^{-1}	6.25×10^{-1}
3.0×10^{1}	4.80×10^{-2}	5.80×10^{-1}	7.22×10^{-1}	5.11×10^{-1}	1.76×10^{-1}	2.26×10^{-1}	3.85×10^{-1}
3.5×10^{1}	3.57×10^{-2}	4.10×10^{-1}	5.34×10^{-1}	3.60×10^{-1}	1.69×10^{-1}	1.69×10^{-1}	---
4.0×10^{1}	---	---	4.28×10^{-1}	2.70×10^{-1}	---	1.39×10^{-1}	2.89×10^{-1}
4.5×10^{1}	---	---	---	1.53×10^{-1}	---	---	1.81×10^{-1}
5.0×10^{1}	1.10×10^{-1}	9.70×10^{-2}	2.72×10^{-1}	1.33×10^{-1}	1.00×10^{-1}	9.70×10^{-2}	1.75×10^{-1}
6.0×10^{1}	7.50×10^{-2}	6.90×10^{-2}	1.45×10^{-1}	9.16×10^{-2}	6.83×10^{-2}	4.35×10^{-2}	8.82×10^{-2}

TABLE A10. SURVIVAL OF GM730 CELLS TO 254 NM RADIATION AT 25° AND 37°C (SEE FIGS. 22, 23)

Experiment Number	21	22	23	24	25
Passage Number	12	15	15	15	16
Plating Efficiency (%)	38	24	13	11	5
UV FLUENCE Jm^{-2}	SURVIVING FRACTION			SURVIVING FRACTION	
5.0×10^{0}	8.32×10^{-1}	---	---	---	7.82×10^{-1}
1.0×10^{1}	7.95×10^{-1}	1.04×10^{0}	8.55×10^{-1}	8.21×10^{-1}	---
1.5×10^{1}	8.11×10^{-1}	---	7.97×10^{-1}	6.32×10^{-1}	6.73×10^{-1}
2.0×10^{1}	7.42×10^{-1}	---	6.39×10^{-1}	3.68×10^{-1}	5.64×10^{-1}
2.5×10^{1}	---	---	4.73×10^{-1}	2.39×10^{-1}	3.52×10^{-1}
3.0×10^{1}	4.81×10^{-1}	3.56×10^{-1}	2.62×10^{-1}	2.31×10^{-1}	2.85×10^{-1}
3.5×10^{1}	2.61×10^{-1}	3.31×10^{-1}	2.10×10^{-1}	1.54×10^{-1}	2.06×10^{-1}
4.0×10^{1}	2.10×10^{-1}	2.15×10^{-1}	1.62×10^{-1}	1.51×10^{-1}	1.27×10^{-1}
4.5×10^{1}	1.04×10^{-1}	---	1.15×10^{-1}	1.25×10^{-1}	8.43×10^{-2}
5.0×10^{1}	---	---	8.31×10^{-2}	1.00×10^{-1}	7.40×10^{-2}
5.5×10^{1}	---	---	6.36×10^{-2}	7.04×10^{-2}	5.70×10^{-2}
6.0×10^{1}	---	$6.44\ 10^{-2}$	3.95×10^{-2}	5.91×10^{-2}	4.49×10^{-2}

TABLE A11. SURVIVAL OF GM730 CELLS TO 313 NM RADIATION AT 0°C. (SEE FIG. 25)

Experiment Number	26	27	28	29	30	31	32
Passage Number	17	13	20	17	14	15	15
Plating Efficiency (%)	41	34	28	19	23	26	43
UV FLUENCE Jm^{-2}	S U R V I V I N G F R A C T I O N						
5.0×10^{3}	---	---	8.04×10^{-1}	9.88×10^{-1}	9.55×10^{-1}	8.99×10^{-1}	9.79×10^{-1}
1.0×10^{4}	8.80×10^{-1}	1.06×10^{0}	7.61×10^{-1}	8.59×10^{-1}	8.95×10^{-1}	7.67×10^{-1}	7.69×10^{-1}
1.5×10^{4}	---	---	5.57×10^{-1}	7.68×10^{-1}	7.91×10^{-1}	---	---
2.0×10^{4}	5.27×10^{-1}	6.67×10^{-1}	6.40×10^{-1}	7.23×10^{-1}	5.72×10^{-1}	5.10×10^{-1}	7.81×10^{-1}
2.5×10^{4}	---	---	5.57×10^{-1}	4.68×10^{-1}	3.83×10^{-1}	3.13×10^{-1}	4.60×10^{-1}
3.0×10^{4}	2.36×10^{-1}	4.19×10^{-1}	4.39×10^{-1}	3.73×10^{-1}	2.44×10^{-1}	2.58×10^{-1}	4.05×10^{-1}
3.5×10^{4}	---	---	---	3.41×10^{-1}	1.44×10^{-1}	1.98×10^{-1}	2.37×10^{-1}
4.0×10^{4}	2.51×10^{-1}	2.41×10^{-1}	1.97×10^{-1}	2.44×10^{-1}	---	1.24×10^{-1}	1.16×10^{-1}
4.5×10^{4}	---	---	---	---	---	7.73×10^{-2}	8.31×10^{-2}
5.0×10^{4}	7.12×10^{-2}	1.23×10^{-1}	5.95×10^{-2}	1.23×10^{-1}	---	4.77×10^{-2}	5.05×10^{-2}
6.0×10^{4}	4.58×10^{-2}	7.14×10^{-2}	---	5.73×10^{-2}	---	2.70×10^{-2}	2.78×10^{-2}

TABLE A12. SURVIVAL OF GM730 CELLS TO 313 NM RADIATION AT 25° AND 37°C (SEE FIGS. 26, 27)

Experiment Number	33	34	35	36	37	38
Passage Number	13	16	15	16	13	18
Plating Efficiency (%)	33	19	22	10	7	11
UV FLUENCE Jm^{-2}	S U R V I V I N G F R A C T I O N			S U R V I V I N G F R A C T I O N		
$5.0x10^{3}$	$8.69x10^{-1}$	---	$6.68x10^{-1}$	---	$7.04x10^{-1}$	$8.30x10^{-1}$
$1.0x10^{4}$	$6.33x10^{-1}$	$7.05x10^{-1}$	$5.99x10^{-1}$	$6.10x10^{-1}$	$4.17x10^{-1}$	$5.26x10^{-1}$
$1.5x10^{4}$	$5.05x10^{-1}$	$4.32x10^{-1}$	---	---	$2.14x10^{-1}$	$2.77x10^{-1}$
$2.0x10^{4}$	$3.68x10^{-1}$	$3.63x10^{-1}$	$2.95x10^{-1}$	---	$1.14x10^{-1}$	$1.91x10^{-1}$
$2.5x10^{4}$	$2.52x10^{-1}$	$2.47x10^{-1}$	$1.52x10^{-1}$	$9.59x10^{-2}$	$9.17x10^{-2}$	$1.26x10^{-1}$
$3.0x10^{4}$	$1.80x10^{-1}$	$1.70x10^{-1}$	$1.43x10^{-1}$	$5.55x10^{-2}$	$7.22x10^{-2}$	$4.80x10^{-2}$
$3.5x10^{4}$	$1.49x10^{-1}$	$1.25x10^{-1}$	$1.09x10^{-1}$	$1.64x10^{-2}$	$4.14x10^{-2}$	$3.74x10^{-2}$
$4.0x10^{4}$	$8.57x10^{-2}$	$1.03x10^{-1}$	$7.50x10^{-2}$	---	$3.10x10^{-2}$	$1.81x10^{-2}$
$4.5x10^{4}$	---	$7.19x10^{-2}$	$3.13x10^{-2}$	---	---	$1.20x10^{-2}$
$5.0x10^{4}$	---	$4.52x10^{-2}$	$2.46x10^{-2}$	---	---	$5.80x10^{-3}$
$5.5x10^{4}$	---	$2.33x10^{-2}$	---	---	---	---
$6.0x10^{4}$	$3.73x10^{-2}$	$1.58x10^{-2}$	---	---	---	---

TABLE A13. SURVIVAL OF GM730 CELLS TO 325 NM RADIATION AT 0° AND 25°C (SEE FIG. 29A)

Experiment Number	39	40
Passage Number	14	14
Plating Efficiency (%)	10	7

UV FLUENCE Jm^{-2}	SURVIVING FRACTION	UV FLUENCE Jm^{-2}	SURVIVING FRACTION
5.0×10^{3}	1.03×10^{0}	1.2×10^{4}	8.96×10^{-1}
1.0×10^{4}	9.45×10^{-1}	2.4×10^{4}	7.08×10^{-1}
1.5×10^{4}	7.60×10^{-1}	3.0×10^{4}	8.13×10^{-1}
2.0×10^{4}	6.13×10^{-1}	3.6×10^{4}	6.16×10^{-1}
2.5×10^{4}	4.67×10^{-1}	4.2×10^{4}	5.49×10^{-1}
3.0×10^{4}	---	4.8×10^{4}	5.43×10^{-1}
3.5×10^{4}	1.83×10^{-1}	5.4×10^{4}	4.79×10^{-1}
4.8×10^{4}	9.67×10^{-2}	6.0×10^{4}	5.12×10^{-1}
5.4×10^{4}	7.33×10^{-2}		
6.0×10^{4}	5.00×10^{-2}		

TABLE A14. SURVIVAL OF GM730 CELLS TO 334 NM RADIATION AT 0° AND 25°C (SEE FIG. 29B)

Experiment Number	41	42	43	44
Passage Number	13	18	13	17
Plating Efficiency (%)	15	5	21	24

UV FLUENCE Jm^{-2}	SURVIVING FRACTION		UV FLUENCE Jm^{-2}	SURVIVING FRACTION	
1.1×10^{4}	8.84×10^{-1}	6.88×10^{-1}	1.0×10^{4}	1.11×10^{0}	8.66×10^{-1}
2.1×10^{4}	7.95×10^{-1}	6.90×10^{-1}	2.0×10^{4}	8.92×10^{-1}	8.53×10^{-1}
3.2×10^{4}	6.23×10^{-1}	5.29×10^{-1}	3.0×10^{4}	1.06×10^{-1}	7.15×10^{-1}
4.3×10^{4}	4.95×10^{-1}	4.12×10^{-1}	4.0×10^{4}	---	8.89×10^{-1}
5.4×10^{4}	2.98×10^{-1}	2.81×10^{-1}	4.5×10^{4}	8.92×10^{-1}	---
6.4×10^{4}	1.57×10^{-1}	1.05×10^{-1}	5.0×10^{4}	7.46×10^{-1}	6.97×10^{-1}
7.5×10^{4}	1.01×10^{-1}	6.52×10^{-2}	5.5×10^{4}	7.67×10^{-1}	---
			6.0×10^{4}	6.43×10^{-1}	6.35×10^{-1}
			7.0×10^{4}	6.81×10^{-1}	---
			8.0×10^{4}	4.84×10^{-1}	---

TABLE A15. SURVIVAL OF AR6LO CELLS TO 365 NM RADIATION AT 25°C IN PBS (SEE FIG. 31A)

Experiment Number	45	46	47	48	49	50
Passage Number	15	15	17	13	15	13
Plating Efficiency (%)	6	8	15	21	11	20
UV FLUENCE Jm^{-2}	S U R V I V I N G	F R A C T I O N		UV FLUENCE Jm^{-2}	S U R V I V I N G	F R A C T I O N
5.0×10^{4}	4.51×10^{-1}	8.17×10^{-1}	7.84×10^{-1}	3.0×10^{4}	7.86×10^{-1}	8.97×10^{-1}	1.14×10^{0}
1.0×10^{5}	3.05×10^{-1}	7.81×10^{-1}	4.66×10^{-1}	6.0×10^{4}	6.67×10^{-1}	7.35×10^{-1}	8.01×10^{-1}
1.5×10^{5}	1.34×10^{-1}	5.20×10^{-1}	3.68×10^{-1}	9.0×10^{4}	6.32×10^{-1}	4.48×10^{-1}	6.17×10^{-1}
2.0×10^{5}	6.59×10^{-2}	2.95×10^{-1}	3.34×10^{-1}	1.2×10^{5}	5.08×10^{-1}	---	6.29×10^{-1}
2.5×10^{5}	6.34×10^{-2}	2.39×10^{-1}	3.08×10^{-1}	1.5×10^{5}	2.20×10^{-1}	3.52×10^{-1}	4.03×10^{-1}
3.0×10^{5}	5.98×10^{-2}	1.35×10^{-1}	2.43×10^{-1}	1.8×10^{5}	---	2.71×10^{-1}	3.98×10^{-1}
3.5×10^{5}	3.54×10^{-2}	1.07×10^{-1}	1.84×10^{-1}	2.1×10^{5}	1.20×10^{-1}	2.14×10^{-1}	2.68×10^{-1}
4.0×10^{5}	1.34×10^{-2}	7.10×10^{-2}	7.45×10^{-2}	2.4×10^{5}	---	1.66×10^{-1}	2.66×10^{-1}
4.5×10^{5}	9.72×10^{-3}	---	7.95×10^{-2}	2.7×10^{5}	1.10×10^{-1}	---	---
5.0×10^{5}	8.50×10^{-3}	---	6.77×10^{-2}	3.0×10^{5}	7.24×10^{-2}	---	1.19×10^{-1}

TABLE A16. SURVIVAL OF AR6LO CELLS TO 365 NM RADIATION AT 25°C IN EMEM AND DMEM (SEE FIGS. 32A, B)

Experiment Number	51	52	53
Passage Number	17	21	18
Plating Efficiency (%)	13	4	14
UV FLUENCE Jm^{-2}	SURVIVING FRACTION	UV FLUENCE Jm^{-2}	SURVIVING FRACTION	UV FLUENCE Jm^{-2}	SURVIVING FRACTION
5.0×10^{4}	6.47×10^{-1}	4.0×10^{4}	8.18×10^{-1}	6.1×10^{4}	6.49×10^{-1}
1.0×10^{5}	6.15×10^{-1}	8.0×10^{4}	6.55×10^{-1}	1.2×10^{5}	4.60×10^{-1}
1.5×10^{5}	3.78×10^{-1}	1.2×10^{5}	5.73×10^{-1}	1.8×10^{5}	2.77×10^{-1}
2.0×10^{5}	1.89×10^{-1}	1.6×10^{5}	4.36×10^{-1}	2.4×10^{5}	1.64×10^{-1}
2.5×10^{5}	1.66×10^{-1}	2.0×10^{5}	3.64×10^{-1}	3.0×10^{5}	8.42×10^{-2}
3.0×10^{5}	8.79×10^{-2}	2.4×10^{5}	2.58×10^{-1}		
3.5×10^{5}	9.13×10^{-2}	2.8×10^{5}	2.18×10^{-1}		
4.0×10^{5}	5.81×10^{-2}	3.2×10^{5}	2.02×10^{-1}		
		3.6×10^{5}	1.20×10^{-1}		
		4.0×10^{5}	1.06×10^{-1}		

TABLE A17. SURVIVAL OF AR6LO CELLS TO 365 NM RADIATION AT 0° AND 37°C (SEE FIGS. 33A, 34A)

Experiment Number	54	55	56	57	58	59	60
Passage Number	15	13	16	12	15	18	14
Plating Efficiency (%)	5	18	10	13	9	16	17
UV FLUENCE Jm^{-2}	S U R V I V I N G	F R A C T I O N					
5.0×10^{4}	6.75×10^{-1}	8.35×10^{-1}	8.96×10^{-1}	9.18×10^{-1}	1.29×10^{0}	8.41×10^{-1}	9.04×10^{-1}
1.0×10^{5}	8.25×10^{-1}	5.13×10^{-1}	6.58×10^{-1}	4.91×10^{-1}	1.03×10^{0}	7.15×10^{-1}	8.62×10^{-1}
1.5×10^{5}	5.65×10^{-1}	2.92×10^{-1}	6.04×10^{-1}	1.96×10^{-1}	8.70×10^{-1}	5.77×10^{-1}	7.25×10^{-1}
2.0×10^{5}	4.13×10^{-1}	2.17×10^{-1}	3.44×10^{-1}	1.36×10^{-1}	4.05×10^{-1}	6.22×10^{-1}	7.78×10^{-1}
2.5×10^{5}	3.54×10^{-1}	1.64×10^{-1}	1.79×10^{-1}	1.27×10^{-1}	1.24×10^{-1}	6.13×10^{-1}	6.23×10^{-1}
3.0×10^{5}	1.56×10^{-1}	1.20×10^{-1}	1.06×10^{-1}	9.09×10^{-2}	8.86×10^{-2}	7.12×10^{-1}	4.14×10^{-1}
3.5×10^{5}	---	3.93×10^{-2}	6.31×10^{-2}	6.27×10^{-2}	4.12×10^{-2}	6.42×10^{-1}	5.73×10^{-1}
4.0×10^{5}	---	1.59×10^{-2}	3.35×10^{-2}	4.09×10^{-2}	2.06×10^{-2}	3.93×10^{-1}	5.23×10^{-1}
4.5×10^{5}	---	1.42×10^{-2}	1.21×10^{-2}	4.07×10^{-2}	9.16×10^{-3}	3.14×10^{-1}	4.94×10^{-1}
5.0×10^{5}	---	6.00×10^{-3}	---	---	3.44×10^{-3}	---	4.55×10^{-1}

TABLE 18. SURVIVAL OF AR6LO CELLS TO 254 NM RADIATION AT 0°, 25° AND 37°C (SEE FIGS. 35A, 36A, 37A)

Experiment Number	61	62	63	64	65	66
Passage Number	14	15	17	14	16	15
Plating Efficiency (%)	7	14	6	15	9	12
UV FLUENCE Jm^{-2}	S U R V I V I N G	F R A C T I O N				
5.0×10^{0}	9.95×10^{-1}	9.70×10^{-1}	---	9.52×10^{-1}	---	9.80×10^{-1}
1.0×10^{1}	6.94×10^{-1}	9.59×10^{-1}	1.02×10^{0}	9.55×10^{-1}	7.03×10^{-1}	6.26×10^{-1}
1.5×10^{1}	7.39×10^{-1}	8.10×10^{-1}	---	7.59×10^{-1}	---	4.65×10^{-1}
2.0×10^{1}	4.74×10^{-1}	7.73×10^{-1}	8.22×10^{-1}	6.99×10^{-1}	7.14×10^{-1}	2.69×10^{-1}
2.5×10^{1}	5.43×10^{-1}	5.93×10^{-1}	6.44×10^{-1}	6.08×10^{-1}	---	2.43×10^{-1}
3.0×10^{1}	3.74×10^{-1}	4.37×10^{-1}	4.08×10^{-1}	3.82×10^{-1}	3.99×10^{-1}	2.49×10^{-1}
3.5×10^{1}	3.38×10^{-1}	1.99×10^{-1}	3.38×10^{-1}	3.09×10^{-1}	---	1.36×10^{-1}
4.0×10^{1}	3.17×10^{-1}	1.70×10^{-1}	2.69×10^{-1}	2.18×10^{-1}	1.63×10^{-1}	---
4.5×10^{1}	---	---	2.00×10^{-1}	1.67×10^{-1}	---	8.79×10^{-2}
5.0×10^{1}	1.79×10^{-1}	7.37×10^{-2}	1.10×10^{-1}	6.70×10^{-2}	8.33×10^{-2}	3.70×10^{-2}
6.0×10^{1}	4.98×10^{-2}	4.48×10^{-2}	5.75×10^{-2}	---	4.06×10^{-2}	1.27×10^{-2}

TABLE A19. SURVIVAL OF AR6LO CELLS TO 313 NM RADIATION AT 0^{o} AND 25^{o}C (SEE FIGS. 38A, 39A)

Experiment Number	67	68	69	70	71
Passage Number	17	15	15	17	15
Plating Efficiency (%)	13	11	20	12	11
UV FLUENCE Jm^{-2}	S U R V I V I N G	F R A C T I O N		S U R V I V I N G	F R A C T I O N
$5.0x10^{3}$	$1.00x10^{0}$	$1.18x10^{0}$	$8.32x10^{-1}$	$8.59x10^{-1}$	$7.91x10^{-1}$
$1.0x10^{4}$	$8.66x10^{-1}$	$9.91x10^{-1}$	$6.44x10^{-1}$	$6.54x10^{-1}$	$4.72x10^{-1}$
$1.5x10^{4}$	$7.22x10^{-1}$	$9.09x10^{-1}$	$5.50x10^{-1}$	$3.75x10^{-1}$	$3.10x10^{-1}$
$2.0x10^{4}$	$6.37x10^{-1}$	$4.42x10^{-1}$	$5.33x10^{-1}$	$2.74x10^{-1}$	$2.94x10^{-1}$
$2.5x10^{4}$	$5.27x10^{-1}$	$4.75x10^{-1}$	$4.54x10^{-1}$	$2.05x10^{-1}$	$1.93x10^{-1}$
$3.0x10^{4}$	$3.67x10^{-1}$	$3.62x10^{-1}$	$2.67x10^{-1}$	$2.46x10^{-1}$	$1.42x10^{-1}$
$3.5x10^{4}$	$1.93x10^{-1}$	$2.71x10^{-1}$	$2.04x10^{-1}$	$1.29x10^{-1}$	$1.28x10^{-1}$
$4.0x10^{4}$	$1.74x10^{-1}$	$1.46x10^{-1}$	$1.64x10^{-1}$	$7.98x10^{-2}$	$7.60x10^{-2}$
$4.5x10^{4}$	$1.28x10^{-1}$	$1.08x10^{-1}$	$1.31x10^{-1}$	---	$4.17x10^{-2}$
$5.0x10^{4}$	$7.67x10^{-2}$	$7.38x10^{-2}$	$9.11x10^{-2}$	$6.23x10^{-2}$	$6.46x10^{-2}$
$5.5x10^{4}$	---	---	$6.47x10^{-2}$	---	$2.41x10^{-2}$
$6.0x10^{4}$	$1.51x10^{-2}$	$6.90x10^{-3}$	---	$3.17x10^{-2}$	---

TABLE A20. SURVIVAL OF AR6LO CELLS TO GAMMA RADIATION (SEE FIG. 40 A)

Experiment Number	72	73	74	75
Passage Number	14	14	17	16
Plating Efficiency (%)	9	13	15	15

GAMMA FLUENCE RADS	SURVIVING FRACTION			GAMMA FLUENCE RADS	SURVIVING FRACTION
5.0×10^{1}	---	7.02×10^{-1}	---	1.3×10^{2}	4.06×10^{-1}
1.0×10^{2}	3.51×10^{-1}	5.69×10^{0}	5.85×10^{-1}	2.6×10^{2}	1.25×10^{-1}
1.5×10^{2}	---	2.71×10^{-1}	---	3.9×10^{2}	5.14×10^{-2}
2.0×10^{2}	1.48×10^{-1}	2.48×10^{-1}	2.24×10^{-1}	5.2×10^{2}	1.81×10^{-2}
2.5×10^{2}	---	9.82×10^{-2}	---	6.5×10^{2}	4.41×10^{-3}
3.0×10^{2}	1.08×10^{-1}	5.37×10^{-2}	8.37×10^{-2}	7.8×10^{2}	1.64×10^{-3}
3.5×10^{2}	---	2.66×10^{-2}	---		
4.0×10^{2}	3.31×10^{-2}	2.32×10^{-2}	3.95×10^{-2}		
5.0×10^{2}	1.70×10^{-2}	1.09×10^{-2}	2.04×10^{-2}		
6.0×10^{2}	---	1.49×10^{-2}	7.91×10^{-3}		
7.0×10^{2}	---	---	2.51×10^{-3}		
8.0×10^{2}	---	---	1.32×10^{-3}		

TABLE A21. SURVIVAL OF GM730 CELLS TO GAMMA RADIATION (SEE FIG. 40B)

Experiment Number	76		77	
Passage Number	12		18	
Plating Efficiency (%)	24		13	
GAMMA FLUENCE RADS	SURVIVING FRACTION		GAMMA FLUENCE RADS	SURVIVING FRACTION
1.30×10^{2}	---		1.0×10^{2}	5.64×10^{-1}
2.60×10^{2}	2.34×10^{-1}		1.5×10^{2}	4.66×10^{-1}
3.25×10^{2}	1.25×10^{-1}		2.0×10^{2}	3.23×10^{-1}
3.90×10^{2}	7.29×10^{-2}		2.5×10^{2}	2.47×10^{-1}
4.55×10^{2}	6.25×10^{-2}		3.0×10^{2}	2.27×10^{-1}
5.20×10^{2}	2.92×10^{-2}		3.5×10^{2}	1.70×10^{-1}
5.85×10^{2}	1.25×10^{-2}		4.0×10^{2}	4.32×10^{-2}
6.50×10^{2}	9.38×10^{-3}		4.5×10^{2}	4.45×10^{-2}
7.80×10^{2}	2.08×10^{-3}		5.0×10^{2}	2.18×10^{-2}
			5.5×10^{2}	8.59×10^{-3}
			6.0×10^{2}	4.62×10^{-3}
			7.0×10^{2}	1.94×10^{-3}

TABLE A22. SURVIVAL OF AR6LO AND GM730 CELLS TO HYDROGEN PEROXIDE TREATMENT (SEE FIGS. 41A, B)

Experiment Number	78	79	80	81
Passage Number	15	16	14	14
Plating Efficiency (%)	4	4	8	8
H_2O_2 CONCENTRATION M	SURVIVING FRACTION		SURVIVING FRACTION	
5	9.21×10^{-1}	1.05×10^{0}	1.00×10^{0}	9.76×10^{-1}
10	7.98×10^{-1}	9.51×10^{-1}	9.67×10^{-1}	8.71×10^{-1}
15	5.00×10^{-1}	4.57×10^{-1}	8.48×10^{-1}	7.26×10^{-1}
20	---	9.84×10^{-2}	6.23×10^{-1}	2.42×10^{-1}
25	8.68×10^{-2}	2.46×10^{-2}	4.22×10^{-1}	1.05×10^{-1}
30	8.72×10^{-3}	8.19×10^{-3}	2.91×10^{-1}	4.08×10^{-2}
35	---	1.60×10^{-3}	6.95×10^{-2}	1.95×10^{-2}
40	---	---	3.90×10^{-2}	7.04×10^{-2}

TABLE A23. SURVIVAL OF AR6LO AND GM730 CELLS TO 365 NM RADIATION AT 25°C IN THE PRESENCE OF 60 μg/ml TROLOX-C IN THE POST-IRRADIATION MEDIUM (SEE FIGS. 43A, B)

Experiment Number	82	83	84	85	86
Passage Number	13	15	13	11	12
Plating Efficiency (%)	25	18	33	48	40

UV FLUENCE Jm^{-2}	SURVIVING FRACTION			UV FLUENCE Jm^{-2}	SURVIVING FRACTION	
3.0×10^{4}	8.39×10^{-1}	9.27×10^{-1}	9.91×10^{-1}	3.3×10^{4}	9.11×10^{-1}	8.61×10^{-1}
6.0×10^{4}	8.96×10^{-1}	9.02×10^{-1}	8.99×10^{-1}	6.7×10^{4}	8.19×10^{-1}	8.19×10^{-1}
9.0×10^{4}	7.70×10^{-1}	7.84×10^{-1}	8.09×10^{-1}	1.0×10^{5}	7.11×10^{-1}	8.32×10^{-1}
1.2×10^{5}	7.60×10^{-1}	6.36×10^{-1}	6.65×10^{-1}	1.3×10^{5}	5.39×10^{-1}	8.25×10^{-1}
1.5×10^{5}	4.49×10^{-1}	6.58×10^{-1}	5.29×10^{-1}	1.7×10^{5}	5.06×10^{-1}	8.52×10^{-1}
1.8×10^{5}	4.02×10^{-1}	4.76×10^{-1}	5.42×10^{-1}	2.0×10^{5}	5.75×10^{-1}	7.76×10^{-1}
2.1×10^{5}	2.43×10^{-1}	4.03×10^{-1}	4.25×10^{-1}	2.3×10^{5}	4.42×10^{-1}	7.26×10^{-1}
2.4×10^{5}	2.89×10^{-1}	3.98×10^{-1}	4.23×10^{-1}	2.7×10^{5}	5.12×10^{-1}	6.58×10^{-1}
2.7×10^{5}	2.29×10^{-1}	5.49×10^{-1}	3.94×10^{-1}	3.0×10^{5}	3.77×10^{-1}	5.48×10^{-1}
3.0×10^{5}	2.09×10^{-1}	3.74×10^{-1}	---	3.3×10^{5}	3.38×10^{-1}	4.60×10^{-1}

TABLE A24. SURVIVAL OF AR6LO CELLS, GROWN IN THE PRESENCE OF 100 μg/ml TROLOX-C OR 100 μg/ml ALPHA-TOCOPHEROL ACETATE, TO 365 NM RADIATION AT 25°C (SEE FIGS. 44A, B)

Experiment Number	87	88	89
Passage Number	14	19	15
Plating Efficiency (%)	19	12	10

UV FLUENCE Jm^{-2}	SURVIVING FRACTION	UV FLUENCE Jm^{-2}	SURVIVING FRACTION	UV FLUENCE Jm^{-2}	SURVIVING FRACTION
4.7×10^{4}	8.04×10^{-1}	4.2×10^{4}	8.61×10^{-1}	5.3×10^{4}	8.23×10^{-1}
9.4×10^{4}	8.16×10^{-1}	8.3×10^{4}	9.28×10^{-1}	9.4×10^{4}	1.00×10^{0}
1.4×10^{5}	7.96×10^{-1}	1.2×10^{5}	1.01×10^{0}	1.4×10^{5}	7.68×10^{-1}
1.9×10^{5}	7.29×10^{-1}	1.7×10^{5}	8.78×10^{-1}	1.9×10^{5}	7.10×10^{-1}
2.3×10^{5}	5.45×10^{-1}	2.1×10^{5}	7.89×10^{-1}	2.4×10^{5}	3.89×10^{-1}
2.8×10^{5}	6.06×10^{-1}	2.5×10^{5}	7.22×10^{-1}	2.8×10^{5}	6.11×10^{-1}
3.3×10^{5}	4.72×10^{-1}	2.9×10^{5}	5.85×10^{-1}	3.3×10^{5}	4.43×10^{-1}
3.8×10^{5}	5.44×10^{-1}	3.3×10^{5}	5.81×10^{-1}	3.8×10^{5}	2.63×10^{-1}
4.2×10^{5}	5.18×10^{-1}	3.8×10^{5}	4.87×10^{-1}	4.2×10^{5}	2.15×10^{-1}
4.7×10^{5}	4.00×10^{-1}			4.7×10^{5}	2.32×10^{-1}

TABLE A25. SURVIVAL OF AR6LO AND GM730 CELLS TO 254 NM RADIATION AT 25°C IN THE PRESENCE OF 60 μg/ml TROLOX-C IN THE POST-IRRADIATION MEDIUM (SEE FIGS. 45A, B).

Experiment Number	90	91	92	93
Passage Number	14	16	12	15
Plating Efficiency (%)	21	14	37	27
UV FLUENCE Jm^{-2}	S U R V I V I N G F R A C T I O N		S U R V I V I N G F R A C T I O N	
$5.0x10^{0}$	$9.29x10^{-1}$	---	$9.46x10^{-1}$	---
$1.0x10^{1}$	$8.32x10^{-1}$	$9.38x10^{-1}$	$8.89x10^{-1}$	$1.03x10^{0}$
$1.5x10^{1}$	$8.81x10^{-1}$	---	$8.37x10^{-1}$	---
$2.0x10^{1}$	$8.11x10^{-1}$	$7.67x10^{-1}$	$6.98x10^{-1}$	$6.22x10^{-1}$
$2.5x10^{1}$	$5.65x10^{-1}$	---	---	---
$3.0x10^{1}$	$6.08x10^{-1}$	$4.07x10^{-1}$	$6.33x10^{-1}$	$3.96x10^{-1}$
$3.5x10^{1}$	$3.29x10^{-1}$	---	$3.26x10^{-1}$	$3.61x10^{-1}$
$4.0x10^{1}$	$2.72x10^{-1}$	$2.67x10^{-1}$	$3.08x10^{-1}$	$2.01x10^{-1}$
$4.5x10^{1}$	$2.35x10^{-1}$	---	$2.16x10^{-1}$	---
$5.0x10^{1}$	$1.39x10^{-1}$	$1.52x10^{-1}$	---	$7.27x10^{-3}$
$6.0x10^{1}$	---	$6.76x10^{-2}$	---	$4.01x10^{-3}$

TABLE A26. SURVIVAL OF AR6LO CELLS TO 365 NM RADIATION AT 25°C IN THE PRESENCE OF 70% D_2O (SEE FIGS. 46A, 49)

Experiment Number	94	95	96	97	98
Passage Number	19	15	20	15	19
Plating Efficiency (%)	4	11	5	16	5
UV FLUENCE Jm^{-2}	S U R V I V I N G F R A C T I O N			S U R V I V I N G F R A C T I O N	
$3.0x10^{4}$	$5.89x10^{-1}$	$5.28x10^{-1}$	$6.91x10^{-1}$	$7.64x10^{-1}$	$6.05x10^{-1}$
$6.0x10^{4}$	$2.08x10^{-1}$	$3.60x10^{-1}$	$4.61x10^{-1}$	$6.26x10^{-1}$	$4.57x10^{-1}$
$9.0x10^{4}$	$1.04x10^{-1}$	$2.12x10^{-1}$	$3.50x10^{-1}$	$2.85x10^{-1}$	$2.22x10^{-1}$
$1.2x10^{5}$	$8.13x10^{-2}$	$1.08x10^{-1}$	$3.13x10^{-1}$	$1.61x10^{-1}$	$1.48x10^{-1}$
$1.5x10^{5}$	$2.68x10^{-2}$	$4.70x10^{-2}$	$1.38x10^{-1}$	$8.70x10^{-2}$	$4.82x10^{-2}$
$1.8x10^{5}$	$2.05x10^{-2}$	$2.88x10^{-2}$	$1.15x10^{-1}$	---	$2.22x10^{-2}$
$2.1x10^{5}$	$4.88x10^{-3}$	$1.04x10^{-2}$	$8.06x10^{-2}$	---	$1.48x10^{-2}$
$2.4x10^{5}$	$4.08x10^{-3}$	---	$3.48x10^{-2}$	---	$7.41x10^{-3}$
$2.7x10^{5}$	$3.66x10^{-3}$	---	$2.16x10^{-2}$	---	$4.63x10^{-3}$

TABLE A27. SURVIVAL OF GM730 CELLS TO 365 NM RADIATION AT 25°C IN THE PRESENCE OF 70% D_2O (SEE FIG. 47A)

Experiment Number	99	100	101	102
Passage Number	12	19	17	17
Plating Efficiency (%)	11	10	7	6

UV FLUENCE Jm^{-2}	SURVIVING FRACTION			UV FLUENCE Jm^{-2}	SURVIVING FRACTION
5.0×10^{4}	7.80×10^{-1}	---	---	6.0×10^{4}	5.86×10^{-1}
1.0×10^{5}	7.32×10^{-1}	5.05×10^{-1}	1.13×10^{0}	1.2×10^{5}	5.96×10^{-1}
1.5×10^{5}	4.57×10^{-1}	---	---	1.8×10^{5}	5.13×10^{-1}
2.0×10^{5}	---	4.55×10^{-1}	5.38×10^{-1}	2.4×10^{5}	4.35×10^{-1}
2.5×10^{5}	3.39×10^{-1}	---	---	3.0×10^{5}	2.44×10^{-1}
3.0×10^{5}	3.20×10^{-1}	1.19×10^{-1}	5.13×10^{-1}		
3.5×10^{5}	2.35×10^{-1}	---	---		
4.0×10^{5}	1.28×10^{-1}	4.75×10^{-2}	1.28×10^{-1}		

TABLE A28. SURVIVAL OF AR6LO AND GM730 CELLS TO 365 NM RADIATION AT 0°C IN THE PRESENCE OF 70% D_2O (SEE FIGS. 48A, B)

Experiment Number	103	104	105	106
Passage Number	14	17	17	18
Plating Efficiency (%)	6	6	9	13
UV FLUENCE Jm^{-2}	SURVIVING FRACTION		SURVIVING FRACTION	
$5.0x10^{4}$	$6.73x10^{-1}$	$7.20x10^{-1}$	$9.42x10^{-1}$	$8.67x10^{-1}$
$1.0x10^{5}$	$5.79x10^{-1}$	$5.40x10^{-1}$	$8.61x10^{-1}$	$6.17x10^{-1}$
$1.5x10^{5}$	$5.10x10^{-1}$	$4.50x10^{-1}$	$4.71x10^{-1}$	$3.35x10^{-1}$
$2.0x10^{5}$	$2.99x10^{-1}$	$3.90x10^{-1}$	$2.88x10^{-1}$	$2.31x10^{-1}$
$2.5x10^{5}$	$2.54x10^{-1}$	$2.10x10^{-1}$	$2.21x10^{-1}$	$1.48x10^{-1}$
$3.0x10^{5}$	$1.85x10^{-1}$	$8.80x10^{-2}$	$1.81x10^{-1}$	$1.49x10^{-1}$
$3.5x10^{5}$	$8.70x10^{-2}$	$7.60x10^{-2}$	$1.23x10^{-1}$	$6.40x10^{-2}$
$4.0x10^{5}$	---	---	$4.40x10^{-2}$	$5.55x10^{-2}$

TABLE A29. SURVIVAL OF AR6LO AND GM730 CELLS TO 254 NM RADIATION AT 25°C IN THE PRESENCE OF 70% D_2O (SEE FIGS. 50A, B)

Experiment Number	107	108	109	110
Passage Number	14	16	19	16
Plating Efficiency (%)	21	14	6	4
UV FLUENCE Jm^{-2}	S U R V I V I N G F R A C T I O N		S U R V I V I N G F R A C T I O N	
$1.0x10^{1}$	$8.75x10^{-1}$	$8.38x10^{-1}$	$6.18x10^{-1}$	$9.46x10^{-1}$
$2.0x10^{1}$	$7.34x10^{-1}$	$7.48x10^{-1}$	$4.12x10^{-1}$	$5.90x10^{-1}$
$3.0x10^{1}$	$6.44x10^{-1}$	$3.94x10^{-1}$	$2.27x10^{-1}$	$4.29x10^{-1}$
$4.0x10^{1}$	$2.81x10^{-1}$	$2.48x10^{-1}$	$1.60x10^{-1}$	$2.04x10^{-1}$
$5.0x10^{1}$	$1.31x10^{-1}$	$1.02x10^{-1}$	$7.89x10^{-2}$	$1.29x10^{-1}$
$6.0x10^{1}$	$9.52x10^{-2}$	$6.62x10^{-2}$	$4.55x10^{-2}$	$5.36x10^{-2}$
$7.0x10^{1}$	---	$2.85x10^{-2}$	---	$1.74x10^{-2}$

TABLE A30. SURVIVAL OF AR6LO CELLS TO BROAD-BAND NEAR-UV RADIATION AT AMBIENT TEMPERATURE (SEE FIG. 52)

Experiment Number	111	112	113	
Passage Number	14	15	17	
Plating Efficiency (%)	14	16	12	
IRRADIATION TIME (min)	S U R V I V I N G F R A C T I O N			MEAN
10	---	---	6.85×10^{-1}	6.85×10^{-1}
15	6.92×10^{-1}	7.10×10^{-1}	8.59×10^{-1}	7.54×10^{-1}
20	---	---	7.72×10^{-1}	7.72×10^{-1}
25	---	---	5.16×10^{-1}	5.16×10^{-1}
30	5.33×10^{-1}	4.10×10^{-1}	4.67×10^{-1}	4.70×10^{-1}
35	---	---	5.05×10^{-1}	5.05×10^{-1}
40	---	---	2.17×10^{-1}	2.17×10^{-1}
45	3.69×10^{-1}	4.70×10^{-2}	1.39×10^{-1}	1.84×10^{-1}
50	---	---	1.00×10^{-1}	1.00×10^{-1}
60	4.70×10^{-3}	8.90×10^{-3}	3.70×10^{-2}	1.69×10^{-2}
70	1.30×10^{-3}	2.50×10^{-3}	---	1.90×10^{-3}

TABLE A31. SURVIVAL OF GM730 CELLS TO BROAD-BAND NEAR-UV RADIATION AT AMBIENT TEMPERATURE (SEE FIG. 52)

Experiment Number	114	115	116	
Passage Number	16	16	18	
Plating Efficiency (%)	12	7	14	
IRRADIATION TIME (min)	S U R V I V I N G F R A C T I O N			MEAN
10	---	---	8.81×10^{-1}	8.81×10^{1}
15	8.43×10^{-1}	9.10×10^{-1}	9.70×10^{-1}	9.08×10^{-1}
20	---	---	8.36×10^{-1}	8.36×10^{-1}
25	---	---	6.62×10^{-1}	6.62×10^{-1}
30	6.65×10^{-1}	8.00×10^{-1}	6.02×10^{-1}	6.89×10^{-1}
35	---	---	6.00×10^{-1}	6.00×10^{-1}
45	2.50×10^{-1}	9.70×10^{-2}	6.37×10^{-1}	3.28×10^{-1}
50	---	---	1.54×10^{-1}	1.54×10^{-1}
60	---	---	1.49×10^{-1}	1.49×10^{-1}
70	3.69×10^{-2}	4.45×10^{-2}	---	4.07×10^{-2}

APPENDIX 9: CLINICAL HISTORY OF PATIENT FROM WHICH AR6LO CELLS ORIGINATED

From the Institute of Dermatology, St. John's Hospital
Hoverton Grove, London

Date of Birth: 4.10.1932

Sex: Male

History: Started 1978, back of hands; 1979 noticed relationship of rash to solar exposure

Monochromator tests: April 1980, monochromator light tests showed abnormal photosensitivity out to 400 nm. Threshold doses for abnormal morphological responses at 300 and 307.5 nm were 10 $mJcm^{-2}$, at 320 nm 0.5Jcm^{-2} and at 340 nm 10 Jcm^{-2}; abnormal morphological responses also obtained with 360 and 400 nm but threshold doses not determined.

Other tests: April, 1980, photo-patch tests done to:

hexachlorophene	-ve
tribromsalicylanilide	-ve
bithionol	-ve
trichlorcarbanilide	-ve
chlorpromazine	+ve

There were weak questionable patch test reactions to a number of substances, e.g. oak moss, "perfume-mix", potassium dichromate, balsam of peru.
Normal (116%) UDS and post-replication repair.

On examination: April, 1980, erythemato-papular eruption on back of hands, face, scalp and neck

REFERENCES

ARLETT, C. F. and HARCOURT, S. A. 1980. Survey of radiosensitivity in a variety of human cell strains. Cancer Res. 40:926-932.

ARLETT, C. F., HARCOURT, S. A. and BROUGHTON B. C. 1975. The influence of caffeine on cell survival in excision-proficient and excision-deficient xeroderma pigmentosum and normal human cell strains following UV-light irradiation. Mutation Res. 33:341-356.

BEN-HUR, E. and RIKLIS, E. 1980. Deuterium oxide enhancement of Chinese hamster cell response to gamma radiation. Radiat. Res. 81:224-235.

BEN-HUR, E., UTSUMI, H. and ELKIND, M. M. 1980. Potentially lethal and DNA radiation damage: Similarities in inhibition of repair by medium containing D_2O and by hypertonic buffer. Radiat. Res. 84: 25-34.

BISBY, R. H. AHMED, S. and CUNDALL, R. B. 1984. Repair of amino acid radicals by a vitamin E analogue. Biochem. Biophys. Res. Commun. 119:245-251.

BLACK, H. S. 1986. Potential involvement of free radical reactions in ultraviolet light-mediated cutaneous damage. Abstracts, 14th Ann. Meet. Amer. Soc. Photobiol. Los Angeles, CA, 22-26 June.

BLACK, H. S. and CHAN, J. T. 1977. Experimental ultraviolet light carcinogenesis. Photochem. Photobiol. 26:183-199.

BLUM, H. F. 1959. Carcinogenesis by Ultraviolet Light, Princeton University Press, New Jersey.

BOTCHERBY, P. K., MAGNUS, I. A. MARIMO, B. and GIANNELLI, F. 1984. Actinic reticuloid--An idiopathic photodermatosis with cellular sensitivity to near ultraviolet radiation. Photochem. Photobiol. 39:641-649.

BRADLEY, M. O. and ERICKSON, L. C. 1981. Comparison of the effects of hydrogen peroxide and X-ray irradiation on toxicity, mutation and DNA damage/repair in mammalian cells (V79). Biochim. Biophys. Acta 654:135-141.

BRUCE, A. K. 1958. Light-induced lysis and carotenogenesis in Myxococcus xanthus. J. Gen. Physiol. 41:693-702.

CABRERA-JUAREZ, E., SETLOW, J. K., SWENSON, P. A. and PEAK, M. J. 1976. Oxygen-independent inactivation of Haemophilus influenzae transforming DNA by monochromatic radiation: Action spectrum, effect of histidine and repair. Photochem. Photobiol. 23:309-313.

CHAMBERLAIN, J. and MOSS, S. H. 1987. Lipid peroxidation and other membrane damage produced in E. coli K1060 by near-UV radiation and deuterium oxide. Photochem. Photobiol. In Press.

CLEAVER, J. E. and BOOTSMA, D. 1975. Xeroderma pigmentosum: Biochemical and genetic characteristics. Ann. Rev. Genet. 9:19-38.

COOHILL, T. 1984. Action spectra for mammalian cells in vitro. IN: Topics in Photomedicine, K. C. Smith, Ed., Plenum Press, New York.

COOHILL, T. P., KNAUER D. J. AND FRY D. G. 1979. The effects of changes in cell geometry on the sensitivity to ultraviolet radiation of mammalian cellular capacity. Photochem. Photobiol. 30:565-572.

COX, R., and MASSON, W. K. 1974. Changes in radiosensitivity during the in vitro growth of diploid human fibroblasts. Int. J. Radiat. Biol. 26:193-196.

CUNNINGHAM, M. L., JOHNSON, J. S., GIOVANAZZI, S. M. and PEAK, M. J. 1985. Photosensitized production of superoxide anion by monochromatic (290-405 nm) ultraviolet irradiation of NADH and NADPH coenzymes. Photochem. Photobiol. 42:125-128.

DANIELS, F. 1963. IN: The First International Conference on the Biology of Cutaneous Cancer. F. Urbach, Ed. National Cancer Institute Monograph No. 10, Washington D. C., pp 407-418.

DANPURE, H. J. and TYRRELL, R. M. 1976. Oxygen-dependence of near UV (365 nm) lethality and the interaction of near UV and X-rays in two mammalian cell lines. Photochem. Photobiol. 23:171-177.

DEGIOVANNI, R. 1960. The effects of deuterium oxide on certain microorgansms. Ann. N. Y. Acad. Sci. 84:644-647.

DELEO, V. A., HANSON, D., WEINSTEIN, I. B. and HARBER, L. C. 1985. Ultraviolet radiation stimulates the release of arachidonic acid from mammalian cells in culture. Photochem. Photobiol. 41:51-56.

DELEO, V. A., HORLICK, H., HANSON, D. EISINGER, M. and HARBER, L. C. 1984. Ultraviolet radiation induces changes in membrane metabolism of human keratinocytes in culture. J. Invest. Dermatol. 83:323-326.

DEMPLE, B. and HALBROOK, J. 1983. Inducible repair of oxidative DNA damage in Escherichia coli. Nature 304:466-468.

DEMPLE, B., HALBROOK, J. and LINN, S. 1983. Escherichia coli xth mutants are hypersensitive to hydrogen peroxide. J. Bacteriol. 153:1079-1082.

DIPLOCK, A. T. and LUCY, J. A. 1973. The biochemical modes of action of vitamin E and selenium: A hypothesis. FEBS Lett. 29:205-210.

DOBA, T., BURTON, G. W., and INGOLD, K. U. 1985. Antioxidant and co-antioxidant activity of vitamin C. The effect of vitamin C, either alone or in the presence of vitamin E or a water-soluble vitamin E analogue, upon the peroxidation of aqueous multilamellar phospholipid liposomes. Biochim. Biophys. Acta 835:298-303.

DONIGER, J., JACOBSON, E. D., KRELL, K. and DIPAOLO, J. A. 1981. Ultraviolet light action spectra for neoplastic transformation and lethality of Syrian hamster embryo cells correlate with spectrum for pyrimidine dimer formation in cellular DNA. Proc. Natl. Acad. Sci. USA 78:2378-2382.

DOUGHTY, C. J. and HOPE, A. B. 1973. Effects of ultraviolet radiation on the membranes of Chara corallina. J. Membrane Biol. 13:185-198.

DRITSCHILO, A., BRENNAN, T., WEICHSELBAUM, R. R. and MOSSMAN, K. L. 1984. Response of human fibroblasts to low dose rate gamma irradiation. Radiat. Res. 100:387-395.

ELKIND, M. M., HAN, A. and CHANG-LIU, C. M. 1978. 'Sunlight'-induced mammalian cell killing: A comparative study of ultraviolet and near-ultraviolet inactivation. Photochem. Photobiol. 27:709-715.

ERIN, A. N., SKRYPIN, V. V. and KAGAN, V. E. 1985. Formation of alpha-tocopherol complexes with fatty acids. Nature of complexes. Biochim. Biophys. Acta 815:209-214.

ERIN, A. N., SPIRIN, M. M., TABIDZE, L. V. and KAGAN, V. E. 1984. Formation of alpha-tocopherol complexes with fatty acids--A hypothetical mechanism of stabilization of biomembranes by vitamin E. Biochim. Biophys. Acta 774:96-102.

FAHRENHOLTZ, S. R., DOLEIDEN, F. H., TROZZOLO, A. M. and LAMOLA, A. A. 1974. On the quenching of singlet oxygen by -tocopherol. Photochem. Photobiol. 20:505-509.

FINAZZI-AGRO, A., DI GIULIO, A., AMICOSANTE, G. and CRIFO, C. 1986. Photohemolysis of erythrocytes enriched with superoxide dismutase, catalase and glutathione peroxidase. Photochem. Photobiol. 43:409-412.

FOOTE, C. S., CHING, T-Y. AND GELLER, G. G. 1974. Chemisty of singlet oxygen - XVIII. Rates of reaction and quenching of alpha-tocopherol and singlet oxygen. Photochem. Photobiol. 20:511-513.

FOOTE, C. S. 1976. IN: Free Radicals in Biology, Vol. II., W.A. Pryor, Ed., Academic Press, New York, pp. 85-133.

FOOTE, C. S. 1979. Quenching of singlet oxygen. IN: Singlet Oxygen. H. H. Wasserman and R. W. Murray, Eds., Academic Press, New York, pp. 139-167.

FREEMAN, B. A. 1984. Biological Sites and Mechanisms of Free Radical Production. IN: Free Radicals in Molecular Biology, Aging and Disease, D. Armstrong et al., Eds., Raven Press, New York.

FREEMAN, S. E., GANGE, R. W., SUTHERLAND, J. C. and SUTHERLAND, B. M. 1986. Action spectrum for pyrimidine dimer formation in human skin. Abstracts, 14th Ann. Meet. Amer. Soc. Photobiol. Los Angeles, CA, 22-26 June.

FRIDOVICH, I. 1975. Superoxide dismutases. Ann. Rev. Biochem. 44:147-159.

FUJIWARA, Y. and TATSUMI, M. 1976. Replication bypass repair of UV damage to DNA of mammalian cells: Caffeine sensitive and caffeine resistant mechanisms. Mutation. Res. 37:91-109.

FURUNO-FUKUSHI, I. and MATSUDAIRA, H. 1985. Mutation induction by tritiated water and effects of deuterium oxide in cultured mouse leukemia cells. Radiat. Res. 103:466-470.

GIANNELLI, F., BOTCHERBY, P. K., MARIMO, B. and MAGNUS, I. A. 1983. Cellular hypersensitivty to UV-A: A clue to the aetiology of actinic reticuloid? Lancet 1:88-91.

GOSKIN, S. A. and FRIDOVICH, I. 1973. Superoxide dismutase and the oxygen effect. Radiation Res. 56:565-569.

GRAMS, G. W. and ESKINS, K. 1972. Dye-sensitized photooxidation of tocopherols. Correlation between singlet oxygen reactivity and vitamin E activity. Biochemistry 11:606-610.

GRIEGO, V. M., WEBB, R. B. and MATSUSHITA, T. 1981. Dependence on stage of growth of mammalian cell sensitivity to near UV irradiation. Photochem. Photobiol. 33:211-214.

HALLIWELL, B. and GUTTERIDGE, J. M. C. 1985. Free Radicals in Biology and Medicine. Clarendon Press, Oxford.

HAN, A., PEAK, M. J. and PEAK, J. G. 1984. Induction of DNA-protein cross-linking in Chinese hamster cells by monochromatic 365 and 405 nm ultraviolet light. Photochem. Photobiol. 39:343-348.

HANAWALT, P. C., COOPER, P. K., GANESAN, A. K., and SMITH, C. A. 1979. DNA repair in bacterial and mammalian cells. Ann. Rev. Biochem. 48: 783-836.

HARIHARAN, P. V. and CERUTTI, P. A. 1977. Formation of products of the 5,6-dihydroxydihydrothymine type by ultraviolet light in HeLa cells. Biochemistry 16:2791-2795.

HATCHARD, C. G. and PARKER, C. A. 1956. A new sensitive chemical actinometer. II. Potassium ferrioxalate as a standard chemical actinometer. Roy. Soc. (London) Proc., A235:518-536.

HIRSCHI, M., NETRAWALI, S., REMSEN., J. F. and CERUTTI, P. A. 1981. Formation of DNA single-strand breaks by near-ultraviolet and gamma-rays in normal and Bloom's syndrome skin fibroblasts. Cancer Res. 41:2003-2007.

HODGES, G. M., LIVINGSTONE, D. C. and FRANKS, L. M. 1973. The localization of trypsin in cultured mammalian cells. J. Cell Sci. 12:887-902.

HOFFMANN, M. E. and MENEGHINI, R. 1979a. DNA strand breaks in mammalian cells exposed to light in the presence of riboflavin and tryptophan. Photochem. Photobiol. 29:299-303.

HOFFMANN, M. E. and MENEGHINI, R. 1979b. Action of hydrogen peroxide on human fibroblast in culture. Photochem. Photobiol. 30:151-155.

HOFFMANN, M. E., MELLO-FILHO, A. C. and MENEGHINI, R. 1984. Correlation between cytotoxic effect of hydrogen peroxide and the yield of DNA strand breaks in cells of different species. Biochim. Biophys. Acta 781:234-238.

HOLLAENDER, A. 1943. Effect of long ultraviolet and short visible radiation (3500-4900 A) on Escherichia coli. J. Bacteriol. 46:531-541.

ITO T., 1978. Cellular and subcellular mechanisms of photodynamic action: The $^1O_2$ hypothesis as a driving force in recent research. Photochem. Photobiol. 28:493-508.

ITO, A. and ITO, T. 1983. Possible involvement of membrane damage in the inactivation by broad-band near-UV radiation in Saccharomyces cerevisiae cells. Photochem. Photobiol. 37:395-401.

ITO, T. and KOBAYASHI, K. 1977. In vivo evidence for the photodynamic membrane damage as a determining step of the inactivation of yeast cells sensitized by toluidine blue. Photochem. Photobiol. 25:399-401.

IVE, F. A., MAGNUS, I. A., WARIN, R. P. and WILSON-JONES, E. 1969. 'Actinic reticuloid'; A chronic dermatosis associated with severe photosensitivity and the histological resemblance to lymphoma. Br. J. Dermatol. 81:469-485.

JACKLE, H. and KALTHOFF, K. 1980. Photoreversible UV-inactivation of messenger RNA in an insect embryo (Smittia spec., Chironomidae, Diptera). Photochem. Photobiol. 32:749-761.

JAGGER, J. 1967. Introduction to Research in Ultraviolet Photobiology. Prentice-Hall, Inc., Englewood Cliffs, New Jersey.

JAGGER, J. 1983. Physiological effects of near-ultraviolet radiation on bacteria. IN: Photochemical and Photobiological Reviews 7, K. C. Smith, Ed., Plenum Press, New York, pp. 1-75.

JAGGER, J. 1985. Solar UV Actions on Living Cells. Praeger Publishers, New York.

JAGGER, J., FOSSUM, T. and MCCAUL, S. 1975. UV irradiation of suspensions of micro-organisms: Possible errors involved in the estimation of average fluence per cell. Photochem. Photobiol. 21:379-382.

JAIN, S. K. 1983. Vitamin E and stabilization of membrane lipid organization in red blood cells with peroxidative damage. Biomed. Biochim. Acta 42:S43-S47.

JOENJE, H., OOSTRA, A. B. and WANAMARTA, A. H. 1983. Cytogenetic toxicity of D_2O in human lymphocyte cultures. Increased sensitivity in Fanconi's ânemia. Experientia 39:782-784.

JOHNSON, B. E. and DANIELS, F. 1969. Lysosomes and the reaction of skin to ultraviolet radiation. J. Invest. Dermatol. 53:85-94.

KANTOR, G. J. 1985. Effects of sunlight on mammalian cells. Photochem. Photobiol. 41:741-746.

KANTOR, G. J. and RITTER, C. 1983. Sunlight-induced killing of nondividing human cells in culture. Photochem. Photobiol. 37:533-538.

KANTOR, G. J. and SETLOW, R. B. 1982. Correlation between inactivation of human cells and numbers of pyrimidine dimers induced by a sunlamp and 254 nm radiation. Photochem. Photobiol. 35:269-274.

KANTOR, G. J., SUTHERLAND, J. C. and SETLOW, R. B. 1980. Action spectra for killing non-dividing normal human and xeroderma pigmentosum cells. Photochem. Photobiol. 31:459-464.

KEARNS, D. R. 1979. Solvent and solvent isotope effects on the lifetime of singlet oxygen. IN Singlet Oxygen, H. H. Wasserman and R. W. Murray, Eds., Academic Press, New York, pp. 115-136.

KELLAND, L. R. 1984. A Study of Near-Ultraviolet Radiation-Induced Damage in Escherichia coli. Ph.D. Thesis, University of Bath.

KELLAND, L. R., MOSS, S. H. and DAVIES, D. J. G. 1983a. An action spectrum for ultraviolet radiation-induced membrane damage in Escherichia coli K-12. Photochem. Photobiol. 37:301-306.

KELLAND, L. R., MOSS, S. H. and DAVIES, D. J. G. 1983b. Recovery of Escherichia coli K-12 from near-ultraviolet radiation-induced membrane damage. Photochem. Photobiol. 37:617-622.

KELLAND, L. R., MOSS, S. H. and DAVIES, D. J. G. 1984. Leakage of $^{86}Rb^+$ after ultraviolet irradiation of Escherichia coli K-12. Photochem. Photobiol. 39:329-336.

KELLOGG, E. W. and FRIDOVICH, I. 1975. Superoxide, hydrogen peroxide and singlet oxygen in lipid peroxidation by a xanthine oxidase system. J. Biol. Chem. 250:8812-8817.

KELLOGG, E. W. and FRIDOVICH, I. 1977. Liposome oxidation and erythrocyte lysis by enzymically generated superoxide and hydrogen peroxide. J. Biol. Chem. 252:6721-6728.

KEYSE, S. M. 1983. The Inactivation of Human Skin Ffibroblasts in Culture by Ultraviolet Radiations. Ph.D. Thesis, University of Bath.

KEYSE, S. M., MOSS. S. H., and DAVIES, D. J. G. 1983. Action spectra for inactivation of normal and xeroderma pigmentosum human skin fibroblassts by ultraviolet radiations. Photochem. Photobiol. 37:307-312.

KEYSE, S. M., MCCALEER, M. A., DAVIES, D. J. G. AND MOSS, S. H. 1985. The response of normal and ataxia-telangiectasia human skin fibroblasts to the lethal effects of far, mid and near ultraviolet radiations. Int. J. Radiat. Biol. 48:975-985.

KLAMEN, D. L. and TUVESON, R. W. 1982. The effect of membrane fatty acid composition on the near-UV (300-400 nm) sensitivity of Escherichia coli K1060. Photochem. Photobiol. 35:167-173.

KOBAYASHI, K. and ITO, T. 1976. Further in vivo studies on the participation of singlet oxygen in the photodynamic inactivation and induction of genetic changes in Saccharomyces cerevisiae. Photochem. Photobiol. 23:21-28.

KOBAYASHI, K. and ITO, T. 1977. Wavelength dependence of singlet oxygen mechanism in acridine orange-sensitized photodynamic action in yeast cells: Experiments with 470 nm. Photochem. Photobiol. 25:385-388.

KONINGS, A. W. T. and RUIFROK, A. C. C. 1985. Role of membrane lipids and membrane fluidity in thermosensitivity and thermotolerance of mammalian cells. Radiation Res. 102:86-98.

KRAEMER, K. H., ANDREWS, A. D., BARRETT, S. F. and ROBBINS, J. H. 1976. Colony-forming ability of ultraviolet-irradiated xeroderma pigmentosum fibroblasts from different DNA repair complementation groups. Biochim. Biophys. Acta 442:147-153.

KRINSKY, N. I. 1979. Biological Functions of Singlet Oxygen. IN: Singlet Oxygen, H. H. Wasserman and R. W. Murray, Eds., Academic Press, New York, pp. 597-636.

KRINSKY, N. I. 1984. Biology and photobiology of singlet oxygen. IN: Oxygen Radicals in Chemistry and Biology, W. Bors, M. Saran, D. Tait, Eds., Walter deGruyter, Berlin, pp. 453-463.

LAVELLE, F., MICHELSON A. M. AND DIMITRIJEVIC, L. 1973. Biological protection by superoxide dismutase. Biochem. Biophys. Res. Commun. 55:350-357.

LEHMANN, A. R. and BRIDGES, B. A. 1977. DNA Repair. Essays in Biochemistry 13:71-117.

LEHMANN, A. R. and KARRAN, P. 1981. DNA repair. Int. Rev. Cytology 72:101-146.

LEHMANN, A. R., KIRK-BELL, S., ARLETT, C. F., HARCOURT, S. A., DE WEERD-KASTELEIN, E. A., KEIJZER, W. and HALL-SMITH, P. 1977. Repair of ultraviolet light damage in a variety of human fibroblast cell strains. Cancer Res. 37:904-910.

LESKO, S. A., TRPIS, L. and YANG, S. U. 1985. Induction of 6-thioguanine-resistant mutants by hyperoxia and gamma-irradiation: Effect of compromising cellular antioxidant systems. Mutation Res. 149:119-126.

LEY, R. D., SEDITA, B. A. and BOYE, E. 1978. DNA polymerase 1-mediated repair of 365 nm-induced single-strand breaks in the DNA of Escherichia coli. Photochem. Photobiol. 27:323-327.

MANDAL, T. K. and CHATTERJEE, S. N. 1980. Ultraviolet- and sunlight-induced lipid peroxidation in liposomal membrane. Radiat. Res. 83:290-302.

MARKLUND, S. L., MIDANDER, J. and WESTMAN, G. 1984a. CuZn superoxide dismutase, Mn superoxide dismutase, catalase and glutathione peroxidase in glutathione-deficient human fibroblasts. Biochim. Biophys. Acta 798:302-305.

MARKLUND, S. L., WESTMAN, G., ROOS, G. and CARLSSON, J. 1984b. Radiation resistance and the CuZn superoxide dismutase, catalase and glutathione peroxidase activities of seven human cell lines. Radiat. Res. 100:115-123.

MCALEER, M. A., MOORE, S. P. AND MOSS, S. H. 1987. Effect of growth temperature on lipid composition and ultraviolet sensitivity of human cells. Photochem. Photobiol. In Press.

MCCORMICK, J. P., FISCHER, J. R., PACHLATKO, J. P. and EISENSTARK, A. 1976. Characterization of a cell-lethal product from the photooxidation of tryptophan: hydrogen peroxide. Science 191:468-469.

MCKEEHAN, W. L., MCKEEHAN, K. A. and HAM, R. G. 1981. The use of low-temperature subculturing and culture surfaces coated with basic polymers to reduce the requirement for serum macromolecules. IN: The Growth Requirements of Vertebrate Cells In Vitro, Waymouth, Ham and Chapple, Eds., Cambridge Univ. Press, pp. 118-130.

MEFFERT, H., DIEZEL, W. and SONNICHSEN, N. 1976. Stable lipid peroxidation products in human skin: Detection, ultraviolet light-induced increase, pathogenic importance. Experientia 32:1397-1398.

MERKEL, P. B., NILSSON, R. and KEARNS, D. R. 1972. Deuterium effects on singlet oxygen lifetimes in solutions. A new test of singlet oxygen reactions. J. Am. Chem. Soc. 94:1030-1032.

MIDDEN, W. R. 1985. Is singlet oxygen responsible for superoxide toxicity? Abstracts 13th Ann. Meet. Amer. Soc. Photobiol. New Orleans, LA, 23-27 June.

MOROWITZ, M. J. 1950. Absorption effects in volume irradiation of microorganisms. Science 111:229-230.

MOSS, S. H. and SMITH, K. C. 1981. Membrane damage can be a significant factor in the inactivation of Escherichia coli by near-ultraviolet radiation. Photochem. Photobiol. 33:203-210.

MURPHY, T. M. and WILSON, C. 1982. UV-stimulated K^+ efflux from rose cells. Counterion and inhibitor studies. Plant Physiol. 70:709-713.

NIGGLI, H. J. and CERUTTI, P. A. 1983. Temperature dependence of induction of cyclobutane-type pyrimidine photodimers in human fibroblasts by 313 nm light. Photochem. Photobiol. 37:467-469.

OHYASHIKI, T., USHIRO, H. and MOHRI, T. 1986. Effects of alpha-tocopherol on the lipid peroxidation and fluidity of porcine intestinal brush-border membranes. Biochim. Biophys. Acta 858:294-300.

OSHINO, N., CHANCE, B., SIES, H. and BUCHER, T. 1973. The role of H_2O_2 generation in perfused rat liver and the reaction of catalase compound I and hydrogen donors. Arch. Biochem. Biophys. 154:117-124.

OZAWA, T. and HANAKI, A. 1985. Spectroscopic studies on the reaction of superoxide ion with tocopherol model compound, 6-hydroxy-2,2,5,7,8-pentamethylchroman. Biochem. Biophys. Res. Commun. 126:873-878.

PACKER, J. E., SLATER, T. F., and WILLSON, R. L. 1979. Direct observation of a free radical interaction between vitamin E and vitamin C. Nature 278:737-738.

PACKER, L. 1978. Protection of environmentally stressed human cells in culture with the free radical scavenger, dl-a-tocopherol. IN: Aging, Carcinogenesis and Radiation Biology--The Role of Nucleic Acid Addition Reactions, K. C. Smith, Ed., Plenum Press, New York, pp. 519-535.

PACKER, L. and SMITH, J. R. 1974. Extension of the lifespan of cultured normal human diploid cells by vitamin E. Proc. Natl. Acad. Sci. 71:4763-4767.

PATHAK, M. A., KRAMER, D. M. and GUNGERICH, U. 1972. Formation of thymine dimers in mammalian skin by ultraviolet radiation in vivo. Photochem. Photobiol. 15:177-185.

PATRICK, G. 1977. The effects of radiation on cell membranes. IN: Mammalian Cell Membranes, Volume 5, G. A. Jamieson and D. M. Robinson, Eds., Butterworth, London pp. 72-100.

PATTON, J. D., ROWAN, L. A., MENDRALA, A. L., HOWELL, J. N., MAHER, V. M. and MCCORMICK, J. J. 1984. Xeroderma pigmentosum fibroblasts including cells from XP variants are abnormally sensitive to the mutagenic and cytotoxic action of broad spectrum simulated sunlight. Photochem. Photobiol. 39:37-42.

PAUL, J. 1975. Cell and Tissue Culture, 5th Ed., Churchill Livingstone, Edinburgh.

PEAK, J. G., FOOTE, C. S. and PEAK, M. J. 1981. Protection by DABCO against inactivation of transforming DNA by near-ultraviolet light: Action spectra and implications for involvement of singlet oxygen. Photochem. Photobiol. 34:45-49.

PEAK, J. G., PEAK, M. J. and MACCOSS, M. 1984. DNA breakage caused by 334 nm ultraviolet light is enhanced by naturally occurring nucleic acid components and nucleotide coenzymes. Photochem. Photobiol. 39:713-716.

PEAK, J. G., PEAK, M. J. and FOOTE, C. S. 1982. Effects of glycerol upon the biological actions of near-ultraviolet light: Spectra and concentration dependence for transforming DNA and for Escherichia coli B/r. Photochem. Photobiol. 36:413-416.

PEAK, J. G., PEAK, M. J., SIKORSKI, R. S. and JONES, C. A. 1985a. Induction of DNA-protein crosslinks in human cells by ultraviolet and visible radiations: Action spectrum. Photochem. Photobiol. 41:295-302.

PEAK, M. J. 1970. Some observations on the lethal effects of near-ultraviolet light on Escherichia coli, compared with the lethal effects of far-ultraviolet light. Photochem. Photobiol. 12:1-8.

PEAK, M. J. and PEAK, J. G. 1973. Protection by histidine against the inactivation of DNA transforming activity by near-ultraviolet light. Photochem. Photobiol. 18:525-527.

PEAK, M. J. and PEAK, J. G. 1975. Protection by AET against inactivation of transforming DNA by ultraviolet light, action spectrum. Photochem. Photobiol. 22:147-148.

PEAK, M. J. and PEAK, J. G. 1980. Protection by glycerol against the biological actions of near-ultraviolet light. Radiat. Res. 83:553-558.

PEAK, M. J. AND PEAK, J. G. 1982. Single-strand breaks induced in Bacillus subtilis DNA by ultraviolet light: Action spectrum and properties. Photochem. Photobiol. 35:675-680.

PEAK, M. J., PEAK, J. G. and WEBB, R. B. 1973. Inactivation of transforming DNA by ultraviolet light. I. Near-UV action spectrum for marker inactivation. II. Protection by histidine against near-UV irradiation: Action spectrum. III. Further observations on the effect of 365 nm radiation. Mutation Res. 20:143-148.

PEAK, M. J., PEAK, J. G. and JONES, C. A. 1985b. Different (direct and indirect) mechanisms for the induction of DNA-protein crosslinks in human cells by far- and near-ultraviolet radiations (290 and 405 nm). Photochem. Photobiol. 42:141-146.

PEREIRA, O. M., SMITH, J. R. and PACKER, L. 1976. Photosensitization of human diploid cell cultures by intracellular flavins and protection by antioxidants. Photochem. Photobiol. 24:237-242.

PETERS, J. 1977. In vivo photoinactivation of Escherichia coli ribonucleotide reductase by near-ultraviolet light. Nature 267:546-548.

PETKAU, A. and CHELACK, W. S. 1974. Protection of Acholeplasma laidlawii B by superoxide dismutase. Int. J. Radiat. Biol. 26:421-426.

POLLARD, E. 1961. Effect of gamma-radiation on Escherichia coli grown in deuterium oxide medium. Nature 192:177-178.

POOLER, J. P. and VALENZENO, D. P. 1979. The role of singlet oxygen in photooxidation of excitable cell membranes. Photochem. Photobiol. 581-584.

PRINCE, E. W. and LITTLE, J. B. 1973. The effect of dietary fatty acids and tocopherol on the radiosensitivity of mammalian erythrocytes. Mutation Res. 53:49-64.

PRYOR, W. A. 1984. Free radicals in autoxidation and aging. IN: Free Radicals in Molecular Biology, Aging and Disease, D. Armstrong, R. S. Sohal, R. G. Cutler, T. F. Slater, Eds., Raven Press, New York, pp. 13-41.

PUCK, T. T., MARCUS, P. I. and CIECIURA, S. J. 1956. Clonal growth of mammalian cells in vitro. Growth characteristics of colonies from single HeLa cells with and without a 'feeder layer'. J. Exptl. Med. 103:273-284.

ROSENSTEIN, B. S. 1984. Photoreactivation of ICR 2A frog cells exposed to solar UV wavelengths. Photochem. Photobiol. 40:207-213.

ROSENSTEIN, B. S. and DUCORE, J. M. 1983. Induction of DNA strand breaks in normal human fibroblasts exposed to monochromatic ultraviolet and visible wavelengths in the 240-546 nm range. Photochem. Photobiol. 38:51-55.

ROSENSTEIN, B. S. and DUCORE, J. M. 1984. Enhancement by bilirubin of DNA damage induced in human cells exposed to phototherapy light. Pediatric Res. 18:3-6.

ROSENSTEIN, B. S. and SETLOW, R. B. 1980. Photoreactivation of ICR 2A frog cells after exposure to monochromatic ultraviolet radiation in the 252-313 nm range. Photochem. Photobiol. 32:361-366.

ROSENSTEIN, B. S., DUCORE, J. M. and CUMMINGS, S. W. 1983. The mechanism of bilirubin-photosensitized DNA strand breakage in human cells exposed to phototherapy light. Mutation Res. 112:397-406.

ROSHCHUPKIN, D. I., PELENITSYN, A. B., POTAPENKO, A. Y., TALITSKY, V. V. and VLADIMIROV, Y. A. 1975. Study of the effects of ultraviolet light on biomembranes--IV. The effect of oxygen on UV-induced hemolysis and lipid peroxidation in rat erythrocytes and liposomes. Photochem. Photobiol. 21:63-69.

ROTHMAN, R. H. and SETLOW, R. B. 1979. An action spectrum for cell killing and pyrimidine dimer formation in Chinese hamster V-79 cells. Photochem. Photobiol. 29:57-61.

ROTHSTEIN, E. L., HARTZELL, R. W., MANSON, L. A. and KRITCHEVSKY, D. 1960. Effects of D_2O on cellular components of mammalian cells grown in tissue culture. Ann. N. Y. Acad. Sci. 84:721-726.

ROZA, L., VAN DER SCHANS, G. P. and LOHMAN, P. H. M. 1985. The induction and repair of DNA damage and its influence on cell death in primary human fibroblasts exposed to UV-A or UV-C irradiation. Mutation Res. 146:89-98.

RUPP, W. D., WILDE, C. E., RENO, D. L. and HOWARD-FLANDERS, P. 1971. Exchanges between DNA strands in UV irradiated E. coli. J. Mol. Biol. 61:25-44.

SAKANASHI, T., SUGIYAMA, M., SUEMATSU, T., HIDAKA, T. and OGURA, R. 1986. Delayed alteration of fluidity in intact cultured B-16 melanoma cells affected by ultraviolet irradiation. Biochem. International 12:341-346.

SAMMARTANO, L. J. and TUVESON, R. W. 1983. Escherichia coli xthA mutants are sensitive to inactivation by broad spectrum near-UV (300-600 nm) radiation. J. Bacteriol. 156:904-906.

SAMMARTANO, L. J. and TUVESON, R. W. 1984. The effects of exogenous catalase on broad spectrum near-UV (300-400 nm) treated Escherichia coli cells. Photochem. Photobiol. 3:607-612.

SAMMARTANO, L. J. and TUVESON, R. W. 1985. Hydrogen peroxide induced resistance to broad spectrum near-ultraviolet (300-400 nm) inactivation in Escherichia coli. Photochem. Photobiol. 41:367-370.

SCARPA, M., RIGO, A., MAIORINO, M., URSINI, F. and GREGOLIN, C. 1984. Formation of alpha-tocopherol radical and recycling of alpha-tocopherol by ascorbate during peroxidation of phosphatidylcholine liposomes. Biochim. Biophys. Acta 801:215-219.

SETLOW, R. B. and CARRIER, W. L. 1964. The disappearance of thymine dimers from DNA, an error correcting mechanism. Proc. Natl. Acad. Sci. (USA) 51:226-231.

SETLOW, R. B. and SETLOW, J. K. 1972. Effects of radiation on polynucleotides. Ann. Rev. Biophys. Bioeng. 1:293-346.

SHIMA, A. and SETLOW, R. B. 1984. Survival and pyrimidine dimers in cultured fish cells exposed to concurrent sun lamp ultraviolet and photoreactivating radiations. Photochem. Photobiol. 39:49-56.

SMITH, J. R. 1981. The Fat-Soluble Vitamins. IN: The Growth Requirements of Vertebrate Cells in Vitro. Waymouth, Ham, and Chapple, Eds., Cambridge Univ. Press, pp. 343-352.

SMITH, K. C. 1964. The photochemical interaction of DNA and protein in vivo and its biological importance. Photochem. Photobiol. 3:415-427.

SMITH, K. C. 1978. Multiple pathways of DNA repair in bacteria and their roles in mutagenesis. Photochem. Photobiol. 28:121-129.

SMITH, P. J. and PATERSON, M. C. 1981. Abnormal responses to mid-ultraviolet light of cultured fibroblasts from patients with disorders featuring sunlight sensitivity. Cancer Res. 41:511-518.

SMITH, P. J. and PATERSON, M. C. 1982. Lethality and the induction and repair of DNA damage in far, mid or near UV-irradiated human fibroblasts: Comparison of effects in normal, xeroderma pigmentosum and Bloom's syndrome cells. Photochem. Photobiol. 36:333-343.

SNEDECOR, G. W. and COCHRAN, W. C. 1967. IN: Statistical Methods, Iowa State University Press, pp. 72-74.

SRIVASTAVA, S., PHADKE, R. S., GOVIL, G. and RAO, C. N. R. 1983. Fluidity, permeability and antioxidant behaviour of model membranes incorporated with alpha-tocopherol and vitamin E acetate. Biochim. Biophys. Acta 734:353-362.

STOIEN, J. D. and WANG, R. J. 1974. Effect of near-ultraviolet and visible light on mammalian cells in culture. II. Formation of toxic photoproducts in tissue culture medium by blacklight. Proc. Natl. Acad. Sci. (USA) 71:3961-3965.

SUTHERLAND, B. M. 1977. Human Photoreactivating Enzymes. IN: Research in Photobiology, A. Castellani, Ed., Plenum Press, New York pp. 307-315.

SUTHERLAND, J. C. and GRIFFIN , K. P. 1981. Absorption spectrum of DNA for wavelengths greater than 300 nm. Radiation Res. 86:399-409.

TAPPEL, A. L. 1968. Will antioxidant nutrients slow aging processes? Geriatrics 23:97-105.

THOMSON, J. F. 1963. Biological Effects of Deuterium. Vol. 19 of International Series of Monographs on Pure and Applied Biology, Pergamon Press, London.

TUVESON, R. W., PEAK, J. G. and PEAK, M. J. 1983. Single-strand DNA breaks induced by 365 nm radiation in E. coli strains differing in sensitivity to near and far UV. Photochem. Photobiol. 37:109-112.

TYRRELL, R. M. 1986. UVA radiation inactivation of human cells--a search for active intermediates. Abstracts, First European Congress of Photobiology, Grenoble, France, 8-12 Sept.

TYRRELL, R. M. 1973. Induction of pyrimidine dimers in bacterial DNA by 365 nm radiations. Photochem. Photobiol. 17:69-73.

TYRRELL, R. M. 1979. Lethal cellular changes induced by near ultraviolet radiation. Acta Biol. Med. Germ. 38:1259-1269.

TYRRELL, R. M. 1985. A common pathway for protection of bacteria against damage by solar UVA (334 nm, 365 nm) and an oxidising agent (H_2O_2). Mutation Res. 145:129-136.

TYRRELL, R. M. and PIDOUX, M. 1986. Endogenous glutathione protects human skin fibroblasts against the cytotoxic action of UVB, UVA and near-visible radiations. Photochem. Photobiol. 44:561-564.

TYRRELL, R. M., LEY, R. D. and WEBB, R. G. 1974. Induction of single-strand breaks (alkali-labile bonds) in bacterial and phage DNA by near-UV (365 nm) radiation. Photochem. Photobiol. 20:395-398.

TYRRELL, R. M., WERFELLI, P. and MORAES, E. C. 1984. Lethal action of ultraviolet and visible (blue-violet) radiations at defined wavelengths on human lymphoblastoid cells: Action spectra and interaction sites. Photochem. Photobiol. 39:183-189.

UENO, A. M., TANAKA, O. and MATSUDAIRA, H. 1984. Inhibition of gamma-ray dose-rate effects by D_2O and inhibitors of poly (ADP-ribose) synthetase in cultured mammalian L5178Y cells. Radiation Res. 98:574-582.

URBACH, F., EPSTEIN, J. H. and FORBES, P. D. 1974. Ultraviolet Carcinogenesis: Experimental, Global and Genetic Aspects. IN: Sunlight and Man, Normal and Abnormal Responses, M. Pathak, L. C. Harber, M. Seiji and A. Kukita, Eds., pp. 259-284.

WAGNER, S., TAYLOR, W. D., KEITH, A. AND SNIPES, W. 1980. Effects of acridine plus near ultraviolet light on Escherichia coli membranes and DNA in vivo. Photochem. Photobiol. 32:771-779.

WANG, D. I. C., SINSKEY, T. J., GEMER, R. E. and DEFILIPPO. 1968. Effect of centrifugation on the viability of Burkitt lymphoma cells. Biotechnol. Bioeng. 10:641-649.

WANG, R. J., STOIEN, J. D. and LANDA, F. 1974. Lethal effect of near-ultraviolet irradiation on mammalian cells in culture. Nature 247:43-45.

WARD, J. F., BLAKELY, W. F. and JONER, E. I. 1985. Mammalian cells are not killed by DNA single-strand breaks caused by hydroxyl radicals from hydrogen peroxide. Radiation Res. **103**:383-392.

WEBB, R. B. 1977. Lethal and mutagenic effects of near-ultraviolet radiation. IN: Photochemical and Photobiological Reviews, K. C. Smith, Ed., Vol. 2., Plenum Press, New York, pp. 169-261.

WEBB, R. B. and BROWN, M. S. 1976. Sensitivity of strains of Escherichia coli differing in repair capability to far UV, near UV and visible radiations. Photochem. Photobiol. **24**:425-432.

WEBB, R. B. and BROWN, M. S. 1979. Action spectra for oxygen-dependent and independent inactivation of Escherichia coli WP2s from 254 to 460 nm. Photochem. Photobiol. **29**:407-409.

WEBB, R. B. and LORENZ, J. R. 1970. Oxygen dependence and repair of lethal effects of near ultraviolet and visible light. Photochem. Photobiol. **12**:283-289.

WEBB, R. B., BROWN, M. S. and TYRRELL, R. M. 1976. Lethal effects of pyrimidine dimers induced at 365 nm in strains of E. coli differing in repair capability. Mutation Res. **37**:167-172.

WEISSMAN, G. and DINGLE, J. 1961. Release of lysosomal protease by ultraviolet irradiation and inhibition by hydrocortisone. Exptl. Cell Res. **25**:207-210

WELLS, R. L. and HAN, A. 1984. Action spectra for killing and mutation of Chinese hamster cels exposed to mid- and near-ultraviolet monochromatic light. Mutation Res. **129**:251-258.

WELLS, R. L. and HAN, A. 1985. Differences in sensitivity between human, mouse and Chinese hamster cells to killing by monochromatic ultraviolet light. Int. J. Radiat. Biol. **47**:17-21.

WITTING, L. A. 1980. Vitamin E and lipid antioxidants in free-radical-initiated reactions. IN: Free Radicals in Biology, W. A. Pryor, Ed., Vol. 4, Academic Press, New York, pp. 295-319.

WOLTERS, H. and KONINGS, A. W. T. 1984. Radiosensitivity of normal and polyunsaturated fatty acid supplemented fibroblasts after depletion of glutathione. Int. J. Radiat. Biol. **46**:161-168.

WOLTERS, H. and KONINGS, A. W. T. 1985. Membrane radiosensitivity of fatty acid supplemented fibroblasts as assayed by the loss of intracellular potassium. Int. J. Radiat. Biol. **6**:963-973.

YOAKUM, G. and EISENSTARK, A. 1972. Toxicity of L-tryptophan photoproduct on recombinationless (rec) mutants of Salmonella typhimurium. J. Bacteriol. **112**:653-655.

YAGI, K., YAMADA, H. and NISHIKIMI, M. 1978. Oxidation of alpha-tocopherol with $^1O_2$: IN: Tocopherol, Oxygen and Biomembranes, C. deDuve and O. Hayaishi, Eds., Elsevier Biomedical Press, Amsterdam.

ZAMANSKY, G. B. 1986. Varying sensitivity of human skin fibroblasts to polychromatic ultraviolet light. Mutation Res. 160:55-60.

ZAMANSKY, G. B., MINKA, D. F., DEAL, C. L. and HENDRICKS, K. 1985. The in vitro photosensitivity of systemic lupus erythematosus skin fibroblasts. J. Immunol. 134:1571-1576.

ZELLE, B., REYNOLDS, R. J., KOTTENHAGEN, M. J., SCHUITE, A. and LOHMAN, P. H. M. 1980. The influence of the wavelength of ultraviolet radiation on survival, mutation induction and DNA repair in irradiated Chinese hamster cells. Mutation Res. 72:491-509.